

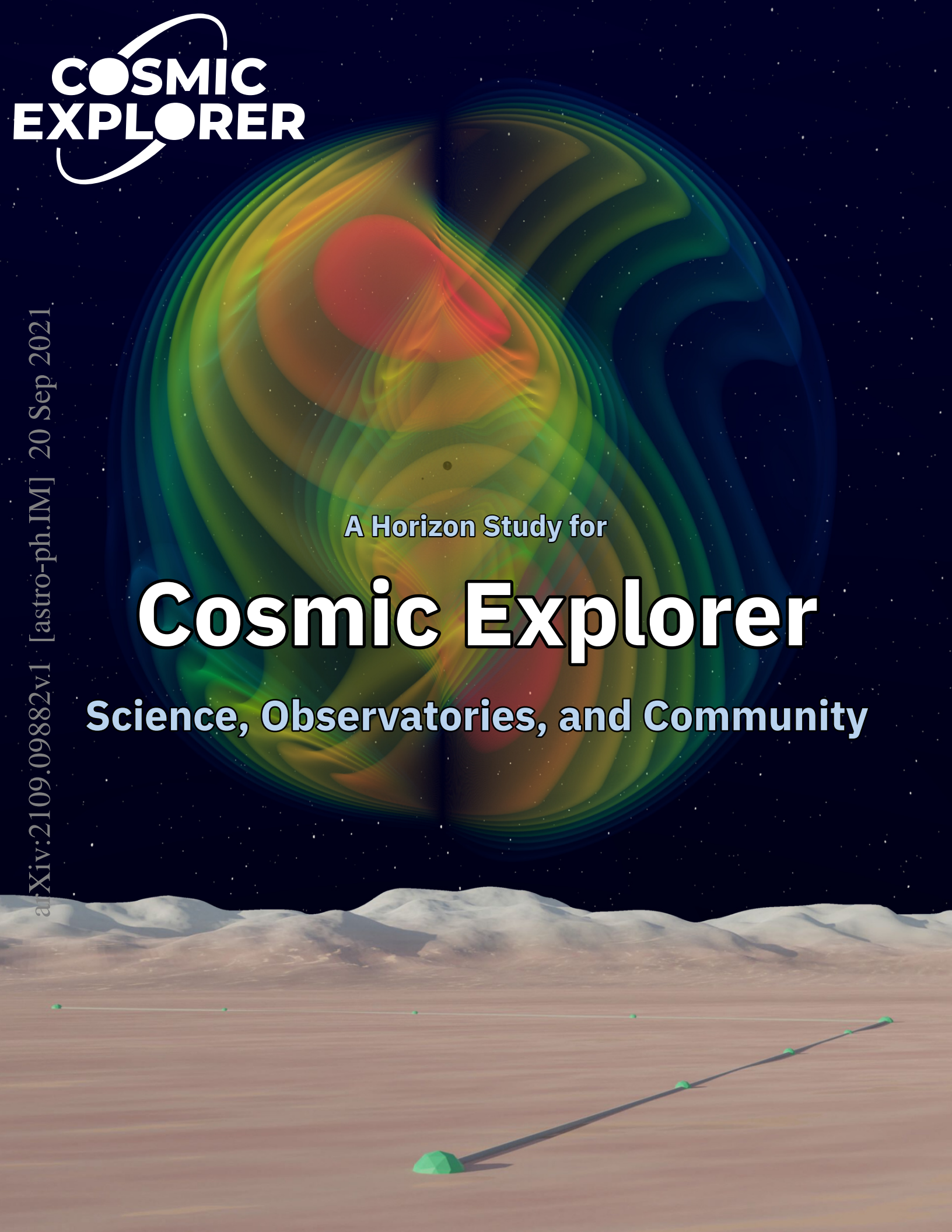
**COSMIC  
EXPLORER**

arXiv:2109.09882v1 [astro-ph.IM] 20 Sep 2021

A Horizon Study for

# Cosmic Explorer

Science, Observatories, and Community



## Authors

Matthew Evans,<sup>a</sup> Rana X Adhikari,<sup>b</sup> Chaitanya Afle,<sup>c</sup> Stefan W. Ballmer,<sup>c</sup> Sylvia Biscoveanu,<sup>a</sup> Ssohrab Borhanian,<sup>d</sup> Duncan A. Brown,<sup>c</sup> Yanbei Chen,<sup>e</sup> Robert Eisenstein,<sup>a</sup> Alexandra Gruson,<sup>f</sup> Anuradha Gupta,<sup>d,g</sup> Evan D. Hall,<sup>a</sup> Rachael Huxford,<sup>d</sup> Brittany Kamai,<sup>h,i</sup> Rahul Kashyap,<sup>d</sup> Jeff S. Kissel,<sup>j</sup> Kevin Kuns,<sup>a</sup> Philippe Landry,<sup>f</sup> Amber Lenon,<sup>c</sup> Geoffrey Lovelace,<sup>f</sup> Lee McCuller,<sup>a</sup> Ken K. Y. Ng,<sup>a</sup> Alexander H. Nitz,<sup>k,l</sup> Jocelyn Read,<sup>f</sup> B. S. Sathyaprakash,<sup>d,m</sup> David H. Shoemaker,<sup>a</sup> Bram J. J. Slagmolen,<sup>n</sup> Joshua R. Smith,<sup>f</sup> Varun Srivastava,<sup>c</sup> Ling Sun,<sup>n</sup> Salvatore Vitale,<sup>a</sup> Rainer Weiss<sup>a</sup>

<sup>a</sup>LIGO Laboratory, Massachusetts Institute of Technology, Cambridge, MA 02139, USA

<sup>b</sup>LIGO Laboratory, California Institute of Technology, Pasadena, CA 91125, USA

<sup>c</sup>Department of Physics, Syracuse University, Syracuse, NY 13244, USA

<sup>d</sup>Institute for Gravitation and the Cosmos, Department of Physics, Pennsylvania State University, University Park, PA 16802, USA

<sup>e</sup>Caltech CaRT, Pasadena, CA 91125, USA

<sup>f</sup>Nicholas and Lee Begovich Center for Gravitational-Wave Physics and Astronomy, California State University, Fullerton, Fullerton, CA 92831, USA

<sup>g</sup>Department of Physics and Astronomy, University of Mississippi, University, MS 38677, USA

<sup>h</sup>Department of Astronomy & Astrophysics, University of California Santa Cruz, Santa Cruz, CA 95064, USA

<sup>i</sup>Department of Mechanical Engineering, California Institute of Technology, Pasadena, CA 91125, USA

<sup>j</sup>LIGO Hanford Observatory, Richland, WA 99352, USA

<sup>k</sup>Max-Planck-Institut für Gravitationsphysik (Albert-Einstein-Institut), D-30167 Hannover, Germany

<sup>l</sup>Leibniz Universität Hannover, D-30167 Hannover, Germany

<sup>m</sup>School of Physics and Astronomy, Cardiff University, Cardiff, UK

<sup>n</sup>OzGrav-ANU, Centre for Gravitational Astrophysics, College of Science, The Australian National University, ACT 2601, Australia

Correspondence: [ce-questions@cosmicexplorer.org](mailto:ce-questions@cosmicexplorer.org)

## Cover Image

The cover image shows an artistic rendering of Cosmic Explorer [credit: Evan Hall (MIT)] beneath a numerical-relativity simulation of a binary black hole emitting gravitational waves [credit: Nils Fischer, Harald Pfeiffer, Alessandra Buonanno (Max Planck Institute for Gravitational Physics), Simulating eXtreme Spacetimes (SXS) Collaboration].



This study was funded by the National Science Foundation.

# Contents

1 Executive Summary 1

2 Purpose and Scope 6

## Science Objectives 8

3 Overview 9

4 Status of Ground-Based Gravitational-Wave Observatories 14

5 Key Science Questions 16

5.1 Black Holes and Neutron Stars Throughout Cosmic Time 16

5.1.1 Remnants of the First Stars 16

5.1.2 Seed Black Holes and Galaxy Formation 17

5.1.3 Formation and Evolution of Compact Objects 18

5.2 Dynamics of Dense Matter 19

5.2.1 Neutron Star Structure and Composition 20

5.2.2 New Phases in Quantum Chromodynamics 22

5.2.3 Chemical Evolution of the Universe 23

5.2.4 Gamma-Ray Burst Jet Engine 24

5.3 Extreme Gravity and Fundamental Physics 24

5.3.1 Nature of Strong Gravity 26

5.3.2 Unusual and Novel Compact Objects 27

5.3.3 Dark Matter and Dark Energy 27

5.4 Discovery Potential 29

5.4.1 Quantum Gravity 32

5.4.2 New Particles and Fields 33

5.4.3 Stochastic Gravitational-Wave Backgrounds 33

## Observatories 36

6 A Science-Driven Design for Cosmic Explorer 37

6.1 Design Concept for Cosmic Explorer 37

6.2 Technology survey 38

<b>7</b>	<b>Optimizing Design Performance Versus Cost</b>	<b>42</b>
7.1	Alternate Configurations	43
7.2	Trade-Study Outline	50
<b>8</b>	<b>Technical Overview and Design Choices</b>	<b>64</b>
8.1	Reference Detector Concept	64
8.2	Site and Facility	72
8.3	Enabling Technologies	77
8.4	Silicon Upgrades	92
8.5	Cost Drivers	94
<b>9</b>	<b>Data Management, Analysis, and Computing</b>	<b>98</b>
9.1	Data Management Plan	98
9.2	Requirements for Open-Data and Analysis	99
9.3	Additional Computational Resources	101
	<b>Community, Organization, and Planning</b>	<b>103</b>
<b>10</b>	<b>CE at the Local and Global Scales</b>	<b>104</b>
10.1	Community Integration and Engagement	104
10.2	Building Strong Relationships with the Local Community	105
10.3	CE as Part of the Scientific Community	108
10.4	Developing a Global Gravitational-Wave Network	111
10.5	A Respectful, Healthy, and Thriving Scientific Community	112
<b>11</b>	<b>Cosmic Explorer Project</b>	<b>114</b>
11.1	Cost Estimates	114
11.2	Timeline	116
11.3	Operations Model	119
11.4	Risk Management	121
11.5	Synergies with Programs at U.S. Funding Agencies	124
11.6	Cosmic Explorer Project Roadmap	125
<b>12</b>	<b>Conclusion</b>	<b>128</b>
	<b>Acknowledgements</b>	<b>129</b>
	<b>Cost and Inflation Estimates</b>	<b>130</b>
	<b>Abbreviations</b>	<b>133</b>
	<b>References</b>	<b>135</b>



# 1 Executive Summary

Gravitational-wave astronomy has revolutionized humanity's view of the universe. Investment in the field has rewarded the scientific community with the first direct detection of a binary black hole merger and the multimessenger observation of a neutron-star merger. Each of these was a watershed moment in astronomy, made possible because gravitational waves reveal the cosmos in a way that no other probe can. Since the first detection of gravitational waves in 2015, the National Science Foundation's LIGO and its partner observatory, the European Union's Virgo, have detected over fifty binary black hole mergers and a second neutron star merger — a rate of discovery that has amazed even the most optimistic scientists.

This Horizon Study describes a next-generation ground-based gravitational-wave observatory: **Cosmic Explorer**. With ten times the sensitivity of Advanced LIGO, Cosmic Explorer will push the reach of gravitational-wave astronomy towards the edge of the observable universe ( $z \sim 100$ ). This Horizon Study presents the science objectives for Cosmic Explorer, and describes and evaluates its design concepts. Cosmic Explorer will continue the United States' leadership in gravitational-wave astronomy in the international effort to build a "Third-Generation" (3G) observatory network that will make discoveries transformative across astronomy, physics, and cosmology.

Major discoveries in astronomy are driven by three related improvements: better sensitivity, higher precision, and opening a new observational window. Cosmic Explorer promises all of these. The nature of gravity means that with a one order-of-magnitude sensitivity improvement over current detectors Cosmic Explorer will see gravitational-wave sources across the history of the universe. With its unprecedented sensitivity, Cosmic Explorer will make discoveries that cannot yet be anticipated, especially since gravitational waves reach into regions of the universe that electromagnetic observations cannot explore. With Cosmic Explorer, scientists can use the universe as a laboratory to test the laws of physics and study the nature of matter. In addition to Cosmic Explorer's extraordinary discovery potential, this Horizon Study focuses on three key science areas in which Cosmic Explorer will make a particularly dramatic impact:

**Black Holes and Neutron Stars Throughout Cosmic Time.** Understanding how the universe made the first black holes, and how these first black holes grew, is one of the most important unsolved problems in astrophysics. Cosmic Explorer will detect gravitational waves from binary black holes and neutron stars out to the edge of the visible universe, providing a view of Cosmic Dawn complementary to that of the James Webb Space Telescope. Cosmic Explorer will see evidence for the first stars by detecting the mergers of the black holes they leave behind. The millions of mergers detected by Cosmic Explorer will map the population of compact objects across time, detect mergers of the first black holes that contributed to seeding the universe's structure, explore the physics of massive stars, and reveal the processes that create black holes

and neutron stars.

**Dynamics of Dense Matter.** While a quantitative theory of nuclei, neutron-rich matter and deconfined quark matter has begun to emerge, understanding the nature of strongly interacting matter is an unsolved problem in physics. By observing many hundreds of loud neutron star mergers and measuring the stars' radii to 100 m or better, Cosmic Explorer will probe the phase structure of quantum chromodynamics, revealing the nuclear equation of state and its phase transitions. Cosmic Explorer's ability to detect and study the hot, dense remnants of neutron star mergers will provide an entirely new way of mapping out the dense, finite-temperature region of the quantum chromodynamics phase space, a region that is currently unexplored. A plethora of multimessenger observations will map heavy-element nucleosynthesis, explain the build-up of the chemical elements that are the building blocks of our world, and explore the physics of the binary-merger engine powering short gamma-ray bursts.

**Extreme Gravity and Fundamental Physics.** Cosmic Explorer's increased discovery aperture will allow it to observe both loud and rare gravitational-wave events — events that will reveal physics of the most extreme gravity in the universe as well as events from unusual and novel objects. LIGO and Virgo are already detecting events that we do not fully understand. With its higher-fidelity detections Cosmic Explorer will reveal the nature of these mysterious sources. Cosmic Explorer will be able to look for the effects of dark matter in the cores of neutron stars and probe the nature of dark energy by looking for its imprint in gravitational-wave signals from the cosmos. Cosmic Explorer's precision observations of black holes could help develop a viable theory of quantum gravity.

Cosmic Explorer's order-of-magnitude sensitivity improvement will be realized using a dual-recycled Fabry–Pérot Michelson interferometer, as in Advanced LIGO. Cosmic Explorer's increased sensitivity comes primarily from scaling up the detector's length from 4 to 40 km. This increases the amplitude of the observed signals with effectively no increase in the detector noise. From the topographical and geological point of view, many sites exist that could accommodate a Cosmic Explorer design with a 40 km detector at facilities in the continental United States. When selecting sites, partnership with the local and regional communities, and Indigenous Peoples, will be of utmost importance to ensure that the presence of a Cosmic Explorer observatory respects the cultural, environmental, socio-economic, political, and other aspects of its host communities. Hazards including earthquakes, floods, storms, and fires must also be considered, especially with the view of a long-lived facility and a changing environment.

There are many design choices that could realize some or all of Cosmic Explorer's wide range of scientific opportunity. The reference concept considered in this Horizon Study is a 40 km detector and a 20 km detector, both located in the United States, with a total estimated cost of \$2061M (2030 USD). Alternative configurations of two 20 km detectors a single 40 km detector are estimated to cost \$1642M (2030 USD) and \$1286M (2030 USD), respectively. (Clearly, the accuracy of these estimates does not warrant the number of digits given here, but they are maintained to ensure consistency with the more detailed breakdowns given in §11.1.) If the project design stage begins in the early 2020s, then Cosmic Explorer's first observing runs could take place in the mid-2030s. As the field moves forward, it will be essential to engage the broadest possible set of scientific stakeholders in Cosmic Explorer's science to define its operational parameters.

This includes defining Cosmic Explorer’s scientific priorities and the best detector technologies, network design, and operational parameters needed to deliver this science.

This Horizon Study includes a preliminary study (summarized in Table 1.1) that shows that although the reference concept can achieve Cosmic Explorer’s science goals without other next-generation gravitational-wave detectors, its scientific output is enhanced when operating as part of an international network. Different configurations for Cosmic Explorer are examined, embedded in a global network that includes the Einstein Telescope, a potential detector in Australia, and the existing second-generation (2G) observatories. The impact of downscoping Cosmic Explorer’s reference design (e.g., to a single 40 km detector) is also investigated. The community is encouraged to use this as a launch point to engage as Cosmic Explorer’s design parameters are developed in the coming years.

This Horizon Study describes a Cosmic Explorer project organization that follows the model successfully employed by LIGO: two US-based Cosmic Explorer facilities constructed in one project, followed by a transition to an operations organization. The project will use well-established methods for addressing technical, managerial and political risks. Cosmic Explorer’s timeline will have distinct stages over several decades: concept development; observatory design and site preparation; construction and commissioning; initial operations; operations at nominal sensitivity; observatory upgrades; and operations. Cosmic Explorer’s facilities are intended to be long-lived, allowing for detector upgrades with technologies yet to be discovered.

The operations stage will embrace daily operations, production of observation data, and low-latency astrophysical searches to produce astronomical alerts. Given the substantial investment and broad community support that will be required to realize a US next-generation gravitational-wave observatory, Cosmic Explorer is planned to be an Open Data facility in its operations phase. In this model, the Cosmic Explorer project is responsible for detector operations, calibration, curation of the detector data streams, and dissemination of detector data and rapid alerts to the scientific community. Cosmic Explorer will generate a data set that provides a unique, rich, and deep view of the universe over its lifetime. An open data approach will facilitate scientific collaboration, maximize the scientific community’s investment in the project, and provide opportunity for scientists from small institutions and historically underrepresented institutions.

Gravitational-wave astronomy is global. As part of a multimessenger network of international gravitational-wave observatories, astro-particle detectors, and telescopes across the electromagnetic spectrum, Cosmic Explorer will precisely localize and study the nature of a multitude of sources. Experiments probing heavy ions and rare isotopes will help Cosmic Explorer determine the physics of dense matter. Gravitational waves are generated by physical processes that are vastly different from those that generate other forms of radiation and particles, and their detections allow us to see into regions of the universe that cannot be observed in any other way. It would be a profound anomaly in astronomy if nothing new and interesting came from Cosmic Explorer’s vast improvement in sensitivity.

With foundations laid by decades of National Science Foundation investment and the work of a large community of scientists, Cosmic Explorer is poised to propel another revolution in our understanding of the universe. The community is invited to join the effort to define, shape, and realize Cosmic Explorer: the future of gravitational-wave astronomy.

# 1 Executive Summary

Science		No CE	CE with 2G			CE with ET			CE, ET, CE South									
Theme	Goals	2G	20	40	20+20	20+40	40+40	20	40	20+20	20+40	40+40	20	40	20+20	20+40	40+40	
Black holes and neutron stars throughout cosmic time	Black holes from the first stars	Gray	Gray	Gray	Yellow	Green	Dark Green	Dark Green	Dark Green	Dark Green	Dark Green	Dark Green	Dark Green	Dark Green	Dark Green	Dark Green	Dark Green	Dark Green
	Seed black holes	Gray	Yellow	Yellow	Green	Dark Green	Dark Green	Dark Green	Dark Green	Dark Green	Dark Green	Dark Green	Dark Green	Dark Green	Dark Green	Dark Green	Dark Green	Dark Green
	Formation and evolution of compact objects	Gray	Yellow	Green	Dark Green	Dark Green	Dark Green	Dark Green	Dark Green	Dark Green	Dark Green	Dark Green	Dark Green	Dark Green	Dark Green	Dark Green	Dark Green	Dark Green
Dynamics of dense matter	Neutron star structure and composition	Gray	Yellow	Green	Dark Green	Dark Green	Dark Green	Dark Green	Dark Green	Dark Green	Dark Green	Dark Green	Dark Green	Dark Green	Dark Green	Dark Green	Dark Green	Dark Green
	New phases in quantum chromodynamics	Gray	Green	Yellow	Dark Green	Dark Green	Dark Green	Dark Green	Yellow	Dark Green	Dark Green	Dark Green	Dark Green	Dark Green	Dark Green	Dark Green	Dark Green	Dark Green
	Chemical evolution of the universe	Gray	Yellow	Yellow	Green	Dark Green	Dark Green	Dark Green	Dark Green	Dark Green	Dark Green	Dark Green	Dark Green	Dark Green	Dark Green	Dark Green	Dark Green	Dark Green
Extreme gravity and fundamental physics	Gamma-ray burst jet engine	Gray	Yellow	Yellow	Green	Dark Green	Dark Green	Dark Green	Dark Green	Dark Green	Dark Green	Dark Green	Dark Green	Dark Green	Dark Green	Dark Green	Dark Green	Dark Green
	Discovery potential	Gray	Gray	Yellow	Yellow	Green	Dark Green	Dark Green	Dark Green	Dark Green	Dark Green	Dark Green	Dark Green	Dark Green	Dark Green	Dark Green	Dark Green	Dark Green
Technical risk		Gray	Red	Light Orange	Light Orange	Light Orange	Light Orange	Red	Light Orange	Light Orange	Light Orange	Light Orange	Light Orange	Light Orange	Light Orange	Light Orange	Light Orange	Light Orange

Table 1.1: This table indicates the accessibility of astrophysical sources that can advance key next-generation science goals. A US Cosmic Explorer consisting of one 20 km observatory, one 40 km observatory, or a pair of observatories of 20 or 40 km length are evaluated in the presence a background network that includes second-generation (2G) gravitational-wave observatories, the European Einstein Telescope (ET), and a 20 km Cosmic Explorer-like detector located in Australia (CE South). For each goal, the colors range from gray (least favorable, science goal not achieved) to green (good, science achievable) and dark green (most favorable). The high-level conclusions of this comparison are summarized in Box 1.1 on the adjacent page and detailed descriptions of the metrics that determine the criteria can be found in §7.2.1. “Technical Risk” illustrates the technical risk associated with each configurations ability to achieve its target sensitivity; light orange is lowest risk, and red is highest risk. We emphasize that this study is a starting point for community input on Cosmic Explorer.

Box 1.1: Impact of Different Detector Configurations on Cosmic Explorer's Science Goals.

Table 1.1 compares the accessibility of the astrophysical sources and observations needed to achieve Cosmic Explorer's Science Goals with different observatories of lengths (20 km or 40 km) operating in different configurations of the global detector network (existing 2G observatories, the Einstein Telescope and an Australian detector CE South).

For each science goal, a gray box indicates that a science goal is not achieved. Green indicates that a science goal will be achieved, with dark green indicating the most favorable configuration for maximizing science from that goal. Yellow indicates that a configuration is unfavorable for achieving a science goal.

Several high-level conclusions can be drawn from this comparison:

- Cosmic Explorer's science goals cannot be accomplished with second-generation detectors.
- Two U.S. Cosmic Explorer observatories of 40 km length, or one observatory of 40 km *and* a second observatory of 20 km length can achieve all science goals without relying on the construction of other next-generation observatories.
- If only one Cosmic Explorer observatory is constructed in the U.S., achieving many of Cosmic Explorer's science goals will require the construction of the Einstein Telescope (ET) in Europe, or a second Cosmic Explorer observatory elsewhere in the world (e.g. CE South). This is due to reduction in the network's ability to measure the distance, inclination, and sky location of mergers.
- Studying new phases of quantum chromodynamics through the hot, post-merger signatures of binary neutron stars is best achieved with a global network that contains a 20 km Cosmic Explorer observatory for optimizing high-frequency sensitivity. This observatory could be in the U.S., in Australia (CE South), or elsewhere.
- Studies of extreme gravity and fundamental physics with gravitational waves is best done with the sensitivity provided by a 40 km Cosmic Explorer observatory.
- In the absence of other next-generation observatories, a Cosmic Explorer consisting of two 40 km observatories is the most favorable configuration for all goals except those involving post-merger physics of neutron stars.
- Under the assumption that the Einstein Telescope is operational, the most favorable Cosmic Explorer configuration is one 40 km observatory and one 20 km observatory.



## 2 Purpose and Scope

The LIGO observatories are continuing to extend their astrophysical reach into new discovery space, but in the coming decade they will reach the limits imposed by their facility size and lifetime. These observatories will be replaced by a new generation of gravitational-wave observatories, known as third-generation (3G) or next-generation observatories, with longer baselines and new infrastructures. The international community's vision for next-generation science is detailed in white papers published by the Gravitational Wave International Committee,<sup>1</sup> and plans toward a next-generation gravitational-wave observatory in Europe, Einstein Telescope, are well underway.<sup>2</sup>

This Horizon Study is part of the development stage of a major-facility project,<sup>3</sup> the US-based next generation gravitational-wave observatory known as Cosmic Explorer (CE). The purpose of this document is to provide a clear vision of the science enabled by CE, a reference concept for the CE instrument and its evolution, and initial cost estimates for its construction and operation. It is intended to inform the scientific community, and the agencies which fund that community, with the goal of providing a foundation for further development of CE in those communities while spurring action toward CE's construction. This document, together with reports from the Gravitational Wave International Committee (GWIC),<sup>4</sup> will form the point of departure for the process leading to the design stage of the Cosmic Explorer Project.<sup>3</sup>

The major science themes that will be addressed by Cosmic Explorer and their associated goals are presented in §§3–5. §6 presents the reference concept for CE based on ground-based laser interferometric detection technology, as well as a discussion of alternative technologies.

Given that funding for the next generation of detectors must be directed so as to maximize the resulting scientific output, this Horizon Study presents a preliminary trade study for CE in §7. This trade study documents the impact of design and funding choices on the scientific output of CE, and in particular on the key science goals presented in §5. Of particular interest are the overall length of the CE arms, since this is the primary cost driver, and the possibility of building multiple observatories in the US. The community is encouraged to use this trade study as a launch point to engage in the development of Cosmic Explorer's design parameters.

With the key scientific objectives and overview of the CE design in hand, the rest of the document focuses on the technology needed to achieve Cosmic Explorer. The technical design concept, and site and infrastructure requirements are presented in §8. A data-management plan, and the human and computational resources needed to deliver open data and multimessenger alerts are presented in §9, along with a survey of the broader computing requirements and analysis costs.

The plans presented in this Horizon Study can only be successful with continued input

from and strong endorsement by the scientific community, and early engagement with local communities, including Indigenous Peoples, at potential observatory locations. The vision of Cosmic Explorer as part of diverse local and global communities, and its anticipated role as part of the global gravitational-wave network, are presented in §10.

§11 presents a cost estimate for CE construction and operation, along with a timeline and management outline for the project. This includes a discussion of technical and project management risk, based on risk management strategies employed by LIGO and other large projects. The timeline starts with ongoing research and development work, and lays out a path to astrophysical observation with CE. Both Initial and Advanced LIGO were delivered on time and on budget and CE will benefit greatly from the experience earned through the LIGO project. The management plan and cost-budget schedule presented here is based upon the successful Advanced LIGO management model, taking into account the lessons learned. Finally, conclusions are reported in §12.



# Science Objectives



### 3 Overview

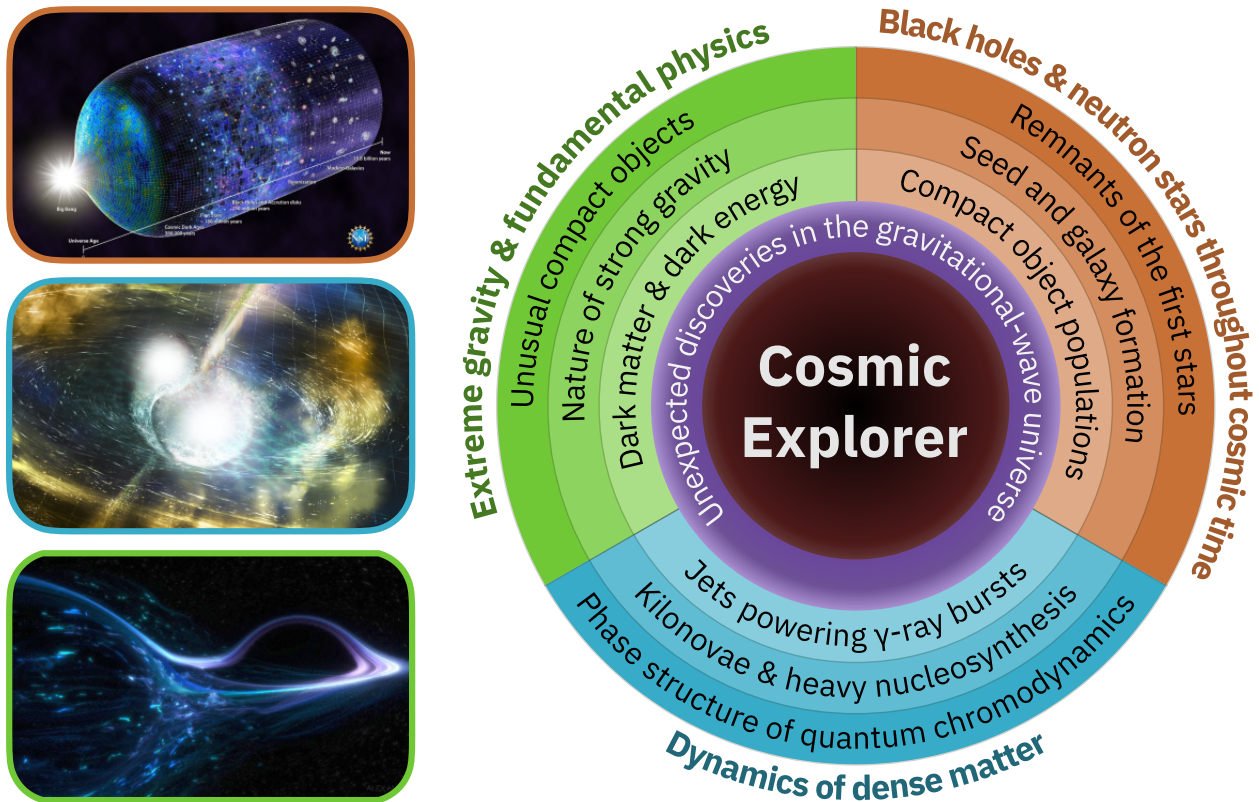


Figure 3.1: Central science themes and objectives that will be addressed by Cosmic Explorer. Cosmic Explorer’s greatly increased sensitivity over today’s detectors provides access to significantly more sources, spread out over cosmic time, as well as high-fidelity measurements of strong, nearby sources. §5 provides a more detailed description of the science enabled by Cosmic Explorer. Descriptions and credits for images to left, from top to bottom: A timeline of the universe, N.R.Fuller, National Science Foundation; Merging neutron stars, Aurore Simonnet, Sonoma State University; Black hole and mystery object, Alex Andrix, independent artist and Virgo/EGO.

The gravitational-wave discoveries by Advanced LIGO and Advanced Virgo have opened a new window on the universe. There is significant international interest in and mobilization toward developing a next generation of ground-based gravitational-wave observatories capable of observing gravitational waves throughout the history of star formation and exploring the workings of gravity at its most turbulent and extreme. Broad and detailed community studies of the potential for a network of such observatories (and its synergy with other types of gravitational-wave observatories and electromagnetic and astro-particle observatories) have been organized

by the Gravitational-Wave International Committee (GWIC) and summarized in a series of white papers.<sup>1</sup> The science case for a next-generation network, extensively described in the GWIC 3G Science Case Report along with a series of 2020 Astro Decadal Survey white papers,<sup>5–9</sup> is highly compelling, and the Einstein Telescope team has independently developed a science case for their planned facility.<sup>10</sup>

Based on these reports and our interactions with the community, we focus in this report on **three central scientific themes** that Cosmic Explorer will address (illustrated in Fig. 3.1):

1. **Black Holes and Neutron Stars Throughout Cosmic Time, §5.1**
2. **Dynamics of Dense Matter, §5.2**
3. **Extreme Gravity and Fundamental Physics, §5.3**

Additionally, we discuss the broad and deep discovery aperture of Cosmic Explorer and its potential for observing unexpected phenomena, §5.4.

Associated with each scientific theme are a number of key objectives. Some of these are achievable by a pair of Cosmic Explorer observatories operating on their own, while others will require an additional observatory or a network to achieve. Similarly, some objectives are certain, based on Cosmic Explorer’s expected performance and what we have already learned about gravitational-wave science, while others are not certain but would provide extraordinary or even revolutionary outcomes. Fig. 3.2 shows the key science objectives for Cosmic Explorer arranged on axes corresponding to these considerations.

A “trade study” of how effectively different variants of Cosmic Explorer could address these science themes, along with a resulting science-driven design concept for Cosmic Explorer, are presented later in §7 and §8. A science traceability matrix describes the measurements required to accomplish the science goals, and the instrument requirements needed to achieve these measurements. This study relies on knowledge that was not available when today’s detectors were designed — e.g., event rates and observations of gravitational-wave sources. In contrast, Cosmic Explorer’s ultimate design will be informed by what the existing observatories have discovered, and will continue to discover, about the gravitational-wave universe. The science traceability matrix reveals that addressing Cosmic Explorer’s science goals will require detectors with a strain sensitivity of  $6 \times 10^{-25} / \sqrt{\text{Hz}}$  at 10 Hz and  $2 \times 10^{-25} / \sqrt{\text{Hz}}$  at 100 Hz; compared to Advanced LIGO, this is an order of magnitude sensitivity improvement at 100 Hz, and opens a new low-frequency gravitational-wave band for observation. This leap in sensitivity between the 2G and 3G detectors, shown in Fig. 3.3 and Fig. 3.4, will expand humanity’s gravitational-wave access from the first nearby discoveries to the majority of stellar-mass black hole and neutron star coalescences in the universe. The current status of the 2G detectors and path toward the next generation is outlined below in §4.



# Cosmic Explorer Science Themes

- Black Holes and Neutron Stars Throughout Cosmic Time
- Dynamics of Dense Matter
- Extreme Gravity and Fundamental Physics
- Discovery Potential

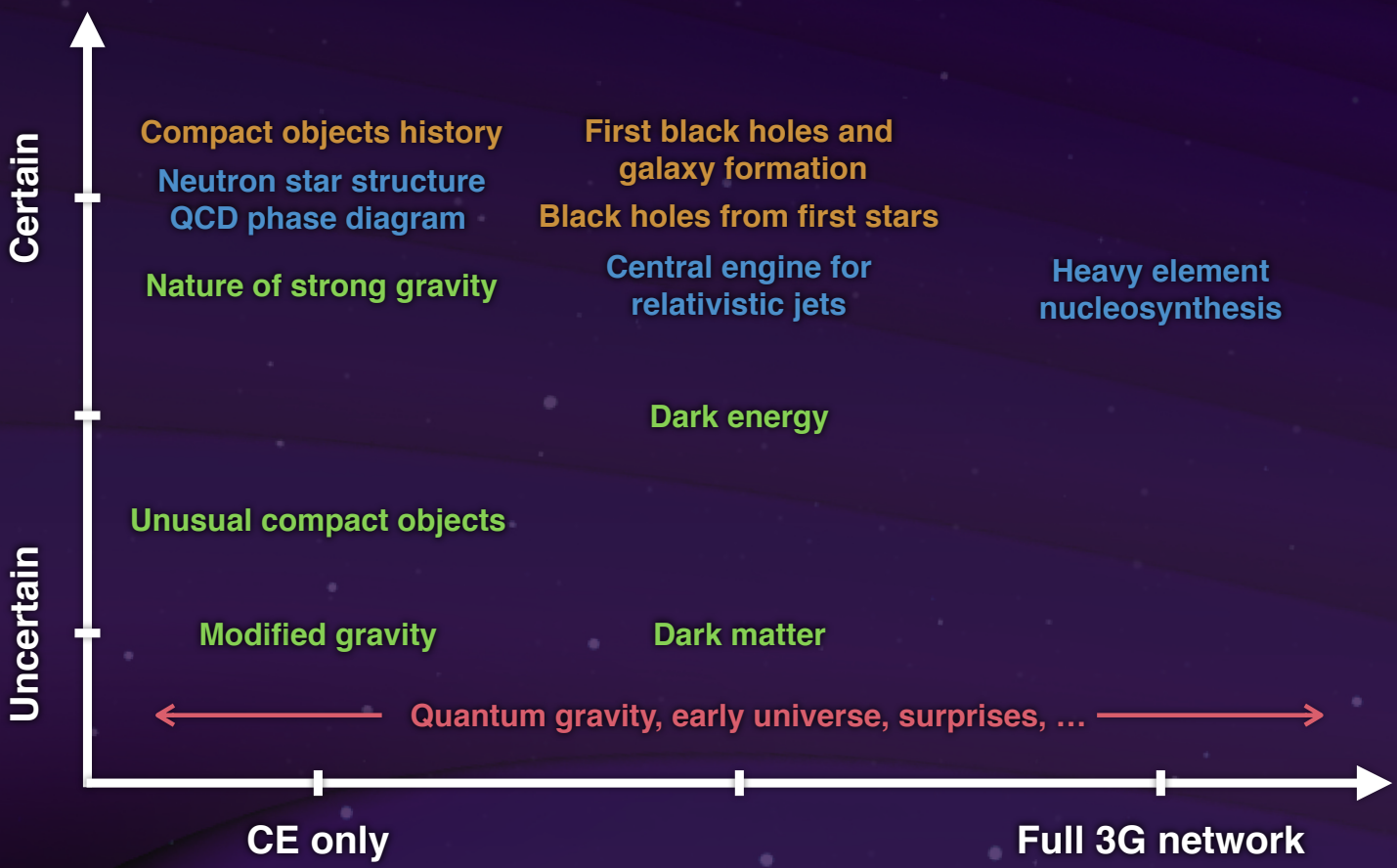


Figure 3.2: The key science objectives for Cosmic Explorer’s central themes, located on axes that qualitatively assess the likelihood of observing gravitational waves related to those objectives, ranging from certain to uncertain, and the number of detectors required to achieve those objectives, ranging from Cosmic Explorer alone (two sites, as described in Box 7.1), through Cosmic Explorer with a second-generation network, to Cosmic Explorer as part of a full third-generation network. The “Discovery Potential” objectives in pink are uncertain and span the space from alone to requiring a full network. Background image is credit ESA, CC BY-SA 3.0 IGO, and was modified.

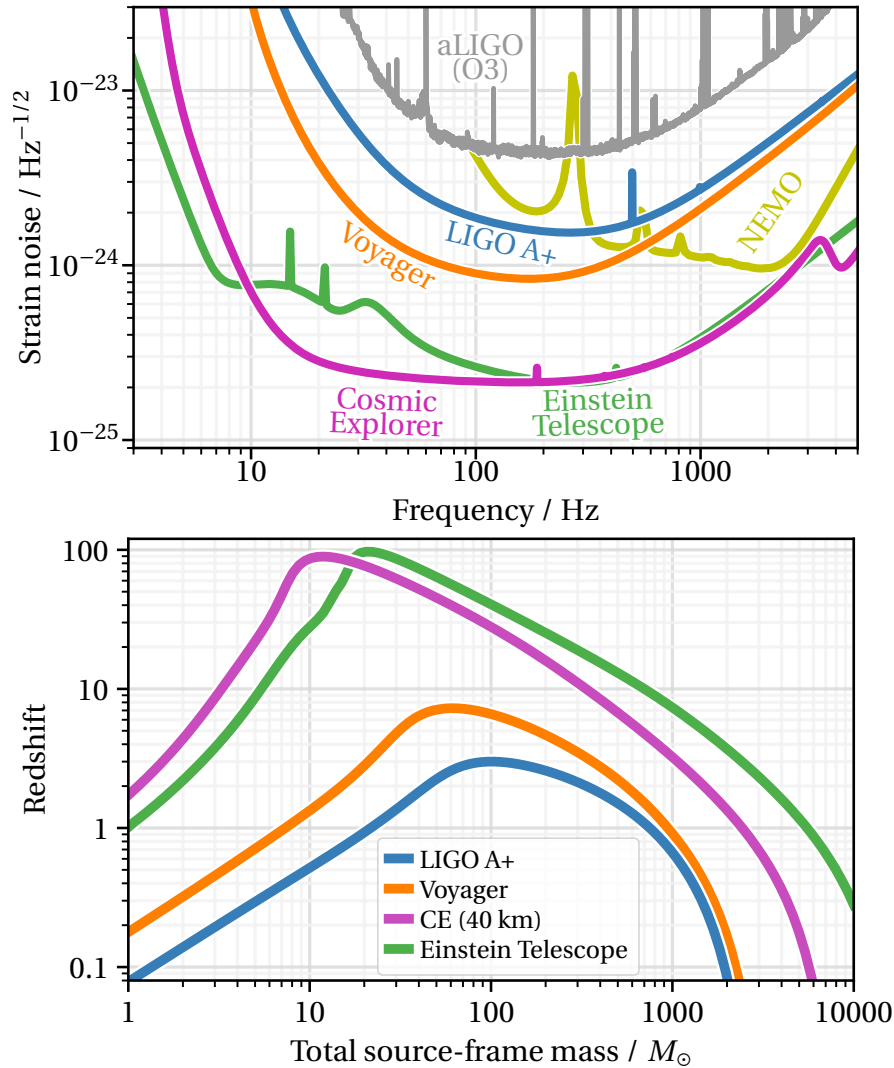


Figure 3.3: *Top*: Amplitude spectral densities of detector noise for Cosmic Explorer (CE), the current (O3) and upgraded (A+) sensitivities of Advanced LIGO, LIGO Voyager, NEMO, and the three paired detectors of the triangular Einstein Telescope (see §4 for observatory descriptions). At each frequency the noise is referred to the strain produced by a source with optimal orientation and polarization. *Bottom*: Maximum redshift (vertical axis) at which an equal-mass binary of given source-frame total mass (horizontal axis) can be observed with a signal-to-noise ratio of 8.<sup>11</sup> Different curves represent different detectors. For binary neutron stars (total mass  $\sim 3M_{\odot}$ ), CE will give access to redshifts larger than 1, where most of the mergers are expected to happen. For binary black holes, it will enable the exploration of redshifts of 10 and above, where mergers of black holes formed by either the first stellar population in the universe (Pop III stars) or by quantum fluctuations shortly after the Big Bang (primordial black holes) might be found.

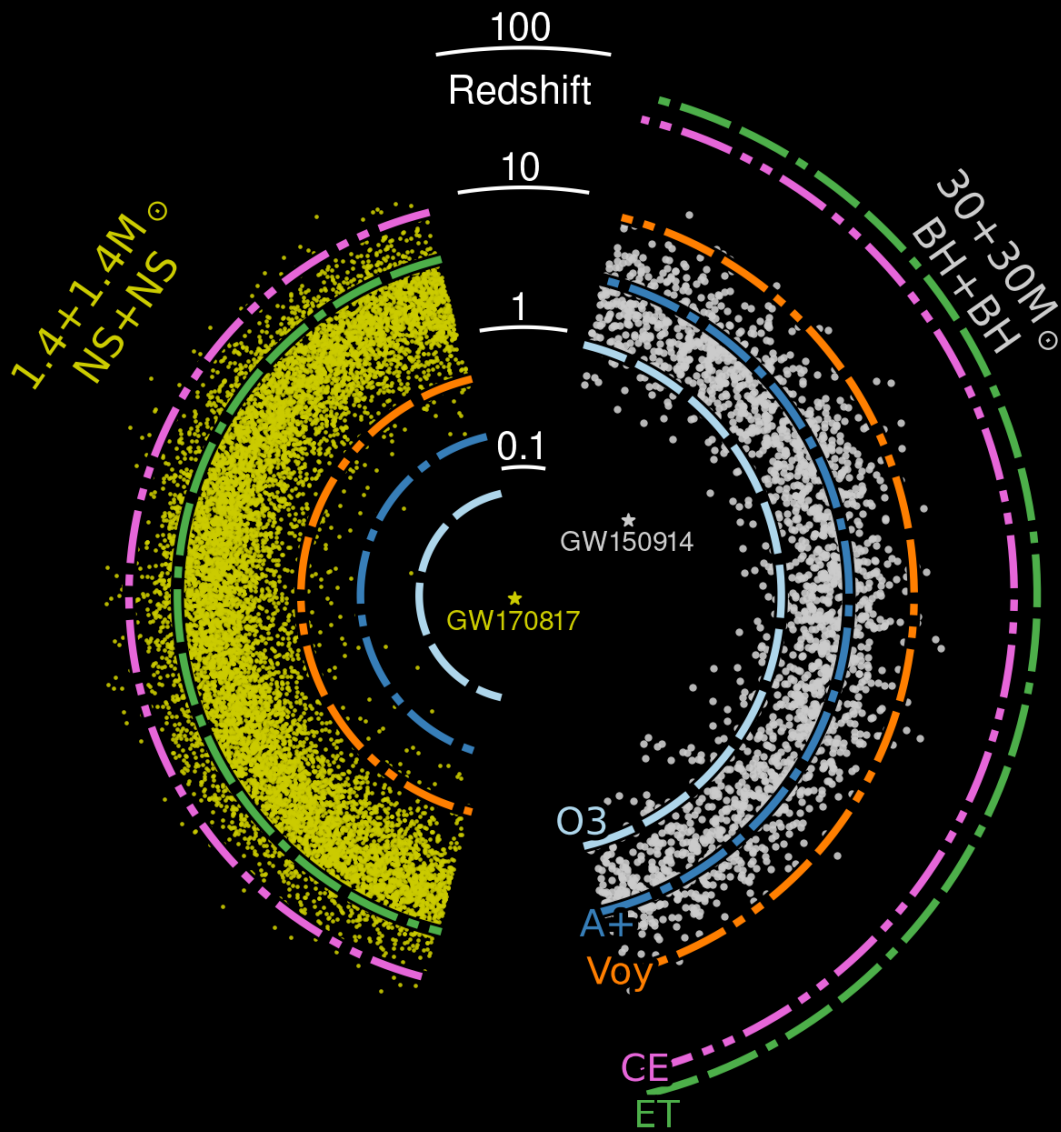


Figure 3.4: Astrophysical horizon of current and proposed future detectors for compact binary systems. As in the bottom of Fig. 3.3, the lines indicate the maximum redshift at which a detection with signal-to-noise ratio 8 could be made. The detectors shown here are Advanced LIGO during its third observing run (“O3”), Advanced LIGO at its anticipated sensitivity for the fifth observing run (“A+”), a possible cryogenic upgrade of LIGO called Voyager (“Voy”), the Einstein Telescope (“ET”), and Cosmic Explorer (“CE”, see §4 for observatory descriptions). The yellow and white dots are for a simulated population of binary neutron star mergers and binary black hole mergers, respectively, following Madau and Dickinson [12] with a characteristic binary merger time of 100 million years.

## 4 Status of Ground-Based Gravitational-Wave Observatories

A century after Einstein’s prediction of gravitational waves, Advanced LIGO<sup>13</sup> debuted this new “sense” for humanity by observing coalescing binary systems of black holes<sup>14–16</sup> with up to tens of solar masses<sup>17</sup> and enabling tests of relativity in the strong gravity regime.<sup>18</sup> In 2017, LIGO and its European partner Virgo<sup>19</sup> inaugurated an era of gravitational-wave multimessenger astronomy by discovering a binary neutron star merger with a gamma-ray-burst counterpart,<sup>20</sup> and rapidly sharing its source location with the broader astronomical community, triggering observations of the system across the electromagnetic spectrum.<sup>21</sup> The scientific goldmine opened by these observations has connected binary neutron star mergers to short gamma-ray bursts, equated the speed of gravity to very precisely that of light,<sup>22</sup> provided a gravitational-wave measure of the local Hubble constant,<sup>23</sup> gave strong clues about the origin of heavy elements,<sup>24</sup> and probed the properties of ultra-dense nuclear matter.<sup>20,25</sup>

These successes of Advanced LIGO were the result of forty years of international collaboration and research and development, from prototypes of increasing scale to the first generation LIGO detectors. These efforts delivered the technology and engineering needed to build the second-generation detectors. They also trained the early-career scientists and engineers who envisioned, built, and are operating these observatories, and fostered a community that is searching for gravitational-wave sources and extracting astrophysical information from these observations.

The LIGO and Virgo observatories have continued to increase their reach and discovery rate, revealing populations of astrophysical events<sup>26–29</sup> and routinely issuing alerts to the broader astronomical community.<sup>30</sup> At its 2020 sensitivity, this network was reporting observations of tens of black hole mergers and of order one merger involving a neutron star per year.<sup>31</sup> At the time of writing, the 2G observatory network is being strengthened by the Japanese KAGRA observatory<sup>32</sup> and by an enhancement to Advanced LIGO known as A+.<sup>33</sup> A planned joint US–India detector, LIGO India,<sup>34</sup> has selected and acquired a site and is awaiting approval from the Indian government. Additionally, progress has been made toward “Voyager” technology to possibly maximize the potential of the existing LIGO facilities by implementing cryogenic silicon optics and suspensions and reducing quantum and Newtonian (gravity gradient) noise.<sup>35,36</sup> Options for lasers, photodiodes, and electro-optics for Voyager’s planned 2  $\mu\text{m}$  operating wavelength, as well as cryogenic engineering solutions to cool the suspended optics, have been identified and will soon be tested in the Caltech 40-m prototype<sup>37</sup> and the European ETpathfinder prototype.<sup>38</sup> LIGO and its partners are providing dramatic and deepening insights into the populations and lifetimes of black holes and the inner workings of neutron stars. However, these 3–4 km detectors

can offer only a glimpse of the full gravitational-wave universe.

Three 3G observatory concepts have emerged. In Europe, plans have solidified for the Einstein Telescope or ET. The first ET Design Report was published in 2011 and updated in 2020.<sup>2</sup> It describes a single-site observatory with 10 km-long arms located 200–300 m underground to reduce seismic motion and Newtonian noise, with low-frequency detectors operated at cryogenic temperatures (10–20 K) to reduce thermal noise and high-frequency detectors using very high laser power and frequency-dependent squeezed light to reduce the impact of the laser light’s quantum noise. In 2021, Einstein Telescope was included in the roadmap of the European Strategic Forum for Research Infrastructures.<sup>39</sup> ET will enter a preparatory phase with construction possible by 2026 and observations by 2035.<sup>40</sup> An Australian detector concept, NEMO,<sup>41</sup> is a 4 km-baseline detector targeting excellent sensitivity in the high frequency band (1–3 kHz) associated with gravitational-waves from the postmerger phase of neutron stars. Cosmic Explorer<sup>42,43</sup> is the planned United States contribution to the next-generation gravitational-wave observatory network and the focus of this study. These observatories will have strong synergy with space-based gravitational-wave observatories, astro-particle detectors, and telescopes across the electromagnetic spectrum.

With that introduction to the detectors, we now turn to a discussion of the scientific opportunities of broad interest that will be opened by Cosmic Explorer.



## 5 Key Science Questions

The key science questions to be addressed by Cosmic Explorer are presented below. The gravitational-wave spectrum is rich with sources, and more scientific opportunities will be explored by the third generation network than described here. This selection was made to focus on the most compelling science that will be accessible with Cosmic Explorer.

### 5.1 Black Holes and Neutron Stars Throughout Cosmic Time

Cosmic Explorer can detect stellar-mass black hole mergers from when the universe was less than 500 million years old. This immense reach will reveal for the first time the complete population of stellar-mass black holes in binaries, starting from an epoch when the universe was still assembling its first stars. Cosmic Explorer will detect hundreds of thousands of black-hole mergers each year, measuring their distances, masses, and spins. These observations will reveal the black-hole merger rate, the underlying star formation rate, how both have changed throughout cosmic time, and how both are correlated with galaxy evolution.

#### 5.1.1 Remnants of the First Stars

The first stars formed when the universe was only a few hundred million years old. With no previous generation of stars to process the primordial gases of the universe, these stars, known as Population III or “Pop III” stars, were almost entirely composed of hydrogen and helium.<sup>44</sup> Due to their pristine composition, they are believed to have been extremely massive, with masses more than a hundred times that of the sun.<sup>45</sup> Despite intensive observational efforts, to date

#### Box 5.1: Key Science Question 1

#### **How have the populations of black holes and neutron stars evolved over the history of the universe?**

Cosmic Explorer will detect gravitational waves from black holes and neutron stars in binaries to redshifts of  $\sim 10$  and above, allowing us to:

- Shed light on Population III stars through the black holes they might have left behind;
- Measure the properties of the first black holes and their role in forming supermassive black holes and galaxies;
- Characterize the populations of compact objects and their evolution.

there are no claims of detection of Pop III stars. Since the rate at which stars burn their nuclear fuel increases dramatically with their mass, it is plausible that no Pop III stars emitted light long enough to be observed in the local universe. The James Webb Space Telescope<sup>46</sup> should be able to observe the very first galaxies in the universe, containing only Pop III stars;<sup>47</sup> though it will be able to and study their role in the epoch of reionization, it will not be able to observe individual stars from this epoch.<sup>48</sup>

After burning their nuclear fuel, Pop III stars, like other stars, may collapse to form compact objects such as black holes. If the mass of Pop III stars is above  $\sim 230 M_{\odot}$ , they should not trigger a pair instability supernova — an explosion that entirely destroys the star, leaving no compact object behind — but instead directly collapse into a black hole with minimal mass loss. Less massive stars might leave behind black holes below the pair-instability supernova mass gap, i.e., with masses up to  $\sim 60 M_{\odot}$ .<sup>49–52</sup> Depending on the initial mass distribution (mass function) of Pop III stars, we expect to find black holes in the early universe with masses of tens to hundreds of solar masses, possibly with a mass-gap between  $\sim 60$  and  $\sim 150 M_{\odot}$  due to pair instability supernovae.<sup>53</sup> Detecting and characterizing the black holes generated by Pop III stars can thus be a powerful method to study the properties of their progenitor stars, including their masses and composition. Knowledge of the mass function of the first generation of stars in the universe could change our understanding of how galaxies formed (see next subsection).

Unfortunately, both existing X-ray telescopes, and those currently proposed for the 2030s (e.g., the Lynx<sup>54</sup> and Athena<sup>55</sup> X-ray observatories) would only be able to detect and measure the mass of supermassive black holes, leaving totally unexplored a region of the mass spectrum that is likely to have been populated by Pop III stars. The LISA gravitational-wave detector<sup>56</sup> will access stellar-mass black holes in extreme mass ratio inspirals up to redshifts of  $\sim 5$ ,<sup>57,58</sup> and IMBHs up to redshifts of  $\gtrsim 10$ . By contrast, Cosmic Explorer can detect stellar-mass black holes to redshifts beyond 10, if they merge in binary systems. Gravitational-wave detectors in the next decade would thus be able to probe a wide range of possible Pop III stars remnants, with Cosmic Explorer targeting the stellar-mass region.

### 5.1.2 Seed Black Holes and Galaxy Formation

Supermassive black holes (SMBHs), with masses of millions to billions of solar masses, are known to exist at the center of most galaxies, significantly impacting the evolution, energetics, and dynamics of their host galaxies.<sup>59,60</sup> The study of galaxy formation is thus intimately related to understanding how and when the central black holes formed — an area of extremely intense research.

A key open question is: how did supermassive black holes form so early in the history of the universe? Compelling evidence shows that SMBHs of billions of solar masses already existed at redshift of  $\gtrsim 7.6$ ,<sup>61</sup> when the universe was only 670 million years old. The relatively short time scale over which SMBHs were produced challenges our understanding of how black holes form and grow. The two main scenarios suggested to explain the presence of high-redshift SMBHs are (1) direct collapse of hydrogen clouds into black holes, followed by gas accretion, and (2)

repeated mergers of smaller black holes through gravitational runaway processes.<sup>62</sup>

If the first black holes in the universe were the remnants of the first generation of stars, as mentioned above they could have masses up to a few hundred solar masses. Repeated mergers of black holes, starting from tens or hundreds of solar masses, passing through the regime of intermediate-mass black holes (IMBHs, in the mass range  $\sim[10^2, 10^5]M_\odot$ ), could eventually result in SMBHs of billions of solar masses. LIGO and Virgo have detected gravitational waves from the merger of two heavy black holes, GW190521, which gave birth to a black hole of  $\sim 150 M_\odot$  at redshift of  $\sim 0.8$ . The merger product might represent the first-ever detection of an IMBH, though a light one. Advanced detectors will observe more of these systems in the next few years, and start measuring their merger rate and mass distribution. Advanced detectors or their upgrades (Fig. 3.3 bottom), however, will not be able to detect a  $100\text{--}100 M_\odot$  IMBH at redshifts larger than 3. By contrast, Cosmic Explorer will be able to observe them to redshifts larger than 10. Measuring the mass function and merger rate of heavy stellar-mass and IMBHs at those redshifts would directly illuminate their role in the formation of SMBHs. Some heavy BBH or IMBH sources could be detected both by LISA and — months to years later — by ground-based detectors,<sup>63</sup> which would significantly improve the estimates of all of the source parameters,<sup>64</sup> including enabling more stringent tests of general relativity.<sup>65</sup> The exciting prospects of gravitational-wave multi-banding have recently been discussed elsewhere.<sup>66</sup>

### 5.1.3 Formation and Evolution of Compact Objects

LIGO and Virgo have detected black holes with masses as light as  $2.5 M_\odot$  (if indeed the lighter component of GW190814 is a black hole<sup>67</sup>) and as heavy as  $150 M_\odot$ .<sup>68</sup> While most of the black hole binaries seem to have small spins (or, more precisely, a small projection of the mass-weighted total spin along the orbital angular momentum,  $\chi_{\text{eff}}$ <sup>69,70</sup>), some systems show large spins, or spins which are misaligned with the orbit.<sup>71</sup> It is unlikely that this variety of parameters can be the result of a single astrophysical formation channel.<sup>31,72</sup> In fact, different formation scenarios are expected to result in different distributions for the masses and spins of the black holes (see Refs. [73–75] for recent reviews). The two channels which are usually expected to produce most black hole binaries are isolated formation in galactic fields<sup>76–80</sup> and dynamical encounters in dense environments (e.g., globular clusters,<sup>81–85</sup> nuclear star clusters, and the disks of active galactic nuclei<sup>86,87</sup>). Dynamical formation may produce heavier black holes than isolated binary evolution due to the possibility of repeated mergers.<sup>88–91</sup> Other parameters of the environment, e.g., the metallicity, also strongly affect the mass of the resulting compact objects.<sup>92</sup> Similarly, the magnitude and orientation of the spins in the binary will depend on where the system formed, and on details of the supernovae explosions that created the black holes.<sup>93</sup> Gravitational-wave measurements of these parameters can aid in understanding where black hole binaries formed, providing precious clues about the evolution and properties of their environments, and thus of galaxies and their surroundings.

While LIGO and Virgo have opened up this new frontier of observational astrophysics, they are also intrinsically limited in their sensitivity. Even in the A+ configuration, LIGO will not be

able to observe black hole binaries at redshifts larger than 3.<sup>a</sup> While still providing significant understanding of the local universe, they will not be able to say much about the production of black holes or their properties earlier in the history of the universe. Precise measurements of the merger rate and mass distribution of merging binaries across a large range of redshifts will make it possible to probe environmental impacts on compact binary yields, delay times between star formation and merger, and ultimately untangle the formation channels and their uncertain physics. Searches for the stochastic signal produced by unresolved sub-threshold binaries will give hints about their high-redshift distribution, but with large uncertainties (compare, e.g., Refs. [94] and [95]). Understanding how the rate and sites of production of black hole binaries evolved across the age of the universe will provide hints about, for example, the evolution of the star formation rate, a quantity which is hard to measure at high-redshift using photons.<sup>12</sup> More importantly, advanced detectors, and the proposed upgrades such as Voyager, would entirely miss black hole mergers at redshifts larger than  $\sim 7$ .<sup>95</sup> This will preclude probing the formation and merger of black holes created by Pop III stars, as described above, and other possible high-redshift channels, e.g., primordial black holes created during the inflationary epoch of the universe. It is only with next-generation detectors like CE that we will be able to understand the efficiency and characteristics of each formation channel that generates black hole binaries, anywhere in the observable universe.

Similar considerations can be made for neutron stars. The discovery of GW190425,<sup>96</sup> a binary neutron star system much heavier than known systems in our galaxy suggests that the astrophysical properties of neutron stars might be more diverse than what has been observed in the Milky Way. Next-generation observatories will provide access to neutron star binaries all the way to redshift  $\sim 10$ , and give us a clear picture of how their parameters vary across cosmic history and galactic environments.

## 5.2 Dynamics of Dense Matter

Neutron stars are made of the densest known matter in the universe and can support incredibly large magnetic fields. The merger of two neutron stars is so cataclysmic that it can produce the brightest electromagnetic emission in the cosmos and trigger the formation of heavy elements like gold and platinum. Six decades after the discovery of neutron stars, we still do not understand how matter behaves at the extreme densities and pressures attained in their cores, or how they can generate magnetic fields a million times stronger than those created on Earth. Cosmic Explorer will detect  $\sim 10^5$  binary neutron star mergers per year out to a redshift of 4, of which  $\sim 10$  are expected to have signal-to-noise ratios above 300. Cosmic Explorer could also detect signals from the 3000 known neutron stars in our Galaxy. The dense-matter science these observations will enable is highlighted in Box 5.2.

<sup>a</sup>This is for  $50\text{--}50 M_{\odot}$  binary black holes. For lighter and heavier systems the horizon will be smaller, as seen in Fig. 3.3.

## Box 5.2: Key Science Question 2

**How does matter behave under the most extreme conditions in the universe?**

Cosmic Explorer will measure gravitational radiation from binary neutron star coalescences and provide the precise source localizations required for multimessenger astronomy, allowing us to:

- Determine the internal structure and composition of neutron stars;
- Explore new regions in the phase diagram of quantum chromodynamics;
- Map heavy element nucleosynthesis in the universe through counterpart kilonovae and distant mergers;
- Reveal the central engine for the highly relativistic jets that power short gamma-ray bursts.

**5.2.1 Neutron Star Structure and Composition**

Neutron stars are excellent astrophysical laboratories for ultra-dense matter. Subtle signatures of the stellar interior are encoded in the gravitational waves emitted when neutron stars coalesce,<sup>97–100</sup> allowing us to probe the fundamental properties and constituents of matter in a phase that is inaccessible to terrestrial experiments.<sup>101</sup> The matter in neutron star cores is so dense that it cannot be described in terms of individual nucleons. It reaches equilibrium as a neutron-rich fluid and may even transition to deconfined quarks at the highest densities.<sup>102</sup> The phase structure of dense matter is shown schematically in Fig. 5.1.

As we enter the Cosmic Explorer era, our understanding of neutron star matter will be informed by current- and near-future observations including gravitational waves,<sup>103–107</sup> X-ray spectra,<sup>108</sup> bursts,<sup>109</sup> and pulsar profile modeling.<sup>110–113</sup> Together, these are expected to yield ~5 % errors on neutron star radii for dozens of sources.

Cosmic Explorer's precision measurements of tidal deformabilities across the neutron-star mass spectrum will constrain the neutron-star radius better than 0.1 km — one part in 100 — for hundreds of systems per year, revolutionizing our knowledge of the equation of state that characterizes the ultradense matter in inspiraling neutron stars. These observations will enable us to distinguish between competing first-principles models for ultra-dense matter<sup>114</sup> and resolve the nature of the phase transition to quark matter,<sup>115</sup> if it occurs in neutron-star cores. Gravitational-wave astroseismology may also emerge from the dynamic excitation of oscillations in the component neutron stars, yielding new insight on their structure and composition,<sup>116–120</sup> including the dense nuclear physics of transport properties such as viscosities and conductivities.

Cosmic Explorer may also observe gravitational waves from spinning neutron stars; quasi-periodic signals lasting for millions of years.<sup>121</sup> Their emission requires nonaxisymmetry, which could be supported by elastic stresses in the crust, deformations due to magnetic fields, thermal asymmetries or unstable oscillations driven by accretion.<sup>121–123</sup> Cosmic Explorer may reveal if



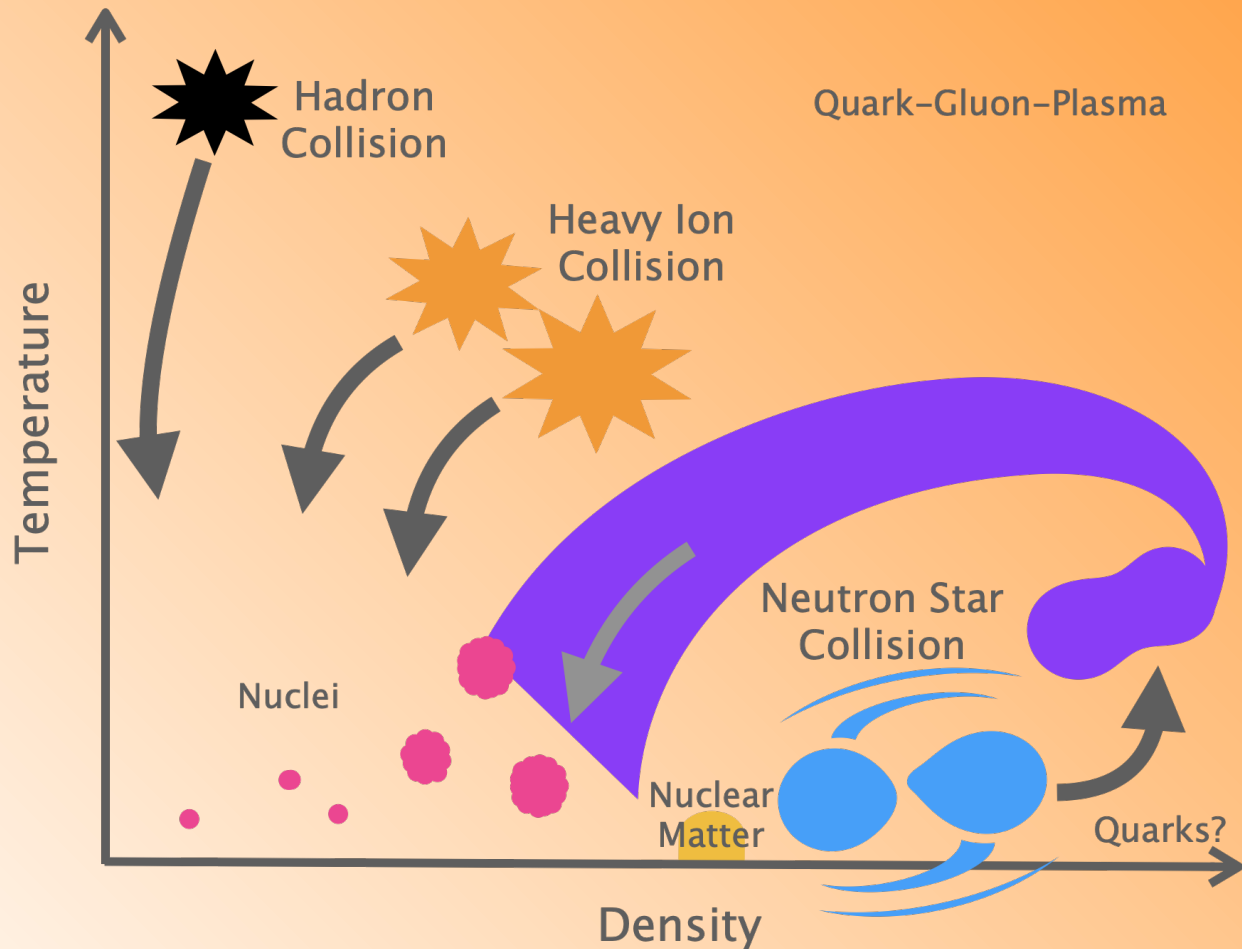


Figure 5.1: Schematic quantum chromodynamic phase diagram. At low densities and temperatures, matter is arranged into nuclei. As the density increases, the nuclei disintegrate into a sea of interacting neutrons and protons, so-called nuclear matter. Terrestrial collider experiments probe dense nuclear matter at high temperature, as it “melts” into a quark-gluon plasma and recombines. In contrast, the compressed cores of neutron stars hold supranuclear-density matter in a cold neutron-rich equilibrium. At the highest densities, phase transitions involving strange particles or quark matter may occur. Gravitational-wave observations of neutron stars explore this low-temperature, high-density phase from the inspiral, and a unique high-temperature, high-density region of the phase diagram after the stars collide. The kilonova counterpart to a neutron star merger traces the r-process nucleosynthesis that transforms neutron-star matter into heavy nuclei.

gravitational waves explain the spin-down rates of millisecond pulsars,<sup>124</sup> and the corresponding ellipticities are within direct detection reach. Gravitational-wave emission could also explain the relatively low spins of accreting neutron stars in low-mass X-ray binaries.<sup>125–127</sup> Observing these long-lived gravitational waves would provide additional insight into the formation and thermal, spin and magnetic field evolution of neutron stars, as well as the properties of the solid crust.<sup>123,128</sup>

### 5.2.2 New Phases in Quantum Chromodynamics

After a binary neutron star merges, oscillations of the hot, extremely dense remnant produce postmerger gravitational radiation. This heretofore undetected signal probes the unexplored high-density, finite-temperature region of the quantum chromodynamic phase diagram. As indicated in Fig. 5.1, this region is inaccessible to collider experiments and difficult to observe directly with electromagnetic astronomy. This is where novel forms of matter are most likely to appear.<sup>129–132</sup> Cosmic Explorer is well-suited to observing postmerger gravitational waves.<sup>133–135</sup> it is expected to detect  $\sim 100$  postmerger signals every year in a 3G network.

Measurements of the dominant postmerger gravitational-wave frequency<sup>136–144</sup> will reveal dense-matter dynamics with finite temperature,<sup>145</sup> rapid rotation<sup>146</sup> and strong magnetic fields.<sup>147</sup> These observations will shape theoretical models describing fundamental many-body nuclear interactions and answer questions about the composition of matter at its most extreme, such as whether quark matter is realized at high densities.<sup>132,148,149</sup> Direct gravitational-wave observations of postmerger remnants will also help determine the threshold mass for collapse of a rotationally supported neutron star,<sup>140,150–153</sup> which has implications for the neutron-star mass distribution,<sup>154</sup> compact binary formation scenarios<sup>155</sup> and predictions for electromagnetic emission from neutron star mergers.<sup>156</sup>

Massive stars undergoing core-collapse supernova also generate gravitational waves from the dynamics of hot, high-density matter in their central regions. Searches for supernova and various other burst-like sources are well-developed.<sup>157–160</sup> Cosmic Explorer will be sensitive to supernovae within the Milky Way and its satellites, which are expected to occur once every few decades.<sup>161</sup> Core collapses should be common enough to have a reasonable chance of occurring during the few-decades-long lifetime of Cosmic Explorer. A core collapse supernova seen by Cosmic Explorer will have a significantly larger signal-to-noise ratio than one seen by current gravitational-wave detectors, and could be detected by a contemporaneous neutrino detector like DUNE<sup>162</sup> giving a spectacular multimessenger event. Detection of a core-collapse event in gravitational waves would provide a unique channel for observing the explosion's central engine<sup>163</sup> and the equation of state of newly formed protoneutron star.<sup>164</sup> Detection of a supernova would be spectacular, allowing measurement of the progenitor core's rotational energy and frequency measurements for oscillations driven by fallback onto the protoneutron star.<sup>165,166</sup> Beyond supernova, gravitational-waves could be generated by other dynamic neutron-star processes such as: accretion, magnetar outbursts, or pulsar glitches, and by the engines of short-duration astrophysical transients such as fast radio bursts. Cosmic Explorer could provide

unique insights into the engine of these events.

### 5.2.3 Chemical Evolution of the Universe

Stellar nucleosynthesis is responsible for the transformation of primordial hydrogen and helium into the light elements, and this elemental history is woven into the gravitational-wave observations described in Section §5.1. The merger rates and mass distributions of black holes and neutron stars over the history of the universe reflect the presence of these elements (‘metallicity’) during star formation<sup>167–169</sup> and provide insight into nuclear reaction rates in massive stars.<sup>170</sup>

A different process must be invoked for elements heavier than iron. The observation of GW170817 and its electromagnetic counterpart established binary neutron star mergers as a key site of heavy element nucleosynthesis.<sup>171</sup> The matter ejected during a merger is hot, dense and neutron-rich, perfectly suited for sustaining rapid neutron capture (r-process) nuclear reactions. These reactions give rise to an optical and infrared afterglow — a kilonova — that can last for days or weeks.<sup>172</sup> Important questions about this picture remain to be answered: is binary neutron star nucleosynthesis the sole, or merely dominant, source of heavy elements in the universe?<sup>173</sup> How do the binary’s properties affect the quantity and composition of the ejected matter?

As part of a third-generation network, Cosmic Explorer will localize  $\sim 20$  binary neutron star mergers in the nearby universe to within  $\sim 0.1$  deg.<sup>2</sup> every year, enabling electromagnetic follow-up to connect gravitational-wave and kilonova observations. Distances and sky localizations for nearby neutron-star and neutron-star/black-hole mergers will identify their host galaxies, allowing the connection between compact binaries and their environment to be closely probed.<sup>174,175</sup> In some cases, early warning of a system likely to produce matter outside the merger remnant can give electromagnetic observatories the advance notice required to capture the earliest moments of the kilonova.<sup>176</sup> Cosmic Explorer will also record essentially all neutron star mergers out to redshift 1, so even poorly localized gravitational-wave events can be connected with independently identified kilonovae from surveys like the Vera C. Rubin Observatory’s LSST and the Roman Space Telescope,<sup>177</sup> enabling follow-up across the electromagnetic spectrum.<sup>178,179</sup> Facilities such as the James Webb Space Telescope,<sup>180</sup> the Extremely Large Telescope,<sup>181</sup> the Giant Magellan Telescope<sup>182</sup> and the Thirty Meter Telescope,<sup>183</sup> will allow us to characterize the nature of the merger through deep imaging and spectroscopy. Precise measurement of the source properties from the inspiral signal will break degeneracies in kilonova models, helping to pin down the rates of specific nuclear reactions. We will learn about the feedback of neutron-star merger nucleosynthesis on stellar and galactic evolution,<sup>184</sup> as well as the conditions under which matter is present in the circumbinary environment.<sup>185</sup> By establishing the rate and distribution of neutron star mergers out to cosmological distances, Cosmic Explorer will also map the history of chemical evolution in the universe beyond the reach of multimessenger astronomy.

### 5.2.4 Gamma-Ray Burst Jet Engine

Gamma-ray bursts are the most energetic electromagnetic phenomena in the universe. Although the connection between the short-duration subclass of these bursts and neutron-star mergers was confirmed by the multimessenger observation of GW170817,<sup>186</sup> the fundamental mechanism that produces this high-energy emission remains to be understood. The features of short gamma-ray burst light curves and spectra suggest that they originate in highly relativistic outflows of matter from the postmerger remnant.<sup>187</sup> However, the central engine powering these relativistic jets is still a matter of debate: is it an accreting black hole, or a strongly magnetized, rotating neutron star (magnetar)?<sup>188,189</sup> Cosmic Explorer will address this question by identifying the gravitational waves associated with all the observable gamma-ray bursts originating in neutron star mergers, thanks to its complete coverage of the binary neutron star population out to a redshift of 1. A third-generation gravitational-wave detector network will measure the inclination angle of each jet, providing a comprehensive view of jet structures,<sup>190–193</sup> the time delay between merger and prompt emission,<sup>194,195</sup> and the nature of afterglow emission.<sup>191</sup> Gravitational-wave information will also distinguish binary neutron star from neutron-star black-hole coalescences, revealing possible phenomenological differences in their gamma-ray emission.<sup>196,197</sup> Future gamma- and X-ray observatories, such as the Einstein Probe,<sup>198</sup> eXTP,<sup>199</sup> ECLAIRs,<sup>200</sup> Athena,<sup>201</sup> THESEUS<sup>202</sup> and TAP,<sup>203</sup> will be critical to increasing the reach for multimessenger follow-up of gravitational-wave sources.

The subset of Cosmic Explorer’s well-localized binary neutron star mergers that produce a long-lived neutron star remnant will teach us about the origin and geometry of the ultra-strong magnetic fields supported by magnetars.<sup>204</sup> The existence of magnetars is known from electromagnetic observations,<sup>205</sup> but the amplification mechanism that allows their magnetic fields to grow so strong is a mystery.<sup>206</sup> Electromagnetic follow-up of these special events will allow magnetohydrodynamic simulations of magnetic field amplification and jet creation to be put to the test. Better knowledge of the magnetic fields neutron star matter can support may shed light on a wide range of photospheric emission phenomena, including radio and gamma-ray pulses.<sup>207</sup>

## 5.3 Extreme Gravity and Fundamental Physics

Cosmic Explorer will reveal the physics of the strongest gravity in the universe in unprecedented detail, thanks to two crucial dividends from Cosmic Explorer’s tremendous advance in sensitivity over current-generation gravitational-wave observatories. First, in three years of operation, a single 40 km Cosmic Explorer observatory, thanks to its increase in sensitivity, particularly at lower frequencies where CE is more than an order of magnitude more sensitive than LIGO A+, would likely detect at least one signal from merging black holes with a signal-to-noise ratio greater than 2700 (the loudest such signal to date, GW150914, had a signal-to-noise ratio of 24). Figure 5.2 illustrates the impact of Cosmic Explorer’s tremendous sensitivity gain by simulating the gravitational-wave strain data a GW150914-like gravitational wave would produce in Cosmic

## Box 5.3: Key Science Question 3

### What is the nature of the strongest gravity in the universe, and what does that nature reveal about the laws of physics?

Cosmic Explorer's observations of loud and rare gravitational waves will reveal the (potentially new) physics of the most extreme gravity in the universe, allowing us to:

- Probe the nature of strong gravity with unprecedented fidelity;
- Discover unusual and (if they exist) novel compact objects impossible to detect today;
- Probe the nature of dark matter and dark energy.

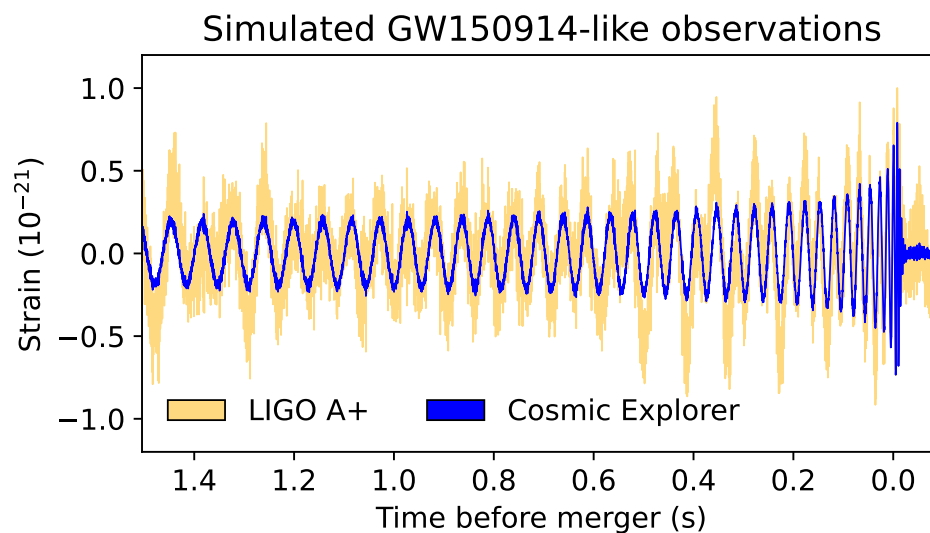


Figure 5.2: Simulated gravitational-wave detector strain measurements for a GW150914-like signal from two merging black holes. The strain is shown as a function of time for the signal superimposed on both simulated Cosmic Explorer noise (blue) and simulated LIGO A+ noise (yellow).

Explorer (and, for comparison, in LIGO A+).

Second, Cosmic Explorer will detect waves from sources too rare for us to observe today: in each year of its operation, Cosmic Explorer will observe approximately 100 000 binary black holes — 2000 times the total number of gravitational waves observed to date from any source.<sup>71,208</sup>

Together, these advances will enable Cosmic Explorer to reveal the nature and nonlinear behavior of the strongest gravity in the universe with incredible clarity, perhaps revealing physics beyond general relativity whose effects are too subtle for us to recognize today. This will open a wide window on fundamental physics. Through possible effects on the gravitational waves it observes, Cosmic Explorer has the potential to shed light on longstanding mysteries in physics, including the unknown natures of dark matter and dark energy. Cosmic Explorer will also reveal the precise nature of the sources of its many observations, uncovering rare black-hole and neutron star binaries and (if they exist) novel impostors that mimic these conventional binaries. Realizing just one of these potential discoveries would revolutionize our understanding

of extreme gravity and fundamental physics.

### 5.3.1 Nature of Strong Gravity

General relativity describes gravity as curvature of a 4-dimensional spacetime.<sup>209</sup> Gravitational-wave detectors are unique in their ability to probe regions of strong spacetime curvature: observations of gravitational waves, beginning with GW150914 *et seq.*,<sup>14,20,26,210</sup> and parallel developments in accurate numerical simulations<sup>211</sup> of binary black-hole coalescences, are giving us a first glimpse of strong spacetime curvature, including constraints on the nature and behavior of strong gravity.<sup>208,212–217</sup>

Detectors on Earth are sensitive to gravitational waves from stellar-mass black holes, which, near their horizons, have stronger spacetime curvature than any other object we have observed. And because the gravitational waves emitted by coalescing binary black holes depend only on the warped vacuum spacetime surrounding the black holes' horizons, these waves present the cleanest opportunity to probe strong gravity's fundamental nature. Making the most of this opportunity is crucial not only for understanding extreme gravity in isolation, but also for understanding its role when combined with matter and electromagnetic fields (as with neutron-star mergers<sup>20</sup>).

So far, although there are many proposed alternatives, all observational and experimental tests are consistent with general relativity.<sup>18,208,212,213,217–219</sup> In particular, the loudest signal from merging black holes to date, GW150914, is in good agreement with general relativity.<sup>220</sup> GW150914 is consistent with the “No-Hair Theorem”<sup>216</sup> at about the  $\sim 10\%$  level: specifically, two inferences of the remnant mass and spin (one via recovering the fundamental ringdown gravitational-wave mode and one overtone, using data as early as the time of peak amplitude, and the other via recovering the fundamental mode using data starting 3 ms after the peak) agree to within  $\sim 10\%$  — evidence to this confidence level that the remnant is a Kerr black hole. GW170817, a binary-neutron-star coalescence<sup>20</sup> accompanied by electromagnetic counterparts,<sup>221</sup> constrained the graviton mass to  $< 4.7 \times 10^{-23} \text{ eV}/c^2$ , provided tight constraints on possible violations of Lorentz and parity invariances, and constrained the gravitational wave speed to light speed within about one part in  $10^{16}$ , ruling out a number of alternative gravity theories that were invoked to explain dark energy.

Cosmic Explorer will test general relativity at unprecedented precision, with the potential to discover physical effects, either predicted by general relativity or by theories beyond general relativity, that are too subtle for current-generation instruments to measure. For instance, unlike today's detectors, next-generation detectors, such as Cosmic Explorer, will be sufficiently sensitive to detect (statistically, from many observations) the gravitational-wave memory effect, which is a change in displacement, predicted by general relativity, that remains after a gravitational wave has passed by.<sup>222</sup> As another example, general relativity has a massless exchange boson (i.e., the graviton); with coincident detection of gravitational waves and gamma-ray bursts at redshifts of  $z \sim 5$ , Cosmic Explorer and its electromagnetic partner observatories would constrain the graviton mass three orders of magnitude better than current observatories. Gen-



eral relativity also is Lorentz invariant, although its experimental confirmation is not as robust<sup>1</sup> as the tremendous accuracy achieved in particle physics,<sup>223</sup> and it is parity invariant, although some quantum-gravity theories (e.g., Ref.<sup>224,225</sup>) predict parity violations. As another example, general relativity satisfies the equivalence principle and has two tensor polarizations for gravitational waves. But alternative theories that, motivated by the low-energy limit of quantum gravity, introduce additional degrees of freedom (such as a scalar field), violate the equivalence principle and lead to additional gravitational-wave polarizations — while modifying compact-binary gravitational-wave emission.<sup>226–228</sup> Discovering even one such violation of general relativity, however small, would revolutionize our understanding of fundamental physics.

### 5.3.2 Unusual and Novel Compact Objects

Cosmic Explorer’s high-fidelity observations of stellar-mass coalescing objects, together with its cosmological reach, will present an excellent opportunity for exploring the nature of merging compact objects. The large number of detected stellar-mass black-hole and neutron-star mergers will likely include uncommon mergers too rare for even upgraded detectors in the current observatories, such as black holes with extremal spin, the inspiral of a neutron star into an intermediate-mass black hole,<sup>229,230</sup> a binary black hole with enough surrounding matter to produce an electromagnetic counterpart,<sup>87,231,232</sup> or binaries with a supernova precursor.<sup>233</sup> Measuring the properties of these rare mergers could revolutionize our understanding of the nature of compact objects.

Cosmic Explorer will also explore with unprecedented clarity whether some compact binaries might contain objects other than black holes and neutron stars. All observations so far are consistent with coalescing black holes and neutron stars, but Cosmic Explorer will probe whether new types of compact binaries<sup>234</sup> exist (e.g., binaries whose constituents include so-called “great impostors”,<sup>235</sup> gravastars,<sup>236–239</sup> boson stars<sup>240,241</sup> quark stars,<sup>242</sup> or Planck stars<sup>243</sup>), as they could have different tidal properties or quasi-normal modes of oscillation. If they do exist, it remains an open question by how much (or how little) the gravitational waves they emit differ from the waves emitted by conventional black-hole and neutron-star binaries.<sup>220,244</sup> At minimum, Cosmic Explorer’s enormously increased sensitivity and throughput will allow detailed tests of the Kerr black hole paradigm,<sup>245–248</sup> a necessary prerequisite for recognizing other kinds of novel compact objects.<sup>234,249</sup> There are, however, black hole mimickers whose inspiral and quasi-normal mode spectrum might be similar to black holes in general relativity but exhibit post-merger signals such as echoes of the ringdown signal due to modified structure of the horizon. And if novel compact objects exist but are rare, Cosmic Explorer’s cosmic reach will greatly increase our potential to observe them.

### 5.3.3 Dark Matter and Dark Energy

Dark matter — one of the major factors that governs the dynamics of the universe — has remained elusive decades after its gravitational influence on baryonic matter was discovered.

And on the largest scales, the universe's expansion is driven by the invisible dark energy whose nature we do not yet comprehend and whose value appears to be too small to be consistent with vacuum energy. The astronomical community is making a substantial, ongoing effort to probe these dark sectors (i.e., dark matter<sup>250</sup> and dark energy<sup>251</sup>).

Gravitational-wave observations present a unique opportunity for synergistic, complementary efforts to better understand dark matter and dark energy. Confirming that the universe appears the same in the gravitational-and electromagnetic-waves would reinforce our degree of belief in cosmological models (in the Bayesian sense), but any departure between the two would be tremendously consequential.

**Dark Matter** Approximately 85 % of the mass in the universe is thought to consist of dark matter.<sup>252</sup> Despite compelling evidence for the existence of dark matter from galaxy rotation curves, gravitational lensing, and the cosmic microwave background, its fundamental nature remains a mystery.<sup>253</sup>

To date, the only observational evidence for dark matter is via their passive gravitational influence on visible matter. Gravitational waves are an exciting new astrophysical probe of dark matter, complementing searches at high-energy colliders and underground direct-detection experiments,<sup>254,255</sup> that might reveal the nature of dark matter in several different scenarios.<sup>256</sup> Cosmic Explorer's greatly improved sensitivity and cosmic reach will enable it to investigate these scenarios. For instance, because of their strong gravitational fields and extreme densities, neutron stars might capture ambient dark matter over time through scattering off nucleons,<sup>257,258</sup> or they might even produce dark matter, thanks to the exceptionally high energies achieved in binary neutron star mergers.<sup>259</sup> If a neutron star were to contain dark matter, the dark matter would affect the neutron star's internal structure and hence its tidal properties.<sup>260</sup> The dark matter concentration would likely depend on the neutron star's age, mass, and environment in this scenario, leading to variations in the neutron-star tidal deformability, maximum neutron-star mass throughout the population, and perhaps the implosion of neutron stars when dark matter forms mini black holes in neutron stars' cores.

There are other possibilities where dark matter might be observable with gravitational waves. Ultra-light bosonic dark matter could become self-gravitating on its own, forming a novel compact object whose properties differ from those of a neutron star.<sup>244,261–263</sup> A significant concentration of ultra-light bosonic dark matter in the vicinity of a black-hole binary could spin down the black holes through superradiance<sup>264–267</sup> to spins below values that are characteristic of the black-hole and boson stars. The spin distribution of detected black holes therefore might reveal the existence of ultralight bosons.<sup>268–270</sup> The cloud itself would produce continuous gravitational waves when it oscillates or a burst of gravitational waves when it collapses.<sup>241,256,268,271</sup> In the former case, level transitions or annihilations in the boson cloud are predicted to emit the continuous gravitational waves monochromatically, with frequency determined by the boson and binary masses.<sup>256</sup> Searches for ultralight dark matter particles via the clouds they create around black holes only assume a coupling through gravity; this type of search would

still be viable even if dark matter does not have any type of electroweak or strong interaction with baryonic matter.

**Dark Energy** More than two thirds of the total energy in the observable universe is dark energy. The accelerating expansion of the universe reveals the ubiquitous nature of dark energy on the largest length scales, but the nature of dark energy remains one of the biggest outstanding mysteries in physics.

Since dark energy interacts only through gravitational interactions, a number of modified theories of gravity beyond general relativity have been proposed as explanations of dark energy. These theories include effects that Cosmic Explorer and its partner gravitational-wave and electromagnetic-wave observatories might detect, if they exist (e.g., Ref.<sup>272</sup> and the references therein, and more broadly, the discussion of the nature of gravity above). For instance, some theories of gravity beyond general relativity predict differences in the observed gravitational-wave and electromagnetic-wave luminosity distances caused by gravitational-wave damping. Cosmic Explorer's cosmic reach puts it in a strong position to search for these effects.

But whether or not Cosmic Explorer observes effects beyond general relativity, it will be well positioned to provide independent observations that complement electromagnetic observations, especially observations that are in tension. For example, gravitational-wave observations can independently address today's tension between the expansion rate of the universe determined by supernova observations and the rate deduced from the cold-dark-matter models that agree with the spectrum of the fluctuations in the cosmic microwave background.<sup>273</sup> Cosmic Explorer's gravitational-wave observations of binary black holes<sup>274</sup> at cosmological distances in particular will be standard sirens. Like standard candles (such as type Ia supernovae), gravitational waves from merging compact binaries provide a reliable measure of distance; specifically, the luminosity distance can be inferred by comparing the observed waves to theoretical model gravitational waveforms (e.g., using the technique of matched filtering<sup>275</sup>). Combining the standard-siren distance with a measure of redshift (either from an electromagnetic counterpart or through statistical methods) will provide measurements of the cosmic expansion history that are independent from conventional measurements using standard candles and the other elements of the standard cosmic distance ladder,<sup>1,276–278</sup> improving our understanding of the dark energy equation of state beyond what would be possible with electromagnetic observations alone (e.g., Fig. 9 of Ref. [279]).

## 5.4 Discovery Potential

Historically, major discoveries in astronomy have been facilitated by three related improvements in detector technology: deeper sensitivity, new bands of observation and higher precision. Improved sensitivity helps sample larger volumes and provide more complete surveys, enabling the discovery of rare events that otherwise do not make the cut, e.g., Type Ia supernovae that eventually led to the discovery of the recent accelerated expansion of the universe. Opening

a new frequency window has been critical to identifying entirely new classes of sources — the cosmic microwave background, quasars and gamma-ray bursts are just the tip of the iceberg examples. Increased precision has often helped discover subtle physical effects or phenomena, e.g., the discrepancy in the Hubble constant inferred from Type Ia supernovae and the Planck mission.

A deeper, wider and sharper observational window Cosmic Explorer will make progress at once in sensitivity, bandwidth and precision, catalyzing unprecedented discovery potential. Gravitational-wave observations will be deeply penetrating, and the signals are generated by physical processes that are vastly different from those that generate other forms of radiation and particles. It would be a profound anomaly in astronomy if nothing new and interesting came from Cosmic Explorer's vast improvement in sensitivity.

Compared to current detectors, Cosmic Explorer will peer far deeper into the universe and considerably widen the observed frequency range, especially to low frequencies. Because gravitational-wave observatories are sensitive to amplitude, which falls off inversely with the distance from the source, a factor ten increase in strain sensitivity is equivalent to a factor ten increase in the *diameter* of a telescope. Cosmic Explorer will thus have dramatically greater discovery potential in a similar way to the “discovery aperture” opened by much larger and more advanced telescopes. Many new telescopes that have greatly expanded our view of the cosmos end up being known for a different and more dramatic discovery than what was predicted in their science cases. The phenomenon of serendipitous discovery has been discussed in articles on exploration of the unknown and serendipitous astronomy,<sup>280,281</sup> some prominent examples being the cosmic microwave background, the discovery of pulsars, Cygnus X-1, and fast radio bursts.

Opportunities for new discoveries Gravitational radiation results from coherent motion of bulk matter and there likely are fewer ways for it to be generated than electromagnetic radiation. However, the gravitational-wave spectrum has already proven to be source rich, with many bright emitters. The fact that we know very little about much of the universe's energy budget promises discoveries of either completely unexplored or highly speculative, but plausible, sources and phenomena. Examples include axionic clouds around black holes, dark matter in the form of sub-solar primordial black hole binaries, stochastic backgrounds from early-universe phase transitions, quantum gravity signatures in the fine structure of black hole horizons or modified boundary conditions. Moreover, gravitational waves often emanate from systems that cannot be observed with electromagnetic astronomy, allowing us to, e.g., probe the dense regions of the earliest epochs of the universe, directly observe the core-collapse supernova mechanism, and explore the nature of dense matter in the interior of neutron stars (see, Fig. 5.3).



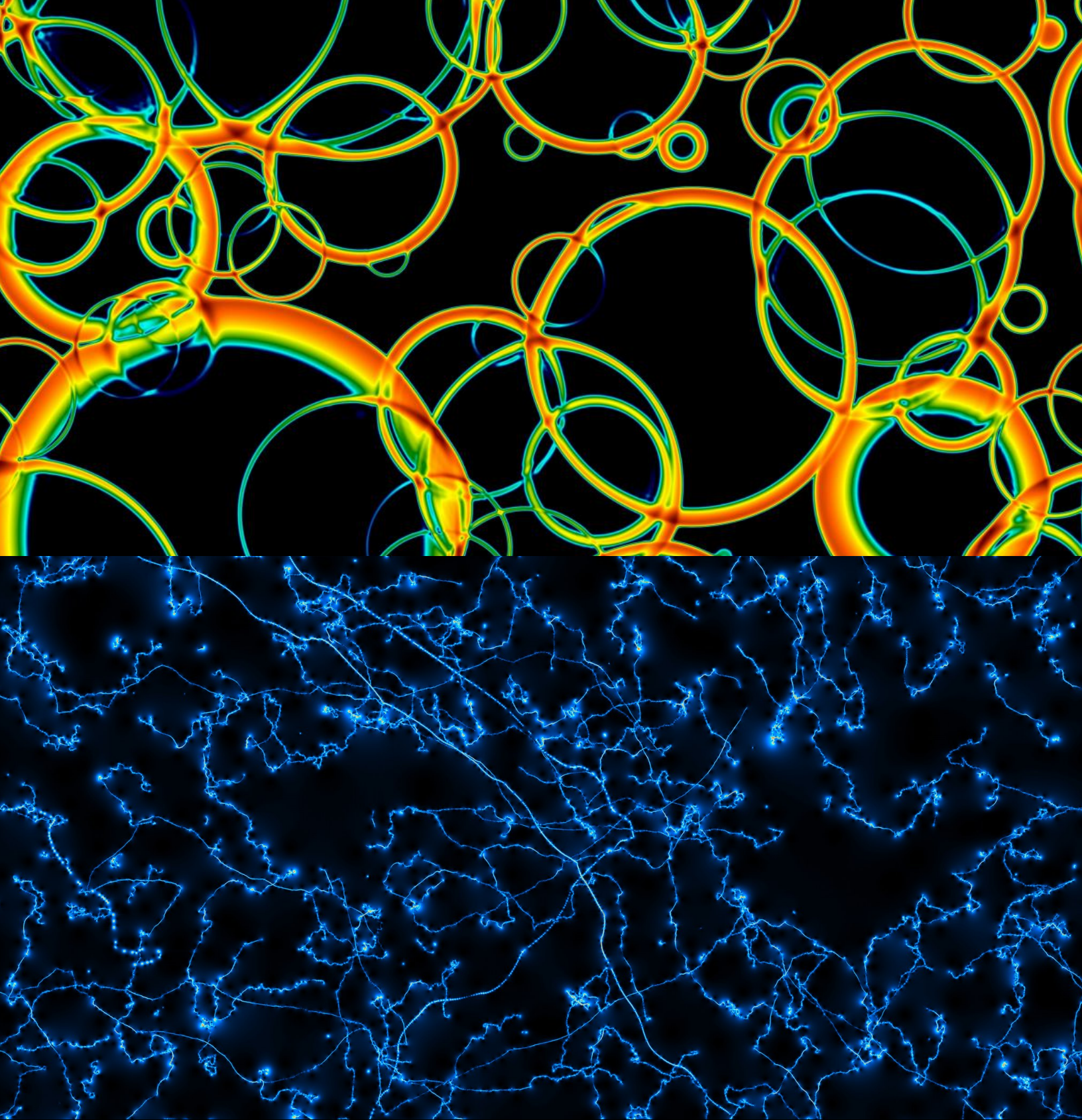


Figure 5.3: Cosmic Explorer’s discovery potential is enabled by increased sensitivity, greater bandwidth, and high-precision measurements. The top image (credit: D. Weir, University of Helsinki) shows bubble collisions in the early universe, and the bottom image (credit: Chris Ringeval, UCLouvain) shows a visualization of cosmic strings, which are topological defects produced following inflation. Both sources could produce stochastic backgrounds detectable by a pair of Cosmic Explorer detectors.

## Box 5.4: Key Science Question 4

### What discoveries might be possible with improved sensitivity, bandwidth and precision measurement?

Cosmic Explorer will have greater sensitivity and bandwidth and measure sources with exquisite precision and help in discoveries in astronomy and fundamental physics:

- Do quantum gravity effects manifest in the structure of black hole horizons?
- What could primeval phase transitions reveal about the energy scales in the Standard Model?
- How would gravitational wave observations help explore new particles and fields?

#### 5.4.1 Quantum Gravity

General relativity and quantum theory, the two founding pillars of modern physics, have both been vindicated time and again by high precision laboratory experiments, astronomical observations and cosmological measurements. Yet, there is no satisfactory theory of quantum gravity to date, but, more critically, general relativity is at odds with the fundamental principles of quantum theory that physical states obey unitary evolution. The latter is brought to bear in the bizarre behavior of black holes that are formed by collapse of matter in pure quantum states and yet when they evaporate by Hawking radiation, which is purely thermal, the observed states are mixed quantum states and information is irretrievably lost.<sup>282</sup> This information paradox that arises in semi-classical gravity is largely suspected to be cured by a quantum theory but every proposal for a quantum theory of gravity violates one or more of the basic tenets of general relativity, e.g., the local Lorentz violation, or its predictions, e.g., the existence of additional polarizations in the radiative field.<sup>228</sup>

It is largely expected that black holes could reveal violations of general relativity in the form of failure of the no-hair theorem as a result of quantum effects near black hole horizons.<sup>283,284</sup> As another example of how Cosmic Explorer might help address open questions in quantum gravity, a recent article states that “there has been a striking realization that physics resolving the black hole information paradox could imply postmerger gravitational wave echoes”.<sup>285</sup> These echoes have not yet been observed,<sup>285–288</sup> but Cosmic Explorer’s extremely high sensitivity could reveal them, should they exist.

The vast cosmological distances, redshifts in excess of  $z \sim 20$ , over which gravitational waves travel will severely constrain violation of local Lorentz invariance and the graviton mass.<sup>228</sup> Such violations or a non-zero graviton mass would cause dispersion in the observed waves and hence help to discover new physics predicted by certain quantum gravity theories. At the same time, propagation effects could also reveal the presence of large extra spatial dimensions that lead to different values for the luminosity distance to a source as inferred by gravitational wave and electromagnetic observations<sup>279,289</sup> or cause birefringence of the waves predicted in certain formulations of string theory.<sup>290,291</sup> The presence of additional polarizations predicted in certain



modified theories of gravity, instead of the two degrees of freedom in general relativity, could also be explored by future detector networks.<sup>228,292</sup>

### 5.4.2 New Particles and Fields

The vast horizon of Cosmic Explorer will help either discover or set stringent limits on the existence of particles and fields on a variety of different scales. The composition of dark matter is largely unknown but it could be composed, at least in part, of ultralight bosons such as QCD axions,<sup>293</sup> dark photons or other light particles,<sup>294</sup> spanning a wide mass range of masses,<sup>293,294</sup> from  $10^{-33}$  eV to  $10^{-10}$  eV. In particular, the Compton wavelength of ultralight bosons in the mass range  $10^{-20}$  eV– $10^{-10}$  eV corresponds to the horizon size of black holes of mass  $10 M_{\odot}$ – $10^{10} M_{\odot}$ . Although these ultralight fields may not interact with other Standard Model particles, the equivalence principle implies that their gravitational interaction with, for instance, black holes, could have observable consequences. For example, bosonic fields whose Compton wavelength matches the horizon scale of an astrophysical black hole could form bound states (often called “gravitational atoms”) around black holes and extract their rotational energy and angular momentum via the mechanism of superradiance.<sup>295,296</sup> This would result in a Bose-Einstein condensate that acts as a source of continuously emitted gravitational waves. Cosmic Explorer would have access to the higher end of the mass range from  $10^{-13}$  eV to  $10^{-10}$  eV, which correspond to QCD axions.

After LIGO’s first discovery of stellar black holes with unusually large masses,<sup>297</sup> primordial black holes were proposed as viable candidate sources, in which case they would also constitute at least a fraction of the dark matter. Searches for subsolar mass black holes have not produced any detections so far, leading to some of the best upper limits<sup>298</sup> on the fraction of dark matter in black holes of mass  $0.2$ – $1.0 M_{\odot}$ . The existence of subsolar black holes would be a definitive proof that they were produced in the primordial universe, as stellar evolution cannot produce black holes below about  $3 M_{\odot}$ . Cosmic Explorer and partner observatories will constrain the fraction of dark matter in such black holes at the level of  $10^{-5}$  of the total budget.

### 5.4.3 Stochastic Gravitational-Wave Backgrounds

A stochastic gravitational-wave background is expected to arise due to the superposition of individually unresolvable gravitational waves of both astrophysical and cosmological origin. The astrophysical backgrounds of stellar-mass compact binary mergers that are the targets of current ground-based gravitational-wave detectors (e.g., Refs. [299–304]) will be nearly entirely resolvable with the next generation observatories, but residual unresolvable signals can contaminate the measurements of much weaker cosmological backgrounds.<sup>305–307</sup> While this poses a computational challenge, recent methods<sup>308</sup> demonstrate that Cosmic Explorer can provide a unique opportunity to probe the early universe with gravitational waves. Standard slow-roll inflationary models are expected to produce a stochastic background with dimensionless energy density  $\Omega_{\text{gw}} \sim 10^{-17}$ ,<sup>309,310</sup> too weak to be directly detected by all but the most

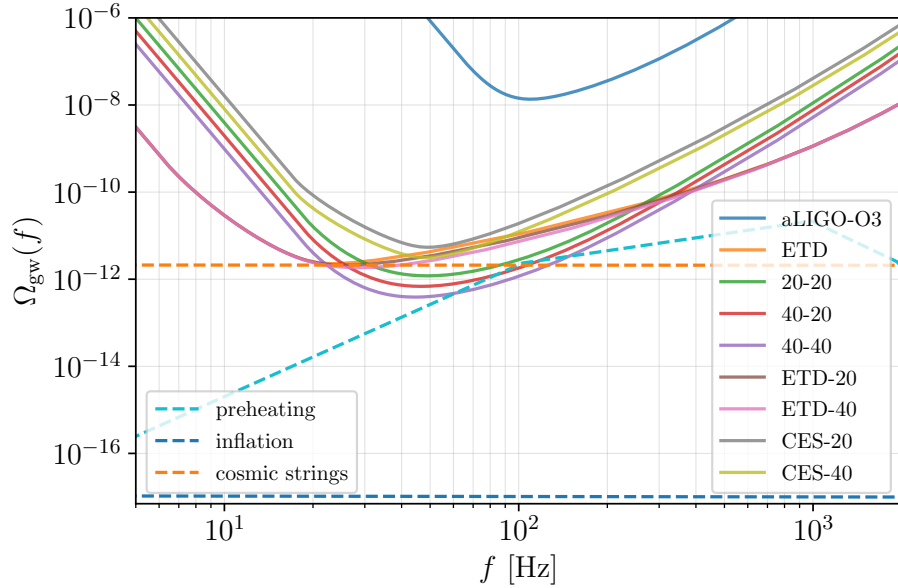


Figure 5.4: Sensitivity of Cosmic Explorer detector networks to stochastic gravitational-wave background compared to that of the three Vs in the Einstein Telescope (ET-D). 20-20, 40-20 and 40-40 correspond to two CE detectors in the US with the numbers indicating the arm length in kilometers. ETD-20, ETD-40 correspond to the sensitivity of an ET array when combined with a CE in the US. Likewise, CES-20 and CES-40 correspond to the sensitivity of a 20 km CE in Australia and a CE in the US. A stochastic background with energy density  $\Omega_{\text{gw}}(f)$  calculated at a reference frequency of 300 Hz would be detected at a SNR of 3 after one year of observing if it crosses the curve for that network.<sup>314</sup> The expected backgrounds for cosmic strings ( $G\mu = 1 \times 10^{-11}$ , with fiducial model parameters from Ref. [315]), preheating (for hybrid inflation occurring at  $10^9$  GeV as calculated in Ref. [316]) and standard slow-roll inflation<sup>313</sup> are shown in dashed lines.

ambitious space-based gravitational-wave detectors.<sup>311,312</sup> However, nonstandard inflationary and cosmological models can produce backgrounds due to processes like preheating, first-order phase transitions, and cosmic strings,<sup>313</sup> all with energy densities within the reach of Cosmic Explorer (see Fig. 5.4).

**Particle Production and Preheating** Following inflation, the universe must undergo a period of particle production during which the inflation field couples to other particle species into which it eventually decays. If this process occurs non-perturbatively, it is called *preheating* (see Refs. [317, 318] for reviews). While the amplitude of the background generated during this process of particle production is expected to be independent of the temperature scale at which it occurs, standard inflationary models predict that it will peak at  $f \sim 10^7 - 10^8$  Hz, well beyond the frequency band of Cosmic Explorer.<sup>319,320</sup> However, for hybrid inflation occurring around  $\sim 10^9$  GeV, the background from preheating peaks in the band of ground-based detectors with an energy density of  $\Omega_{\text{gw}} \sim 10^{-11}$ , which is detectable with Cosmic Explorer.<sup>316,321,322</sup> Even a non-detection of such a background could be used to constrain the physics and temperature scale of particle production in the early universe.

**Cosmic Strings** Cosmic strings are one-dimensional topological defects produced in spontaneous symmetry breaking phase transitions following inflation.<sup>323</sup> When a string folds upon itself, it produces a loop, which oscillates under its tension, emitting gravitational waves in a series of harmonic modes.<sup>324–326</sup> Cusps and kinks are formed when cosmic string loops intersect.<sup>327,328</sup> These string features emit higher frequency bursts of gravitational radiation<sup>329</sup> whose superposition creates a stochastic gravitational-wave background accessible to ground-based gravitational-wave detectors.<sup>330,331</sup> The spectrum of the background depends on the cosmic string tension,  $G\mu$ , and the loop model, among other parameters.<sup>332,333</sup> The current generation of ground-based gravitational-wave detectors has placed the most stringent upper limit on the string tension to date,  $G\mu \lesssim 4 \times 10^{-15}$ ,<sup>159</sup> using a loop model based on Ref. [334], distinct from the model of Ref. [316] shown in Fig. 5.4. Cosmic Explorer will allow us to probe tensions that are several orders of magnitude smaller, offering a window into beyond-the-standard-model physics at the highest energies.

**Electroweak Phase Transition** Phase transitions in the early universe, such as the decoupling of the electromagnetic and weak forces, can also produce a stochastic gravitational-wave background under some modifications of the Standard Model if they are strongly first order,<sup>335–338</sup> i.e., if there is a discontinuity in the first derivative of the free energy during the transition. In this scenario, gravitational waves are emitted due to the collision of bubbles of the new phase<sup>339,340</sup> and due to the anisotropic stresses generated by magnetohydrodynamical turbulence and discontinuities in the shocked plasma surrounding the expanding bubbles.<sup>341–344</sup> A first-order electroweak phase transition also has implications for electroweak baryogenesis, which could provide an explanation for the cosmic baryon asymmetry.<sup>345</sup> The peak frequency of the stochastic background energy density spectrum depends on the energy scale of the transition, with a transition occurring at  $10^9$  GeV producing a background peaking in the frequency band of ground-based gravitational-wave detectors.<sup>309,346</sup> Such a background is expected to have an amplitude of  $\Omega_{\text{gw}} \sim 10^{-12 \pm 2}$ , within the range of Cosmic Explorer.<sup>347,348</sup> The detection of a cosmological stochastic background by Cosmic Explorer would represent the accomplishment of one of the most ambitious goals of gravitational-wave astronomy, and even a non-detection would allow for constraints on beyond-the standard-model physics at energies orders of magnitude larger than those accessible with particle accelerators.



# Observatories

## 6 A Science-Driven Design for Cosmic Explorer

Achieving the science goals laid out in §3 requires a gravitational-wave observatory capable of reliably measuring the strain from mergers in the band between a few hertz and a few kilohertz with a peak sensitivity of approximately  $3 \times 10^{-25} / \sqrt{\text{Hz}}$ . This strain sensitivity guarantees that remnant mergers from the first stars are still observable (Fig. 6.1, adapted from Ref. [95]). The upper limit of the frequency band is dictated by the highest frequency signals expected from the lightest known compact objects: neutron stars. The lower edge of the frequency band of any terrestrial detector is dictated by the seismic motion of the detector and by Newtonian noise, the coupling of seismic and atmospheric fluctuations through direct Newtonian gravity. Since seismic and Newtonian noise are displacement noises, the low-frequency strain sensitivity can be improved by lengthening the detector arms.

Since gravitational-wave detectors are essentially antennas, the highest frequency of interest also sets the ideal scale of the antenna: a few tens of kilometers for signals at a few kilohertz, about ten times the size of existing detectors.

### 6.1 Design Concept for Cosmic Explorer

The interferometric technology used in current gravitational-wave detectors such as Advanced LIGO and Virgo is the most mature and it forms the basis for the Cosmic Explorer detector concept. In addition to the discussion of interferometric technology in §6.2.1, in this section we also briefly discuss potential alternative technologies: space-based interferometers in §6.2.2, atom interferometers in §6.2.3, and torsion pendulum detectors in §6.2.4.

The scale of the facility required to achieve the science goals outlined in §3 represents a major investment. We therefore plan for this facility to have a lifespan of about 50 years and the flexibility to host a number of iterations of detector designs. This will allow funding agencies to capitalize on future research and development breakthroughs, should the operational life-span of CE be extended beyond the initial mandate (which is expected to be 20 years).

The technology to be installed when the Cosmic Explorer observatories are built features the lowest possible technical risk to achieve the most readily accessible science goals. The corresponding detector is largely a scaled-up version of current room-temperature, fused-silica-based interferometers, with some incremental improvements in non-critical technologies (see §8.3). This will be followed by a sequence of planned upgrades that incorporate currently less developed technologies as they become available (see §8.1). In addition to the planned upgrade path to achieving the CE target sensitivity and science goals, a second path involving 2  $\mu\text{m}$  lasers

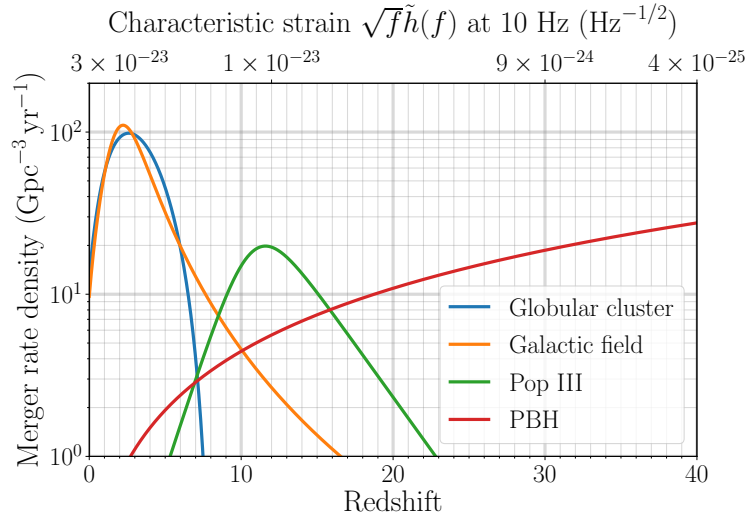


Figure 6.1: Merger rate densities of a few representative populations of compact objects as a function of redshift. Galactic field and globular cluster formation are expected to produce both binary black holes (BBHs) and binary neutron stars, while the other channels will only produce BBHs. The curves for galactic field, globular cluster and Pop III formation are taken from Ng et al.,<sup>95</sup> and are based on population synthesis analyses by Refs. [349–351]. The primordial black hole (PBH) merger rate is taken from Refs. [352, 353]. The top axis gives the characteristic strain calculated at 10 Hz (as measured in the detector frame) of an optimally oriented  $30\text{--}30 M_{\odot}$  BBH placed at the corresponding redshift indicated on the bottom axis. Here the characteristic strain is defined as  $\sqrt{f}|\tilde{h}(f)|$ , where  $\tilde{h}(f)$  is the Fourier transform of the gravitational-wave signal. The strain does not follow a simple linear trend with redshift due to (1) the non-linear relation between luminosity distance and redshift<sup>354</sup> and (2) the fact that if the source is far enough, what will be observed at 10 Hz are the merger and the ringdown.

and cryogenic silicon mirrors (a.k.a. “Voyager technology” or simply “2  $\mu\text{m}$  technology”) is discussed as a potential alternative should the incremental approach based on current technology encounter unexpected challenges. Beyond its role as a technology alternative for the Cosmic Explorer science goals presented here, 2  $\mu\text{m}$  technology may present an opportunity for maximizing the output of the Cosmic Explorer observatories in the future. While 2  $\mu\text{m}$  technology is much less mature than the currently deployed 1  $\mu\text{m}$  technology, this technology, or some other future detector technology that has not yet been conceptualized, may eventually allow the CE observatories to push toward the fundamental physical limits of the facility (see §8.4).

## 6.2 Technology survey

Here we survey a number of potential technologies for detecting gravitational waves: ground-based laser interferometry (which we choose as the technology for the CE reference concept), space-based interferometry, atom interferometry, and torsion bars. We also look at the cryogenic silicon-based upgrade proposal Voyager for the currently existing LIGO observatories. A comparison of low-frequency terrestrial gravitational wave detection methods was also given by Harms et al.<sup>355</sup>



### 6.2.1 Ground-Based Laser Interferometry

All direct detections of gravitational waves to date have been made with laser interferometers, more specifically Michelson interferometers enhanced with optical cavities in a so-called “dual-recycled Fabry–Pérot Michelson” (DRFPMI) configuration. Astrophysically sensitive laser interferometers of this type are the result of a global R&D effort spanning four decades: whereas early laboratory prototypes in the 1980s achieved peak strain sensitivities of about  $10^{-19} / \sqrt{\text{Hz}}$  at kilohertz frequencies,<sup>356</sup> the current kilometer-scale detectors achieve peak strain sensitivities better than  $10^{-23} / \sqrt{\text{Hz}}$  down to several tens of hertz.

The Cosmic Explorer reference concept (§8.1) adopts the DRFPMI interferometer as the working technology. This design builds on the success of the existing DRFPMI research program, aiming to extend the sensitivity of this class of laser interferometers by one more order of magnitude, achieving peak strain sensitivities better than  $10^{-24} / \sqrt{\text{Hz}}$  down to 5 Hz. This sensitivity improvement is due to a combination of longer interferometer arm cavities, realizable in the 2030s at new facility, and a set of technology improvements that can be achieved in the 2020s and 2030s.

Other laser interferometer topologies have been proposed for gravitational wave detection.<sup>357,358</sup> However, none of these topologies will achieve cosmological reach unless, as with the Cosmic Explorer DRFPMI design, a combination of longer facilities and technology improvements is assumed. Moreover, these interferometer topologies are still in the laboratory prototyping phase: compared to the DRFPMI program, any program needed to realize these alternate topologies carries more risk and cannot leverage as much existing R&D. The Cosmic Explorer facility however would be able to accommodate a corresponding upgrade should one of these topologies turn out to be beneficial. This is particularly true for an above-ground facility like Cosmic Explorer, where significant changes to the observatory’s vertex and end stations are possible.

### 6.2.2 Space Missions

Gravitational-wave interferometry is also being pursued for implementation in space, with a science program that is largely complementary to that of ground-based gravitational-wave interferometers. The first anticipated space mission, LISA,<sup>359</sup> is scheduled to launch in the mid-2030s, and other missions include TianQin,<sup>360,361</sup> Taiji<sup>362</sup> and DECIGO.<sup>363,364</sup> Going into space has the advantage of much longer laser path lengths (2.5 million kilometers, in the case of LISA), as well as the absence of terrestrial force noise. On the other hand, laser power limitations and diffraction loss limit the achievable arm power, and hence the shot noise sensitivity of space-based laser interferometers is less than terrestrial detectors. These characteristics make space missions most suitable for detections in the sub-hertz band. Space missions will detect the mergers of intermediate-mass and supermassive black holes, as well as extreme mass-ratio mergers of stellar-size objects and massive black holes. They will observe stellar-mass binary systems only in their early inspiral phase. Notably, space missions will not observe neutron-star

postmerger signals. On the other hand, space missions will be able to observe some early-inspiral stellar-mass systems months to years before they are observed in terrestrial detectors. Such joint ‘multi-band’ observations can potentially set tighter limits for some tests of general relativity. The planned dates for the LISA mission, with observation starting in the late 2030s, mesh well with Cosmic Explorer’s schedule promising interesting multi-band observations.

### 6.2.3 Atom Interferometry

Atom interferometers have been proposed as tools to detect gravitational waves via gradiometric measurement.<sup>365–369</sup> In a typical proposed setup atom interferometers are used as interferometric inertial references, taking the place of test masses in conventional gravitational-wave interferometers. Two or more such atom interferometers are separated along a baseline and interrogated by a common laser. Pulses from that laser serve as splitter, mirrors and recombiner for the individual atom interferometers, and additionally pick up a phase modulation due to a gravitational wave passing through the baseline. This puts challenging constraints on the laser phase front that need to be met to achieve interesting sensitivities. For reference, the initial sensitivity goal for the MAGIS-100 experiment, using state-of-the-art parameters for projection, is about  $5 \times 10^{-15} / \sqrt{\text{Hz}}$  between 0.3 Hz and 3 Hz<sup>366</sup>.

Even with orders-of-magnitude improvements in atomic flux and with baselines exceeding 10 km, the audio-band strain sensitivity of these gradiometers is limited by atomic shot noise to a level that does not surpass the sensitivity already achieved by laser interferometers. Instead, the proposed sensitivity improvement over ground-based laser interferometers occurs in the decihertz band, where the seismic noise coupling is suppressed because the atom clouds are in free-fall. As such, an atomic gradiometer operating at the shot-noise limit is sensitive primarily to compact binaries in the range  $[10^3, 10^4]M_{\odot}$ , potentially extending to redshifts of a few.

Though the direct seismic noise is suppressed, atomic gradiometers are still sensitive to seismic and atmospheric fluctuation through Newtonian coupling in much the same way as laser interferometers. This Newtonian noise drives many of the proposed experiments to assume underground operation over a long (kilometer-scale) baseline, coupled with other techniques such as noise subtraction with auxiliary sensors and the use of dozens of atom interferometers to exploit the different spatial correlation properties of gravitational waves and Newtonian noise. Even so, mitigating Newtonian noise at decihertz frequencies, which is a prerequisite for shot-noise-limited operation of the instrument, will require a challenging research program due to the greater strength of geophysical noise below 1 Hz and the greater number of processes that produce it.<sup>370,371</sup>

### 6.2.4 Torsion Pendulums

Laser interferometry can be used to search for gravitational-wave-induced fluctuations in the angle between two bars, suspended from their centers of mass as torsion pendulums. Such a torsion bar antenna design offers some cancellation of mechanical noise. The characteristic

length scale of the detector is set by the size of the bars, which in the TOBA proposal<sup>372,373</sup> is 10 m; this proposal additionally assumes cryogenic operation underground. The design sensitivity is of the order  $10^{-20} / \sqrt{\text{Hz}}$  above 1 Hz, which is several orders of magnitude less sensitive than ground-based interferometric detectors. Torsion bar detectors are also affected by Newtonian noise, although the coupling geometry is slightly different. Interestingly, this might make torsion bar detectors the most promising local sensors for directly measuring Newtonian noise, potentially assisting Newtonian noise mitigation in other gravitational-wave detector designs.

### 6.2.5 Voyager

Voyager is the name for a proposed cryogenic silicon upgrade intended to maximize the reach of the existing LIGO facilities.<sup>35</sup> Efforts toward Voyager are currently focused on the research and development needed for cryogenic silicon and 2  $\mu\text{m}$  technology. The implementation of Voyager in the LIGO facilities would lead to increased gravitational-wave detection rates and significantly improved astrophysics. However, the unproved nature of the optics needs extensive development. The 4 km baseline would also constrain the future. Voyager would not reach the era of first stars or achieve the full set of goals envisioned for CE (see Table 7.3). Voyager would be a demonstration of technology that could be used to upgrade Cosmic Explorer, yielding important performance information in detectors significantly more sensitive than other possible technology prototypes.

## 7 Optimizing Design Performance Versus Cost

In this section we explore a range of Cosmic Explorer designs and the impact of design choices on the scientific output of CE and the 3G network. The objective of this exploration is to ensure that resources expended in construction of the CE facility are put to good use, i.e., to optimize the science-per-dollar spent on CE.

We start by creating a science traceability matrix, shown in Table 7.2, that maps the three primary science objectives described in §5 to the observations needed to realize each objective in terms of a specific measurement and its requirements. Measurement requirements are then mapped to the instruments and instrument requirements. We then identify a reference configuration for CE (see Box 7.1) that can meet all of these requirements, and discuss a number of variants of this configuration (see §7.1). These variants differ principally in the length and number of CE facilities in the US, since these are the primary cost drivers. This is followed by a presentation of the impact of these alternatives on CE’s ability to achieve its key science goals. A summary of the results of this section is given in Table 7.3.

### Box 7.1: Cosmic Explorer Reference Concept.

*The Cosmic Explorer concept consists of two widely-separated L-shaped observatories in the United States — one with 40 km long arms and another with 20 km arms.*

This concept maximizes the scientific output as the 40 km detector can be optimized for deep broadband sensitivity, while the 20 km detector is capable of tuning its sensitivity to the physics of neutron stars after they have merged. To enable accurate source localization and coverage and to ensure sufficient transient noise rejection, the observatories should not be co-located. To ensure that wave polarizations can be well distinguished, the observatories should not be parallel.

Two US observatories can accomplish all of the CE science goals independent of additional international next-generation gravitational-wave observatories — though CE will reach its maximum potential as part of a next-generation network. This concept also takes advantage of efficiencies associated with simultaneous construction (as well as commissioning and operation) of two sites within the US, as done by LIGO.

Facility capabilities differ more than might be expected by a simple arm-length scaling of the signal’s strength. In particular, the free spectral range of long-arm facilities ( $c/2L_{\text{arm}} \approx 3.7$  kHz for a 40 km detector) begins to limit the flexibility of the observatories to target high-frequency signals such as the postmerger phase of neutron-star mergers. The frequency of postmerger

gravitational waves varies substantially within current matter uncertainties and with the masses of the merging stars.<sup>374</sup> As we better understand the population of neutron-star mergers and the properties of dense matter, we can tune the sensitivity of a shorter 20 km detector for optimal postmerger physics,<sup>41,135</sup> for example by focusing on frequencies characteristic of a hadron-quark phase transition.<sup>148</sup> To compare facilities, we include reference tunings optimized for inspiral and postmerger observation.

## 7.1 Alternate Configurations

This section describes variants which differ somewhat from the reference configuration of two L-shaped observatories, one with 40 km long arms and another with 20 km arms (see Box 7.1). For the reasons discussed in the following sub-sections, the variants involving one or two observatories of either 20 km or 40 km are carried forward into the subsequent trade-study discussion in §7.2.

### 7.1.1 Shorter Arms (10, 20 and 30 km) and Optical Tunings

Reducing the length of the interferometer arms is a clear means of reducing the cost of a CE facility. As the reference concept was chosen for maximum scientific output, this cost reduction must come at the expense of scientific output.

Table 7.1 shows the scalings of fundamental noises as the detector length  $L$  is varied. In all cases, the strain-referred noise from the geophysical and thermal sources is the same or worse as  $L$  is reduced. The shot noise, which is the dominant noise source near and above 100 Hz, is shaped not only by the length of the detector, but also by its optical configuration. For a given length  $L$ , we identify two optical configurations of interest. First, we identify a “compact-binary optimized” configuration, where the detector’s shot noise is tuned to give the best sensitivity below 1 kHz, where stellar-mass binaries inspiral and merge. Second, we identify a “postmerger optimized” configuration, where the detector’s shot noise is tuned to give the best sensitivity around 2–3 kHz, at the expense of sensitivity below 1 kHz; this configuration will best capture late-time signals from the aftermath of neutron star mergers. It is possible to convert the detector from one configuration to the other by replacing a small number of optical components, with no facility modification required.

The compact-binary optimized and postmerger optimized detector configurations are shown in Fig. 7.1 as a function of arm length. Evidently, for  $L = 40$  km there is only a modest difference between the two configurations. However, for a 20 km facility the difference is significant, showing a clear trade-off to be made between the science goals. It is noteworthy that the 30 km option appears to be “the worst of both worlds” in that it cannot be tuned to high frequencies, and its sensitivity at low frequency is not as good as a longer facility.

We stress that for a given detector length, the trade-off between these two optimized configurations is *not* built into the facility and thus not a long-term choice. We expect to periodically



Noise	Scaling	Remarks
Coating Brownian	$1/L^{3/2}$	Fixed cavity geometry
Substrate Thermo-Refractive	$1/L^2$	Fixed cavity geometry
Suspension Thermal	$1/L, 1$	Horizontal, vertical noise
Seismic	$1/L, 1$	Horizontal, vertical noise
Newtonian	$1/L$	
Residual Gas Scattering	$1/L^{3/4}$	Fixed cavity geometry
Residual Gas Damping	$1/L$	
*Quantum Shot Noise	$1/L^{1/2}$	Fixed bandwidth
*Quantum Radiation pressure	$1/L^{3/2}$	Fixed bandwidth

Table 7.1: Scalings of fundamental noises with arm length  $L$ , referred to astrophysical strain.<sup>375</sup> The test mass radii of curvature are varied to hold the arm cavity geometry fixed. In the case of the quantum shot and radiation-pressure noises (\*), the given scalings are for a fixed detector bandwidth, but these noises could instead be optimized in a number of different ways — hence the “compact-binary optimized” and “postmerger optimized” curves in Fig. 7.1.

switch detector configurations (e.g., observe in compact-binary mode for a year, then observe in postmerger mode the following year), since this requires only minor modifications to the detector and does not require facility modification. Furthermore, the postmerger optimized sensitivity shown in Fig. 7.1 is only one of a continuum of options available: in a 20 km facility, for instance, any frequency between 1 and 3 kHz can be targeted, and the target frequency can be changed between observing runs.

### 7.1.2 Multiple Interferometers

The current reference concept for Cosmic Explorer includes two facilities that are geographically separated while still being located in the United States. While the reference maximizes the scientific output of CE, alternate configurations may involve one, two or three detectors which may or may not be colocated.

**One Large CE versus Two Smaller CEs** It is apparent that a 40 km facility will cost more than a 20 km facility, and one might imagine that two of the smaller facilities can be built for a price similar to that of a single larger detector. (This is not true; see §8.5.) The merits of a longer detector lie in the scaling of various noises with length (see Table 7.1), while those of multiple detectors lie in the freedom to sample different gravitational-wave polarizations and to geographically separate the detectors to improve localization of sources. For CE, where the arm-length approaches the wavelength of the gravitational waves of interest for some science goals, the bandwidth of the detector is also an important consideration. Thus, the impact of choosing a single detector over a pair of detectors will be different for different science goals.

As a simplified example in which high-frequency free spectral range effects are not a concern, consider two 10 km facilities versus a single 20 km facility. When tuned to a broadband

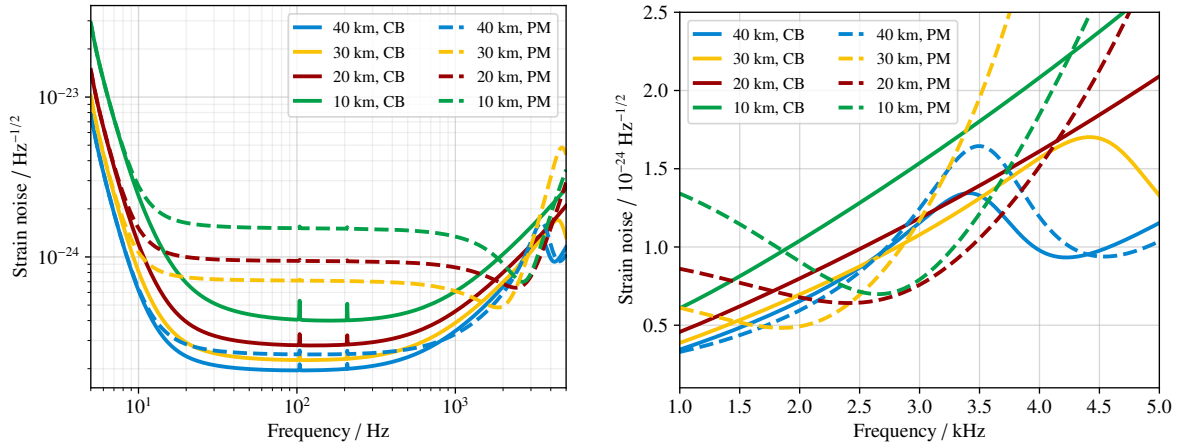


Figure 7.1: Amplitude spectrum of the detector noise as a function of frequency for the four Cosmic Explorer lengths considered in this comparative performance study. PM denotes the postmerger optimized configuration and CB denotes the compact-binary optimized configuration. The plot on the left shows the broadband sensitivity and the plot on the right shows the benefits of the postmerger optimized configurations at high frequencies.

configuration, quantum shot noise will dominate in most of the detection band. If we keep the quantum noise tuned to the same fixed bandwidth, from Table 7.1 we can see that these two configurations will give similar results (i.e., both a factor of  $\sqrt{2}$  more sensitive than a single 10 km facility). At lower frequencies, where quantum radiation pressure, coating Brownian noise, and Newtonian noise are dominant, the longer detector will provide superior performance. The same is true for mid-frequencies if we tune the quantum noise to trade bandwidth for low- and mid-frequency performance. This consideration, combined with the fact that cost is not simply proportional to arm length, drives us to consider long detectors, and is the reason why the CE reference concept revolves around matching the detector to the gravitational-wave wavelength relevant to our science goals.

This brings us back to the original question: one large observatory, or two smaller ones? In §7.2 we consider combinations of 20 km and 40 km observatories and the merits of each depend on the science question being answered. Broadly speaking, when operating without international partners (e.g. Einstein Telescope or CE South in Australia), having two Cosmic Explorer detectors is critical for many science goals (see Table 7.3). However, when operating as part of a global network, the sensitivity advantage of a 40 km observatory outweighs the benefit from the additional detector in a two 20 km configuration (see Table 7.3) for most science goals. As previously noted a single 40 km observatory is also somewhat less expensive than a pair of 20 km observatories (see Table 11.1). A single 20 km observatory would clearly be the worst of the considered Cosmic Explorer configurations (see Table 7.3 and §11.4).

**Two Interferometers in a Single Vacuum Envelope** Given the expense of building a CE observatory, one might expect that housing multiple interferometers in the same vacuum envelope would allow for greater sensitivity and flexibility with relatively little added cost. Putting both

a 20 km and a 40 km CE in the same beamtubes, for instance, appears to yield an observatory capable of simultaneously optimizing compact-binary and postmerger science. The Initial LIGO Hanford Observatory did, in fact, operate with two interferometers in the same beamtubes, albeit for different reasons.

Unfortunately, this approach requires that the clear aperture of the beamtubes be large enough to put the interferometer optics side-by-side with enough separation to avoid mechanical and optical interactions between the detectors. This, in turn, requires that the beamtube diameter be roughly doubled to house two interferometers, which leads to a number of practical and economical challenges.

The immediate practical issue is that CE, which has a characteristic beam diameter of several tens of centimeters along its entire length, already requires the largest pipe diameter and vacuum hardware (e.g., gate valves) commonly made. A special process would be required to produce many kilometers of larger diameter pipe and special orders would be required for all beamtube related hardware. The second issue is that a tube with diameter  $2D$  requires twice as much material per unit length as two tubes each with diameter  $D$ , since the pipe wall thickness required to support atmospheric pressure must increase linearly with diameter in order to maintain the same safety margin (or else a more sophisticated manufacturing process, e.g., stiffening rings or corrugated pipes, is required).<sup>376</sup> These factors combined would increase the cost of the vacuum system by more than a factor of 2, making separate vacuum systems a clearly superior approach. Using separate vacuum systems also avoids potential optical interactions between the interferometers — a problem which plagued the initial LIGO Hanford Observatory.

One approach that could work is to “time multiplex” the vacuum system. That is, to build an observatory that can operate as either a 20 km *or* a 40 km CE by building mid-stations (20 km from the vertex) capable of housing test-masses. The mid-station mirrors could be installed when dense matter science motivates the 20 km postmerger-optimized configuration. The advantages of this configuration are relatively small, but so is the additional expense, so it may be the best option if only one observatory can be built.

**Side-by-Side Interferometers** While the previous discussion makes it clear that putting multiple interferometers in the same vacuum envelope will not reduce cost, there remains the possibility of placing two interferometers side-by-side in the same observatory. This approach could potentially save some fraction of the civil engineering cost of CE (26% of the total) relative to building two separate observatories. It also has the advantage of reducing the overall project footprint, and thus its impact on the land and environment.

The disadvantages of this approach are clear: both detectors measure only one gravitational-wave polarization, and there is no additional sky localization information offered by the second detector. This would result in a significant compromise on the science goals: much like having only a single detector, CE would be dependent on the rest of the next-generation network in order to deliver on many science goals (see Table 7.3).

**Three-Detector Triangle** Another option is to build a single triangular facility comprised of three side-by-side detectors, which is the baseline design of the Einstein Telescope. Such a facility is sensitive to both the + and  $\times$  polarization of incoming gravitational waves. As a rough metric, we can compare the signal-to-noise performance of such a three-detector triangular facility to two single-detector L-shaped facilities with nonparallel arms, which jointly would be sensitive to both polarizations.

For a circularly-polarized overhead signal, a three-detector triangular facility of length  $L$  on a side collects the same signal-to-noise ratio as two L-shaped single-detector facilities each with arm length  $L' = \frac{9}{8}L$  and oriented at  $45^\circ$  relative to one another, assuming in both cases the detectors are shot-noise limited with the same bandwidth, and otherwise have identical parameters.<sup>a</sup> This means that instead of laying out a triangular facility with total arm length  $3L$ , laying out two L-shaped facilities of the same overall sensitivity would require a total arm length  $4 \times \frac{9}{8}L = 4.5L$ . However, since each detector in the triangular facility requires a separate vacuum envelope, the triangular facility would require  $6L$  of vacuum tube, while the two L-shaped facilities would require only  $4.5L$ . The relative expense of these options will depend on the details of the sites and local construction costs, but it is unclear that the decrease in total arm length when building a triangle (relative to two L's) will ever be sufficient to outweigh the added expense of manufacturing, housing, and operating a longer total vacuum envelope and an extra interferometer. (In CE, the vacuum system makes up 34% of the cost, the detector 26%, and the civil work 26%, which suggests that a triangular facility would cost at least as much as two L-shaped facilities with the same sensitivity.)

In light of the above, it is clear that building a three-detector triangular facility is not advantageous relative to two co-located L-shaped facilities, except possibly in an environment where excavation costs entirely dominate the facility cost, which is not the case for CE. Furthermore, with two L-shaped facilities there is the clear advantage that the facilities can be separated by a long baseline, as with the current LIGO facilities, and thereby achieve better sky localization than a single triangular facility. This option is also favorable in that it only requires two interferometers to be built and operated, rather than three interferometers as in the triangular design, thereby reducing maintenance and operations costs.

<sup>a</sup>Suppose the triangular facility has a side length of  $L$ , so that each of the three detectors has an arm length  $L$  and an opening angle of  $60^\circ$ . If a circularly polarized signal with strain amplitude  $h_+ = h_\times \equiv h$  is incident from directly overhead, then the total signal-to-noise ratio of the triangular facility is  $\rho_\Delta(L) = \frac{3}{2}\rho(L)$ , where

$$\rho(L) = \left( 4 \int df \frac{h^2}{S_h^{(L)}(f)} \right)^{1/2} \quad (7.1)$$

is the signal-to-noise ratio that would be accumulated by a single detector also of length  $L$  with  $90^\circ$  opening angle, and  $S_h^{(L)}(f)$  is the strain noise power spectral density of such a detector.

Conversely, two L-shaped facilities of length  $L'$  oriented at  $45^\circ$  relative to one another would collect a total signal-to-noise ratio of  $\rho_{\perp\vee}(L') = \sqrt{2}\rho(L')$ . Assuming that the detector parameters, including the bandwidth, are the same in both the triangular and L-shaped cases, and assuming the signal occurs in a frequency range dominated by shot noise, the detector noises are related by  $S_h^{(L')} = (L/L')S_h^{(L)}$ .<sup>375</sup> Equality of the signal-to-noise ratios  $\rho_\Delta(L)$  and  $\rho_{\perp\vee}(L')$  is then achieved for  $L' = \frac{9}{8}L$ .

Table 7.2: Science traceability matrix for the science goals identified for Cosmic Explorer in this Horizon Study. This matrix illustrates the flow-down of Cosmic Explorer’s high-level science goals, through the measurement objectives and requirements needed to accomplish these goals, to the minimum required instruments and the corresponding projected instrument performance. The instruments chosen here are the minimum set needed for Cosmic Explorer alone to realize each science goal. We emphasize that this study is a starting point for community input to the final design of Cosmic Explorer and encourage the community to provide input to expand and refine Cosmic Explorer’s science traceability matrix.

Science Objectives	Measurement Objectives	Measurements	Instruments	Projected Instrument Performance
<b>Black holes and neutron stars throughout cosmic time.</b>	<p>Observe black holes formed by Population III stars.</p> <p>Determine if supermassive black holes at <math>z \sim 8</math> are built from hierarchical mergers of smaller black holes.</p> <p>Determine the formation and evolution channels of black holes and neutron stars formed at <math>z &lt; 4</math>.</p>	<p>Detect tens of binary black hole mergers at <math>z &gt; 10</math> and measure their redshifts better than 10 %.</p> <p>Detect thousands of binary black hole mergers at <math>z &gt; 8</math> and measure their redshifts better than 20% and source frame mass better than 10 %.</p> <p>Detect tens of thousands binary black hole mergers up to redshift of 4 and measure their redshifts to better than 5 % and source frame mass to better than 10 %.</p>	<p>A 40 km and a 20 km Cosmic Explorer.</p> <p>Two 20 km Cosmic Explorer, or a 40 km and a 20 km Cosmic Explorer.</p> <p>Two 20 km Cosmic Explorer, or a 40 km and a 20 km Cosmic Explorer.</p>	<p>Two detectors with strain sensitivity better than <math>1 \times 10^{-24} \sqrt{\text{Hz}}</math> below 10 Hz, increasing to no more than <math>2 \times 10^{-25} \sqrt{\text{Hz}}</math> up to 50 Hz.</p> <p>Two detectors with strain sensitivity better than <math>1 \times 10^{-24} \sqrt{\text{Hz}}</math> below 10 Hz, increasing to no more than <math>3 \times 10^{-25} \sqrt{\text{Hz}}</math> up to 500 Hz.</p> <p>Preferably two detectors with strain sensitivity better than <math>5 \times 10^{-25} \sqrt{\text{Hz}}</math> from 10 Hz to 500 Hz.</p>
<b>Dynamics of dense matter.</b>	<p>Measure the structure and composition of neutron stars.</p> <p>Explore the high density, finite temperature phase space of quantum chromodynamics.</p> <p>Trace the chemical evolution of the universe using multi messenger observations of neutron star mergers.</p> <p>Connect the properties of binary neutron star mergers to the physics of the relativistic jets powering short gamma-ray bursts.</p>	<p>Measure the neutron star radius to within <math>&lt; 100</math> m across the full mass range of neutron stars and all plausible nuclear equations of state.</p> <p>Detect neutron star post-merger remnants with a signal-to-noise ratio <math>&gt; 8</math> with measurement of merging object’s masses to better than 1 %.</p> <p>Detect and localize neutron star mergers to <math>1 \text{ deg}^2</math> and 1 % in distance at least two minutes prior to merger.</p> <p>Detect mergers and measure binary inclination to within 1 % for neutron star mergers out to <math>z \sim 2</math>.</p>	<p>A 40 km Cosmic Explorer, or two 20 km Cosmic Explorer.</p> <p>A 20 km Cosmic Explorer, or two 40 km Cosmic Explorer.</p> <p>Two 20 km Cosmic Explorer, or a 40 km and a 20 km Cosmic Explorer, and electromagnetic observatories.</p> <p>Two 20 km Cosmic Explorer, or a 40 km and 20 km Cosmic Explorer, and gamma-ray burst satellites.</p>	<p>Strain sensitivity better than <math>3 \times 10^{-25} \sqrt{\text{Hz}}</math> between 20 Hz to 400 Hz, rising to no more than <math>6 \times 10^{-25} \sqrt{\text{Hz}}</math> at 1.5 kHz.</p> <p>High frequency strain sensitivity better than <math>1 \times 10^{-24} \sqrt{\text{Hz}}</math> between 2–4 kHz.</p> <p>Two detectors with strain sensitivity better than <math>5 \times 10^{-25} \sqrt{\text{Hz}}</math> from 20 Hz to 2 kHz.</p> <p>Two detectors with strain sensitivity better than <math>5 \times 10^{-25} \sqrt{\text{Hz}}</math> from 20 Hz to 2 kHz.</p>
<b>Extreme gravity, fundamental physics, and discovery potential.</b>	<p>Study the nature of strong gravity, search for unusual or novel compact objects, explore the implications of quantum gravity, and probe dark matter and dark energy.</p>	<p>Open the largest possible discovery space in gravitational-wave strain sensitivity with a network that is sensitive to both polarizations of the gravitational-wave signal.</p>	<p>A 40 km and a 20 km Cosmic Explorer, preferably two 40 km Cosmic Explorer detectors.</p>	<p>At least one 40 km Cosmic Explorer facility with strain sensitivity better than <math>2 \times 10^{-25} \sqrt{\text{Hz}}</math> across the widest possible frequency band, tunable to <math>1 \times 10^{-25} \sqrt{\text{Hz}}</math> in a narrower band.</p>



Science		No CE	CE with 2G					CE with ET					CE, ET, CE South				
Theme	Goals	2G	20	40	20+20	20+40	40+40	20	40	20+20	20+40	40+40	20	40	20+20	20+40	40+40
Black holes and neutron stars throughout cosmic time	Black holes from the first stars	Gray	Gray	Gray	Yellow	Green	Dark Green	Dark Green	Dark Green	Dark Green	Dark Green	Dark Green	Dark Green	Dark Green	Dark Green	Dark Green	Dark Green
	Seed black holes	Gray	Yellow	Yellow	Green	Dark Green	Dark Green	Dark Green	Dark Green	Dark Green	Dark Green	Dark Green	Dark Green	Dark Green	Dark Green	Dark Green	Dark Green
	Formation and evolution of compact objects	Gray	Yellow	Green	Dark Green	Dark Green	Dark Green	Dark Green	Dark Green	Dark Green	Dark Green	Dark Green	Dark Green	Dark Green	Dark Green	Dark Green	Dark Green
Dynamics of dense matter	Neutron star structure and composition	Gray	Yellow	Green	Dark Green	Dark Green	Dark Green	Dark Green	Dark Green	Dark Green	Dark Green	Dark Green	Dark Green	Dark Green	Dark Green	Dark Green	Dark Green
	New phases in quantum chromodynamics	Gray	Green	Yellow	Dark Green	Dark Green	Dark Green	Yellow	Yellow	Dark Green	Dark Green	Dark Green	Dark Green	Dark Green	Dark Green	Dark Green	Dark Green
	Chemical evolution of the universe	Gray	Yellow	Yellow	Green	Dark Green	Dark Green	Dark Green	Dark Green	Dark Green	Dark Green	Dark Green	Dark Green	Dark Green	Dark Green	Dark Green	Dark Green
Extreme gravity and fundamental physics	Gamma-ray burst jet engine	Gray	Yellow	Yellow	Green	Dark Green	Dark Green	Dark Green	Dark Green	Dark Green	Dark Green	Dark Green	Dark Green	Dark Green	Dark Green	Dark Green	Dark Green
	Discovery potential	Gray	Gray	Yellow	Yellow	Green	Dark Green	Yellow	Dark Green	Dark Green	Dark Green	Dark Green	Dark Green	Dark Green	Dark Green	Dark Green	Dark Green
Technical risk			Red	Light Orange	Light Orange	Light Orange	Light Orange	Red	Light Orange	Light Orange	Light Orange	Light Orange	Light Orange	Light Orange	Light Orange	Light Orange	Light Orange

Table 7.3: This table indicates the accessibility of astrophysical sources that can advance key next-generation science goals. A US Cosmic Explorer consisting of one 20 km observatory, one 40 km observatory, or a pair of observatories of 20 or 40 km length are evaluated in the presence a background network that includes second-generation (2G) gravitational-wave observatories, the EU Einstein Telescope (ET), and a 20 km Cosmic Explorer-like detector located in Australia (CE South). For each goal, the colors range from gray (least favorable, science goal not achieved) to green (good, science achievable) and dark green (most favorable). Longer, more sensitive detectors are generally better, and a network is required for many science goals. For example, studying black holes from the first stars requires a 40 km detector that can see black holes at  $z \gtrsim 10$  in a network that can measure both gravitational-wave polarizations to accurately measure the holes' redshifts. Only observations of neutron star post-merger signatures benefit from a 20 km detector. The higher bandwidth of the 20 km observatory allows for better narrow-band tuning for this particular source, although only one detector needs to be in this configuration. Detailed descriptions of the metrics that determine the criteria can be found in §7.2.1. The final row, labeled “Technical Risk”, represented the technical risk associated with each configurations ability to achieve its target sensitivity; light orange is lowest risk, and red is highest risk. We emphasize that this study is a starting point for community input on Cosmic Explorer.

## 7.2 Trade-Study Outline

The optimization of CE design in the context of a variety of potential future global gravitational-wave detector networks is a complex task. The process used to perform this optimization is referred to herein as a “trade study” since we are looking for trade-offs which are likely to maximize the scientific output of CE both in the near-term and integrated over the lifetime of the facility. This section gives a brief outline of the trade study, while leaving a full technical description to the literature.<sup>377–380</sup>

The trade study considers the performance of CE design variants both in the context of the existing 2G detector network, and in the presence of representative next-generation facilities. Specifically, nine detector locations are considered in this study: the five 2G detector sites, including LIGO India (Hingoli, India), and four representative sites for the 3G detectors. Since the locations of future detectors are unknown, we choose locations which we expect are plausible based on geophysical considerations, knowing that the exact location of a detector has little impact on network performance.<sup>378</sup> The Einstein Telescope’s reference location is set to be the same as Virgo, while the three possible Cosmic Explorer locations C, N, and S are set to be sites in Idaho (USA), New Mexico (USA), and New South Wales (Australia). The spread of these locations around Earth is shown in Fig. 7.2. The right-hand plot in Fig. 7.2 provides a graphical summary of 2G and 3G detector generations and design concepts considered at each location. The Cosmic Explorer sensitivity curves used in the trade-study are shown in Fig. 7.1. For the sake of brevity, we include results for only 20 km and 40 km Cosmic Explorer configurations although the results are available, and will be made public online, for other arm lengths.

Many different performance metrics are used in the trade-study to capture network perfor-

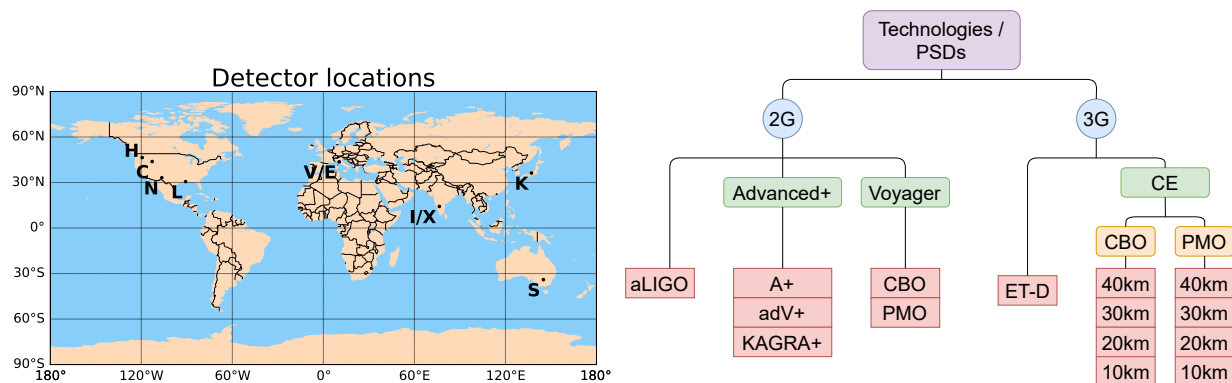


Figure 7.2: The left plot shows detector locations considered in this trade study while the right plot is a graphical summary of the choices available for installing detectors of different arm lengths and sensitivities at various locations. The LIGO A+, AdVirgo+, KAGRA+, and Voyager detectors are located at the 5 existing sites (labeled H, L, V, K and I). Since its actual future location is unknown, but certainly in Europe, the Virgo site is used as our reference location for the Einstein Telescope. Cosmic Explorer facilities are considered at three possible locations, two in the US (C and N), and one in Australia (S). For each instance of CE in the US, a variety of configurations are considered (encoded as different power spectral densities, PSDs, and shown on the right side, under the green CE label). These include arm lengths from 10 to 40 km and compact-binary or postmerger optimizations (CBO or PMO).

mance and its impact on scientific output.<sup>377–380</sup> A key ingredient in almost all performance metrics is the rate of events expected to be observed by different detector networks as a function of redshift. Based on observations so far, the local (i.e.,  $z \ll 1$ ) merger rates inferred for the population of binary neutron stars (BNS) and binary black holes (BBH) are  $\mathcal{R}_{\text{BNS}} = 320 \text{ Gpc}^{-3} \text{ yr}^{-1}$  and  $\mathcal{R}_{\text{BBH}} = 23.8 \text{ Gpc}^{-3} \text{ yr}^{-1}$ ,<sup>31</sup> broadly consistent with expectations from multiple astrophysical formation channels.<sup>381</sup> Fig. 7.3 plots the cosmic merger rate as a function of redshift for the two source populations. This rate model begins with a Madau–Dickinson star-formation rate as a function of redshift,<sup>12</sup> and then accounts for the characteristic time delay from binary formation to merger, including the effects of metallicity for BBHs.<sup>95</sup>

The component masses of the BNS population are chosen to be Gaussian distributed with mean  $1.34 M_{\odot}$ , standard deviation  $0.15 M_{\odot}$ , minimum mass  $1 M_{\odot}$ , and maximum mass  $2 M_{\odot}$ . The primary masses of the BBH population are chosen to follow the so-called POWER LAW + PEAK distribution<sup>382</sup> with lower and upper cutoffs at  $4.59$  and  $86.22 M_{\odot}$ , while the secondary mass is sampled uniformly between the lower cutoff and the primary mass component. This deviation from the original POWER LAW + PEAK model allows for the examination of a broader mass ratio range with the BBH population.

### 7.2.1 Impact on Key Science Goals

To assess the impact of Cosmic Explorer design choices on our capacity to accomplish the science goals described in §5, we identify a set of performance metrics for each science goal and then evaluate the capability of Cosmic Explorer. We perform this evaluation for several scenarios, with Cosmic Explorer either in the presence or absence of other detectors. Box 7.2 summarizes the main conclusions of this study, and Box 7.3 summarizes the key observation rates for Cosmic Explorer.

### 7.2.2 Black Holes and Neutron Stars Through Cosmic Time

**Remnants of the First Stars** The most sensitive astronomical telescopes (e.g., JWST) will be sensitive to objects at a maximum redshift  $z \sim 30$ , some 100 Myr after the Big Bang, while the first stars in the universe could have formed even earlier, a mere 30 Myr after the Big Bang or  $z = 70$ . The network of ET and two CE facilities with at least one 40 km facility will be sensitive to such redshifts and beyond. Binaries of black hole remnants of first stars could be observed by the 3G network. Decisively inferring that the observed sources are remnants of first stars requires an accurate measurement of their redshift. This can be done either using the whole population of detected sources, and showing that it contains a high-redshift merger peak, or by proving that individual sources have merged at redshifts higher than what is expected from other astrophysical channels.

The first approach was followed by Ng et al.<sup>95</sup> where it was shown that a network of 2 CE and one ET could reveal a peak of mergers from Pop III remnants at redshift of  $\sim 12$  (see also Fig. 6.1 above). Given the computational cost of that type of analysis, here we use a simpler

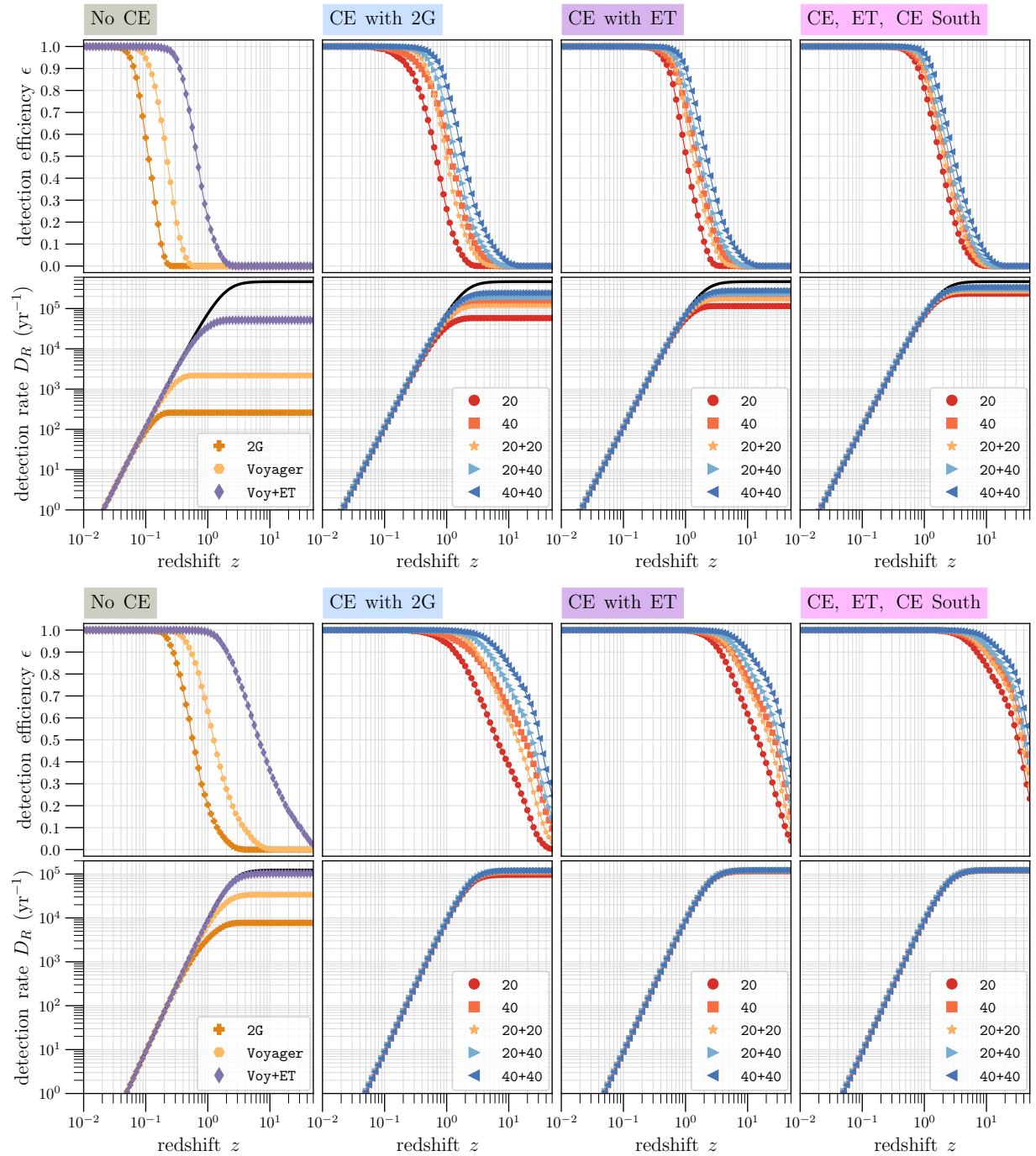


Figure 7.3: The detection efficiency (top and third rows) and the cumulative detection rate from the galactic field binaries (second and fourth rows) of events with signal-to-noise ratio greater than 10 for binary neutron stars (top two panels) and binary black holes (bottom two panels). For a given redshift  $z$ , the detection efficiency  $\epsilon$  is defined as the ratio of the number of detected sources to the total number of sources (shown as solid, black lines in the third and bottom rows) out to that distance. The networks are exactly as in Table 7.3.

Box 7.2: Questions addressed by the trade study, and their answers in brief.

In addition to a general science-per-dollar optimization, we also use the trade study as a means of answering the following frequently asked questions:

- Is it better to build one large CE, or two smaller ones?  
*Science goals requiring excellent source localization drive the strong desire for a network of detectors. The significantly increased broadband sensitivity of a 40 km detector is advantageous for science goals that require high signal-to-noise observations. Compared to one 40 km observatory, two 20 km observatories are somewhat more expensive (see §7.1.2). The 40 km + 40 km and the 40 km + 20 km configurations had the best performance in the study. Because of cost considerations and the tunability advantage for neutron star post-merger signal the reference configuration was chosen as the 40 km + 20 km configuration. (see Table 7.3).*
- Should a second CE be built in the US, internationally, or both?  
*Having a long separation between observatories is favorable for localizing and characterizing gravitational-wave sources, so if only two CE observatories are built it is best for the second to be located far away (e.g., in Australia). However, two observatories in the US can be separated by a sufficient distance to precisely localize a large number of sources, making the key science goals accessible (see Table 7.3).*
- Would a triangular Einstein Telescope-like design make sense for CE?  
*A triangular configuration is not advantageous in places where above-ground construction is feasible (e.g., US and Australia, see §7.1.2).*
- To what degree are our key science goals dependent on the global detector network?  
*This question drives much of the complexity of our trade study, and the answer is graphically captured in Table 7.3. The short answer is: the key science goals are achievable with the reference CE configuration (one 40 km and one 20 km observatory), while a network of three or more next-generation detectors will increase the rate at which these goals are achieved.*

figure-of-merit based on individual sources. Specifically, we focus on the fraction of events merging at redshifts  $z \geq 10$  with fractional redshift uncertainty smaller than some threshold. As shown in Fig. 6.1, the peak of mergers from Pop. III remnants is expected to happen at  $z \sim 12$  (though significant uncertainty exists). Meanwhile, the main two late-universe populations, formation in galactic fields or dynamical formation in globular clusters,<sup>b</sup> do not contribute significantly to the total merger rate for redshifts above  $\sim 9$  (Fig. 6.1). Our rough figure of merit is thus the number of BBH sources for which the statistical uncertainty in redshift is better than 10%. This is an uncertainty for which the posterior distribution for the redshift of a black hole binary that merges at the lowest redshift we consider, i.e., 10, would exclude  $z < 9$  with  $1\sigma$  level. For black holes whose true redshift is higher than 10, this criterion is conservative in the sense that even an uncertainty larger than 10% could be sufficient to exclude  $z < 9$ . We find that no network without at least two 3G detectors can satisfy our criterion. A network with only one

<sup>b</sup>Other formation channels have been proposed, e.g., nuclear star clusters, young star clusters and mergers in the disk of active galactic nuclei. Here we focus on globular clusters and galactic fields merely because they have been extensively studied in the literature.



## Box 7.3: Observation Rates for Compact Binaries with Cosmic Explorer.

Cosmic Explorer's ability to detect<sup>a</sup> large numbers of compact binaries out to large cosmological distances is driven by the low-frequency sensitivity of the 40 km detector. In one year of observations, such a detector will:

- Observe 300 000 binary neutron star mergers (one every 100 seconds),
  - including 80 % of all mergers within  $z = 1$ , allowing association with EM transient surveys,
  - of which 5 will have  $\text{SNR} > 300$ , providing access to postmerger physics,
  - for thousands will provide distance and sky localization with more than 10 minutes of early warning,
  - and will observe half of all mergers out to  $z = 10$ , allowing association with gamma-ray bursts and charting the history of supernovae and merger time delays;
- Observe 100 000 binary black hole mergers from galactic field population (one every 5 minutes),
  - of which 8 will be nearby ( $z < 0.1$ ) with median SNR of 600 and exceeding an SNR of 2700 for the loudest source,
  - and 60 000 will be at cosmological distances  $z > 2$  (inaccessible to current networks whose most distant sources are  $z \sim 1$ ) and have median SNR of 20 (i.e., with SNR similar to GW150914 in Advanced LIGO).
  - and 10 000 will be at cosmological distances  $z > 4$  and have median SNR of 18.

<sup>a</sup>We use signal-to-noise ratio greater than 10 as detection criteria.

3G detector (Einstein Telescope or Cosmic Explorer) could *detect* some sources at  $z \geq 10$ , but the associated redshift uncertainty would be too large to definitively prove the merger did not happen at smaller redshifts. A network with two 40 km Cosmic Explorer optimized for compact binaries detection<sup>c</sup> would detect roughly 200 sources per year that satisfy our criterion. That number improves by ten folds ( $\sim 2000$  sources) if the network is augmented to also include Einstein Telescope. This increase is due to the superior polarization resolving power of multiple detectors. In Table 7.3 we mark in yellow networks that yield at least 10 viable sources per year, and in light (dark) green networks that give access to at least 50 (100) viable sources per year. Details are available in a technical note.<sup>383</sup>

**Black Hole Seeds and Galaxy Formation** If supermassive black holes at  $z \sim 8$  were built from hierarchical mergers of smaller black holes at higher redshifts we should detect lighter black hole mergers at higher redshifts and heavier ones at lower redshifts. This requires not only the

<sup>c</sup>For all science goals involving populations of compact binaries, low frequency sensitivity is more important than sensitivity above  $\sim 500$  Hz. Therefore, the postmerger-optimized setting is not thoroughly discussed here.

capability of measuring the redshift of a BBH source, but also its source-frame mass. We stress that precise measurement of the source-frame mass does in turn require a precise measurement of the source redshift. This is because gravitational-wave detectors measure redshifted mass parameters, which are  $(1+z)$  times larger than the astrophysically interesting source-frame quantities.<sup>309</sup> Therefore, we expect that networks with more detectors will do better at measuring source-frame masses.<sup>384,385</sup>

Our figure-of-merit to quantify the ability of a network to track the growth of black holes across cosmic history will be the number of sources for which the source-frame chirp mass and the redshift can be measured at least as well as what has been reported for GW190521. This source is one of the most interesting found to date in advanced detector data, being composed of two very heavy stellar mass black holes, one of which might lie in the pair instability mass gap (see §5.1). Its formation pathway is not certain, but it might be the result of previous-generation black hole mergers.<sup>386</sup>

We would like our 3G network to be able to characterize similar sources with equal or higher precision, at high redshifts, from 4 to 10. Quantitatively, this requires a  $1\sigma$  uncertainty on the estimation of the source-frame chirp mass of  $\sim 10\%$  or better, and a  $1\sigma$  uncertainty on the estimation of the redshift of  $\sim 20\%$  or better.

We find that at least two 3G detectors are needed. For example, a network of two 20 km CEs (both compact-binary-optimized) will provide access to  $\sim 1100$  viable sources per year. Networks which can more precisely resolve the two polarizations of gravitational-wave signals can yield significantly higher numbers of sources that satisfy our criterion. An Einstein Telescope and a 40 km compact-binary-optimized Cosmic Explorer would detect  $\sim 3000$  viable sources per year, while the best network we consider (ET, CE South and two 40 km compact-binary-optimized CEs, i.e. ET plus three CE detectors) would yield nearly 10000 sources per year.

In Table 7.3 we mark in yellow networks that can detect at least 50 viable sources per year, and in light (dark) green networks that give access to at least 500 (2000) viable sources per year. Details are available in a technical note.<sup>383</sup>

**Formation and Evolution of Compact Objects** While the extremely high redshift universe will teach us about primordial black holes and black holes from the first generation of stars, most of the black holes in the universe are produced and merge at redshifts smaller than 4. To characterize the evolution and formation channels of these black holes one needs a large number of black hole binaries with precise measurement of redshifts and intrinsic parameters. The figure of merit we use is the number of detected sources whose source-frame chirp mass is measured to a  $1\sigma$  uncertainty of 10 % or less, and whose redshift is measured to a  $1\sigma$  uncertainty of 5 % or less. However, we only consider sources up to redshift of 4.

As one might expect, even networks without a Cosmic Explorer can yield some viable sources per year, for example a network of 3 Voyager detectors can detect  $\sim 230$  viable sources per year. While a single 40 km Cosmic Explorer with 2G detectors can find  $\sim 3000$  viable sources per year, that number becomes 15000 if two 20 km CEs are used. This highlights that when the BBHs of

interest are at redshifts of few, instead of  $> 10$ , having two 20 km CE detectors is more beneficial than having a single larger detector. In turn this is due to the superior polarization resolving power of larger networks. The same pattern is observed even when ET is included. A network of ET and a 40 km CE finds 27 000 sources per year, while a network of ET and two 20 km CEs finds 36 000. Adding a CE South increases the number of viable sources by less than 10 %.

In Table 7.3 we mark in yellow networks that can yield at least 250 viable sources per year, and in light (dark) green networks that give access to at least 2500 (25 000) viable sources per year. Details are available in a technical note.<sup>383</sup>

### 7.2.3 Dynamics of Dense Matter

**Neutron Star Structure and Composition** Cosmic Explorer’s ability to probe the structure and composition of neutron star matter is tied to the precision with which the 3G detector network can measure masses and tidal deformabilities from inspiral gravitational waves. In order to achieve a milestone in our knowledge of the neutron-star equation of state at zero temperature, masses and tidal deformabilities must be measured precisely enough to constrain the stellar radius to within 0.1 km across the full neutron-star mass spectrum. As the measurability of these parameters is essentially dictated by the inspiral SNR, this will require hundreds of observations of loud binary neutron star mergers. Adopting an SNR of 100 as the threshold above which we expect an informative tidal signature in the measured waveform, we assess the relative performance of different Cosmic Explorer configurations and networks for this science goal by comparing the yearly number of loud binary neutron star mergers they detect.

The cumulative number of binary neutron star detections per year with  $\text{SNR} > 100$  is plotted as a function of redshift in the top left panel of Fig. 7.4 for the different networks; the redshift horizon for detection of these loud sources is between  $z = 0.1$  and  $0.4$ , depending on the network. For this science goal, the primary driver of relative performance is the number of 40 km Cosmic Explorer detectors in the network: all else being equal, a 40 km Cosmic Explorer clearly outperforms a 20 km one for this metric. For instance, a single 40 km Cosmic Explorer will observe  $\sim 80$  binary neutron star mergers per year with SNR in excess of 100 when embedded in a 2G background network, compared to  $\sim 30$  for a single 20 km detector. Similarly, a 2G network augmented with two 40 km Cosmic Explorers can observe five times as many loud binary neutron star mergers as a single 40 km detector, and four times as many as two inspiral-optimized 20 km detectors. (Optimization for the postmerger signal is detrimental to this science goal, as a postmerger-optimized 20 km Cosmic Explorer detects only about half as many loud binary neutron star mergers as the inspiral-optimized one.) The performance of a heterogeneous 40 km-20 km Cosmic Explorer network is intermediate between the 40 km-40 km and 20 km-20 km pairs. The addition of a third 3G detector to the network — whether ET, or a 20 km Cosmic Explorer South facility — boosts the detection rate significantly: two 40 km Cosmic Explorers plus ET will detect  $\sim 600$  loud binary neutron star mergers per year, while even two 20 km Cosmic Explorers plus ET will capture in excess of 100 such mergers per year.

Hence, the return on this science goal can be maximized with two 40 km Cosmic Explorer

detectors. The rate of loud binary neutron star merger detections would be enhanced by the presence of ET or Cosmic Explorer South in the network, but the science target could still be fully achieved with two 40 km detectors (or, indeed, one 40 km detector and one 20 km detector) in a 2G background network. A single Cosmic Explorer detector of either length is also a viable choice, provided the global detector network includes ET; without ET, however, a single 20 km Cosmic Explorer would fail to deliver most of this science on its own. To discretize the performance assessment, in Table 7.3 we mark in light (dark) green networks that are expected to detect at least 50 (200) binary neutron star inspirals with signal-to-noise ratio above 100 per year. Networks marked in yellow meet this inspiral signal-to-noise ratio criterion at a rate of 1–50 per year.

**New Phases in Quantum Chromodynamics** Cosmic Explorer’s capacity to map the phase structure of quantum chromodynamics with neutron-star merger observations will depend on the 3G detector network’s sensitivity to the postmerger signal. In order to break new ground in our understanding of the equation of state in the finite-temperature regime, postmerger gravitational waves must be captured above a signal-to-noise threshold of 8 for several neutron-star mergers, so as to permit measurements of the dominant postmerger frequency.

In contrast to the inspiral signal, the postmerger signal is better captured by a 20 km Cosmic Explorer detector than a 40 km detector because it can be tuned for increased sensitivity in the relevant kilohertz frequency range. A postmerger-optimized 20 km detector will make 60–70 postmerger observations per year, whether operating in a 2G background network or with Einstein Telescope. A single 40 km Cosmic Explorer in a 2G background network would likely miss half of those signals. The optimal performance is achieved when pairing the 20 km postmerger-optimized Cosmic Explorer with a second Cosmic Explorer detector of either 20 km or 40 km; we can then expect ~110 postmerger detections (~140 if Einstein Telescope is also in the network) per year. Although the trade study shows that a network of two 40 km Cosmic Explorer detectors may nominally return ~70 postmerger observations per year, such a network has a greater risk of missing the postmerger signal altogether because its high-frequency sensitivity is not tunable and the precise value of the dominant postmerger frequency depends on the uncertain neutron star equation of state.

In Table 7.3 we mark in light (dark) green networks that are expected to detect at least 50 (100) postmerger signals per year. Networks marked in yellow are expected to detect more than one postmerger signal per year.

**Chemical Evolution of the Universe** The evolution of heavy elements in the universe can be traced by observing hundreds of neutron-star mergers out to cosmological distances. The complete picture will be built up from multimessenger observations of the sources, particularly prompt electromagnetic observations over the entire spectrum accessible to ground- and space-based telescopes. The key to rapid electromagnetic follow-up is precise localization of the sources, preferably before merger. Since the signal can last for hours in the sensitivity window of Cosmic Explorer if it is loud enough, it will in many cases be possible to provide alerts about

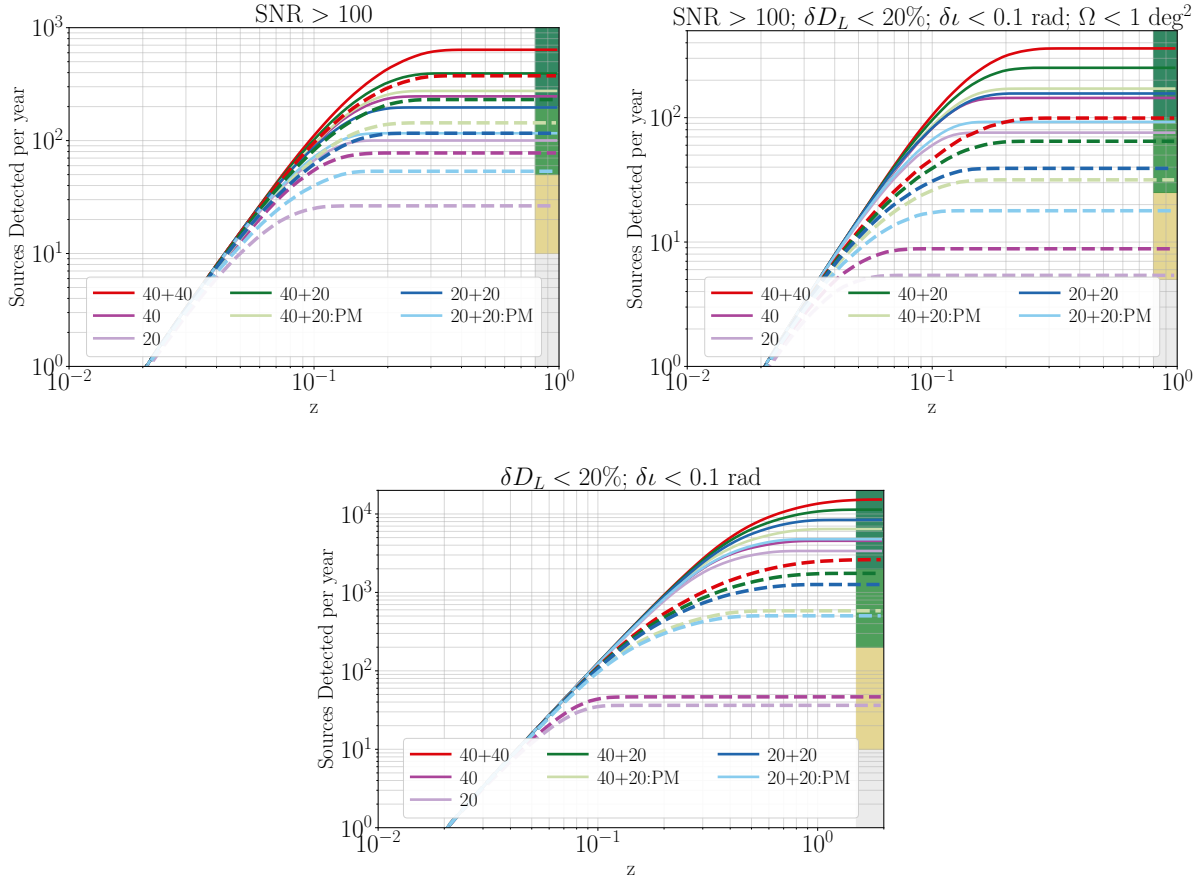


Figure 7.4: Cumulative number of detected BNS mergers satisfying criteria relevant to the Dynamics of Dense Matter science goals as a function of redshift, after one year of observation by different CE networks. Dashed curves refer to a 2G background network, while solid curves include ET in the network. A network’s ability to achieve a given science goal is assessed based on the cumulative number of detections across all redshifts, with the colors in Table 7.3 corresponding to the colored bins shown along the right edge of the plot. *Top left:* BNS mergers detected with SNR above 100, a threshold for an informative tidal signature in the signal. Networks that detect 50 (respectively, 200) such mergers per year can achieve (ensure the best return on) the Neutron Star Structure and Composition science goal. *Top right:* Subset of the BNS mergers with SNR above 100 that are localized to within 1 deg<sup>2</sup> on the sky and 20 % uncertainty in distance, while having their inclination  $\iota$  constrained to better than  $\pm 0.1$  in  $\cos \iota$ ; these criteria allow for early warning of the merger, targeted electromagnetic follow-up and the breaking of distance and inclination degeneracies in emission models. Networks that capture 25 (respectively, 100) mergers per year according to these criteria can achieve (ensure the best return on) the Chemical Evolution of the Universe science goal. Virtually all of the sources satisfying the SNR criterion are detected within a redshift of  $z = 0.5$ ; sources satisfying only the sky area and inclination criteria can be detected out to  $z \approx 2$ . *Bottom:* BNS mergers with distance measured to within 20 % and inclination to within  $\pm 0.1$  in  $\cos \iota$ , such that they track the sources’ redshift evolution out to  $z \approx 2$  and break degeneracies in electromagnetic emission models. Networks that make 200 (2000) such detections per year can achieve (ensure the best return on) the Gamma-Ray Burst Jet Engine science goal.



an imminent merger several minutes ahead of time. Electromagnetic telescopes can then slew to source and observe the prompt emission of electromagnetic waves in the aftermath of the merger. Additionally, a precise measurement of the binary's inclination angle is important for determining whether it is being viewed face-on or edge-on. If detected, postmerger gravitational waves would also help connect the merger remnant's properties to emission models. To evaluate the ability of the various detector networks to achieve this science goal, we examine the yearly number of binary neutron star detections satisfying a combination of metrics: SNR greater than 100, for early warning of the merger; a sky localization of less than  $1 \text{ deg}^2$ , to enable identification of electromagnetic counterparts; and a distance uncertainty of less than 20 % and an inclination uncertainty of less than  $\pm 0.1$  in  $\cos i$ , to break degeneracies in emission models.

The yearly number of SNR  $> 100$  binary neutron star mergers localized to  $1 \text{ deg}^2$  in sky area and 20 % in distance, with a  $\pm 0.1$  measurement of inclination  $\cos i$ , is plotted in the top right panel of Fig. 7.4 for the different networks. A key factor governing a network's performance is the number of 3G detectors it includes: those with a single one detect fewer than 10 signals satisfying the combined criteria per year, while those with two or three can respectively detect up to a hundred or several hundred per year. Because of ET's especially good low-frequency sensitivity, networks that include ET are particularly advantageous for localizing sources on the sky. Given that a single 40 km Cosmic Explorer detects loud, well-localized mergers at about twice the rate of a 20 km detector, all else being equal, networks that include 40 km detectors outperform their 20 km counterparts. Thus, for example, a single 40 km Cosmic Explorer paired with ET performs as well as the three-detector network consisting of two 20 km Cosmic Explorers plus ET, making  $\sim 150$  such detections per year. For comparison, two 40 km Cosmic Explorers embedded in a 2G background network detect  $\sim 100$  equivalent mergers per year.

The signals loud enough to give early warning of the merger while satisfying the distance, inclination and sky area constraints will only be detected out to  $z \approx 0.3$ . However, mergers with lower SNR can be detected out to  $z \approx 2$  while meeting the other criteria. The quantitative performance of the various networks without the early warning criterion is documented in,<sup>387</sup> but their relative performance is essentially the same as in the lower panel of Fig. 7.4, which omits both the SNR and sky area targets. When emphasizing the reach of well-localized neutron-star observations out to cosmological distances, rather than the prospect of early warning, the most important factor is simply the number of 3G detectors in the network.

In terms of distance measurements, inclination constraints and sky localization, the post-merger-optimized 20 km detectors are less effective than their inspiral-optimized counterparts. On the other hand, the inclusion of a postmerger-optimized detector in the network increases the odds of associating postmerger gravitational waves with inspiral and electromagnetic observations. This would help relate the postmerger dynamics, and the lifetime of the remnant in particular, to the features of the electromagnetic emission. For this science goal, the trade-off in converting one inspiral-optimized 20 km Cosmic Explorer to a postmerger-optimized one is roughly a factor of two reduction in the number of detections satisfying the combined criteria.

Consequently, the optimal detector network for this science goal would involve two 40 km Cosmic Explorer detectors, preferably with a third 3G detector such as Einstein Telescope.

However, any network with three 3G detectors has the ability to fully achieve the science goal (as does the ET plus 40 km Cosmic Explorer network). Choosing one of the three detectors to be a 20 km postmerger-optimized Cosmic Explorer increases the prospect of joint electromagnetic, inspiral and postmerger gravitational wave observations, and is a viable option as the overall network performance is enough to compensate for the mild loss in localization and early warning capabilities. A single Cosmic Explorer detector could not achieve this science goal on its own. In Table 7.3, networks colored in light (dark) green will make detections satisfying the joint criteria at least 25 (100) times per year. Yellow networks cannot achieve these criteria at a similar rate, but nonetheless detect at least 5 such sources per year.

**Gamma-Ray Burst Jet Engine** The properties of the gamma-ray burst ensuing after a neutron star merger are largely determined by the remnant, which forms the central engine for launching and driving relativistic jets. To make associations between gamma-ray bursts and gravitational-wave events, a 3G detector network will need to capture a large fraction of the population of merging neutron stars out to the horizon  $z \sim 2$  of future gamma-ray observatories, while measuring the distance to these mergers precisely, so as to provide a reasonably complete gravitational-wave catalog for identifying counterparts. Additionally, to break degeneracies in emission models, it is crucial to measure the source inclination precisely. Postmerger gravitational-wave observations are also desirable for this science goal, as they can reveal the nature of the remnant and help establish its connection to the physics of the jets. To compare the different Cosmic Explorer configurations and networks for this science goal, we investigate their ability to detect binary neutron star mergers satisfying distance and inclination criteria out to cosmological distances. As in the previous subsection, we target 20 %-level uncertainty in the distance measurement, and  $\pm 0.1$  uncertainty in the measurement of  $\cos i$  for the inclination.

In Fig. 7.4, the lower panel plots the cumulative number of binary neutron star mergers whose distance is measured to 20 % and whose inclination is constrained to  $\pm 0.1$  in  $\cos i$  as a function of redshift for the networks we consider. The performance for this science goal is most sensitive to the background network: all of the networks that include ET outperform those that rely on a 2G background. For example, a single 20 km Cosmic Explorer operating in tandem with ET will observe  $\sim 3000$  mergers per year satisfying the distance and inclination criteria, compared to  $\sim 40$  per year operating alone. The best-performing network with a 2G background, two 40 km Cosmic Explorers, will make  $\sim 2500$  such observations per year. The number of 3G detectors in the network also controls the redshift horizon out to which the sources' distance and inclination can be constrained precisely: for networks with two (respectively, three) 3G detectors, it is  $z \sim 1$  (2), compared to  $z \sim 0.1$  for a single Cosmic Explorer detector. Within a given background network, two Cosmic Explorer detectors are better than one, and the 40 km configuration outperforms the 20 km one for distance and inclination measurements, all else being equal.

While a network consisting of two 40 km Cosmic Explorer detectors plus ET would detect the greatest number of sources ( $\sim 1.5 \times 10^4$  per year) satisfying the distance and inclination

constraints, a network that includes a postmerger-optimized 20 km detector would have a better chance of observing postmerger gravitational waves in conjunction with a fraction of the gamma-ray bursts. This can be done without drastically compromising the distance and inclination measurement precision. For example, substituting a postmerger-optimized 20 km Cosmic Explorer in place of one of the 40 km detectors will still result in ~6000 observations with precisely determined distances and inclinations per year.

Thus, from the point of view of supplying a complete catalog of gravitational-wave observations to associate with gamma-ray bursts, two 40 km Cosmic Explorers operating in conjunction with ET or Cosmic Explorer South is the optimal network for this science goal. However, a heterogeneous Cosmic Explorer network involving one postmerger-optimized 20 km detector is an advantageous choice because of the prospect for joint postmerger, inspiral and gamma-ray observations. A global network involving at least two (and preferably three) 3G detectors is critical for this science goal: a single Cosmic Explorer cannot achieve the required coverage in redshift with a 2G background network. In Table 7.3, the networks colored light (dark) green will make 200 (2000) yearly detections of binary neutron star mergers that are well-constrained in distance and inclination out to cosmological distances. The networks colored yellow will make between 1 and 200 such detections per year, all of which are restricted to the local universe.

#### 7.2.4 Extreme Gravity and Fundamental Physics

**The Nature of Strong Gravity** Gravitational-wave observations of merging black holes encode the nature of the strongest gravity in the universe — the gravity near the horizon of a stellar-mass black hole. Observations of merging black holes with current-generation detectors are giving us a first look at the nature and behavior of strong gravity. So far, all of these observations are consistent with general relativity’s picture of two (initially Kerr) black holes merging into a remnant Kerr black hole, within the experimental noise and theoretical uncertainty of the form of the emitted gravitational waves.

But evidence of new, revolutionary physics has often been first evident in small deviations from conventional expectations. How much we can learn about strong gravity from a gravitational-wave observation thus depends on the strength of the gravitational-wave signal compared to detector noise. The higher the signal-to-noise ratio of an observation, the clearer is the resulting view of the underlying gravitational physics, and the greater potential for discovery.

A Cosmic Explorer detector will give us a solid opportunity far beyond the first look that even the best current-generation detector network could give. For instance, in each year of its operation, a single, 40 km, Cosmic Explorer detector would observe roughly 8 merging black holes that are approximately at least as close to Earth as GW150914 (redshift  $z < 0.1$ ), the loudest gravitational-wave observation from merging black holes so far, with half having signal-to-noise ratios greater than about 600 and the top 10 % having signal-to-noise ratios greater than 2700. In contrast, half the observations with a second-generation network using A+ (Voyager) technology would have a signal-to-noise ratio greater than about 70 (150), with the top 10 % of signals having signal-to-noise ratios greater than about 280 (610).

A 40 km Cosmic Explorer detector in a network including at least one other next-generation detector would be especially favorable for revealing the nature of strong gravity. In a network with three 3G detectors (two 40 km Cosmic Explorers and one Einstein Telescope), for instance, the top 10 % of binary black holes closer than  $z = 0.1$  would have signal-to-noise ratios greater than 4100. Also, including more than one next-generation interferometer enables better measurement of the gravitational waves' polarization, including any potential scalar or vector polarizations that would indicate physics beyond general relativity. A network of next-generation detectors that each have arm lengths no longer than 20 km would be almost as favorable but would not be quite as sensitive a probe of the nature of gravity, because the 20 km detector's sensitivity is not quite as good in the most sensitive frequency band.

**Unusual or Novel Compact Objects** Third-generation detectors have the potential to unmask novel objects, including objects potentially masquerading as black holes or neutron stars, by providing precise strain measurements that can be compared with theoretical predictions. Voyager would be capable of giving us a first look at rarer compact binaries, and it also has the potential to give a first look at novel compact objects, if they not only exist but are also sufficiently nearby to be in Voyager's range and sufficiently distinct from black holes and neutron stars that they do not require the signal-to-noise ratios that only detectors in next-generation observatories can achieve. Even a single next-generation observatory would give a much more solid picture of rare, conventional compact binaries: one Cosmic Explorer detector would observe all of the binary-black-hole mergers in the observable universe (about 100 000 observations per year) and would observe nearby mergers with very high signal-to-noise ratios, which corresponds to a greater opportunity to recognize an observation as being unusual.

Similar considerations as for probing the nature of strong gravity apply here: a Cosmic Explorer with 40 km instead of 20 km arms, as part of a network with more than one next-generation detector, would be especially favorable. The 40 km arm length would deliver the highest signal-to-noise ratios, which would enable us to better recognize unusual or novel compact binaries. More than one next-generation detector would be especially favorable for finding unusual or novel compact binaries, because they would increase our confidence in observations of faint unusual or novel compact binaries, and because they would provide polarization information not accessible to a single detector.

**Dark Matter and Dark Energy** The strength that any signature that dark matter or dark energy might have on gravitational-wave observations is unknown. Current-generation detectors have so far not found signatures of dark matter, and they lack the cosmic reach to provide insight into dark energy through cosmic variations in the observed population of compact objects.

To look for such potential effects, a 40 km Cosmic Explorer as part of a network with multiple next-generation detectors would be most favorable. A 40 km detector would have the highest sensitivity, which would have the best potential to reveal subtle signatures of dark matter, dark energy, or quantum gravity. And a network with more than one next-generation detector will

be necessary to observe some of the proposed effects, such as additional gravitational-wave polarizations or standard sirens that rely on multimessenger observations. While some of the proposed effects, such as gravitational-wave echoes, would not necessarily require a network with more than one next-generation detector, such a network would still increase our confidence in detecting faint imprints that dark matter, dark energy, and quantum gravity might have on gravitational-wave observations.



## 8 Technical Overview and Design Choices

The LIGO and Virgo instruments have opened a new window on the universe, but they are, like Galileo’s first telescope, just sensitive enough to observe the brightest sources. Today the Advanced LIGO detectors see signals roughly weekly; when the “A+” upgrade is mature in 2025, it will deliver roughly ten detections per week. The key science questions presented in §3 are only answerable by making observations with significantly higher fidelity over a wider frequency band, and by observing more distant sources. As described in §6, this requires new facilities with longer baselines and detectors with an order of magnitude greater sensitivity in the audio frequency band. This section provides a technical overview of the Cosmic Explorer observatory that can deliver that sensitivity, including the sites, infrastructure, and vacuum systems. It also outlines the key technologies that will require research and development to enable the CE science goals. Finally, the key drivers of project costs are discussed.

### 8.1 Reference Detector Concept

The Cosmic Explorer reference detector concept is a dual-recycled Fabry–Pérot Michelson interferometer (DRFPMI) scaled up to use 40 km or 20 km long arms (see Box 7.1). The longer arm length will increase the amplitude of the observed signals with effectively no increase in the noise. Although there are areas of detector technology where improvements will lead to increases in the sensitivity and bandwidth of the instrument relative to the existing LIGO detectors, the dominant improvement will come from the order-of-magnitude increase in length.

The interferometers installed in the Cosmic Explorer observatories will evolve as the technologies and science evolve. The first two decades of Cosmic Explorer evolution are sketched Fig. 11.1. Like LIGO and Advanced LIGO, CE’s sensitivity is expected to improve with time thanks to technology upgrades and commissioning effort. Parts of the CE nominal design may not be installed before the CE observatories begin collecting data. These “planned upgrades”, to be installed as the technology becomes available, include: low-loss readout of high-fidelity squeezed states of light (§8.3.5), adding seismometer arrays to subtract fluctuations in the local gravity (§8.3.9), and improved sensors for seismic isolation relative to what is expected to be available at the time of construction (§8.3.8).

To minimize the required technical development, the initial CE detectors will use the Advanced LIGO detector design, including its A+ upgrades, scaled as needed in size, along with some advances to improve the low frequency sensitivity. This provides a straightforward approach to significant improvement using tested technology with relatively low risk. The planned upgrades

will then proceed when possible given availability of new technologies and when maximally beneficial to the scientific output of the observatories. That is, the upgrades can all be performed in parallel at one or both observatories, or sequentially at one observatory at a time to avoid long downtimes.

A second technology capable of achieving (and possibly surpassing) the target sensitivity of CE has also been identified. This approach uses technology currently being developed for the LIGO Voyager detector, consisting of a 2  $\mu\text{m}$  laser and cryogenic silicon test masses, and will only be required if a major problem is encountered with scaling up current technology. Research is ongoing to understand if the 2  $\mu\text{m}$  design also offers a path to higher laser power and thus sensitivity beyond the CE target (§8.4).

### 8.1.1 Overview

A simple Michelson interferometer measures the strain of a passing gravitational wave by measuring the difference in time for light to traverse two more-or-less perpendicular arms, at the end of which are mirrors serving as test masses. So that these test masses are free from external horizontal forces in the frequency band of interest, they are suspended from pendulums (which also isolate them from seismic noise as discussed further below). The relative phase accumulated by the light in each arm is modulated by a passing gravitational wave and the ensuing power modulation at the antisymmetric port is measured with photodetectors. Practically, the common mode rejection of a Michelson interferometer provides some suppression of laser frequency and intensity noises.

The DRFPMI, shown in Fig. 8.1, improves on the simple Michelson interferometer in several ways. First, input test masses are added to each arm to make Fabry–Pérot cavities. This increases the power stored in the arms, which decreases the quantum shot noise. Second, a “power recycling mirror” added to the symmetric port further increases the power stored in the interferometer and provides passive filtering of laser noise. Finally, a “signal extraction mirror” added to the antisymmetric port forms a “signal extraction cavity.” The bandwidth of the interferometer can be tuned to enhance the sensitivity relevant for a particular science case by simply changing the reflectivity of this mirror. For example, the sensitivity to post-merger physics can be improved as shown in Fig. 7.1, though other tunings can improve the low frequency sensitivity instead.

The other major subsystems of the interferometer are described in the following sections. Figure 8.1 shows this reference concept including these major subsystems and Table 8.1 presents the key design parameters. The estimated spectral sensitivity of Cosmic Explorer and the limitations imposed by the fundamental noise sources are shown in Fig. 8.2.

### 8.1.2 Quantum Noise Reduction

Quantum vacuum fluctuations entering the antisymmetric port of the interferometer will be the dominant limit to the sensitivity of Cosmic Explorer above 20 Hz. Quantum mechanics requires

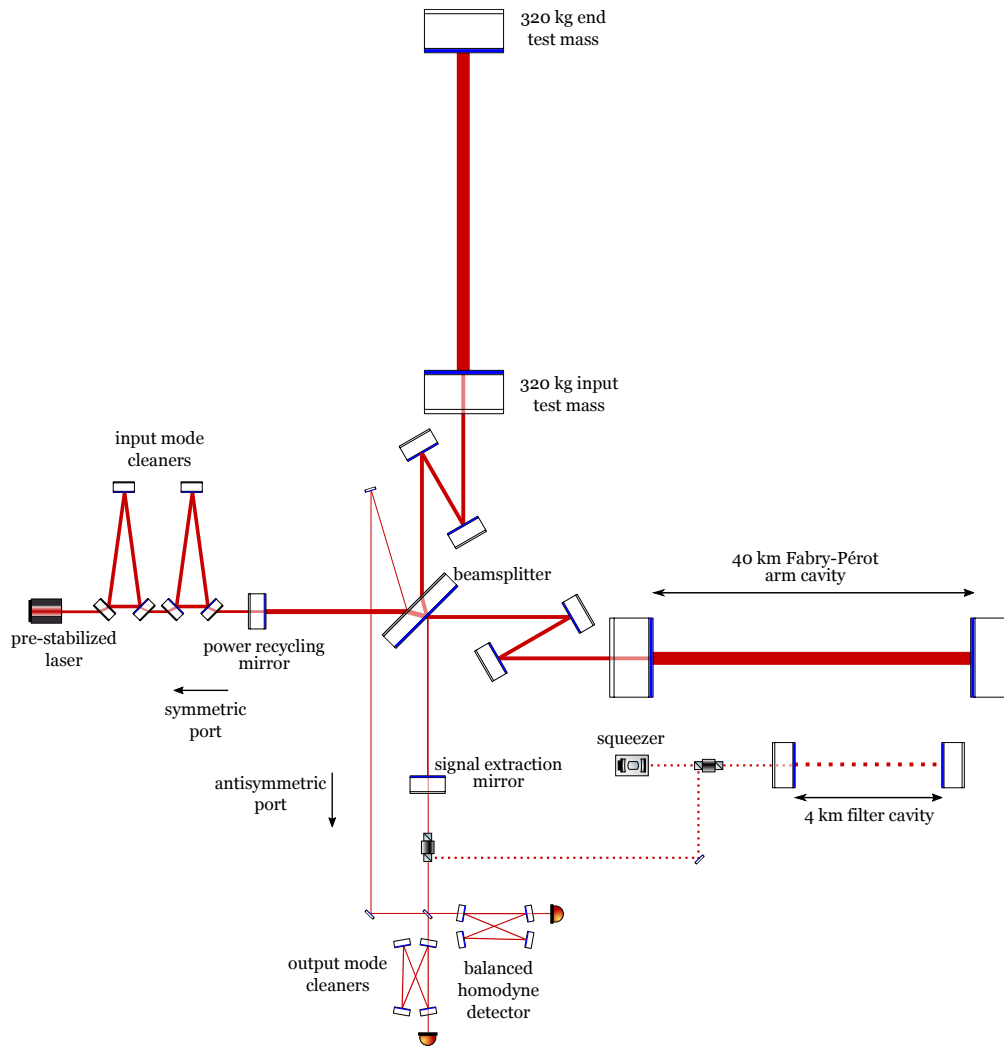


Figure 8.1: Simplified optical layout of the Cosmic Explorer reference detector concept for the 40 km implementation. The input and end test masses form the two arm cavities which, together with the beamsplitter, power recycling mirror, and signal extraction mirror, comprise the core of the dual-recycled Fabry–Pérot Michelson interferometer as described in §8.1.1. As described in §8.1.5, the light carrying the gravitational wave signal is spatially filtered and read out from the antisymmetric port by a balanced homodyne detector comprised of two photodiodes and output mode cleaners; a high power laser is injected into the symmetric port of the interferometer after passing through two input mode cleaners which assist in producing a frequency and intensity stabilized beam with a spatially clean mode. The squeezer generates squeezed vacuum states which are reflected off of a filter cavity and injected into the antisymmetric port to provide broadband quantum noise reduction as described in §8.1.2. The beamsplitter is shown with the high-reflective surface facing the antisymmetric port rather than the laser, unlike current detectors, to minimize loss in the signal extraction cavity, but careful analysis of thermal effects is needed before finalizing the design.

every mode of the electromagnetic field to have a minimum zero-point energy. These vacuum fluctuations enter any open port of the optical system.<sup>a</sup> Radiation pressure noise dominates

<sup>a</sup>Vacuum fluctuations entering the symmetric port contribute noise to the common mode, rather than the differential mode which carries the gravitational wave signal.

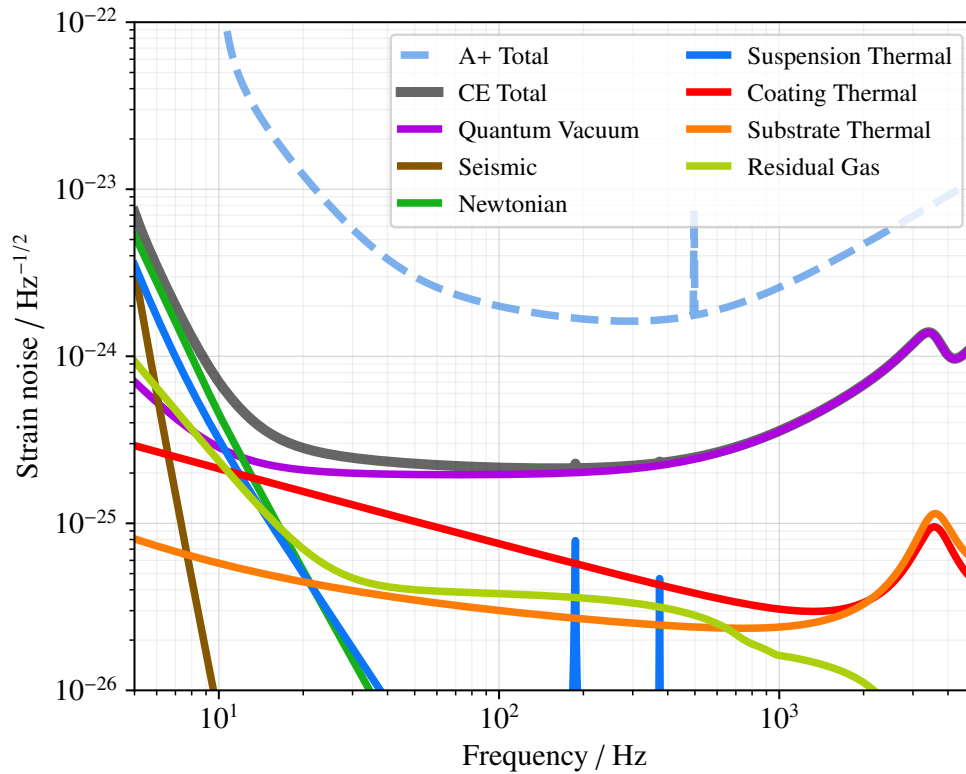


Figure 8.2: Estimated spectral sensitivity (solid black) of Cosmic Explorer and the known fundamental sources of noise that contribute to this total (colored curves). The design sensitivity of LIGO A+ is also shown in dashed blue.

at low frequencies where fluctuations in the vacuum field amplitude quadrature beat with the main laser field to produce a fluctuating radiation pressure force on the mirrors. At higher frequencies, it is the beating of the vacuum field fluctuations in the orthogonal phase quadrature with the main laser field, shot noise,<sup>b</sup> that directly limits the accuracy with which the phase can be measured.<sup>388–390</sup>

While Heisenberg’s uncertainty relation dictates the fundamental limit below which the vacuum fluctuations cannot be reduced, fluctuations in one quadrature can be reduced at the expense of increasing the fluctuations in the orthogonal quadrature, leading to “squeezed states.”<sup>391</sup> As with Advanced LIGO,<sup>392</sup> Cosmic Explorer will use a nonlinear crystal pumped with a laser at twice the frequency of the main laser, known as a degenerate optical parametric amplifier, to produce the correlations necessary to generate such squeezed vacuum states and inject them into the antisymmetric port. In this way, radiation pressure noise can be reduced by injecting states with decreased uncertainty in the amplitude quadrature, at the expense of increased phase uncertainty and shot noise. Similarly, shot noise can be reduced by injecting

<sup>b</sup>This shot noise arising from the beating of the vacuum fluctuations entering the antisymmetric port with the main laser is a truly intrinsic phase noise of the optomechanical system. It is distinct from the related technical noise, also referred to as shot noise, where phase noise is produced by excess light incident on a photodiode beating with vacuum fluctuations.

	Quantity	Units	LIGO A+	CE	CE (2 $\mu\text{m}$ )
	Arm length	km	4	40	40
	Laser wavelength	$\mu\text{m}$	1	1	2
	Arm power	MW	0.8	1.5	3
	Squeezed light	dB	6	10	10
	Susp. point at 1 Hz	$\text{pm}/\sqrt{\text{Hz}}$	10	0.1	0.1
Test masses	Material		Silica	Silica	Silicon
	Mass	kg	40	320	320
	Temperature	K	293	293	123
Suspensions	Total length	m	1.6	4	4
	Total mass	kg	120	1500	1500
	Final stage blade		No	Yes	Yes
Newtonian noise	Rayleigh wave suppr.	dB	0	20	20
	Body wave suppr.	dB	0	10	10
Optical loss	Arm cavity (round trip)	ppm	75	40	40
	SEC (round trip)	ppm	5000	500	500
	BNS horizon redshift		0.19	8.3	11.7
	BBH horizon redshift		2.7	41	41
	BNS SNR, $z = 0.01$		75	1260	1460
	BNS warning, $z = 0.01$	min	4	103	103

Table 8.1: Key design parameters and astrophysical performance measures for the LIGO A+ and 40 km Cosmic Explorer detectors. The astrophysical performance measures assume a  $1.4\text{--}1.4M_{\odot}$  binary-neutron-star (BNS) system and a  $30\text{--}30M_{\odot}$  binary-black-hole (BBH) system, both optimally oriented. “BNS warning” is the time before merger at which the event has accumulated a signal-to-noise ratio (SNR) of 8.

states with decreased uncertainty in the phase quadrature at the expense of increased amplitude fluctuations and radiation pressure noise. However, since radiation pressure dominates at low frequencies and shot noise dominates at high frequencies, injecting squeezed vacuum with a fixed ratio of amplitude to phase uncertainty necessitates a trade-off between reducing quantum noise at high and low frequencies.

The frequency dependence required to achieve broadband quantum noise reduction can be achieved by reflecting the squeezed vacuum state generated by the parametric amplifier off of an extra optical cavity detuned from resonance, known as a filter cavity, before it is injected into the interferometer.<sup>389,393,394</sup> Cosmic Explorer will use such a 4 km long filter cavity to produce a frequency dependent squeezed state that rotates from amplitude squeezing at low frequencies to phase squeezing at high frequencies at the appropriate rate to achieve 10 dB of broadband quantum noise reduction. The net noise reduction depends on the optical losses in the system, which are expected to be reduced as upgrades are made to the detector.



### 8.1.3 Optics and Coatings

Cosmic Explorer will use large 320 kg test masses made into highly reflective mirrors through the use of thin-film coatings consisting of alternating layers of high and low refractive-index materials. The more massive test masses serve to reduce quantum radiation pressure noise and, as a practical matter, they must be wide enough to accommodate the large diameter beams of a nearly diffraction limited 40 km long arm cavity.

The CE test masses will use the LIGO A+ technology, scaled up for their larger size. The substrate is fused silica, chosen for its low mechanical loss and correspondingly low thermal noise at room temperature, and low optical absorption at 1  $\mu\text{m}$ . The low refractive-index layers of the coatings will be silica; the high index layers are yet to be determined. These coatings must have low mechanical loss to reduce their thermal noise, yet this thermal noise is still non-negligible below  $\sim 60$  Hz. The desire to reduce this noise is one factor motivating the use of cryogenics as an alternative technology as discussed in §8.1.8.

### 8.1.4 Seismic Isolation and Suspensions

Each of the four Cosmic Explorer test masses will be suspended by a quadruple pendulum to isolate them from seismic disturbances.<sup>395</sup> The suspensions provide passive  $1/f^8$  filtering of seismic noise above their mechanical resonance frequencies. The suspensions themselves will be mounted on inertial seismic isolation systems which provide additional active and passive suppression of seismic noise.<sup>396</sup>

To minimize thermal noise, the final suspension stage is fabricated monolithically from fused silica, with the test mass suspended from the penultimate mass by fused silica fibers.<sup>395</sup> The top two masses of the suspensions are steel and are suspended by steel wires.

To reduce the vertical suspension resonances, and thus both the vertical seismic noise and thermal noise which couple into the arm length due to the Earth's curvature, each of the first three stages is suspended from steel blade springs attached to the stage above. Unlike the LIGO suspensions, however, a set of silica blade springs is added for the final stage instead of bonding the suspension fibers directly to the penultimate mass.

The inertial seismic isolation systems are similar to those of Advanced LIGO<sup>396</sup> but with improved inertial and position sensors. It is assumed that incremental improvements will allow Cosmic Explorer to initially achieve a threefold improvement over Advanced LIGO at 10 Hz and a tenfold improvement at 1 Hz. Novel six-dimensional inertial isolators with optical readout will be used to achieve an additional threefold improvement at 10 Hz and tenfold improvement at 1 Hz to achieve the final Cosmic Explorer sensitivity. The status of this technology is described in §8.3.8.

### 8.1.5 Input and Output

The laser source for Cosmic Explorer is similar to that of LIGO and begins with a 1  $\mu\text{m}$ , 1–2 W seed laser. This is amplified by a multi-stage amplifier to produce the full input power of up to 200 W. Together with some laser intensity and frequency stabilization and some cleaning of the spatial mode of the laser, this comprises the pre-stabilized laser.<sup>397</sup> The light from the pre-stabilized laser is then sent through two triangular cavities known as input mode cleaners to provide further laser frequency stabilization and cleaning of the spatial mode. The frequency stabilization scheme used in LIGO relies on a single mode cleaner, but the longer arms of Cosmic Explorer require a new control scheme which, while possible to implement with a single mode cleaner, greatly benefits from two.<sup>398</sup> The light exiting these mode cleaners, required to be  $\sim 140\text{W}$  to reach the goal of 1.5 MW arm power with the expected optical loss, is then injected into the main interferometer at the back of the power recycling mirror.

The gravitational wave signal is imprinted on the light exiting the interferometer from the signal extraction mirror. This signal is measured using a balanced homodyne detector with a local oscillator derived from a few hundred milliwatts of light extracted from the beamsplitter. The spatial mode and frequency content of the signal and local oscillator are cleaned by two bow-tie cavities known as output mode cleaners before being detected with high quantum-efficiency photodiodes.

### 8.1.6 Newtonian Noise Mitigation

Fluctuations in the gravitational attraction between the test masses and the environment, known as “Newtonian noise”,<sup>371</sup> are a significant low frequency noise source for Cosmic Explorer.

Seismic waves are one source of Newtonian noise. Cosmic Explorer will initially suppress noise from Rayleigh surface waves by a factor of two in amplitude. After planned upgrades, it will suppress Rayleigh waves by a factor of ten and will additionally suppress the Newtonian noise from body waves by a factor of three. A combination of several techniques may be employed to achieve these goals. One technique is to use seismometer arrays to estimate the seismic field near the test masses and to subtract its effects from the gravitational wave strain data.<sup>399</sup> Another approach is to directly reduce the coupling of seismic waves to the test mass by modifying the density of the material below each mass<sup>400</sup> or intentionally deflecting or dissipating them with architected materials or seismic metamaterials.<sup>401–406</sup> These techniques are discussed in detail in §8.3.9.

Cosmic Explorer is also affected by Newtonian noise due to density fluctuations in the atmosphere at infrasonic frequencies. The reference concept does not include any suppression of Newtonian infrasound noise, since it is unknown if the technology needed to do so would be mature by the 2040s. This is the dominant source of Newtonian noise after the seismic contributions have been suppressed.

### 8.1.7 Computing and Controls

Holding the detector at its stable, astrophysically sensitive operating point requires feedback control on a large number of degrees of freedom, such as the relative distances and angles between the suspended optics. Additionally, bringing the detector to its operating point requires a multi-step locking scheme. Similar to LIGO,<sup>407</sup> Cosmic Explorer will use a hybrid digital and analog real-time data acquisition and controls system, along with automated supervision of the detector locking. The digital system will also provide near real time calibration and astronomical alerts.

Because of their susceptibility to environmental conditions and the time required for the locking process, current gravitational-wave interferometers have roughly 75 % availability; the CE designs will strive to improve upon this. The greatest improvement in observing time will likely come from reducing the time required to achieve lock, e.g., with a fully deterministic locking scheme and feed-forward thermal compensation, and from improving the instrument's robustness to environmental disturbances, particularly from high seismicity and wind.

### 8.1.8 2 $\mu\text{m}$ Cryogenic Silicon as an Alternative Technology

Since it is possible that a major problem prevents the LIGO A+ technology from achieving the Cosmic Explorer design sensitivity, and to retain the possibility of surpassing this goal in the future, it is prudent to continue research into the technology being developed for LIGO Voyager, namely cryogenic silicon test masses and a 2  $\mu\text{m}$  laser.

One concern for the nominal 1  $\mu\text{m}$  technology is potential roadblocks to achieving 1.5 MW power in the arm cavities. The presence of particulates in the test mass coatings that absorb the laser power and thermally deform the mirrors has been an obstacle to achieving the design power in Advanced LIGO.<sup>408</sup> While progress has been made in addressing this issue, which must also be solved for A+ to reach its sensitivity goal, it is not expected to be a significant issue for the cryogenic silicon technology due to the high thermal conductivity of silicon. Other thermal effects may also limit the achievable arm power for the 1  $\mu\text{m}$  technology. The power absorbed in the test mass coatings and substrates, for instance, creates both a thermoelastic deformation of the mirror surface and a thermally induced lens. Both effects produce wavefront distortions which must be corrected with adaptive optics.<sup>409</sup> While research is still needed into methods of doing so with the 2  $\mu\text{m}$  technology, the magnitude of these distortions should be smaller than in the 1  $\mu\text{m}$  technology.

Another motivation for research into the 2  $\mu\text{m}$  technology is the fact that coating Brownian noise is a non-negligible noise source from roughly 10 to 100 Hz for the 1  $\mu\text{m}$  technology. Even if the thermal effects associated with the 1  $\mu\text{m}$  technology are overcome and more power can be stored in the arm cavities, coating Brownian noise may prevent significant improvement beyond the current design. Brownian noise from promising coatings for the 2  $\mu\text{m}$  technology can be roughly a factor of 2.5 lower in comparison. Furthermore, while both technologies achieve similar performance with the long arms of Cosmic Explorer, the 1  $\mu\text{m}$  technology becomes less

attractive for arms significantly shorter than 20 km. If, however, the more speculative crystalline GaAs/AlGaAs coatings are used instead of the amorphous A+ coatings for the 1  $\mu\text{m}$  technology, both technologies would again have similar performance for shorter arm lengths.

## 8.2 Site and Facility

Several important factors must be considered when identifying sites suitable for hosting a Cosmic Explorer facility. The site must satisfy the requirements described in §8.2.1 in order to reach design sensitivity, and sites with favorable topography can significantly decrease the cost of civil engineering work needed to accommodate the beamtubes as is discussed in §8.5.1. Other site selection considerations are discussed in §8.5.3.

The Cosmic Explorer building design and construction can be based upon those used for LIGO, with future research into considerations such as aerodynamic building shapes, wind fences, and other vibration reduction engineering such as berms. Operating the existing LIGO observatories has taught us the importance of designing facilities that have more immunity to environmental noise. As much as possible, equipment and personnel that cause vibration, acoustic, infrasound, and electromagnetic disturbances should be located far from the most sensitive equipment, for example in out-buildings near to the corner and end stations. In addition to the buildings housing the CE detector infrastructure, CE will require laboratories, warehouses, mechanical and electrical workshops, and offices, as well as meeting spaces for users and visitors. These buildings should be close enough to allow access to the CE site, but far enough away that they do not significantly couple anthropogenic noise into the detector. Access roads will be needed, and access to rail would be advantageous, especially for delivery of the vacuum pipe.

### 8.2.1 Site and Facility Requirements

**Ambient seismicity** Ground motion directly impacts the sensitivity of Cosmic Explorer, including from seismically induced fluctuations in the local gravitational field. This gravitational influence on the detector test masses cannot be screened or shielded, though it can be partially ameliorated with data subtraction techniques, by altering the properties of the ground near the test masses, and by selecting a low-seismicity site. The current estimate of the Cosmic Explorer sensitivity assumes a Rayleigh-wave-dominated ground motion with amplitude  $1 (\mu\text{m}/\text{s}^2)/\sqrt{\text{Hz}}$ . Based on US seismic surveys, this ground acceleration target is not particularly onerous, and the overall seismicity at the site is likely to be dominated by local machinery above 5 Hz. A dedicated seismic survey for Cosmic Explorer must establish both the overall ground motion amplitude above 5 Hz, as well as the partitioning of the field into its bulk and surface wave components.

Additionally, experience from existing long-baseline laser interferometers shows that high seismicity negatively impacts the controllability of the instrument, leading to downtime and decreased sensitivity. It is therefore important to survey the ground motion down to 10 mHz to

understand the requirements on the seismic isolation system.

**Ambient infrasound** Acoustic waves also impact the Cosmic Explorer sensitivity by generating local gravity fluctuations. The Cosmic Explorer sensitivity model assumes an ambient acoustic spectrum of  $1 \text{ mPa}/\sqrt{\text{Hz}}$ , which is in line with the median spectrum from long-term global infrasound surveys. A dedicated infrasound survey for Cosmic Explorer must be careful to disentangle the effect of wind confusion noise.

**Geotechnical issues** Any potential site will require a geotechnical investigation to assess its suitability and to arrive at a precise cost estimate for the construction of a CE observatory. In addition to standard civil-engineering aspects, this assessment will need to evaluate the potential for seismic engineering as discussed in §8.3.9.

**Ambient environment** Long-term measurements of the environment are required to determine the variation in noise arising from the weather (for example, wind and thunderstorms) or from anthropogenic origins (such as cars and trains). Susceptibility to natural disasters such as flooding, earthquakes, or hurricanes must also be evaluated.

**Environmental stewardship** Throughout the construction of Cosmic Explorer very careful attention will be given to preserving the local environment — both its living ecosystems and its non-living components.

Possible alterations of the ecosystem might include interference with migratory or mating patterns, the extinction of local flora and fauna, or the introduction of damaging invasive species. Such problems can be caused by chemical or thermal pollution, negligent construction, or waste disposal practices. Therefore, a thorough environmental impact study will be necessary to identify, constrain, and remediate such effects. This will be done with the active participation of the local community as well as state and federal governing agencies.

While respect for the environment is essential throughout the lifetime of the facility, it is especially important during the initial construction phase and during facility decommissioning. During the operations phase, the potential for harm is smaller but still requires careful monitoring.

### 8.2.2 Vacuum System

As with all interferometric gravitational-wave detectors, ultrahigh vacuum (UHV) is necessary in Cosmic Explorer to reduce path-length fluctuation of the light traveling down the arms and to reduce mechanical damping on the detector's core optics. The vacuum system is additionally responsible for shielding the interferometer from acoustic noise and thermal noise from the atmosphere. While the vacuum techniques developed for the LIGO detectors are adequate



Beamtube diameter	48 in (122 cm)
Beamtube thickness	$\frac{1}{2}$ in (13 mm)
Beamtube material	mild steel
Beamtube BRDF	$10^{-3} \text{ sr}^{-1}$
Hard close gate valves	10, partitioning into 10 km sections
Soft close gate valves	32, partitioning into 2 km subsections
2000 L/s ion pumps	40, one for each subsection
Roughing pumps	40, one for each subsection
non-evaporable getters	distributed throughout
6 in pumping ports	one every 250 m
Baffle aperture	100 cm
Baffle BRDF	$10^{-3} \text{ sr}^{-1}$

Table 8.2: Reference parameters for the Cosmic Explorer vacuum system for a 40 km facility. Fig. 8.3 shows a schematic of how the vacuum system is broken up into 10 km subsections.

for Cosmic Explorer, there is room for improvement and value engineering (§8.3.1). Nominal parameters of the Cosmic Explorer vacuum system are given in Table 8.2.

The vacuum practices used with the test mass chambers of Cosmic Explorer will need to be improved relative to those for current LIGO chambers to reduce pumpdown times after in-chamber detector work. Besides increased pumping capacity, it may be necessary to heat the walls of the test mass chambers to increase the evaporation rate (known as baking), especially in the case that the mirrors are cryogenically cooled and need protection from condensation. For both the chambers and beamtubes, the hydrogen pumping speed can easily be augmented by titanium sublimation or non-evaporable getter pumps.

**Residual gas pressure requirements** The pressure requirements in the beamtubes and in the test mass chambers are set by the effect of two different processes. Fluctuations of the gas column density in the beamtubes induces a phase noise when the light scatters off the residual gas molecules,<sup>410</sup> while the residual gas in the chambers exerts a force noise directly on the test masses.<sup>411,412</sup> The gas force noise has a  $1/f^2$  frequency dependence and is important at low frequencies, while the gas scattering noise is constant in frequency up to a cutoff frequency determined by the time for a molecule to cross the beam (see Fig. 8.2). Reaction masses are used in LIGO for electrostatic force actuation on the test masses, and the resulting squeezed film damping from their close proximity to the test masses increases the total damping noise.<sup>412</sup> This excess noise is not considered here since it is assumed that CE will use a different actuation scheme where this effect is negligible.

The vacuum system requirements for the partial pressures of each species are broken up into a set of requirements that must be met and a set of goals to strive for. The requirements on the beamtube pressures are that the gas scattering noise is at least a factor of five below the design sensitivity, and the requirements on the chamber pressures are that the gas damping noise is at least a factor of three below the design sensitivity. The goals on the pressures in both

the beamtubes and chambers are that the residual gas noise is a factor of ten below the design sensitivity at all frequencies. In the absence of a malfunction or poor vacuum practice, such as leaks in the vacuum system or inadequate cleaning of vacuum components, achieving the low partial pressures necessary to meet these requirements will be most challenging for hydrogen, water, nitrogen, and oxygen. We thus allow these four species to saturate these requirements with each contributing one quarter to the total. Hydrocarbons could potentially make a large contribution to the noise since they are massive and have large polarizabilities. Keeping their pressures low enough to have a negligible contribution to the total noise also ensures that they do not contaminate the mirror and cause excess optical loss. These pressure requirements and goals are summarized in Table 8.3.

Species	Beamtubes			Chambers	
	Req / torr	Goal / torr	LIGO Achvd / torr	Req / torr	Goal / torr
He	$1.3 \times 10^{-9}$	$3.4 \times 10^{-10}$		$8.8 \times 10^{-10}$	$7.9 \times 10^{-11}$
H <sub>2</sub>	$3.3 \times 10^{-10}$	$8.3 \times 10^{-11}$	$3.4 \times 10^{-9}$	$3.1 \times 10^{-9}$	$2.8 \times 10^{-10}$
Ne	$1.8 \times 10^{-10}$	$4.5 \times 10^{-11}$		$3.9 \times 10^{-10}$	$3.5 \times 10^{-11}$
H <sub>2</sub> O	$3.0 \times 10^{-11}$	$7.6 \times 10^{-12}$	$2.3 \times 10^{-12}$	$1.0 \times 10^{-9}$	$9.4 \times 10^{-11}$
O <sub>2</sub>	$2.1 \times 10^{-11}$	$5.3 \times 10^{-12}$	$2.0 \times 10^{-13}$	$7.8 \times 10^{-10}$	$7.0 \times 10^{-11}$
N <sub>2</sub>	$1.9 \times 10^{-11}$	$4.7 \times 10^{-12}$	$1.0 \times 10^{-13}$	$8.3 \times 10^{-10}$	$7.5 \times 10^{-11}$
Ar	$6.7 \times 10^{-12}$	$1.7 \times 10^{-12}$	$9.0 \times 10^{-14}$	$2.8 \times 10^{-10}$	$2.5 \times 10^{-11}$
CO	$5.8 \times 10^{-12}$	$1.4 \times 10^{-12}$	$2.0 \times 10^{-12}$	$3.3 \times 10^{-10}$	$3.0 \times 10^{-11}$
CH <sub>4</sub>	$4.8 \times 10^{-12}$	$1.2 \times 10^{-12}$	$2.2 \times 10^{-11}$	$4.4 \times 10^{-10}$	$4.0 \times 10^{-11}$
CO <sub>2</sub>	$2.8 \times 10^{-12}$	$6.9 \times 10^{-13}$	$4.0 \times 10^{-13}$	$2.7 \times 10^{-10}$	$2.4 \times 10^{-11}$
Xe	$6.3 \times 10^{-13}$	$1.6 \times 10^{-13}$		$1.5 \times 10^{-10}$	$1.4 \times 10^{-11}$
100 u H <sub>n</sub> C <sub>m</sub>	$8.9 \times 10^{-14}$	$2.2 \times 10^{-14}$		$1.8 \times 10^{-10}$	$1.6 \times 10^{-11}$
200 u H <sub>n</sub> C <sub>m</sub>	$1.7 \times 10^{-14}$	$4.2 \times 10^{-15}$		$1.2 \times 10^{-10}$	$1.1 \times 10^{-11}$
300 u H <sub>n</sub> C <sub>m</sub>	$6.2 \times 10^{-15}$	$1.5 \times 10^{-15}$		$1.0 \times 10^{-10}$	$9.2 \times 10^{-12}$
400 u H <sub>n</sub> C <sub>m</sub>	$3.1 \times 10^{-15}$	$7.6 \times 10^{-16}$		$8.8 \times 10^{-11}$	$7.9 \times 10^{-12}$
500 u H <sub>n</sub> C <sub>m</sub>	$1.7 \times 10^{-15}$	$4.3 \times 10^{-16}$		$7.9 \times 10^{-11}$	$7.1 \times 10^{-12}$
600 u H <sub>n</sub> C <sub>m</sub>	$1.1 \times 10^{-15}$	$2.8 \times 10^{-16}$		$7.2 \times 10^{-11}$	$6.5 \times 10^{-12}$

Table 8.3: Cosmic Explorer residual gas requirements and goals. The requirements are that the total gas scattering noise is a factor of five below the design sensitivity and that the total gas damping noises are a factor of three below the design sensitivity. The goals are that the total residual gas noise is a factor of ten below the design sensitivity everywhere. See text for details. The pressures achieved in the Advanced LIGO beamtube are also shown for comparison.<sup>413</sup> The H<sub>2</sub> pumping speed can easily be augmented by titanium sublimation or non-evaporable getter pumps to reach the required pressures in both the chambers and beamtubes.

**Ultra-high-vacuum beamtubes** The vacuum tubing for Cosmic Explorer will be separated into 10 km sections, which are independently pumped. Each section is further divided into 2 km subsections for outgassing and leak hunting as shown in Fig. 8.3. The ends of the 10 km sections will require fully capable gate valves but the 2 km subsections need only the equivalent of light

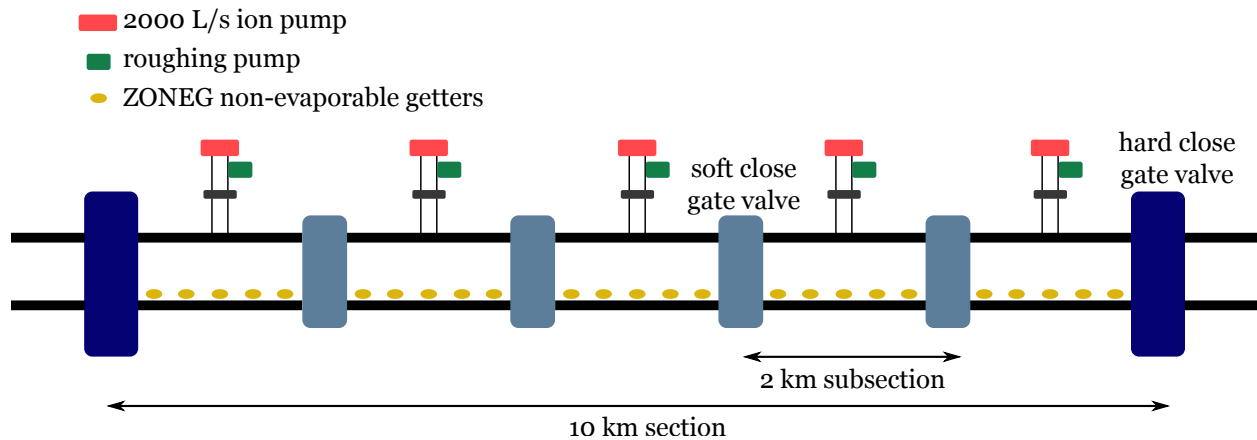


Figure 8.3: Schematic of a 10 km beamtube section. Each 10 km section can be pumped and serviced independently. The ends of the section are determined by commercial 48 in (122 cm) gate valves with elastomer O-rings that can withstand an atmospheric pressure from either side. The 2 km subsections are separated by soft-close gate valves used for separating regions with small pressure differences during some bake operations and for diagnostics. 6 in pumping ports (not shown) are located every 250 m and can be used for leak hunting and diagnostics or while pumping down.

weight shutters to aid in the initial commissioning and operational leak checking. These shutters can be allowed to leak between subsections by as much as  $10^{-3}$  L/s and do not have to bear atmospheric loads. We call this a “soft” close valve which should be significantly lower in cost than the “hard” close valves used at the ends of the 10 km sections. The soft close valves could be magnetically actuated and will not require penetrations in the vacuum envelope.

**Test mass chambers** Each test mass suspension will be enclosed in a UHV chamber. An option that will be considered is to separate the bottom two stages of the suspension (consisting of the test mass and penultimate mass) from the upper stages. This will enable the stages to be separately accessed, and can shield the test masses from materials with high outgassing. The feasibility of doing this in a manner that both withstands atmospheric loads and maintains the necessary vibration isolation needs to be investigated. Even if this can be accomplished, achieving the goal pressures in the chambers will be more challenging than in the beamtubes since high temperature bakes are not possible in order to protect the components housed in the chambers and since they will need to be opened periodically to make modifications to the detector. The other core optics, such as the beamsplitter, will also be housed in UHV chambers though the requirements on these are not as stringent.

**Requirements due to scattered light** Light scattered out of the interferometer can scatter off the beamtube and reenter the interferometer. In this way, motion of the beamtube can be converted to noise on the light circulating in the interferometer and thus noise at the gravitational-wave readout. Calculations show that 120 cm diameter beamtubes with 100 cm baffle apertures are sufficient to keep noise due to scattered light a factor of ten or more below the nominal sensitivity of Cosmic Explorer.<sup>414,415</sup> See §8.3.13 for a broader discussion of the scattered light mitigation

research required for CE.

### 8.3 Enabling Technologies

Technology	2G	CE facility	initial CE	CE	CE (2 $\mu\text{m}$ )
Ultrahigh-Vacuum Systems	Green	Yellow	Grey	Grey	Grey
Large, High-Purity Mirror Substrates	Green	Grey	Orange	Orange	Red
Low-Loss Mirror Coatings	Yellow	Grey	Yellow	Yellow	Orange
Optical Wavefront Control	Yellow	Grey	Yellow	Yellow	Yellow
High-Fidelity Squeezed States of Light	Yellow	Grey	Yellow	Orange	Red
High-Power Ultrastable Laser	Green	Grey	Yellow	Orange	Orange
Low-Noise Suspensions	Green	Grey	Orange	Orange	Red
Inertial and Position Sensors	Green	Grey	Orange	Red	Red
Seismic Arrays and Engineering	Green	Yellow	Orange	Orange	Orange
Environmental Monitoring	Green	Grey	Yellow	Yellow	Yellow
Low-Noise Cryogenics	Grey	Grey	Grey	Orange	Orange
Low-Noise Control Systems	Yellow	Grey	Orange	Red	Red
Calibration Techniques	Yellow	Grey	Orange	Orange	Orange
Scattered Light Mitigation	Green	Grey	Yellow	Orange	Orange

Table 8.4: Summary of required research and development activities for Cosmic Explorer. The columns in the table indicate whether the activity involves primarily the near-future second generation (2G) detectors, i.e., A+, the CE facility, the initial Cosmic Explorer sensitivity (initial CE), the target Cosmic Explorer sensitivity (CE), or a realization of the target sensitivity using the 2  $\mu\text{m}$  technology (CE (2  $\mu\text{m}$ )). Technology readiness is indicated by green (ready), yellow (nearly ready), orange (requiring modest research), and red (requiring significant research).

The reference detector concept for Cosmic Explorer is largely based on the evolution of technology currently deployed in LIGO and other gravitational-wave detectors. Clearly, this evolution of technology will not happen without direction, effort and funding. This section identified areas where research and development are required to realize the target Cosmic Explorer sensitivity.

The timeline for Cosmic Explorer, which includes a collection of planned upgrades, is constructed so as to follow the expected technology development over the next two decades. Development areas are enumerated in Table 8.4 and discussed in the following sections, along with the research required to advance them. To ensure the continuity of gravitational-wave astronomy, it is critical that these development efforts are well supported while the current generation of observatories are still operational. In addition to ensuring that CE will achieve its full potential, many of the technologies required for CE may also be used to enhance existing observatories. This research will take place in collaboration with other projects like ETpathfinder<sup>38</sup> and the Caltech 40 m prototype.<sup>37</sup>

### 8.3.1 Research on Reducing the Cost of Ultrahigh Vacuum Systems

Roughly 34% of the cost of CE resides in the ultrahigh vacuum (UHV) system needed for the beamtubes and vacuum chambers. While the vacuum technology used in LIGO could be used to meet the goals for CE, ongoing research indicates that significant cost savings may be available, and as such LIGO vacuum technology serves as a backup strategy should new techniques not be realized. In particular, the research described below aims to develop technology that could meet the CE requirements and reduce the cost of UHV systems from the estimate of around \$520 million for duplication of the LIGO approach to less than \$340 million.

**Techniques to eliminate high temperature bakes** The outgassing of adsorbed water is a well established problem in UHV technology. The binding energy of water to the surface has a broad distribution with a peak around 1 eV ( $10^4$  K). The time it takes a water molecule to evaporate from the surface at a fixed temperature is exponentially dependent on the binding energy. The molecules with low binding energy evaporate quickly while the tightly bound ones can take years (even centuries) to evaporate. The distribution of binding energies leads to a  $1/t$  dependence in the outgassing rate of gas species at a fixed temperature as a function of time  $t$ . Gases that do not adsorb, such as nitrogen and oxygen, usually pump out of a system exponentially while water remains as a long term contributor to the residual gas pressure. A standard method to remove water from a system is to heat the walls (“bake”) to increase the evaporation rate. In LIGO the beamtubes were heated to 150 °C for three weeks while the water was pumped out of the system with 6000 L/s cryopumps placed every 250 m along the tube. The overall bakeout costs were \$9 million in 1994 dollars for 16 km of tubing and, as discussed in §8.5, would conservatively cost \$62M (2021 USD) for the 80 km of tubing required for a 40 km CE and nearly \$100M project-wide for the 2-observatory reference concept. This cost was dominated by the electricity needed for the bake and motivates research to establish if there are more economical methods.

One method is to use lower temperature bakes with modest pumping capacity for longer durations. Modeling suggests that this could reduce the water outgassing to levels that meet the CE requirements in the beamtube. Another technique is to use a moving external heater with dry flush gas to remove water from a tube. The process would take place before the tube is evacuated and involves passing the dry gas through the tube while heating the tube to between 145 to 200 °C with a movable external ring oven about a meter long. The gas density and flow rate are adjusted to keep the water entrapped in the gas from diffusing back as the oven is slowly moved from one end of the tube to the other in the direction of the gas flow. The temperature of the tube in the short region under the ring heater can be significantly higher than in a full bake which reduces the emission time of the tightly bound water and allows shorter dwell time for the ring heater at each point along the tube. It would take about 14 days to complete the bake for one 2 km subsystem. CERN is looking into a system using inductive rather than radiative heating.

A test planned for LIGO (and important for both LIGO and CE) is the ability to backfill a large vacuum system that has been under UHV conditions with a dry gas and recover UHV conditions



without a bake — a situation that might occur after an accident or necessary repair is made. Modeling indicates that with dry gas filters now available it should be achievable.

**Mild steel instead of stainless steel beamtubes** Low carbon steel is a quarter to a third the cost of stainless steel with comparable mechanical properties. For many years it has not been considered a satisfactory material for UHV due to some faulty measurements in the 1950s. Standard production techniques now produce carbon steel with 0.1–0.3 % of the entrapped hydrogen and comparable water outgassing than most stainless steels.<sup>416</sup> Recent preliminary measurements at CERN and NIST have provided additional evidence for the low hydrogen outgassing but more research is needed to verify these findings and to develop the practical techniques necessary to use mild steel in UHV. The cost estimates presented in §11.1 assume the use of mild-steel beamtubes.

**Beamtube coatings** Coating the interior of the beamtubes with a material that has a low binding energy for water would reduce the time needed to bake the beamtubes. Ongoing research by metallurgists indicates that the dark oxide that forms on carbon steel (magnetite,  $\text{Fe}_3\text{O}_4$ ) may have a lower binding energy for water, but this needs to be tested. This naturally forming oxide, similar to “gun bluing”, could be generated on both the internal and external surfaces of the beamtubes to both lower binding energies and prevent oxidation (rust). It may also be worth looking into using hydrophobic silicon coatings for the internal surface, and considering the oil-industry standard epoxy coating for the external surface.

**Soft-close gate valves for leak hunting** Each beamtube is broken up into 10 km long sections separated by hard close gate valves, and each of these is further broken up into five 2 km subsections separated by soft close gate valves. 48 in (122 cm) diameter gate valves for UHV service are commercially available from VAT and other sources. They cost \$150 000 to \$200 000 and are able to seal a vacuum system from atmospheric leakage to better than  $10^{-7}$  L/s as well as to withstand the atmospheric pressure load. However, in the event that a leak develops in the a beamtube, an uninterrupted 10 km segment will make finding the problem challenging. Experience from LIGO shows that 2 km sections are manageable for leak-hunting, and development of less expensive soft-close valves which are used only in the event of a leak could result in significant cost savings for the CE project. The cost estimates presented in §11.1 assume the availability of such soft-close valves at 40 % of the cost of a hard-close valve for a project-wide savings of roughly \$4M.

**Nested system** In the event that the water outgassing cannot be reduced sufficiently to meet the CE requirements it becomes useful to investigate another option. There are engineering and operational advantages to separating the functions of maintaining a space against the atmospheric pressure load from that of reducing the residual gas to the levels of UHV. One promising concept uses a nested vacuum system with an outer shell of carbon steel tubing and an inner tube of thin wall aluminum.<sup>417</sup> If the research shows the nested system is favored, it

will be useful to develop an annular soft close valve that separates the inner and outer systems for outgassing and UHV operations and opens quickly in the event of a pressure increase in the outer system.

### 8.3.2 Large, High-Purity Mirror Substrates

Cosmic Explorer requires large and high-quality optical substrates for the main interferometer mirrors (a.k.a. test masses). The Cosmic Explorer test masses will be much heavier than the current Advanced LIGO mirrors (320 kg instead of 40 kg) in order to reduce quantum radiation pressure noise, suspension thermal noise, and all technical force noises. Furthermore, due to the larger diffraction-limited beam size, the Cosmic Explorer mirrors must have a diameter of more than 50 cm in order to hold round-trip optical losses from aperture effects to the parts-per-million level.<sup>375</sup>

**Large silica optics** The fused silica test masses used for CE will be roughly twice the diameter of those in Advanced LIGO (70 cm instead of 34 cm), again to reduce diffraction loss from the large beams. Such large volume masses are thought to be achievable with excellent optical properties. However, a careful engineering design, specification, and characterization of the optics will need to be carried out as with Advanced LIGO.<sup>418</sup> The GWIC 3G R&D report<sup>1</sup> calls out the importance of the homogeneity of the index of refraction for silica optics, which may be a significant challenge for the CE beamsplitters and input test masses due to their large diameter.

**Large silicon optics** The material of choice for the 2  $\mu\text{m}$  technology test mass substrates is silicon for the reasons outlined in Ref. [35]. Silicon has low Brownian noise at cryogenic temperatures (unlike fused silica), its thermoelastic noise vanishes at 123 K where its coefficient of thermal expansion goes to zero, and this temperature is compatible with high optical power. The diameter of the silicon mirrors for CE will be at least to 80 cm since 2  $\mu\text{m}$  diffraction limited beams are larger than 1  $\mu\text{m}$  beams. There is currently no production process which can produce substrates of this size of sufficient purity for CE (see §8.4). Furthermore, there is some evidence that polishing silicon surfaces can increase their optical absorption.<sup>419</sup> Further work is required to develop a production process compatible with CE requirements and to test whether a silicon surface can be polished to the specifications without resulting in surface absorption.

**Polishing and surface figure** Scattered light continues to be a significant source of noise for the current generation of gravitational-wave detectors. Continued improvements in surface polishing of large optics would help to reduce the level of scattered light from the optical surfaces. Estimates of the noise from scattered light for CE suggest that the required surface polish is comparable to that already achieved in Advanced LIGO for spatial scales below a few cm.<sup>415</sup> However, due to the larger CE beam size, it is necessary to ensure that this level of surface uniformity can be achieved up to spatial scales of several tens of cm. See §8.3.13 for a broader discussion of the scattered light mitigation research required for CE.

### 8.3.3 Low-Loss Mirror Coatings

**1  $\mu\text{m}$  Coatings** Current Advanced LIGO coatings are alternating layers of  $\text{SiO}_2$  and  $\text{Ti:Ta}_2\text{O}_5$  (nearly quarter wavelength) Bragg stacks, deposited via ion-beam sputtering. Research is underway to improve upon the mechanical loss and optical properties of these for A+. The Cosmic Explorer 1  $\mu\text{m}$  technology will require A+-like low-mechanical-loss coatings, scaled to larger substrates, and with excellent purity to minimize scattering and absorption. Cosmic Explorer will benefit from current research aimed at improving the A+ coatings. Because the room-temperature mechanical loss of the current low-index material ( $\text{SiO}_2$ ) is quite low, significant effort is focused on identifying a high-index material with lower mechanical loss. Doped germanium is a promising coating for A+, potentially offering a factor of 2 reduction in coating thermal noise.<sup>420</sup> While much more speculative than amorphous coatings, crystalline GaAs/AlGaAs<sup>421</sup> could provide even lower coating thermal noise if they can be scaled to the size of Cosmic Explorer optics. Because coating thermal noise will be a contributing noise source for Cosmic Explorer, additional gains beyond the state of the art in the coming years will be of great benefit.

Anomalous absorption from small defects in the Advanced LIGO test mass coatings has proven to be a major challenge and limitation the sensitivity of the instruments via degradation of the cavity buildup.<sup>408</sup> Research to solve this problem is currently a major focus for LIGO coatings, and clearly it must be solved for Cosmic Explorer as well.

**2  $\mu\text{m}$  Coatings** The 2  $\mu\text{m}$  coating technology will build off research and development toward LIGO Voyager and shows promise to offer improved thermal noise performance over the 1  $\mu\text{m}$  technology. The baseline assumed is “Voyager” coatings, scaled to 80 cm diameter and operated at 123 K. While it is expected that this area will benefit from significant further research, promising candidates for such coatings have already been identified, including amorphous  $\text{SiO}_2/\text{Si}$ <sup>422</sup> and crystalline GaAs/AlGaAs.<sup>421</sup> Development efforts are also needed toward scaling up from the current state-of-the-art of 10 cm and 34 cm for crystalline GaAs/AlGaAs<sup>421</sup> and amorphous coatings, respectively.

**Conductive Coatings** Silica is an insulator, and hence charge can build up on its surface. This has been an issue in Advanced LIGO, so it will be important to limit the amount of charge that is able to build up on the Cosmic Explorer optics.<sup>423</sup> With R&D underway on slightly conductive overcoatings and with the experience of charge control in LIGO to capitalize on, charge is not expected to be a major issue for CE.

### 8.3.4 Optical Wavefront Control

Even at the sub-part-per-million level of optical absorption achieved in the current Advanced LIGO mirror coatings, thermal lensing and thermal expansion induced by the high laser power circulating in the arm cavities (1.5–3 MW for Cosmic Explorer) will lead to significant changes of the optical mode in the interferometer. In addition, any anomalous absorption from small

defects (see §8.3.3) will make the problem significantly worse. If not corrected, the resulting wavefront distortions lead to excess scattering in the arm cavities, limit the power build-up, and degrade the interferometer contrast at the readout port. Furthermore, the distorted optical modes will no longer match the output mode cleaner cavity, nor the mode of the non-classical squeezed vacuum injected from the dark port to reduce the interferometer quantum noise (see §8.3.5) — unsqueezed quantum vacuum will leak into the interferometer, reducing the sensitivity gain from squeezing the quantum noise.

In order to achieve the mode-matching requirements and the high levels of frequency dependent squeezing in CE, active wavefront control actuators will be indispensable for the readout optics leading to the output mode cleaner, for the squeezed vacuum injection optics and filter cavity, as well as for the test masses themselves. New technologies are under development for active wavefront control and mode-matching for the A+ upgrade. These have direct applicability to CE with its even stricter optical loss requirements.

### 8.3.5 High-Fidelity Squeezed States of Light

Squeezed states of light are used to reduce quantum noise in current gravitational-wave detectors and this technology will also be used in Cosmic Explorer, initially at modest levels of noise reduction with planned upgrades expected to bring CE to its target sensitivity (see §8.1.2). Frequency-independent squeezing is employed in the current Advanced LIGO<sup>392</sup> and Advanced Virgo<sup>424</sup> detectors, and has reached 6 dB of noise reduction in GEO600.<sup>425</sup> Frequency-dependent squeezing has been achieved by reflecting squeezed light off of filter cavities as described above,<sup>426,427</sup> and a 300 m filter cavity is now being installed at the LIGO sites for the A+ upgrade. These two demonstrated technologies set the baseline 6 dB of frequency-dependent squeezing for the initial CE target. Research and development is needed to reach the required 10 dB of frequency-dependent squeezing, down to about 10 Hz, for the final CE design and to demonstrate this also at 2  $\mu\text{m}$  laser wavelength.

The level of noise reduction by squeezing, in decibels, is limited to  $10 \log_{10}(2\theta_{\text{rms}} + \Lambda)$ , where  $\theta_{\text{rms}}$  is the rms phase noise of the squeezed field, and  $\Lambda$  is the total effective optical loss experienced by the field, in both cases accounting for all mechanisms starting from the generation of the field, its propagation through all optical elements of the detector, and its conversion to current in the photodiode. 10 dB of noise reduction can be achieved assuming baseline values of  $\theta_{\text{rms}} \lesssim 10 \text{ mrad}$  and  $\Lambda \lesssim 8\%$ . The effective squeezing losses have some broadband contributions as well as some frequency dependent contributions due to the optical cavities of the interferometer and quantum filter cavity. Here it is assumed that the contributions to the total loss are mostly broadband: 1 % from the squeezer, 2 % from the Faraday isolators, 1 % from the photodiodes, 1 % from the output mode cleaner, 1 % from the pickoff mirrors, and 1 % from mode mismatch; finally, frequency-dependent cavity effects contribute an additional 1 %, thereby totaling 8 % total loss. The following paragraphs provide an overview of the R&D needed to achieve these loss levels.

**Squeezer design** The existing design of in-vacuum squeezers used by Advanced LIGO,<sup>428,429</sup> which yields 2 % internal cavity losses, is nearly sufficient for the Cosmic Explorer requirements, and only incremental improvements are needed to achieve the CE loss target of 1 %.

Research to demonstrate squeezing at 2  $\mu\text{m}$ , where similar design constraints apply, is ongoing.<sup>430</sup> The main differences are related to the eventual coating performance and crystal losses achievable at the longer wavelength.

**Low-loss Faraday isolators** Low-loss Faraday isolators are now used in Advanced Virgo<sup>431</sup> and Advanced LIGO. These demonstrate 0.5–1 % loss per pass of the squeezed light. The current design of a filter cavity requires a minimum of four total passes through Faraday isolators. An additional fifth pass is used in Advanced LIGO to add optical isolation, but can be avoided with improved isolation and scattered light mitigation. Minor improvement is required to bring the isolator losses down to a total of 2 % given the four required isolator passes.

**High Quantum-Efficiency Photodetection** Achieving 1 % loss from photodiodes requires photodiode quantum efficiencies  $\gtrsim 99\%$ . While this level of quantum efficiency has already been achieved for 1  $\mu\text{m}$  light, it is a serious challenge for 2  $\mu\text{m}$  light requiring significant R&D, but there are no known fundamental obstacles to achieving this performance.<sup>35</sup> Promising candidate technologies are described in Ref. [35] and include extending the InGaAs detectors used for 1  $\mu\text{m}$  light as well as developing HgCdTe and InAsSb detectors.

An alternative method is to add parametric amplification, with strict requirements on its efficiency, to the output of the interferometer, possibly by adding another squeezer unit.<sup>388,432,433</sup> This amplifies both the optical signal and quantum noise, preserving the signal-to-noise ratio, and lower quantum efficiency photodiodes may then be used without penalty. The integration requirements of such an optical parametric amplifier, and its pump light, have so far not been fully studied. However, the balanced homodyne readout of the A+ upgrade to LIGO shares a number of requirements that are likely to translate to the parametric amplified readout scheme.

**Filter cavity** Low-frequency design and high-mass mirrors give Cosmic Explorer a very low “standard quantum limit” (SQL) crossover frequency where the quantum noise has equal contributions from photon shot noise and quantum radiation pressure noise. It is necessary for the squeezed state to rotate from amplitude squeezing to phase squeezing at this frequency in order to achieve broadband quantum noise reduction, and this will be accomplished with a 4 km filter cavity with a finesse of  $\sim 4000$ , based on the 60–70 ppm losses achieved in the Advanced LIGO arm cavities. A 4 km filter cavity length is necessary to prevent the loss-induced dephasing of the cavity from limiting the allowable injected squeezing.<sup>434</sup>

The additional design constraints for controlling squeezing with a 40 km interferometer can be alleviated given more research into the scheme proposed in Ref. [435], which uses the filter cavity itself as a low-noise phase reference for the squeezed light.



**Constraints due to the Integration of Subsystems** In Advanced LIGO, some of the interferometer alignment signals are sensed at the antisymmetric port using a 1 % transmissive mirror. Additionally, the filter cavity also samples 1 % of the power for alignment control. For Cosmic Explorer, these transmissivities should ideally be avoided or reduced, which will impact the overall controls design of the instrument. This will require research given that the alignment sensing and controls need to achieve the low frequency sensitivity goals of Cosmic Explorer.

Additionally, there are integrative constraints for the squeezer and filter cavity involving the total optical isolation, the length and alignment noises which must be suppressed, and the sensing noise injected by the control systems. Improved seismic isolation will reduce the required control bandwidth and offset the requirements imposed by the lower frequency sensitivity of the CE detectors. A more detailed design study is required.

**Core Optics** Optical losses in an interferometer limit the enhancement due to squeezing, independent of other aspects of the system.<sup>436</sup> In Cosmic Explorer, the loss in the signal extraction cavity (see Fig. 8.1) directly limits the high-frequency sensitivity of the detector and thus the postmerger science it can perform. Above the detector bandwidth, the low transmission of the CE signal extraction mirror causes a large enhancement of losses within the signal extraction cavity, approximately  $4\epsilon_{\text{SEC}}/T_{\text{SEM}}$  where  $T_{\text{SEM}}$  is the transmissivity of the signal extraction mirror and  $\epsilon_{\text{SEC}}$  is the loss in the signal extraction cavity. While these resonantly-enhanced losses reach their maximum above the instrument bandwidth, they are sufficiently large that the losses within the signal extraction cavity must be minimized, so they do not degrade the detector performance within the signal band. This includes all of the anti-reflection coatings of vertex optics such as the input test masses, compensation plates, and beamsplitter. Additionally, there is loss in the high-reflection coatings of the telescope optics within the signal extraction cavity. While compensated in other optics, the refractive index inhomogeneities in the substrate of the beamsplitter cannot currently be compensated using surface polishing, due to the non-normal incidence of the beam, and must be analyzed to consider its contribution to the squeezing losses.

At high frequencies, the resonant “dips” in the 20 km instrument noise at 2–4 kHz, which depend on the arm length, signal extraction cavity length, and signal extraction mirror transmissivity, depend on the internal cavity losses. Full optimization of the squeezing level for postmerger signals requires a careful analysis not only of the instrument response, but also of the losses to squeezing, as the two mostly, but not entirely, align at those high frequencies. Furthermore, it is the loss in the signal extraction cavity that limits both the depth of these dips and the frequencies to which they can be tuned, so it is especially important to the 20 km science case that these losses be kept low.

**Mode Matching** The squeezed states will interact with a sequence of optical cavities: the squeezer’s optical parametric amplifier, the filter cavity, the interferometer, then finally the output mode cleaner. Achieving loss of  $< 2\%$  in squeezing due specifically to mismatch (at all

frequencies<sup>434</sup>) will require the design of the output optics and squeezer to be extremely mindful not only of curvature mismatch, but astigmatism and higher order aberrations as well. The overall curvature mismatch can be corrected using active wavefront control,<sup>437,438</sup> as is planned for LIGO. Research is needed into control and mitigation of astigmatism in the telescope designs, and the ability to measure and quantify wavefront errors in-situ using auxiliary beams and detectors should also be improved.

The need for higher-order aberration correction may prove necessary to match the squeezer beam to the interferometer, given that the interferometer has contrast defect and distortion from heating. More modeling is necessary to establish those needs.

### 8.3.6 High-Power Ultrastable Laser

Cosmic Explorer will use a similar laser source as that of LIGO, known as the pre-stabilized laser, consisting of a seed laser, laser amplifier, some frequency and intensity stabilization, and some reduction of higher order mode content.<sup>397</sup> The CE requirements on laser frequency noise incident on the interferometer are estimated to be  $7 \times 10^{-7} \text{ Hz}/\sqrt{\text{Hz}}$ . The frequency stabilization scheme currently employed by LIGO relies on using the common mode arm cavity as the ultimate frequency reference; however, this scheme cannot achieve the frequency noise requirements for CE across the entire detection band due to its ten times longer arms. A new scheme using two suspended modecleaners can achieve these requirements without relying on the arms as a reference<sup>398</sup> and is used as the reference concept for CE. While the second mode cleaner is not strictly necessary to meet the frequency stabilization requirements, it simplifies the intensity stabilization, can reduce the complexity of the pre-stabilized laser, and reduces other technical noises.

After passing through the mode cleaners, CE will require  $\sim 140 \text{ W}$  to be injected into the interferometer to reach the nominal  $1.5 \text{ MW}$  arm power given the expected optical loss. This level of output power has already been demonstrated in stabilized continuous-wave lasers.<sup>439</sup> If the alternative  $2 \mu\text{m}$  technology were employed, a significantly higher power of  $\sim 280 \text{ W}$  would be needed to reach the nominal  $3 \text{ MW}$  of arm power. The technology available at  $2 \mu\text{m}$  is much less advanced than  $1 \mu\text{m}$  technology, and considerable research and development toward ultrastable  $2 \mu\text{m}$  laser sources<sup>440</sup> and their high power amplification is needed.

### 8.3.7 Low-Noise Suspensions

As described in §8.1.4, each of the four test masses will be suspended by quadruple pendulum suspensions similar to those currently employed by LIGO. The reference concept for both technologies is a  $4 \text{ m}$  long suspension chain of total mass  $1500 \text{ kg}$ . It is believed that such suspensions can be achieved and supported by scaling up current Advanced LIGO systems.

Increasing the mechanical compliance of the suspensions — in all six degrees of freedom — is key to reduce seismic and thermal noises. More compliant suspensions produce lower frequency mechanical resonances, and displacement noises are passively filtered above these frequencies.

The mechanical loss of the suspension material determines the magnitude of the suspension thermal noise.

Developing highly stressed suspensions is critical for two reasons. First, this provides the opportunity to increase the suspension compliance. Second, it increases the fundamental and harmonic frequencies of the high- $Q$  transverse vibrational (“violin”) modes of the suspensions, which degrade the sensitivity in a narrow ( $\sim 1/Q$ ) band around the mode frequencies, thus reducing the number of modes in the detection band. The development status of highly stressed materials for the two technologies is discussed below.

**Silica** The gravitational-wave community has much experience with manufacturing highly stressed fused silica suspension fibers using a fiber pulling technique.<sup>441</sup> Tapered fibers are used in order to reduce thermoelastic noise at the ends of the fiber where the most bending, and therefore the most loss, occurs. The end radius is chosen to cancel the two contributions to thermoelastic loss — one from thermal expansion and one from the temperature dependence of the Young modulus. A smaller radius is chosen to maximize the stress along the length of the fiber. The maximum stress in the Advanced LIGO silica fibers is 800 MPa,<sup>395</sup> which provides a safety factor of about six for the breaking stress of fibers realized at the time the LIGO suspensions were designed.<sup>442</sup> Recent advances in these fabrication techniques allow for fibers to be manufactured with working stresses of 1.2 GPa, which provides a safety factor of about three.<sup>443</sup> While these fiber fabrication techniques are mature, no fused silica blade springs have been manufactured to date, and this is a critical area of R&D necessary to meet CE’s low frequency sensitivity goals. The current design for both stages of the silica technology calls for 1.2 GPa fiber stress and 800 MPa blade spring stress.<sup>415</sup>

**Silicon** Since the alternative silicon realization of CE operates at the zero-crossing of the thermal expansion coefficient, it is not possible to cancel the thermoelastic noise as is done for the fused silica fibers. Therefore, silicon suspensions would use silicon ribbons with dimensions chosen to maximize the stress along the entire length of the ribbon. Silicon ribbon fabrication is not well developed and the experiments most relevant to manufacturing suspensions find that the tensile strength of ribbons depends on the surface treatment and edge quality with average breaking stresses measured ranging from 100 to 400 MPa, and individual samples observed as high as 700 MPa.<sup>444,445</sup> Silicon blade springs have yet to be developed. While larger stresses have been observed in other applications, the alternative silicon based concept for CE assumes 400 MPa of stress in both the fibers and blade springs.<sup>415</sup>

### 8.3.8 Inertial and Position Sensors

Cosmic Explorer will benefit greatly from research and development into low-noise inertial and position sensors. Such sensors will enable improvements in seismic isolation and suspension control, both of which enhance the low-frequency sensitivity of Cosmic Explorer, and thereby

improve its localization, early warning, and/or high-redshift detection capabilities for compact binaries.

As described in §8.1.4 above, the seismic isolation for the initial CE target assumes a moderate improvement over current technology:  $0.1 \text{ pm}/\sqrt{\text{Hz}}$  at 10 Hz, which is threefold better isolation than Advanced LIGO, and  $1 \text{ pm}/\sqrt{\text{Hz}}$  at 1 Hz, which is tenfold better than Advanced LIGO.<sup>415</sup> Promising technologies to achieve this include combining the mechanics of a conventional geophone (GS13) with an interferometric proof mass readout.<sup>446</sup> The noise below 1 Hz is residual ground motion that comes from the inclusion of a position sensor signal to lock the suspension point to the ground on long timescales (a technique known as “blending”). Additionally, the horizontal inertial sensing is susceptible to contamination from ground tilt, and should therefore be paired with low-noise tiltmeters.<sup>447</sup> This is motivated by studies at LIGO Hanford that have shown that ground tilt couples significantly to the strain readout of the interferometer even after active seismic isolation.<sup>448</sup> Lowering the tilt coupling, along with mitigating Newtonian noise fluctuations from the atmosphere, is an important motivator for carefully designed buildings.<sup>449</sup> Further research in all of these areas is warranted.

Subsequent upgrades are planned to achieve a more significant isolation improvement: an additional threefold improvement at 10 Hz and tenfold improvement at 1 Hz. A number of efforts are underway to meet this challenge worldwide.<sup>450–453</sup> Moreover, improved low-frequency noise of the inertial sensors leads to less reliance on the low-frequency position sensor signals, thereby lessening the contamination from residual ground motion.

### 8.3.9 Seismometer Arrays and Seismic Engineering

Without mitigation, Newtonian noise from seismic waves would limit the low-frequency sensitivity of Cosmic Explorer. As stated in §8.1.6, Newtonian noise produced from surface seismic waves will need to be suppressed by a factor of ten and noise produced from body waves by a factor of three through a combination of careful facility design and sensor based noise cancellation. A combination of several techniques can be employed to achieve these goals, outlined in Ref. [415], and briefly discussed below.

**Low-density materials** Newtonian noise may be reduced by lowering the overall material density near the test mass.<sup>400</sup> This is achieved in the facility design by having recesses (e.g., a basement) or low-density building materials (e.g., Geofam) near/under the test masses, and/or by locating the test masses well above the ground level (e.g., on the second floor).

**Seismic metamaterials and architected structures** Seismic waves can be deflected or dissipated before they reach the test masses with intentionally designed structures. Seismic metamaterials are architected structures that can reduce surface wave propagation, using above-ground resonators, buried resonators, inclusions, and/or exclusions.<sup>401–406</sup> While more detailed studies will be needed on the feasibility of employing this technology, the CE facility is expected to incorporate at least the simplest of these techniques into its design.

Seismometer array subtraction Newtonian noise can be subtracted from the detector's strain data by estimating the local seismic field with an array of seismometers.<sup>399</sup> A recent proof of principle experiment demonstrated a tenfold suppression in the range 10–20 Hz,<sup>448</sup> though more research is needed to meet the Cosmic Explorer low frequency requirements down to 5 Hz.

The above techniques largely rely on modeling wave propagation through homogeneous media. Future studies on wave propagation through inhomogeneous media, such as stratified soil, natural topological structures, etc., will need to be conducted to ensure that these techniques are capable of reaching design sensitivity in a given seismic noise environment.

### 8.3.10 Environmental Monitoring

Monitoring of non-gravitational-wave disturbances from the environment, using an array of instruments located at the sites as well as information from global monitoring, has been critical for ground-based gravitational-wave observatories to date. The main purposes of environmental monitoring are localizing and mitigating sources of noise, assuring that the contribution of ambient environmental noise is kept below the background noise of the detectors or subtracted from the detector strain data, and validating candidate gravitational-wave signals by ruling out potential sources of terrestrial origin.<sup>454</sup>

For Cosmic Explorer, Newtonian noise will place more stringent requirements on acoustics, particularly infrasound (sound at frequency less than 20 Hz).<sup>415</sup> CE will thus require a careful measurement strategy, and potentially a reduction strategy, for infrasound. Ideally, Cosmic Explorer will employ sensors that measure the atmospheric pressure down to  $0.1 \text{ mPa}/\sqrt{\text{Hz}}$  at 10 Hz, and can disentangle the acoustic field from turbulent pressure fluctuations. Subtraction of infrasonic Newtonian noise with sensor arrays faces a number of uncertainties,<sup>371</sup> and as such the Cosmic Explorer sites should be selected, and facilities constructed, so as to minimize infrasonic noise.

Requirements for the facility magnetic spectrum and coupling to the CE electronics and sensitive equipment have not yet been set. However, magnetic coupling in current detectors has required significant monitoring and mitigation, so we expect this to also be the case for CE. For example, Schumann resonances, electromagnetic resonances between the Earth's surface and the ionosphere that are excited by lightning, will require careful measurement and perhaps subtraction.<sup>455</sup>

### 8.3.11 Low-Noise Cryogenics

A centerpiece of the alternative  $2 \mu\text{m}$  Voyager technology, as well as Einstein Telescope, is the use of crystalline silicon at cryogenic temperatures for the test masses and the lowest stages of the suspensions. The Japanese detector KAGRA, currently under construction, will use cryogenics and sapphire test masses to achieve similar objectives. KAGRA and ET will operate at 20 K, while Voyager operates at 123 K. The latter was chosen because it not only offers some reduction of



thermal noise, but is also a zero crossing value for the thermal expansion coefficient of crystalline silicon<sup>456</sup> and thus eliminates two major limitations to performance: thermoelastic noise and thermal aberrations from light absorption within the optics.

A challenge for the cryogenic operation of Cosmic Explorer will be to accurately ( $\pm 2$  K)<sup>415</sup> hold the optics and suspensions at their target temperature without introducing additional noise through vibrations, acoustics, or Newtonian noise coupling. Techniques under consideration, but requiring more study, to control deviations from the target temperature include: using the vibrational eigenmodes of the test masses as temperature sensors;<sup>457</sup> and injecting small localized heat modulation to the test masses and minimizing the induced displacement. For both, thermal radiation could likely be used to actuate the temperature.

It is likely that a radiative cooling approach such as that envisioned for Voyager<sup>36</sup> would be used for CE. This involves a movable heat link that comes into contact with the test mass only during initial cool down, to speed up heat extraction, and then radiative cooling only to maintain the test mass and suspension temperature during operations. However, there are open questions such as: What are the key drivers of the overall heat budget?; What are the requirements on temperature, length (tens of meters?), and material/coating properties for the radiation shields that stop the cold optics from seeing the warmer tube and environment?; Will each core optic and suspension require a dedicated cryostat? What is the most promising cryogenic technology (e.g., pulse-tube cryocoolers in phase opposition (such as in ET) or Gifford-McMahon)?; How will vibrations be mitigated?; and what techniques (such as helium gas cool-down or retractable contacts) will be used to provide high cool-down speeds? These questions will be addressed in more detail in the design phase of the CE project, and in light of Voyager technology research developments.

### 8.3.12 Calibration Techniques

Like current gravitational-wave detectors, Cosmic Explorer will need a calibration apparatus to turn the raw detector data into an estimated strain time series. The greater sensitivity of Cosmic Explorer compared to today's detectors, coupled with the expected improvement in theoretical waveform accuracy (see §9), will result in calibration requirements more stringent than those of Advanced LIGO and Virgo. In today's detectors, the systematic error in the calibration is a few percent in amplitude and a few degrees in phase across the sensitive band; the 68 % uncertainty on the error estimate is 10 % in amplitude and 1° in phase, and a few tens of microseconds in intersite timing.<sup>458–463</sup> The error and uncertainty are small enough that astrophysical parameter estimation is limited by noise in the detectors, rather than the calibration.<sup>464–469</sup>

The exact calibration requirements for Cosmic Explorer are not known, but are likely to be significantly below 1 % accuracy so as to not limit the astrophysical output of CE. Such accuracy in calibration will enable an estimate of the Hubble constant with a 0.2 % uncertainty over five years via multimessenger observations with telescopes such as the Vera Rubin Observatory.<sup>470</sup> This calibration accuracy will also extend tests of general relativity, reducing the chance of calibration errors being mistaken for false-positive deviations of the observed signal waveforms

from theory.<sup>467</sup> Pushing these levels of accuracy to frequencies of a few kilohertz will allow tighter constraints on the equations of state of neutron stars through observations of their postmerger phase.<sup>106</sup> Extending the accuracy to below 20 Hz will improve CE's ability to probe the crust and magnetic fields of rapidly rotating isolated neutron stars.<sup>471</sup> Continued research is required to assess whether improvement beyond these bounds, and in particular frequency regions, may be required for other sources.

Research and development is required to extend the calibration techniques of today to reach these stringent requirements. Currently, the level of systematic error is estimated using offline measurements; these measurements encompass the detector's response to displacement of its test masses, the test masses' response to control forces, and the detector's sensor and actuator signal processing electronics.<sup>458,459</sup> The offline measurements are paired with online measurements of a few slowly-varying time-dependent parameters.<sup>472,473</sup> These measurements are compared with a frequency-dependent model of the detector and its control system, and this model is used to produce the strain time series. The systematic error in this calibration is limited by theoretical accuracy of the model, the residual error between the measured and modeled frequency-dependent components, and the uncertainty in the detector's absolute displacement reference or "calibration standard", used to measure some of the model components.<sup>459</sup> Each of these areas need to be improved to ensure the required systematic error.

The primary calibration standards for the current detectors are so-called photon calibrators, which use power-modulated laser light from auxiliary lasers to drive the test masses with radiation pressure.<sup>474,475</sup> The reflected light is measured by photodiodes traceable to the National Institute of Standards and Technology (NIST), thereby enabling highly accurate estimates of the radiation force on the test masses. These systems already produce displacement with amplitude uncertainty of 0.5%.<sup>476</sup> Improving the photon calibrator systems to the accuracy level required for CE (perhaps < 0.1%) should be possible with anticipated improvements in laser power standards from the global network of national metrology institutes (including NIST)<sup>477,478</sup> and the reduction of other practical limiting systematics to the systems.<sup>476</sup>

In addition to photon calibrators, other supplemental calibration standards are being considered. Options include using existing subsystems of the detectors themselves, such as frequency modulation of the primary laser<sup>479</sup> or the use of auxiliary lasers,<sup>480</sup> or measurements based on the laser wavelength with the detector temporarily configured as a simple Michelson interferometer.<sup>480–482</sup> The use of gravitational-wave sources themselves as calibration standards (sometimes referred to as astrophysical calibration) has been studied and demonstrated; however, the accuracy of these methods will not be competitive with photon calibrators, even for 3G detectors.<sup>483,484</sup> Other direct force options such as spinning gravitational calibrators (Newtonian calibrators) have demonstrated promising accuracy in early prototypes<sup>485,486</sup> and recent work suggests that a combination of photon and gravitational calibrators could achieve an absolute accuracy of 0.17%.<sup>487</sup>

Work will also be needed to improve the accuracy of the detector's modeled response to gravitational-wave strain. For example, (1) developing methods to characterize the full dual-recycled Fabry–Pérot Michelson response, with losses, to surpass the accuracy of past approxima-

tions,<sup>467,488–493</sup> (2) taking into account the multi-input multi-output complexity of the auxiliary control systems to better account for cross-coupling,<sup>423,458</sup> and (3) going beyond long-standing assumptions for how gravitational waves interact with the detectors, such as the long-wavelength approximation.<sup>488,489</sup>

Producing the estimate of the systematic error function at a given time, from offline measurements, is time-consuming and inherently more uncertain than directly measuring the error by comparing displacement made by an absolute reference in real time. To date, the desired observational duty factor has trumped characterizing the detector’s calibration error, as high accuracy and precision were not of paramount importance. As such, many months are spent reconstructing the error estimate for all time in post-processing, after the strain data is recorded, and follow-up characterization measurements can be made. Research is underway to find methods of continual characterization while retaining observation time; this includes leveraging noise subtraction techniques already demonstrated to improve the detector sensitivity.<sup>494,495</sup> In this way, the 68% confidence interval on the systematic error will then only be limited by the uncertainty in the absolute reference(s) used to create the characterization signal and data integration time. Identifying and reducing the systematic error itself may still be time consuming. However, newly developed data analysis techniques may sufficiently marginalize over them if armed with precise quantified knowledge of these errors,<sup>468,469</sup> and other calibration pipeline development may yet yield full frequency-dependent correction of the well-characterized systematic error function in low-latency.

While all of this research and development is a challenge, the path appears clear to deliver the required precision in a timely manner for Cosmic Explorer.

### 8.3.13 Scattered Light Mitigation

Noise from light that is scattered out of the main laser beams has been a persistent issue for current gravitational-wave detectors.<sup>496,497</sup> While scattered light reduction was included in the design of the advanced detectors, much effort has been devoted to diagnosing and fixing light scattering issues after installation.<sup>454,498,499</sup> Scattered light effects, which are often driven by seismic motion, will be particularly important to address in order to ensure the excellent low-frequency performance of Cosmic Explorer. It is thus important that a scattered light mitigation design that incorporates the best practices and lessons learned from the 2G experience be developed for Cosmic Explorer. Three main areas of concern are discussed below.

Light scattered from the coated test masses can reflect off of moving elements, such as the beamtube walls and baffles, and recombine with the main cavity laser mode giving rise to additional phase noise in the readout.<sup>500</sup> For this reason, baffles were installed along the beamtubes of the 2G detectors to deflect and absorb scattered light. Light scattering from the test masses has two main sources: roughness of the coated surfaces, which is responsible for most of the scattering at small angles; and point defects on the surfaces that show up as “bright spots” and are responsible for most of the scattering at large angles. The noise contribution to Cosmic Explorer surface roughness scattering can be estimated following Sec. 2.2 of Ref. [414]. Setting a

noise requirement that is a factor of ten below the CE design sensitivity at all frequencies, and assuming a beamtube diameter of 120 cm (as discussed in §8.2) point scattering into the baffled arms was found to be an insignificant noise source for Cosmic Explorer.<sup>415</sup>

A related and potentially important consideration is light from the main cavity mode being clipped by the moving baffles in the beamtubes, leading to modulated diffraction that causes phase noise in the readout. Several approaches to this problem are being investigated, including modal simulations and analytic solutions. While progress is being made, and preliminary results indicate that this coupling mechanism will not be problematic for CE, no firm estimates have yet been produced.<sup>501</sup>

Additionally, an evolution and front-loading of the stray light control work done for the 2G detectors will be needed for Cosmic Explorer. In Advanced LIGO, for example, it was necessary to incorporate dozens of baffles and beam dumps specifically designed, using ray-tracing software, to intercept significant stray light.<sup>502</sup> Some baffles also required better seismic isolation and damping of resonant motion.<sup>454</sup> Significant design work is called for to identify and eliminate scatter and stray beams associated with the many optical and mechanical components of CE, along with continued R&D into low-scatter materials and coatings that could reduce the levels of stray light.

## 8.4 Silicon Upgrades

The prospect of using the 2  $\mu\text{m}$  cryogenic silicon technology with higher arm powers than in the nominal design is a strong motivation for continued R&D into this technology. Here we briefly examine the limits to which this technology can be pushed, and then show that it could be used to approach the sensitivity limits imposed by the Cosmic Explorer facility.

Since the cryogenic Cosmic Explorer test masses would be radiatively cooled, a strict limit on the achievable arm power is imposed by the requirement that the power absorbed in the test masses does not exceed the radiative cooling power.<sup>35</sup> The main sources of heat are the power absorbed in the high-reflectivity (HR) optical coatings and the power absorbed in the input test mass substrates, which in turn depends on the absorption of the silicon crystal.

There are two methods of producing silicon crystals<sup>35</sup> and, as discussed in §8.3.2, producing the large 80 cm diameter silicon CE test masses is one of the most challenging tasks for the 2  $\mu\text{m}$  technology. The magnetically stabilized Czochralski method can produce the largest crystals — up to 45 cm in diameter today. This is the baseline design for Voyager. The float zone technique has only realized crystals up to 20 cm in diameter, but they are more pure than magnetically stabilized Czochralski crystals and therefore have lower absorption. Since in either case it will likely be necessary to bond multiple silicon crystals together to make the CE test masses, it is reasonable to consider float-zone silicon. Silicon absorption of 5 ppm/cm has been measured at 1550 nm wavelength<sup>503</sup> and can be taken as a starting point for the substrate absorption of a float zone CE test mass.

The emissivity of the test mass barrel can likely be made nearly 1 either by coating it with a

high emissivity coating or with a broadband anti-reflective coating. The emissivities of the HR and antireflective (AR) optical coatings are unknown at this time. Assuming emissivities of 0.95, 0.75, and 0.9 for the barrel, HR, and AR surfaces, respectively, a Cosmic Explorer using float-zone silicon could possibly achieve 12 MW arm power while satisfying the heat budget, assuming the coatings have 1 ppm absorption. Thermal lensing in the input test mass substrates<sup>504</sup> would likely not be an issue at this power.

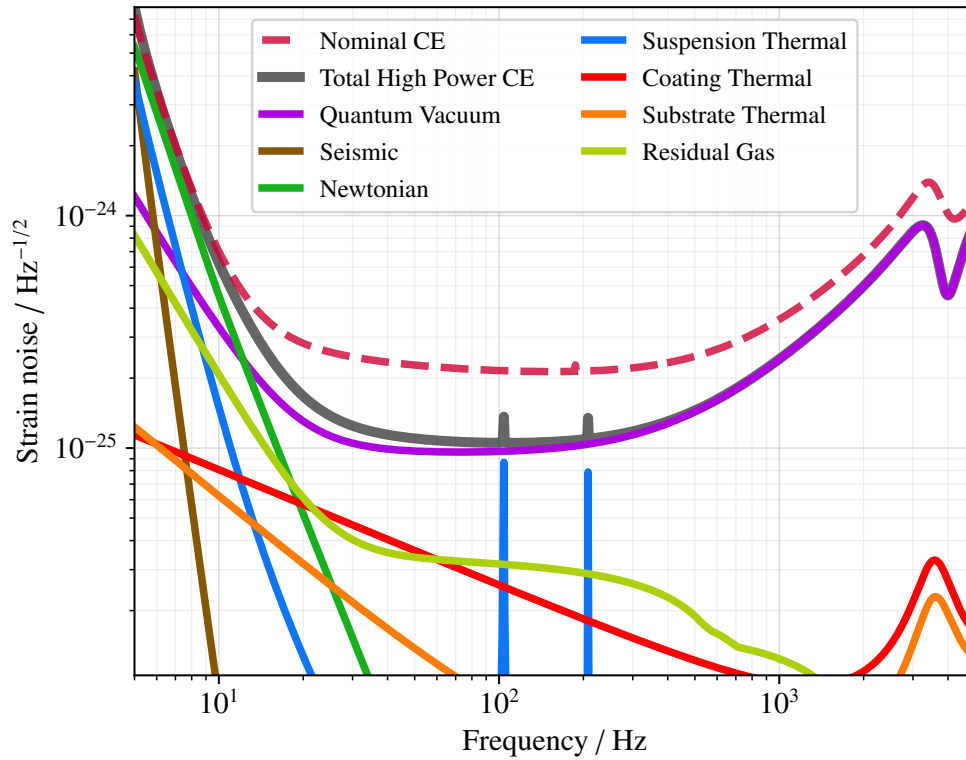


Figure 8.4: Noise budget for a high power silicon Cosmic Explorer with 12 MW arm power.

Such an interferometer would be roughly a factor of two more sensitive than the nominal design from about 30 to 300 Hz. The noise budget for such an interferometer is shown in Fig. 8.4. The high frequency sensitivity is not significantly improved by going to higher power because it is dominated by loss in the signal extraction cavity (SEC), which is enhanced by the arm cavity finesse  $\mathcal{F}$ . The finesse is increased in proportion to the arm power so as to satisfy the heat budget by reducing the power absorbed in the input test mass substrates. Quantum noise at high frequencies is proportional to  $P_{\text{arm}}^{-1/2}$ . Since the noise due to SEC loss is proportional to  $\sqrt{\mathcal{F}/P_{\text{arm}}}$ , it is effectively constant when the power is increased in this manner, while the other quantum noises, dominant below  $\sim 300$  Hz, are reduced as  $P_{\text{arm}}^{-1/2}$ .

The ultimate limits to the achievable sensitivity of any future detector that a given facility can support are usually taken to be the sum of the residual gas and Newtonian noises. If we add to this list 500 ppm SEC loss, the broadband sensitivity of a high power interferometer shown in Fig. 8.4 reaches this limit below  $\sim 10$  Hz, where it is limited by Newtonian noise, and above



~600 Hz, where it is limited by SEC loss. It is possible to find a “mid-frequency” tuning which reaches a peak sensitivity of  $7 \times 10^{-26} / \sqrt{\text{Hz}}$  around 100 Hz at the expense of sensitivity above about 400 Hz. It is not possible to find tunings with a resonant dip at higher frequencies due to SEC loss. Therefore, improving the high frequency sensitivity ( $\gtrsim 600$  Hz) beyond that shown in Fig. 8.4 requires some combination of reducing SEC loss below 500 ppm, reducing the silicon substrate absorption, reducing the coating absorption (which may become necessary), and increasing the emissivities of the test masses.

## 8.5 Cost Drivers

The initial cost estimate for CE presented in §11.1 is based on actual costs from LIGO construction, the Advanced LIGO upgrade, and the work of professional civil engineering and metallurgy consultants. The exercise of developing this cost estimate brought to the fore a set of cost-drivers which impact the technical design and scientific output of a Cosmic Explorer observatory. The following sections describe the primary cost-drivers and their relationship to CE performance: arm length, beamtube material and diameter, and observatory location. Notably, the cost of the detectors installed in the Observatories is not a major cost driver.

### 8.5.1 Arm Length

The length of an observatory’s arms is the most fundamental feature in determining its potential scientific output (see Table 7.1 and Box 7.1). As such, arm length is generally increased in the measure possible to the optimal length dictated by the science goals and thus automatically becomes the principal cost-driver for any gravitational-wave observatory.

Many of the costs associated with arm length are simply proportional to the length. Examples of this are: the road which goes along the beamline and provides access to the beamtube, the electrical utilities which run alongside the beamtube, the slab which supports the beamtube, the beamtube enclosure, and the beamtube itself. All of these civil engineering costs are largely location independent (generally within 10 % of the national average, and often a few percent lower than the average for the reference sites considered for CE). The sum of all costs which are simply proportional to length is 55 % of the cost of a 40 km facility and 43 % of the cost of a 20 km facility.

The cost of excavation and transportation is not included in the above list of civil engineering costs because it is highly location dependent, and generally not proportional to the length of the facility. As a concrete example, consider a large dry lake bed (e.g., the Bonneville Salt Flats along interstate 80 west of Salt Lake City, UT). The surface at such a location follows the geoid almost perfectly: meaning that it follows the curvature of the Earth and has constant altitude. The arms of a gravitational-wave observatory must, however, be straight lines since laser beams do not curve with the Earth’s geoid. The curvature of the Earth is such that the elevation at the center of a 40 km long straight line is 30 m lower than the ends. Preparing such a site would require

excavating almost 10 million cubic meters of soil, and transporting it more than 10 km on average (i.e., from the center to the ends), at a cost of very roughly \$100 million (highly dependent on geology). For a “flat” site like this, the volume of excavation required grows with arm length squared, and the transportation distances grow with length, such that the total cost grows with arm length to the third power (i.e., a 40 km facility would cost *8 times* that of a 20 km facility).

The flat-site example drove significant interest in finding sites which minimize excavation and transportation costs.<sup>505</sup> Such sites are slightly bowl-shaped with an elevation profile roughly 30 m higher at the ends than in the middle. There are a number of wide “valleys” that fit this description in the western states, and picking a location and orientation well can vastly reduce excavation and transportation costs. However, this search for topographically favorable sites clearly showed that the number of advantageous and available sites decreases rapidly with arm length, meaning that excavation costs for a 20 km observatory may be less than a 5 % of the total observatory cost, while for a 40 km observatory they are likely to remain near 10 % of the total simply because there are fewer 40 km sites to choose from.

### 8.5.2 Beamtube Material and Diameter

The laser light propagating along the arms of a gravitational-wave detector must travel in ultrahigh vacuum to avoid the noise associated with polarizable atoms and molecules traversing the laser beams (see Box 7.1). This fundamental performance driver is the reason that the LIGO facilities are among the largest ultrahigh vacuum systems ever built. The cost of this vacuum system, utilizing the research described in §8.3.1, will be roughly 34% of the cost of a CE facility, and approximately one third of that is required to produce the beamtubes, making the choice of beamtube material and size an important cost driver.

As discussed in §8.2.2, a wide variety of factors come into play when designing a vacuum system. While CE could use the LIGO vacuum system design with only minor modifications, ongoing research into the vacuum properties of steel suggest that mild carbon steel will provide superior performance at lower-cost.<sup>506</sup> This is the material used by the oil industry for pipelines, so it is well characterized and readily available in a range of diameters up to 48 in (122 cm). The standard pipeline wall-thickness of  $\frac{1}{2}$  in (13 mm) is sufficient to support the atmospheric load without stiffening rings (required in the current LIGO design), making manufacturing relatively simple. (Note: Shifting to thinner walls to save material actually increases cost, since this requires a non-standard process at the foundry.)

Scattered light is a potentially limiting technical noise source for gravitational-wave detectors, as observed in LIGO and Virgo. Initial estimates of scattering in the CE arms indicate that 48 in beamtubes are sufficient to ensure that this technical noise will not be limiting for CE. Calculations of scattering in the CE arms are ongoing with the objective of developing a detailed baffling strategy for CE, based on the baffles currently used in LIGO (see §8.3.13 for more detail).

### 8.5.3 Choice of Site

As mentioned above, the location of an observatory can have a significant impact on its cost. In addition to topography and geology, which determine the type of excavation (i.e., digging, or blasting) and the amount of transportation required, there are a variety of other factors that must be considered. A few prominent features are listed below, informed by the experience with LIGO-US and LIGO-India site identification.

**Local Community** A CE observatory will inevitably have a significant impact on the landscape, environment and the local community. As such *the local community must be included in any site selection process from the beginning*. This issue is of paramount importance for CE and §10.2 is dedicated to it.

**Environmental Impact** The long L-shaped footprint of a CE facility may have environmental impacts on resident and migratory animal populations. When searching for potential CE sites one should expect that many topographically favorable locations will be eliminated by environmental constraints (e.g., sage grouse leks in Idaho), and that some construction costs will be expended to accommodate animal populations (e.g., wildlife bridges).

**Land Acquisition** Sites which are favorable for CE are vast open spaces with relatively flat terrain, and as such they tend to be either very remote, already in use (as national parks, military facilities, etc.), or both. In some cases, this can facilitate land acquisition for CE (e.g., if the land is federally owned), or make it unfeasible (e.g., if the space is a national monument). Land acquisition may also be difficult in areas that are mostly private land due to the length of the CE arms, which may cross many individual plots.

A potential site could be unsuitable if the land cannot be acquired or its acquisition would greatly increase the cost of the project. Though Cosmic Explorer will be a surface facility, attention must be paid to, e.g., severed mineral rights, to avoid underground activity that negatively impacts the instrument performance.

**Natural Hazards** Certain potential sites could be disqualified due to unacceptably high probability of catastrophic natural disaster (flood, fire, etc.). In addition to consulting the historical record (e.g., the 100-year flood level), the potential impact of climate change on the suitability of a location must also be considered.

**Surrounding Infrastructure.** Some otherwise promising sites may be disqualified if they are hard to access or frequently rendered inaccessible (e.g., due to inclement weather). The absence of anthropogenic noise sources (e.g., industry, wind farms) must be assured for the lifetime of CE. Not all potential sites will be located close enough to critical infrastructure (e.g., roads, utilities) required to construct and operate the facility, and building such infrastructure may be prohibitively expensive.

**Proximity to cities** In addition, while some candidate sites tend to be remote, they must be sufficiently close to social infrastructure (hospitals, schools, etc.) to sustain an effective workforce.

## 9 Data Management, Analysis, and Computing

### 9.1 Data Management Plan

Given the substantial United States Federal Government investment and broad community support that will be required to realize a U.S. third-generation gravitational-wave detector, Cosmic Explorer is planned to be an Open Data facility. To realize this goal, both the construction and operations budgets must contain sufficient funding to support personnel and computing for the rapid release of high-quality, calibrated gravitational-wave strain data and alerts for events of interest. Development of Cosmic Explorer will include the creation of a Data Management Plan that will describe the technical implementation of user access mechanisms throughout the life cycle of Cosmic Explorer, guidelines for the use of data products, and publishing rights. The full data management plan will be developed in consultation with input from U.S. and international stakeholder funding agencies, the instrument development team, and the broader scientific community. Although there are significant differences in the type and scale of the data sets, the data policies of the NSF/DOE Vera C. Rubin Observatory and NASA's Fermi Gamma-Ray Space Telescope provides an excellent baseline for Cosmic Explorer's data management plan. This Horizon Study outlines the following principles for Cosmic Explorer's data management plan:

1. The data management plan should maximize the science output of the funding agencies' and science community's investment in the project.
2. There should be no reserved science; all types of scientific endeavors are open to all individuals and membership of any group or collaboration does not convey exclusive rights to any particular area of research.
3. Open data facilitates scientific collaboration, enriches research and advances analytical capacity to inform decisions.
4. Open data supports and ensures access for junior scientists.
5. Open data supports scientists from small institutions and historically underrepresented institutions.

To achieve these goals, the Cosmic Explorer data set will be released as open data as quickly as possible (i.e., as close to real time as possible) once construction ends and operations begin.



Cosmic Explorer will generate a data set that provides a unique, rich, and deep view of the universe over its lifetime. However, in comparison to e.g., the Rubin Observatory data set, the volume of Cosmic Explorer's data is remarkably small considering its scientific potential. Almost all of the scientific information from an interferometric gravitational-wave detector is contained in a one-dimensional time series, with calibration information and additional metadata that describes these data. Whereas the Rubin Observatory is expected to generate  $\sim 20$  terabytes of data each night, the size of Cosmic Explorer's primary data set will be  $\sim 20$  gigabytes per day. An additional  $\sim 2$  terabytes of control and monitoring data will be recorded each day for a single interferometer. The size of alert data packets containing timing, sky location, and source properties (e.g., masses and spins) for detected compact-object mergers is less than 1 gigabyte per day, assuming of order one hundred alerts per day. We anticipate no significant technical challenges to releasing these data to the user community in real time.

The challenges of realizing open data for Cosmic Explorer are (1) ensuring that project construction costs have sufficient funding for the human resources needed to develop the infrastructure to deliver open data to the community, and (2) ensuring that the operation budget has sufficient funds to calibrate, clean and release the gravitational-wave time series with appropriate detector metadata and as quickly as possible. Funding will be needed for personnel to develop, deploy, and manage the generation of astronomical alerts for compact-object mergers, and to provide support to the user community. Given the critical nature of these tasks, they should not be subject to a separate entity supported by third-party funding or separate grants; they should be included in the construction and operation budgets, as appropriate.

Open release of Cosmic Explorer's data will allow the broadest possible use of the Cosmic Explorer facility, while keeping the scope of the project at a reasonable level. All data will be released with a liberal open license. Reuse, redistribution, and the dissemination of derivative data products will be allowed and encouraged. To aid in the use of Cosmic Explorer data by the public, all software developed for and data produced by Cosmic Explorer will be publicly released and thoroughly and clearly documented. All data will use standard, open formats whenever such formats exist. §9.2 and §9.3 discuss the requirements for computing expected to be with the scope of the project, as well as the broader scope of computing that will be pursued by the wider community.

## 9.2 Requirements for Open-Data and Analysis

To deliver the science goals described in §5.1–§5.3, the Cosmic Explorer project will need to provide:

1. Management and curation of the detector data throughout the life cycle of the project.
2. Near-real time production of a calibrated, cleaned gravitational-wave strain data set with metadata describing the quality of these data.
3. Production of low-latency alerts for the merger of compact-object binaries.

4. Operation and support of a Cosmic Explorer Data Access Center for dissemination and support of open data.
5. Periodic publication of catalogs describing the events observed in a given period.

Data management and the production of low-latency analysis required to deliver alerts and prepare the data product releases for the community will be in scope for the project — neither of these tasks present significant computational challenges, as described below. Approximately ten FTEs will be needed to perform tasks related to data preparation, alert generation, data curation, and user community support during the operations phase of the project.

The bandwidth of the control systems required to operate Cosmic Explorer does not differ significantly from that of Advanced LIGO. As in Advanced LIGO, the cost of the digital detector control systems is not expected to be a significant fraction of the cost of the instrument. Since the number of Cosmic Explorer control and data channels will be similar to that of Advanced LIGO, we expect data rates of 2 Tb per day of detector operation. Storage and dissemination of data of this scale is a solved problem with current technology.

The sensitivity of Cosmic Explorer will be an order of magnitude better than that of Advanced LIGO at 100 Hz and two orders of magnitude better at 10 Hz. Cosmic Explorer’s detector noise increases rapidly below 10 Hz and at 3 Hz the detector is five orders of magnitude less sensitive than it is at 10 Hz. For a broad-band source such as inspiraling compact objects, there is very little signal-to-noise below 7 Hz; over 99.5 % of the signal-to-noise lies above 7 Hz. A binary neutron star waveform starting at this frequency lasts 77 minutes from the time that it enters the detector’s sensitive band to coalescence. For a waveform of this length, the Doppler frequency modulation due to the diurnal and orbital motion is  $(\Delta f / f) \sim 10^{-8}$  and can be neglected in search algorithms.<sup>507</sup> Several search algorithms already exist that can search for waveforms of this length in a computationally efficient manner.<sup>508–510</sup> The number of templates required in a matched filter search scales as a function of the bandwidth of the detector and not the overall strain sensitivity.<sup>511</sup> Consequently, a matched filter search for binary neutron stars with component masses between 1 and  $3 M_{\odot}$  using current data-analysis algorithms only requires a factor of three times more template in its bank than required by Advanced LIGO.<sup>512</sup> Again, this is a scale of computing that is accessible by current technology (using either CPUs or GPUs); implementing searches for the rapid identification of compact-object merger events will be straightforward a decade from now.

The computational cost of parameter measurement scales with the number of sources observed. While this is expected to increase by three orders of magnitude with respect to Advanced LIGO, there already exist algorithms that can measure the parameters of, e.g., a binary neutron star (sky location, masses, and spins) within 20 minutes of detection for Advanced LIGO using 32 cores of a current processor.<sup>513–515</sup> Although Cosmic Explorer will detect events at a significantly higher rate than Advanced LIGO, the time-frequency volume of these events is relatively sparse in the data set and so Cosmic Explorer data analysis will not be confusion limited (as is the case, e.g., for LISA white dwarf sources). Consequently, there are no major obstacles to measuring binary parameters for the generation of alerts.<sup>516</sup> Increasing the speed of parameter estimation

from detection to time-to-release for catalogs over present-day analysis primarily requires development of data-analysis pipelines to automate tasks currently performed by humans, e.g., hand-checking of convergence for detected events.

While the computational challenges are straightforward and the necessary algorithms are already being explored, there is still significant algorithm, code, and infrastructure development needed to realize the scientific potential of Cosmic Explorer; these developments will allow a richer and more efficient approach to low-latency analysis in the Cosmic Explorer era. Adopting the open data paradigm for Cosmic Explorer will: allow greater access to data; opening possibilities to build upon and create new research from publicly accessible data and alerts; facilitate research across disciplines and foster new collaborations; help to ensure universal participation in Cosmic Explorer's science without barriers that can prevent the participation of underrepresented groups; and ensure compliance with funding agency mandates.

### 9.3 Additional Computational Resources

An open data model for Cosmic Explorer leaves the community free to pursue a wide range of science goals using human and computational resources that they obtain through the normal process of obtaining research funding and computational resources. These projects include but are not limited to: searches for sources of gravitational waves beyond compact-object mergers; low-latency analysis for gravitational waves e.g., from core collapse supernovae; re-analysis of events or data using new waveform models; analysis of populations of events; and comparison of signals to numerical models of sources.

Searches for unmodeled transient sources with Cosmic Explorer are likely to be challenging but will not require significant computational resources. The most computationally challenging analysis will be the all-sky search for continuous waves from pulsars. The scale is set by the need to search over pulsar frequency, the pulsar's spin down rate, and the sky location of the source (due to the Doppler modulation induced by the Earth's motion over the integration period). Although the computational cost of this search does not depend on the detector sensitivity, broad parameter space searches for continuous gravitational waves are likely to remain bound by computational power due to the extremely fine grid needed to search the target signal space. At fixed computational power, the development of more sensitive search algorithms and the use of new computing hardware will be pivotal to fully exploit the improved reach of Cosmic Explorer.

A significant effort will be needed to develop waveforms that will be accurate enough for third-generation gravitational wave detectors. The accuracy necessary to avoid biasing interpretation of an observation scales with the square of the observation's signal-to-noise-ratio. While the loudest observations of merging black holes and neutron stars to date have signal-to-noise ratios of  $\approx 30$ , Cosmic Explorer's observations will include detections with signal-to-noise ratios in the thousands. These loud signals are among the most critical for realizing our science objectives, and interpreting them without bias will require inspiral-merger-ringdown waveform models

substantially more accurate than today’s state of the art.<sup>517,518</sup>

Additionally, most current neutron star merger simulations are still not carried out with realistic microphysics, and full explorations of the parameter space of neutron star mergers are extremely challenging computationally. These issues are illustrated, for example, in the disagreement between multimessenger constraints on the lower limit of the neutron star radius that use different numerical simulations of neutron stars merging in GW170817. Also note that only a handful of high-accuracy neutron star merger waveforms exist today — and these are not accurate enough for Cosmic Explorer.<sup>519</sup>

Significant progress needs to be made over the next decade to ensure that waveforms of sufficient accuracy and that span a large enough parameter space are in hand to deliver the promise of Cosmic Explorer’s science case. For instance, achieving sufficiently accurate gravitational waveforms will likely require next-generation numerical-relativity codes that will take full advantage of the high-performance computing facilities that will be available in the 2030s.





# Community, Organization, and Planning



## 10 Cosmic Explorer at the Local and Global Scales

The Cosmic Explorer project will develop observatory designs with a multi-dimensional approach that creates synergy with its respective local, scientific, and global communities. This includes designing the physical and virtual infrastructure so that it will serve the broader goals of community integration and engagement by developing interpersonal relationships among members of these communities. Early and ongoing engagement with communities connected with Cosmic Explorer, from local to global, will be crucial to the project's success.

In 2020 the GWIC 3G Community Networking Subcommittee published a report that identifies potentially interested scientific communities for third-generation gravitational-wave projects.<sup>4</sup> The GWIC report also outlines a communication and outreach plan for engaging the relevant communities, and delivers concrete recommendations for next-generation gravitational-wave projects. This section describes specific actions already taken toward these recommendations, and plans for realizing others in the future.

The report identifies engagement with the public as key to the success of the coming observatories, just as it has been for the existing observatories. However, third-generation gravitational-wave observatories come at a time of growing public awareness of the social impact of large scientific projects and facilities, and Cosmic Explorer must consider how to engage the public in this era. Crucially, Cosmic Explorer must identify and connect with all communities that have a potential interest in the observatory, particularly focusing on local communities who will be impacted by its presence. This step lays the foundation for the critically important need to build positive and mutually beneficial relationships with those communities.

### 10.1 Community Integration and Engagement

As Cosmic Explorer is a new astrophysical observatory, there is an opportunity to reimagine the human-focused portion of the observatory, by designing the facility to strengthen the interaction between everyone who uses and visits it while highlighting the contribution of the local community to the Cosmic Explorer effort. The model currently used is to implement community engagement plans;<sup>520</sup> some include the construction of science education centers, as in Louisiana and Western Australia.<sup>521,522</sup> These efforts have drawn significant local and global public interest. Cosmic Explorer will build upon this model by facilitating an even tighter integration between scientists and the public.

In designing a facility that brings scientists and the public together, Cosmic Explorer can look to other scientific installations, such as Fermilab's Wilson Hall, which combines staff offices with

public gathering spaces. Beyond purely scientific outreach activities, Wilson Hall hosts cultural activities, such as art exhibitions, thus embedding itself in the fabric of the local community. Additionally, the architecture of the Fermilab facility itself is designed intentionally to conserve and restore the surrounding environment.<sup>523</sup> Another example of a successful meeting and exhibition space is the ‘Imiloa Astronomy Center in Hawaii,<sup>a</sup> which presents the astronomical knowledge of the local Native Hawaiian community alongside the astronomical observatories in Hawaii, and emphasizes the community presence by (for example) translating all materials into the local Indigenous language.<sup>524–526</sup> By looking to these examples, the Cosmic Explorer facility can be a place for scientific workshops, community activities, teach-ins (such as the work of Karletta Chief in the Navajo Nation<sup>527</sup>) and exhibitions happening under one roof in a welcoming environment.

## 10.2 Building Strong Relationships with the Local Community

The Cosmic Explorer concept is based on observatories on the grandest of scales. These observatories’ activities will not happen in a vacuum: they will impact the landscape in which they are built and will change the lives of people in nearby communities. The Cosmic Explorer project will address issues surrounding observatory impact on the land, environment, and host community carefully, intentionally, and as an opportunity to build a mutually beneficial long-term relationships with its host communities.

Cosmic Explorer cannot be built and operated without ongoing local consent, which could disintegrate if the project does not actively work to maintain a positive relationship with the local communities. Cosmic Explorer will first need to work to identify all relevant communities, including Indigenous communities, to ensure that the consent is comprehensive and meaningful. Having identified these communities, Cosmic Explorer will integrate Indigenous leadership (elders and community leaders) and local community leaders at large into the leadership structure of Cosmic Explorer, to ensure there is continuous engagement around future directions of the project. This integration could, for example, take the form of a community-based oversight committee, representative of the project’s hosts, neighbors, and other local communities, with decision making power (e.g., the ability to enter into binding arbitration) over any project decision that impacts the land, environment or community. Importantly, this leadership structure must truly represent the perspectives of the community and cannot serve as a substitute for it. The Cosmic Explorer project will request funding from private partners and federal, state, and local agencies to engage with the community and Indigenous peoples. Such inclusion in the project and the broader scientific community is crucial for maintaining broad consent for the project. This support might include, for example, funding scholarships for undergraduate students and fellowships for graduate students and postdoctoral scholars drawn from local demographic and Indigenous populations. Ultimately the specific form of support will depend on the community’s needs, which can only be ascertained after proper

<sup>a</sup>[imiloahawaii.org](http://imiloahawaii.org)

relationships are established.

These actions reflect Cosmic Explorer's need to prioritize community involvement in a fundamentally new way compared to previous physics and astronomy projects. Having multiple members from local communities serving on the leadership boards of the project — including Indigenous leadership, local community groups, and others — will be necessary during all stages of the project. The Cosmic Explorer project must start by building respectful and meaningful relationships from the outset, evolving into permission for land use, continuing integration and collaboration during commissioning and operations, and importantly ensuring accountability for agreements throughout the lifetime and decommissioning of the observatories.

### 10.2.1 Indigenous Communities

All lands within the United States are the ancestral home lands of Indigenous Peoples.<sup>528</sup> Establishing mutually beneficial relationships with these communities is important to the project's success. Failing to establish meaningful relationships with Indigenous communities has led to friction, delays, and public backlash for several astronomical projects, including the Mount Graham International Observatory, the Kitt Peak National Observatory, and the Thirty-Meter Telescope.<sup>529,530</sup> The contentious relationships between these projects and Indigenous communities has a negative impact on the communities themselves, who often are working from previous negative experiences with academic, scientific, and technical projects.<sup>531–533</sup> As the process to find a site for Cosmic Explorer begins, the Cosmic Explorer project will first learn the history of each potential site. The project will then connect with networks of tribal councils and leaders to learn the most respectful ways to engage. If there is a desire for ongoing engagement, the project will work to build and maintain a relationship with the community.

Building these relationships will be a core driver in the way the project engages with the local community.<sup>534</sup> A community's willingness to host an observatory will depend critically on the relationships built and the competency the project demonstrates around the community's heritage, ancestry, values, and culture. The Cosmic Explorer project schedule will include the time to learn together about how an observatory could achieve mutually beneficial relationships consistent with the community's priorities. The Cosmic Explorer project management and site search teams will make a conscious effort to build these relationships so that dialog and consent may follow. To gain experience, the project management and site search teams will study previous examples of the impact of large astronomical facilities, and large government and industrial facilities more broadly, on Indigenous communities. For example, the teams will work to understand the full spectrum of views around the local impact of the Thirty Meter Telescope, including those of the astrophysics community, the local Hawaiian community, and those in both communities, in order to understand how the disconnect between the communities arose.<sup>530,535</sup> The Cosmic Explorer team will invest in internal and external development with respect to Indigenous Peoples. Where appropriate, this investment will be enabled by partnerships with federal, state, local, and private agencies, and involve existing institutions such as local universities. We envision that the development work will include, but not be limited

to, the following:

1. The Cosmic Explorer project will demonstrate to the Indigenous community its commitment to understanding their culture and cultural practices.
2. The project will conduct cultural impact studies that involve the local Indigenous community as part of any site-selection process, with the goal of ensuring that the project is aware of and respectful toward locations of cultural significance at the earliest possible stage of the process.
3. Indigenous communities often have protocols — e.g., practices of respect and ceremony at physical locations. As the Cosmic Explorer project will be a guest in local host communities, the project will learn about these practices and create space for their perpetuation.
4. As part of developing lasting and mutually beneficial relationships, the Cosmic Explorer project will seek out appropriate opportunities to integrate Indigenous wisdom into its research plans, such as in the case of environmental monitoring. Indigenous cultures have millennia of history and experience specific to their ancestral land and the environment, making this a clear opportunity for working together to build mutual respect and trust.<sup>536</sup>
5. Cosmic Explorer will invite the involvement of its Indigenous hosts more broadly in order to highlight their presence at the observatory. The exact nature of this involvement will depend on the host community's needs and values but may include, for example, language preservation — e.g., using Indigenous names for parts of the observatory and notable discoveries, and translating descriptions of discoveries into Indigenous languages.<sup>525,537–539</sup> This genre of activity in particular is an opportunity for federal, state, local, and private partners to involve themselves.
6. Cosmic Explorer will work to eradicate anti-Indigenous rhetoric from the gravitational-wave community and ensure that it is not creating a hostile environment for anyone in the local community seeking to engage or for Indigenous scholars who join the gravitational-wave astrophysics community.
7. Cosmic Explorer will elevate anti-racist work around Indigenous communities in the gravitational-wave community, including improving cultural competency, researching how to utilize language that is respectful of Indigenous communities and their relationship to land, and building on relationships and partnerships that are already in place. These actions should lead to a collaborative environment that is intentionally structured to avoid the perpetuation of racist practices.
8. As a commitment to the stewards of the lands, Cosmic Explorer must be in continuous dialogue about what procedures match the practices of the host Indigenous community. For example, during the construction phase, how and where to put the land once it is moved must be mutually agreed upon.<sup>536</sup> During the planning and decommissioning

phases, dialogue on what returning the land looks like to the host community must be discussed, budgeted, and fully achieved, and will be codified in Cosmic Explorer's long-term facility plans (as required by, for example, the NSF MREFC guide). The Cosmic Explorer project must ensure that nothing is abandoned and everything is accounted for.

Taken together, the above points show the necessity of the Cosmic Explorer community developing positive relationships with local communities with historically longstanding land tenure. This comes at a time when funding agencies such as the NSF are increasingly recognizing the importance of strengthening such relationships.<sup>540</sup>

### 10.2.2 The Local Community at Large

The Cosmic Explorer project will work to cultivate a positive relationship with additional groups in local communities, importantly starting before a site is chosen, and continuing through the lifetime of the project. The success of the project will rely on the members of the community being invested and involved in CE. Members of the community will be integral to the project as members of the CE staff, collaborators on local projects, educational partners, and colleagues in local governance. Cosmic Explorer will engage with local communities at forums including public libraries, local government offices, schools, colleges and universities.

Throughout the site search process, Cosmic Explorer will reach out to local educational institutions and develop partnerships to integrate participation of their students, scientists, and educators with CE science and outreach. This partnership may include science education research, sharing science and technology development with the public, and outreach to a broad audience in the surrounding regions, following examples such as the Southern University/LIGO partnership in Louisiana.<sup>541</sup>

In parallel, Cosmic Explorer will initiate conversations at other local hubs such as public libraries and community centers, starting during the site identification process and continuing during the project and observatory lifetime, to build and maintain local relationships.

## 10.3 Cosmic Explorer as Part of the Scientific Community

The Cosmic Explorer project will only succeed with wide and explicit engagement and support by all levels of the scientific community. As the project moves forward, it will work to ramp up the frequency and depth of this engagement and support.

### 10.3.1 In the Gravitational-Wave Community

In the context of completing this Horizon Study, preliminary steps toward integrating Cosmic Explorer into the gravitational-wave community are already underway, including the following:



- Cosmic Explorer’s membership in the Gravitational-Wave International Committee (GWIC).<sup>542</sup> This membership enables Cosmic Explorer to participate in the coordination of projects covering ground interferometers, space interferometers, and pulsar timing arrays. Membership also enables Cosmic Explorer to provide updates to GWIC and to the Gravitational-Wave Agencies Correspondents (GWAC) to inform the funding agencies covering the broad scope of gravitational-wave research.<sup>543</sup>
- Presentations and outreach to communities, including those at meetings of the LIGO–Virgo–KAGRA Collaboration, ET Collaboration, Pulsar Timing Array, and LISA Consortium;
- Organization of a one-day meeting in Summer 2020 between the teams associated with Einstein Telescope, NEMO and Cosmic Explorer;
- Organization of the First Cosmic Explorer Meeting, a five-day remote conference that was held in October 2020 with broad community participation to discuss the technical design and the science case for CE;
- Formation of the Cosmic Explorer Consortium<sup>544</sup> in October 2020 to provide an open and efficient way for members of the broader physics and astronomy communities to contribute to the conceptualization, design, and future use of CE. Already the consortium has more than 300 members and has begun two monthly remote meetings, one devoted to instrumental research and development and another devoted to astrophysics; and
- Participation in discussions, plenaries, and technical talks at international Dawn Meetings.

### 10.3.2 In the Physics Community

The Horizon Study team has worked to raise the profile of Cosmic Explorer within the wider physics community through the following:

- Participation in discussions, plenaries, and technical talks at American Physical Society meetings;<sup>545,546</sup>
- Invitations through the APS Division of Gravity to join the Cosmic Explorer Consortium and research meetings;
- Participation in the DOE Snowmass2021 effort through committee leadership (Adhikari and Sathyaprakash) and through a Letter of Interest:
  1. “Cosmic Explorer: The Next-Generation U.S. Gravitational-Wave Detector”, S. Ballmer, P. Fritschel, Cosmic Explorer, LIGO Laboratory<sup>547</sup>

### 10.3.3 In the Astronomy Community

The Horizon Study team has worked to raise the profile of Cosmic Explorer within the wider astronomy community through the following:

- Participation in the Astro2020 Decadal Survey through two white papers:
  1. D. Reitze et al., “Cosmic Explorer: The U.S. Contribution to Gravitational-Wave Astronomy beyond LIGO”, *Bull. Am. Astron. Soc.* **51**, 035 (2019)
  2. D. Reitze et al., “The US Program in Ground-Based Gravitational Wave Science: Contribution from the LIGO Laboratory”, *Bull. Am. Astron. Soc.* **51**, 141 (2019)

### 10.3.4 In the Scientific Community

The Horizon Study team has worked to raise the profile of Cosmic Explorer within the wider scientific community through the following:

- Launching a Cosmic Explorer website<sup>b</sup> to increase visibility and opportunities for engagement in the CE community;
- Communicating Cosmic Explorer science with the public through social media about upcoming meetings, science goals, and opportunities;
- Discussing Cosmic Explorer at SACNAS conferences, which includes scientists across all STEM disciplines;
- Amplifying the Cosmic Explorer Plans in Science Magazine: A. Cho, “Giant detectors could hear murmurs from across universe”, *Science* **371**, 1089–1090 (2021).

### 10.3.5 Current and Future Work

This Horizon Study document serves as a reference to communicate plans and gather input and feedback. Through the current NSF funding supporting this study, the Cosmic Explorer team has already initiated efforts toward education and public outreach. All of the PIs have made Cosmic Explorer a focal point in their presentations to the public, and many of them have begun incorporating Cosmic Explorer technology and science into their classes. The project has strong engagement by graduate students and has been engaging undergraduate researchers in small but increasing numbers. These students have presented their research at their universities and in public settings.

Beyond the initial phases described above, this document will be employed to re-engage and expand discussions with members of the gravitational-wave, physics, astronomy, scientific affinity groups, and Indigenous leadership communities, including the LIGO, Virgo, and

<sup>b</sup><https://cosmicexplorer.org/>

KAGRA Scientific Collaborations, Einstein Telescope, LISA, DECIGO, NanoGrav, CMBS4, the APS Division of Gravitational Physics, AAS, the DOE Snowmass, the APS Forum on Diversity & Inclusion, AAS Committee on the Status of Minorities in Astronomy, SACNAS, AISES, to name a few. Building on the preliminary phases of community engagement described above, the Cosmic Explorer project will begin to operationalize recommendations from the Horizon Study, expecting that engagement with the broader communities will increase steadily as the Cosmic Explorer Project moves forward.

## 10.4 Developing a Global Gravitational-Wave Network

The discussion in §§3–5 of the observational science that is possible with the next generation of gravitational-wave observatories illustrates the great value added were these detectors to operate in concert as a global network.

The ground-based gravitational-wave community has recognized the imperative to form a globally coherent effort, and has made some progress toward that outcome. One of the deliverables of this Horizon Study has been to contribute to this goal. A series of NSF-supported meetings<sup>550–554</sup> began in 2015 to start planning for the future. These meetings have helped guide the development of the LIGO interferometers, specifically establishing “A+” as an upgrade to the 4 km detectors. They have served as valuable forums for discussion of further improvements to the present 4 km baseline LIGO observatories, and to discuss CE and other next-generation observatories, and have helped cultivate ideas for an Australian detector that would focus mostly on studies of the coalescence phase of neutron stars (NEMO<sup>41</sup>).

Presently, the Einstein Telescope and Cosmic Explorer are the candidate next-generation observatories in Europe and the United States. Assuming that CE and ET are realized, they could naturally form the basis of the 3G network, as Advanced LIGO and Advanced Virgo do now for the 2G network. Should other facilities of suitable capability come online, they too could participate. An effective 3G network would be a coordinated partnership that seeks to leverage the investments in each independent observatory to create great value added. Optimally, it would consist of three (or more) 3G detectors, geographically distributed on the globe to provide good localization of sources on the sky.

When envisioning international partnerships for Cosmic Explorer, we will learn from the success of the LIGO Scientific Collaboration (LSC). The LSC has data sharing and data analysis agreements, through memoranda of understanding, with Virgo and KAGRA. Also, the GEO collaboration, with its GEO600 detector, is a member of the LSC, as is OzGrav. Through this mechanism, leaders from the LIGO, Virgo, KAGRA, and GEO600 detector groups participate in the Joint Run Planning Committee to coordinate observing runs. These partnerships have been crucial for enabling and extracting the most information possible from the first observations of gravitational waves and especially the sky localization enabling multimessenger astronomy.

In parallel, the Gravitational-Wave International Committee (GWIC)<sup>542</sup> chartered a subcommittee to study detector astrophysical and instrumental science.<sup>555</sup> Hundreds of scientists

worldwide participated in providing in-depth analyses of the observational science and discussions of the instrumental opportunities and challenges. The documents were improved by reviews from both experts in the field and by members of the Gravitational-Wave Agencies Correspondents (GWAC) and are publicly available on the GWIC web pages.<sup>1,543</sup> This GWIC 3G endeavor enriched and updated the CE and ET science cases, and helped prioritize and focus the instrumental development. GWIC remains actively engaged in coordinating the world-wide effort and will sponsor further collaborative activities.

There remains a strong incentive for each of the major projects to form consortia which are focused internally. Einstein Telescope has formed a Consortium<sup>556</sup> which is providing technical and scientific support for its proposal, and the Cosmic Explorer Consortium is also active (§10.3.1). However, the experience with the current observatories demonstrates the synergy, efficiency, and scientific value of close coordination at all levels. Recognizing this, the CE and ET efforts are coordinated through exchange of members in their organizing committees, and via informal interactions at meetings in our field: Dawn, GWADW, Amaldi, GWPAW.

The CE team greatly values closer links between the CE and ET projects, and as early as is feasible. This will allow common technical developments, minimize independent parallel work, and could possibly lead to economies of scale. In the longer term, it is clear that the greatest scientific return will come from joint planning for running and upgrades and from joint analyses of data. The nature of this global governance is yet to be determined, but value in significant coordination is clear.

Historically, the gravitational wave community has built strong partnerships across many institutions, mainly in North America, Europe, Australia, Japan and India. Into the 2030s, we will expect to see a shift into a more developed and connected global scientific community. Cosmic Explorer will facilitate opportunities for broader geographic participation so that scientists across Africa, the Americas, Asian, and Pacific Island nations can be welcomed into the global gravitational-wave community.

## 10.5 Cultivating a Respectful, Healthy, and Thriving Scientific Community

Innovation excels when diverse minds across many axes of identity can thrive. The National Science Foundation has identified gender identity, race, color, ethnicity, (dis-)ability, socioeconomic status, sexual orientation, language, nationality, age, religion, veteran status, and family structure as some of the attributes of a diverse and high-performing workforce that will best advance science.<sup>557</sup> The Cosmic Explorer project will continuously and comprehensively work to address all axes of diversity. As the project builds capacity around each axis of diversity, it will understand how people may intersect multiple groups. Cosmic Explorer will build competency on what impacts each demographic and work to ensure that each population has access to participation and is represented and respected for their contributions in every aspect of the project's work. This requires comprehensive yearly planning, continuous engagement

and regular assessment on whether those goals are achieved.

As Cosmic Explorer continues to ensure fruitful engagement with its global partners, it will continue to invest in learning respectful cultural practices and designing our workflows and schedules based on this. Beyond seeking input from the physics and astronomy communities, Cosmic Explorer will seek to learn best practices from different organizations that have set up thriving diverse global institutions. The project will also ensure support exists to engage with outside consultants and facilitators to help grow our awareness around the most effective ways to do this.



# 11 Cosmic Explorer Project

This section presents cost estimates, a project timeline, an operations model, and an outline of the project management that would be brought to bear in the project phase of Cosmic Explorer.

## 11.1 Cost Estimates

The cost estimate for CE presented here is based on actual costs from LIGO construction and the Advanced LIGO upgrade. Since the CE observatories are significantly longer than LIGO, we have revised the estimated civil engineering costs with the guidance of a professional civil engineering consultant (Eric Riegel, TruE Consulting), and we have engaged a professional metallurgy consultant (Dan Henkel, Rimkus) to help us find approaches to beamtube construction that simultaneously reduce cost and increase performance. The technical impact of design-choice cost-drivers is discussed in §8.5.

Adapting the historical LIGO construction and upgrade costs to CE required a few extrapolations: costs which depend on the length of the observatory must be scaled appropriately, design changes due to lessons learned and research that has been done since LIGO was built must be incorporated, and inflation and shifts in the market prices of materials must be accounted for. The CE cost estimate was broken down into four top-level categories: civil engineering, vacuum system, detector, and project costs. Each of these estimates include materials and labor, as well as management and design costs (see Table 11.1).

The civil engineering costs were estimated *ab initio* by our civil engineering consultant, Eric Riegel, in consultation with LIGO engineers (including Fred Asiri, the civil engineer in charge of the original LIGO construction). These estimates were cross-checked against scaled LIGO costs. Civil engineering accounts for 26% of the total estimated project cost (see Table 11.2).

The vacuum system cost estimate is based on recent work done by Rainer Weiss as part of the *NSF Workshop on Large Ultrahigh Vacuum Systems for Frontier Scientific Research Instrumentation*<sup>558</sup> (NSF award 1846124). This estimate was, in turn, based on extrapolation from LIGO costs, along with updates for current material prices and new technologies. Vacuum systems account for 34% of the total estimated project cost.

Experience from the Advanced LIGO upgrade was used to estimate the cost of design, construction, and installation of a CE detector. Adjustments were made for sub-systems which will be significantly different, such as the mirror suspension system, and for systems which were not part of the Advanced LIGO upgrade (e.g., the squeezed light source). The detectors account for 26% of the total estimated project cost.

## Cosmic Explorer Cost Estimates, \$(M) 2030 USD

<b>Observatory Costs</b>	<b>20 km</b>	<b>40 km</b>	<b>Project Level Costs</b>	
<i>Management</i>			<i>Project Wide</i>	
Civil Engineering	15	29	Management	25
Vacuum System	21	38	Coordination	6
Detector	22	22	Computing	13
<i>Total</i>	<i>58</i>	<i>89</i>	<i>Total</i>	<i>44</i>
<i>Site Specific Design</i>			<i>Common Design</i>	
Civil Engineering	3.2	3.2	Civil Engineering	19
Vacuum System	0.8	0.8	Vacuum System	8
Detector	1.2	1.2	Detector	6
<i>Total</i>	<i>5.2</i>	<i>5.2</i>	<i>Total</i>	<i>33</i>
<i>Realization</i>			<b>Project Level Total</b>	
Civil Engineering	148	293		<b>77</b>
Vacuum System	210	383	<b>Contingency</b>	
Detector	225	225	20 km Observatory	129
<i>Total</i>	<i>583</i>	<i>901</i>	40 km Observatory	199
<b>Observatory Total</b>	<b>646</b>	<b>995</b>	Project Level	15

**Grand Total for Reference Concept (2 Observatories) 2061**

Table 11.1: Cost estimate for the Cosmic Explorer Project reference concept (one 40 km and one 20 km observatory), in millions of 2030 US dollars (see §12 for 2021 USD). The cost estimate includes design, materials, construction, installation and project management for the civil engineering (buildings, roads, etc.), the vacuum system, and the detector. The cost of alternate configurations can be estimated by adding the associated observatory costs to the project-level costs (e.g., \$1642 M 2030 USD for two 20 km observatories, or \$1286 M 2030 USD for a single 40 km observatory).

The project-level costs, including management, were estimated based on the Advanced LIGO experience. This includes separate management estimates for each of the other cost categories, as well as project-level costs such as computing and communication, travel and shipping between observatory locations (collectively labeled “Coordination” in Table 11.2). The project-level and management costs account for 14% of the total estimated project cost.

Some significant uncertainties remain to be resolved in this cost estimate. An essentially irreducible uncertainty of roughly 20 % results from changes in the market prices of raw materials, especially steel for the vacuum system. Furthermore, a more complete design of the facility, vacuum system and detector will be required to improve the cost estimates for these components. Finally, about half of the cost of civil engineering is in excavation and site dependent costs that introduce some uncertainty in that portion of the estimate. These uncertainties will be addressed as the Cosmic Explorer timeline becomes clearer, the design phase progresses, and the site selection process converges.

## 11.2 Timeline

The Cosmic Explorer timeline spans multiple decades and takes place in distinct stages: development; observatory design and site preparation; construction and commissioning; initial operations; planned upgrades; operations at nominal sensitivity; future observatory upgrades and operations.

**Development** The development stage for Cosmic Explorer began in 2013, and has resulted in many relevant publications within the gravitational-wave community. This stage will continue after the completion of this document and its endorsement by the scientific community that Cosmic Explorer will serve. This phase is one in which the community engagement work must expand in scope as described in §10, our understanding of the key science goals discussed in §5 will deepen, and the enabling technology discussed in §8.3 can be further developed by the instrument community.

As noted in §10, building competence around, and relationships with, Indigenous Peoples is a long-term endeavor that will be critical to the success of CE and must commence as soon as possible. This work can, and must, begin before a site is selected and may begin even before any specific sites are considered by making contact with national Indigenous Peoples organizations (e.g., SACNAS). By opening the conversation with national Indigenous Peoples organizations, the relationship building process can expand to include learning about Indigenous communities, and eventually reaching out to specific community leaders and seeking permission to engage in a dialog about potential locations for a Cosmic Explorer observatory.

The technical development described §8.3 is also important to ensuring that the investment in Cosmic Explorer facilities is most effectively utilized, and the CE science goals are achieved. Development of the technologies summarized in Table 8.4 will require planning and funding, roughly at the level of \$15 M over 4 years.<sup>42</sup> This effort may overlap with the Conceptual Design phase, depending on the relative timelines of CE project funding and the various research efforts.

Top-Level Costs	\$(M) 2030 USD	Percent
Civil Engineering	528	26
Vacuum System	712	34
Detector	540	26
Management, Design, Project	283	14
<b>Grand Total (2 Observatories)</b>	<b>2062</b>	<b>100</b>

Table 11.2: Top-level cost breakdown for Cosmic Explorer, excluding operating costs, in millions of 2030 US dollars and including 20 % contingency. Inflation is computed in then-year USD for a project starting in 2027 and completing in 2035 with a typical ramp up and ramp down, which is numerically equivalent to 2030 USD (see §12 for more info and for estimates in 2021 USD).

**Observatory Design and Site Preparation** The project begins with dedicated funding for Cosmic Explorer design and passes through all phases of the MREFC process.<sup>3a</sup> In addition to the design phases for the CE observatories (conceptual, preliminary, final), this preparatory stage will include prototype construction for the CE vacuum system and a nationwide search for and research about potential observatory sites. This will result in the selection of observatory construction locations (“site selection”): a process that we expect will be led by the relevant funding agencies. Two or more years will be required to build relationships with local communities and to obtain the necessary permits for construction, making it imperative that this work be done in parallel with technical and civil design efforts. The total time estimated for this phase of the project is 7 years.

**Construction and Commissioning** While some overlap between design and construction is possible, the vast majority of the technical and civil designs will need to have finished their final design phases before funds can be appropriated for construction. The civil works required for a Cosmic Explorer observatory will require at least three years, and potentially more depending on the particulars of the site. Installation of the detector and subsystem commissioning can occur to some degree in parallel with civil works (i.e., as soon as the corner and end buildings are finished). However, commissioning of each detector to the point of acceptance (i.e., transition to operations) will require at least one year after construction is complete, making the estimated time for this phase of the project 6 years.

**First Operations Phase** Once the CE detectors are operational, the project will transition to the Operations Stage. This will follow the successful model developed by LIGO: interleaved commissioning and observation, with observation periods growing in duration as the detector matures. Observational campaigns will also be coordinated with other gravitational-wave observatories, potentially including Einstein Telescope and/or Cosmic Explorer South. In parallel with detector operations, preparations for the planned upgrades will be underway, as described in §8.1. The duration of this phase depends on commissioning progress, upgrade readiness, and the success of the observation campaigns, and as such is somewhat flexible: 5 years is a plausible duration. By this phase, we expect that the community-focused aspect of the facility (§10.1) will also be operational; depending on the nature of the facility, this could include the arrangement of exhibits, workshops or other programs of community interest.

**Upgrade Phase** The upgrade of the CE detectors to their nominal configuration will bring increased sensitivity and full access to the key science goals described in §5. Some upgrades (see §8.1) can be performed with relatively little disruption of observation (e.g., seismometer array installation), while other may require significant down-time (e.g., upgrading seismic isolation systems). To allow for installation and commissioning of the new sub-systems, interleaved with

<sup>a</sup><https://www.nsf.gov/bfa/lfo/>

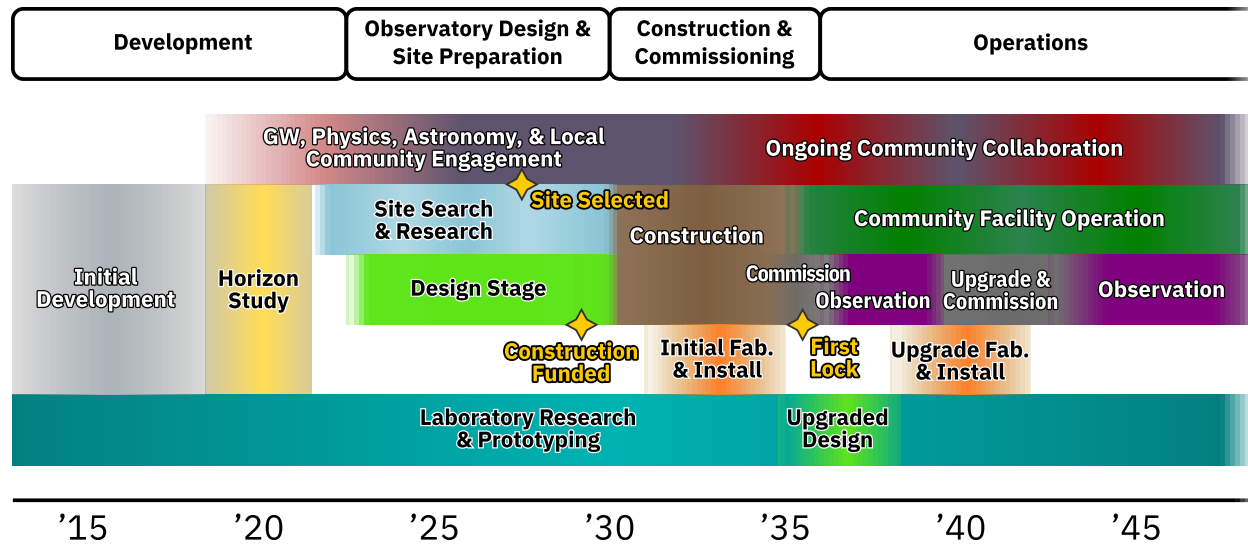


Figure 11.1: A top-level timeline showing a phased approach to Cosmic Explorer, as described in §11.2. The eventual divestment from the facility is not indicated.

observation, this phase may last as long as 4 years. The upgrades of the CE observatories may, depending on the needs of the scientific community, happen simultaneously or sequentially.

**Second Operations Phase** The second operations phase envisioned in this Horizon Study will presumably occur in the presence of other next-generation gravitational-wave detectors, and as such will result in ground-breaking high-fidelity access to gravitational-wave sources from throughout the universe. The duration of this phase is not specified here.

**Future Work** Though the commitment to fund Cosmic Explorer will likely be based on a 20-year duration, the Cosmic Explorer facilities are intended to be long-lived, with a nominal 50-year lifetime. While this is too far into the future for meaningful speculation about particular technologies, the CE facility design allows for improvements in fundamental noises, such as quantum and thermal noise, well beyond the CE target sensitivity (see Fig. 8.4). As such, the CE observatories will accommodate continuous improvements to detector technology and scientific output.

Eventually the CE facility will reach the later stages of its life cycle and be divested. It is thus important to begin planning from the outset, as recommended for large facilities,<sup>3</sup> to engage the scientific and local communities in divestment decisions and to anticipate costs. Some questions to be considered are whether the facilities could live on with new stewardship or be dismantled and cleaned up and how these decisions could strengthen the relationships fostered with the local community.



## 11.3 Operations Model

Following the successful example of LIGO, the Cosmic Explorer construction project will have a well-defined scope which leads into the commissioning and then operations phases. The hand-off could be defined as the point at which all installation at the Observatory is complete, and acceptance of the subsystems following a successful stand-alone test campaign has been completed. The first goal of the operations and maintenance phase would be to commission the instruments to reach a useful initial astrophysical sensitivity and sufficiently robust operations, along with the ability to produce high-quality and well-calibrated astrophysical data and alerts to the broader astronomical community. Achievement of this goal leads into a phase of alternating periods of observations and detector improvements, following the successful model employed by the current gravitational-wave network.

We anticipate an open data model for Cosmic Explorer in which strain data and astronomical triggers would be released immediately to the public (see §9.1). The data distribution and associated computing infrastructure will thus be key aspects of the operations model.

The organizational and staffing model for accomplishing the Cosmic Explorer Operation and Maintenance is provided below, based on the LIGO Laboratory Operations for the Advanced LIGO Phase. There will be persons who play roles in several groups, and many will change their focus according to the phase of activity (repairs, upgrades, commissioning, observing).

1. A *detector group*, consisting of engineers and scientists who specialize in various detector subsystems and electronics. This group will be responsible for maintaining, testing, documenting, and repairing controlled detector configurations with a focus on optimizing data quality and uptime. This group will also be responsible for operating the detectors.
2. A *commissioning group*, largely scientists, will commission and test the instruments and establish new detector configurations, with a focus on improving their performance.
3. A *systems engineering group*, largely engineers, will set technical standards and approve changes in controlled configurations, with a focus on system trades.
4. A *calibration and data quality group* of scientists and engineers will ensure the data are ready for astrophysical interpretation. These individuals will work with commissioners to find and resolve sources of instrumental and environmental noise, and will vet the data to correct, mark, and/or edit data as needed to allow the subsequent analysis to be made by the scientific community.
5. An *observation coordination group* of scientists will plan and coordinate observations with the gravitational-wave and astronomical network and interface with the broader scientific community on issues related to observations.
6. An *analysis, data, and computing group*, focused on the cybersecurity, computing, low-latency analysis for astronomical alerts, maintaining catalogs of observations, curating

and disseminating open data, and running a “Help Desk” to facilitate the use of CE by the broader scientific community.

7. A *facilities group*, responsible for maintaining the physical infrastructure of the observatories. Staffing will include significant vacuum expertise, and civil, electrical, and grounds engineers and technical support.
8. A *management group*. Each site will have a lightweight management and business group, enabling safety, procurements, shipping, human resources support, and top-level direction. For the target configuration of two Cosmic Explorer Observatories, one of the two observatory sites will carry management common to the two sites to minimize costs and maximize synergy between the sites.
9. An *community engagement and integration group* responsible for promoting integration of the CE observatories into the local community, arranging programs and exhibits at the community-focused facility, and with engaging the public at large. This includes building and maintaining synergistic relationships with local Indigenous Peoples, publishing broadly accessible versions of high-impact scientific results which inspire community engagement, and translating these materials into Indigenous languages.

External advisory committees will be established to (1) aid in technical management and evolution of the observatories, (2) coordinate with the greater scientific community and help guide the timing and trades of observation vs. commissioning, and (3) ensure that each observatory maintains healthy relationships with local communities, including Indigenous Peoples.

The scope for the operations of Cosmic Explorer can be estimated based on extrapolation from the LIGO Laboratory operations. As described above, significant staff will be required to properly operate, maintain, and incrementally commission the detectors. The two-detector configuration of CE would profit, as LIGO does, from some economy of scale for technical and management staff; the single detector approach would allow some reduction but not a factor of two. The vertex and end stations are expected to be similar in size and complexity to the LIGO buildings. The first detector to be installed will be comparable in electronic, mechanical, and optical systems, and will require staff comparable to LIGO’s to maintain it. The vertex and end-station vacuum systems for the initial detector will also be similar to LIGO; if the 2  $\mu\text{m}$  technology requiring cryogenics is used, there will be some increased operating complexity. The vacuum system will be 5 to 10 times greater in length and volume, but a great majority is passive once installed. There will be greater maintenance needs to inspect and maintain the tube, foundation, and protective cover. There will be a significant increase — roughly a factor three — in the staffing and operating expenses for this larger vacuum system and civil infrastructure, bringing them to roughly 40 % of the total operations cost (see Table 11.3).

A significant difference in project scope for Cosmic Explorer compared to Advanced LIGO is the staffing associated with delivering Cosmic Explorer data and alerts to the scientific community. In an Open Data model, data will need to be calibrated and conditioned to the point that it

<b>Yearly Operations Cost Estimates</b>	<b>\$(M) 2030 USD</b>	<b>Percent</b>
Facilities	22.5	30
Vacuum Systems	9.6	13
Detector	21.1	28
Analysis, Data, and Computing	9	12
Management	7.1	9
Community Engagement	5.9	8
<b>Grand Total (2 Observatories)</b>	<b>75.3</b>	<b>100</b>

Table 11.3: Estimated yearly operations costs for Cosmic Explorer with two observatories, based on Advanced LIGO and scaled for CE facility sizes, in millions of 2030 US dollars (see §12 for 2021 USD). Operations costs for a CE project with a single observatory would be roughly 30 % less. This estimate is for observatory operations *only* and does not include research for instrument upgrades.

can be interpreted for observational science without expert knowledge of the instrument and the data imperfections, which must be documented. Operations staff will also have responsibility for the production and dissemination of low-latency alerts for known multimessenger sources. These activities will require a dedicated group of people whose sole job is preparing data and performing initial analysis.

It is assumed that the research and development of new detectors will be supported by proposals to funding agencies; the staff at the CE observatories would be members of groups proposing for upgrades and new detectors, complemented by many in the greater scientific community.

## 11.4 Risk Management

Successful risk management starts with a careful examination of the project requirements and the construction and engineering responses in place to meet them. This examination leads to a good understanding of potential risk factors and their impact on the project. It is a common practice among large projects to establish a “risk registry” for perceived problem areas so that potential major issues are identified early and resolved, and that the project remains on schedule. For example, the Risk Registry and Risk Management Plan for Advanced LIGO will serve as a guide to Cosmic Explorer.<sup>559,560</sup> In the next two subsections we present the main technical and management risk factors that will form the starting point of Cosmic Explorer’s risk management plan.

### 11.4.1 Technical Risk

Unproven technologies (cf. §8.3) and identification of appropriate sites constitute the largest technical risk factors for the project. Cosmic Explorer will rely on the proven room temperature fused-silica-optic technology of Advanced LIGO operating at a wavelength of 1064 nm; fortunately, the success of Advanced LIGO establishes that this technology is extremely mature. As

with LIGO, the Cosmic Explorer sensitivity will continue to improve through a series of planned upgrades.

The main technical risk factors are fairly limited. The ones we have identified so far are:

1. *Risk of acquiring site(s) with adequate space and no excess noise that could compromise interferometer sensitivity and performance* (cf. §8.2.2). Finding appropriate site(s) that have not only adequate space for Cosmic Explorer, but also provide a low seismic noise background for the observatory is key to the Cosmic Explorer design. Initial surveys of North America suggest that it is possible to find adequate sites, and a detailed site survey as part of a design study can guarantee that the current seismicity of candidate sites is acceptable. But acquiring the required continuous piece of land from potentially numerous previous owners can be difficult and poses an obvious project risk. An excellent relationship with Indigenous communities and neighboring land owners is essential. Thus the land acquisition will have to be managed carefully. Possible urban encroachment on the site(s) over the lifespan of the observatory also will have to be managed.
2. *Risk associated with the vacuum system* (cf. §8.2.2). An adequate vacuum system is clearly technologically feasible. However, the significant increase in required vacuum volume compared to the Advanced LIGO detectors makes the vacuum system the driving cost factor for the project. A more cost-effective vacuum system construction is desired, and requires additional research.

To mitigate the project risk ahead of construction it is essential that a vacuum system prototype be built at the engineering design stage. Ideally this prototype would be constructed by the company that will get the contract for the vacuum system. It would also be useful to prototype a test mass chamber due to its complexity. Prototypes similar in spirit were constructed as part of initial LIGO.

3. *Risk associated with larger test masses not achieving design specifications*. While almost all technology from Advanced LIGO could be directly installed in a larger facility, the longer arm lengths do require an increase in optics size compared to Advanced LIGO, beyond the capability of current coating facilities. Together with issues related to small absorbers in the test-mass mirror coatings encountered in Advanced LIGO, this puts the manufacturing capability of optics for Cosmic Explorer at a critical spot. Achieving the optics and coatings design specifications is essential for reaching the design circulating laser power (1.5 MW) and thermal noise. Addressing this risk will require a significant investment in proof-of-principle optics (see §8.3).
4. *Risks associated with a 20 km detector*. Losses in the signal extraction cavity limit the high frequency sensitivity of a 20 km CE observatory; specifically, they reduce the depth of the resonant dip in the post-merger tuned configuration. Since the high frequency sensitivity is a key science driver for a 20 km Cosmic Explorer detector, there is also added technical risk for this 20 km post-merger tuning configuration arising from any excess

signal extraction cavity loss. The low frequency optimized tuning is not limited by the excess loss in the signal extraction cavity. Compared with a 40 km detector, many technical noise sources are also closer to limiting the sensitivity for a 20 km. Thus, we realize that the overall risk of having a single 20 km detector is significantly higher than a single 40 km detector. The technological challenges and the corresponding risk to CE detectors are discussed in (cf. §8.3).

5. *Risk due to an inadequate number of electromagnetic follow-up observatories.* Part of Cosmic Explorer's scientific promise is to provide sky localization and early warning for neutron star merger events. Thus the availability of a sufficient number of well-performing satellites, observatories and telescopes (X-ray, optical, radio, neutrino) is critical for reaping the full scientific benefit from Cosmic Explorer. Scheduling observation runs to maximize overlap with followup assets can mitigate that risk.
6. *Environmental risks:* As a facility designed for a 20+ year life span, rare but violent events such as floods, violent storms and earthquakes pose a significant but hard to predict risk for the project. The site selection, facility and instrument design will have to accommodate these risk factors.
7. *Malicious risks:* Sufficient site security, in the form of video monitoring, digital surveillance and physical barriers (locked entrances and fencing), will be needed to protect against both unintentional accidents and intentional sabotage. Infrastructure such as power lines, the vacuum system and the computer grid may be tempting targets for bad actors.

We have also identified the alternative technology being developed for the LIGO Voyager detector consisting of cryogenic silicon optics operating at a wavelength of 2  $\mu\text{m}$  which could be installed after the initial observing phase if a major problem is found which prevents the Advanced LIGO technology from reaching the sensitivity goals (cf. §8.1.8). This technology could also be used to surpass the nominal CE sensitivity in the future (cf. §8.4).

### 11.4.2 Management Risk

The management risk for a large project like Cosmic Explorer is to a large extent related to the deployment and organization of human resources to address the technical and engineering challenges of the project. This includes adequate financial backing and coordination to ensure that resources and scheduling are adequate to the task.

As described in §11.6, Cosmic Explorer project management will be accomplished using standard project management practices. A team of project management professionals will be tightly integrated into the project engineering and systems integration group. The use of monitoring software (e.g., Primavera, used by Advanced LIGO) and a resource-loaded schedule will help to identify areas which may have significant risk. The risk registry described in §11.4 will be critical in managing problem areas and their potential effects on project costs and schedule.

For Cosmic Explorer, there is potential for significant management risk in at least three areas: (1) publicity risk associated with site acquisition; (2) where new technology is required to achieve performance goals (cf. §8.3); and (3) international partnerships that may be established as part of the core Cosmic Explorer project and the wider 3G network.

1. The construction of Cosmic Explorer requires the acquisition of a large, continuous, L-shaped piece of land. While for most of this land the construction impact will be limited to allowing a path for the vacuum system, this land acquisition will impact local land owners and Indigenous communities. Thus, especially in the age of social media, a meaningful and genuine relationship with local communities is absolutely essential for the success of the project. The ground work for these relationships needs to be laid early on in the project, well ahead of any attempt to acquire permission to build at a particular location.
2. Potential loss of the expertise required to design, build and commission Cosmic Explorer. Through the lifespan of Initial and Advanced LIGO the NSF has invested in building up that technical, scientific and engineering expertise in the form of the LIGO laboratory staff scientists and engineers, as well as associated research groups across the country. That pool expertise forms a national asset, the loss of which would set back Cosmic Explorer significantly. It is thus of particular importance to sustain this expertise during the transition from current detectors (Advanced LIGO, A+) to Cosmic Explorer.
3. International partnerships can present difficult complexities in several ways, including: the length of time needed to put them into place; the probable need for negotiations between high levels of government; differing costing protocols between countries (making cost assessments difficult to compare); ensuring that a single management structure has adequate authority; and differing work rules. Similar issues can arise also between states and funding agencies within the U.S., though they are usually more easily managed.

## 11.5 Synergies with Programs at U.S. Funding Agencies

Cosmic Explorer's unique capabilities to explore extreme gravity and to search for new physics complement the priorities and planned missions of several funding agencies in the United States. (A comprehensive description of the "European Strategy for Particle Physics" is available in the 2020 Physics Briefing Book.<sup>254</sup>)

1. NSF: The Divisions of Astronomy<sup>561</sup> (AST, \$250M 2019 Current Plan) and Physics<sup>562</sup> (PHY, \$285M 2019 Actual), and the Office of Polar Programs<sup>563</sup> (OPP, \$398M 2019 Actual) all make large investments in the study of black holes, stellar evolution, nuclear physics, dark energy and dark matter. Instruments such as LIGO, IceCube, the Event Horizon Telescope, and optical and radio telescopes are located at many sites around the world, including the South Pole.



2. DOE: The DOE program<sup>564</sup> in High Energy Physics (HEP, \$1.01B 2019 request) comprises: the Energy Frontier, the Intensity Frontier and the Cosmic Frontier. The intellectual basis for the program is described in the 2014 “P5” report.<sup>565</sup> The overall science focus is on the Higgs boson, neutrino mass, dark matter, cosmic acceleration and “exploring the unknown.” The “Cosmic Frontier” program (\$75.5M 2019 request) supports the ongoing Fermi/GLAST, AMS, HAWC, DES and eBOSS experiments. It is constructing the Rubin Observatory and DESI for research into dark energy, and LZ and SuperCDMS-SNOlab for dark matter searches. Via the SPT-3G it explores the CMB to study cosmic acceleration and neutrino properties (with NSF). There is also an extensive program in cosmic-ray and gamma-ray research (AMS, HAWC). Nuclear Physics programs of the Office of Science, such as the Facility for Rare Isotope Beams (FRIB), actively develop connections to nuclear astrophysics.<sup>566</sup>
3. NASA: The Astrophysics Program<sup>567</sup> (\$1.496B 2019 request) plays the lead role in eight operating missions (e.g., Hubble, FGST, NICER, TESS), and five in development (e.g., JWST, WFIRST). It is a partner in the development of Euclid and LISA. The NASA Physics of the Cosmos program focuses on dark matter and dark energy, the evolution of galaxies and stars, and matter and energy in extreme environments. The LISA program<sup>568</sup> in GW research is closely tied to LIGO/Virgo, and possibly to Cosmic Explorer and the European Einstein Telescope.<sup>569</sup>

## 11.6 Cosmic Explorer Project Roadmap

In proceeding with the Cosmic Explorer Project, we will draw on the successful experience and expertise of the LIGO Lab and the lessons learned during LIGO’s planning, construction, and operation. The LIGO Lab now has a long history of delivering on time and on budget, has been well operated and managed, and has delivered important scientific discoveries. The LIGO Lab has consistently received high ratings for its leadership and management. As a result of these attributes, morale within the LIGO Lab has generally been very high. We recognize this quality as one of the greatest assets to any project and one which must be preserved for Cosmic Explorer.

We also recognize that the CE Project is significantly larger in scale and will require greater sophistication in the Project organization, and a larger breadth of participation and support in the project.

In planning the next steps for the Project, three resources have been of particular value:

- The NSF Major Facilities Guide (MFG).<sup>3</sup>
- The book chapter on “Planning, managing, and executing the design and construction of Advanced LIGO”<sup>570</sup> by David Shoemaker, who led the Advanced LIGO Project. This chapter was written with future projects in mind to provide experience, generalizations, and lessons learned from both Initial and Advanced LIGO.

- Advice and experience shared by the management and staff of LIGO, other gravitational-wave observatories world-wide, and other large-scale scientific facilities.

The Cosmic Explorer Project will proceed along the guidelines provided in the Major Facilities Guide. In broad outline, these are to:

- collect feedback from the broad scientific community on the match of the Cosmic Explorer concept and capability with their needs and interests, using the Horizon Study as a basis for discussion. In this process the parties (individuals and institutions) interested in engaging substantively in the next Project phases can be identified. Partnership arrangements and international participation will be informally explored.
- collect feedback from the NSF, and address any specific shortcomings to ensure that the NSF can correctly consider the Project; feedback on next steps will be welcome.
- cast the Horizon study into the form of a Project Execution Plan, and start to address those elements most in need of refinement. Several of these elements follow.
- establish the core of a Project Office, and within it a system engineering activity.
- establish a plan to create an accurate, detailed, costed baseline project description that provides the project performance goals, the technical aspects of the facility, its estimated cost and the time required for completion. This will become the *Reference Design* for the project. This essential document provides the point of departure for measuring progress accurately and for assessing cost, schedule and technical performances.
- establish an orderly process for implementing project changes even at an early conceptual phase, and maintain an accurate record of them as they occur.
- identify potential critical and near-critical paths through the schedule. Ensure that early effort is allocated to assess these activities to firm up estimates, and explore mitigation where possible.
- develop a plan for identifying and managing risk (*cf.* §11.4)
- research and document “lessons learned” during the construction of LIGO, Advanced LIGO and A+, as well as from observatories constructed outside the U.S. (GEO, KAGRA, LIGO India, Einstein Telescope) and other large facilities (e.g., the Thirty Meter Telescope).
- draft a Scope Management Plan and explore scope contingency responses to anticipate means to explore savings from potential de-scoping options, and find decision points for exercising options.
- establish robust means of communication with the external physics and astronomy communities and the public.

- collaborate with other relevant Projects (e.g., Einstein Telescope) to leverage technical and scientific opportunities whenever possible.
- establish and maintain a strong community engagement and integration program with the objective of building synergistic relationships with local communities at potential Observatory sites, including Indigenous Peoples.

These activities will be focused (and iteratively tuned) with a target of creating a technical development roadmap with estimates of funding and more detail on the magnitude of the challenges associated with technical development work. A goal will be to support a critical review by mid-decade to enable a detailed engineering design study.

The pace and character of this followup activity will depend on the funding available to the Project. Seeking that funding will be one of the first activities to follow the completion of the Horizon Study.

## 12 Conclusion

This Horizon Study has described a path forward for realizing Cosmic Explorer, a next-generation, ground-based gravitational-wave observatory in the United States. By drawing on two decades of international effort to scale up the proven technology that has enabled humanity's first observations of gravitational waves, Cosmic Explorer will extend our gravitational-wave vision to the farthest reaches of the universe.

In this study, we have described a science-driven design for Cosmic Explorer and have considered how to optimize the design performance versus the cost. We presented a technical overview of the detectors and a roadmap to the research and development required to achieve them. We have further examined the organization, planning, and community engagement that will be necessary to design, build, and operate Cosmic Explorer.

During the next few years, we will welcome feedback from the National Science Foundation, the National Research Council, and from the gravitational-wave community; their guidance and endorsement will be critical to the success of the next generation of gravitational-wave science in the United States. We aspire for this study to prepare the way, through the next two decades, for the ultimate design, construction, and operation of Cosmic Explorer.

Continued funding to develop enabling technologies, grow the CE community and build relationships with potential observatory host communities is crucial to preparing the CE Project for critical review in the mid-2020s. If CE is determined to be technically ready, of interest and timely, we expect that a thorough design study will begin, leading to a complete design and construction plan that will be funded in the late-2020s.

Once operational, its cosmic reach and exquisite sensitivity will enable Cosmic Explorer to revolutionize our understanding of the universe while continuing the United States' leadership in gravitational-wave science. Cosmic Explorer will observe black holes and neutron stars throughout cosmic time, probe the nature and behavior of the densest matter in the universe, and explore the universe's most extreme gravity and open questions in fundamental physics. As part of an international next-generation gravitational-wave network, Cosmic Explorer would couple these advances in gravitational-wave astronomy with the future of electromagnetic and particle astronomy.

## Acknowledgements

We would like to thank the National Science Foundation for supporting this study through the collaborative awards NSF–1836814, NSF–1836779, NSF–1836702, NSF–1836809, and NSF–1836734. We also thank the Australian Research Council, who provided funding through grant CE170100004, as well as the MathWorks, Inc., and the Heising-Simons foundation. We would also like to thank the members of this study’s advisory panel, Patrick Brady, Kathryn Daniel, Gabriela González, Vicky Kalogera, Harald Lück, David Reitze, Sheila Rowan, and Jim Yeck, for their advice and helpful suggestions throughout the study. Furthermore, we are very grateful to the gravitational-wave community and especially the Gravitational-Wave International Committee, both for their work toward the next generation of gravitational-wave observatories and for their feedback on this study.

The authors, as a group and individually, acknowledge the ancestral homelands we were on during the creation of this work.<sup>a</sup> The authors acknowledge Indigenous Peoples as the traditional stewards of the land, and the enduring relationship that exists between them and their traditional territories. We acknowledge the longer history of these lands and our place in that history, and we pay our respects to the Indigenous land caretakers past, present, and emerging. The MIT authors acknowledge our presence on the traditional, ancestral, and unceded territory of the Wampanoag and Pawtucket Nations. The Syracuse University authors acknowledge with respect the Onondaga Nation, firekeepers of the Haudenosaunee, the Indigenous peoples on whose ancestral lands Syracuse University now stands. The Pennsylvania State University campuses are located on the original homelands of the Erie, Haudenosaunee (Seneca, Cayuga, Onondaga, Oneida, Mohawk, and Tuscarora), Lenape (Delaware Nation, Delaware Tribe, Stockbridge-Munsee), Shawnee (Absentee, Eastern, and Oklahoma), Susquehannock, and Wahzhazhe (Osage) Nations. The Penn State authors acknowledge and honor the traditional caretakers of these lands and strive to understand and model their responsible stewardship. The University of Mississippi authors recognize and acknowledge that their university is on the historic Homeland of the Chickasaw Nation. The Caltech and Cal State Fullerton authors acknowledge and offer our respect to past and present Gabrielino-Tongva people and their unceded ancestral lands, including the Los Angeles Basin where Caltech and Cal State Fullerton stand today. The U.C. Santa Cruz authors acknowledge that the land on which the university stands is the unceded territory of the Awaswas-speaking Uypi Tribe.

Finally, the PIs on the grants that funded this work are deeply grateful to the graduate student and postdoctoral scholar co-authors who worked tirelessly to make this Horizon Study a reality.

<sup>a</sup>We are grateful for the work of Native Land Digital (<https://native-land.ca>) for the resources they have provided.

## Cost and Inflation Estimates

This appendix describes the inflation estimates that went into the cost tables presented in §11. This is done in two parts: first, the cost tables are presented in 2021 USD, and then the process used to compute the “2030 USD” estimates is described.

### 1 Cost Estimates in 2021 USD

The following cost tables represent the same content as the ones presented in §11.1 and §11.3. The only difference is that they are presented in 2021 USD, i.e. without any attempt to estimate future inflation rates.

<b>Top-Level Costs</b>	<b>\$(M) 2021 USD</b>	<b>Percent</b>
Civil Engineering	422	26
Vacuum System	569	34
Detector	432	26
Management, Design, Project	227	14
<b>Grand Total (2 Observatories)</b>	<b>1650</b>	<b>100</b>

Table 1: Top-level cost breakdown for Cosmic Explorer including 20 % contingency, but excluding operating costs, in millions of 2021 US dollars. The content of this table is the same as Table 11.2, but with no attempt to estimate future inflation.

<b>Yearly Operations Cost Estimates</b>	<b>\$(M) 2021 USD</b>	<b>Percent</b>
Facilities	18	30
Vacuum Systems	7.7	13
Detector	16.9	28
Analysis, Data, and Computing	7.2	12
Management	5.7	9
Community Engagement	4.7	8
<b>Grand Total (2 Observatories)</b>	<b>60.2</b>	<b>100</b>

Table 2: Estimated yearly operations costs for Cosmic Explorer with two observatories, based on Advanced LIGO and scaled for CE facility sizes, in millions of 2021 US dollars. The content of this table is the same as Table 11.3, but with no attempt to estimate future inflation.



## Cosmic Explorer Cost Estimates, \$(M) 2021 USD

Observatory Costs	20 km	40 km	Project Level Costs	
<i>Management</i>			<i>Project Wide</i>	
Civil Engineering	12	23	Management	20
Vacuum System	17	31	Coordination	5
Detector	18	18	Computing	10
<i>Total</i>	47	72	<i>Total</i>	35
<i>Site Specific Design</i>			<i>Common Design</i>	
Civil Engineering	2.5	2.5	Civil Engineering	15
Vacuum System	0.7	0.7	Vacuum System	7
Detector	0.9	0.9	Detector	5
<i>Total</i>	4.1	4.1	<i>Total</i>	27
<i>Realization</i>			<b>Project Level Total 62</b>	
Civil Engineering	118	234		
Vacuum System	168	306		
Detector	180	180		
<i>Total</i>	466	720		
<b>Observatory Total</b>	<b>517</b>	<b>796</b>	<b>Contingency</b>	
			20 km Observatory	103
			40 km Observatory	159
			Project Level	12

**Grand Total for Reference Concept (2 Observatories) 1649**

Table 3: Reproduction of the cost estimate presented in Table 11.1, but here in millions of 2021 US dollars (i.e., with no attempt to estimate future inflation). The cost estimate includes design, materials, construction, installation and project management for the civil engineering (buildings, roads, etc.), the vacuum system, and the detector. The cost of alternate configurations can be estimated by adding the associated observatory costs to the project-level costs (e.g., \$1314 M 2021 USD for two 20 km observatories, or \$1029 M 2021 USD for a single 40 km observatory).

## 2 Inflation Estimates for Cosmic Explorer Project

The cost tables in §11 are given in “2030 USD”. This is intended to give the reader access to dollar values representative of what the Cosmic Explorer Project will cost in then-year dollars assuming the timeline show in Fig. 11.1. The spending profile used for this computation is drawn from experience with other large projects, including LIGO construction and the Advanced LIGO upgrade. In our estimation, spending on the CE project begins with the Conceptual Design phase of the MREFC process in 2024, peaks in the years around 2030 with observatory construction, and ramps-down to zero in 2035 as the Project enters the Operations phase. Inflation in the years from 2022 to 2035 is assumed to be 2.3 % per year. Since spending peaks around 2030, the total project cost is inflated by an amount which is numerically equivalent to the estimated inflation from 2021 to 2030: roughly 25 %. Rather than presenting cost estimates in §11 in then-year dollars, which would add significant complexity and indicate a level of precision that we feel is unwarranted at this stage, we simply inflate all values by 25 % and label these inflated

## Cost and Inflation Estimates

estimates as 2030 USD. In recognition of the uncertainty in this estimate, especially in light of the COVID-19 pandemic, the previous section presents values in 2021 USD.

## Abbreviations

<b>2G</b>	Second generation of gravitational-wave detectors
<b>3G</b>	Third generation of gravitational-wave detectors
<b>A+</b>	LIGO A+ upgrade
<b>AAS</b>	American Astronomical Society
<b>AISES</b>	American Indian Science and Engineering Society
<b>APS</b>	American Physical Society
<b>BBH</b>	Binary black hole
<b>BNS</b>	Binary neutron star
<b>BRDF</b>	Bidirectional reflectance distribution function
<b>CBO</b>	Compact-binary-optimized detector configuration
<b>CE</b>	Cosmic Explorer
<b>CERN</b>	European Organization for Nuclear Research
<b>DECIGO</b>	Decihertz Gravitational-Wave Observatory
<b>DOE</b>	Department of Energy
<b>ET</b>	Einstein Telescope
<b>EOS</b>	Equation of state
<b>GWAC</b>	Gravitational-Wave Agencies Correspondents
<b>GWADW</b>	Gravitational-Wave Advanced Detector Workshop
<b>GWIC</b>	Gravitational-Wave International Committee
<b>GWPAW</b>	Gravitational-Wave Physics and Astronomy Workshop
<b>IMBH</b>	Intermediate-mass black hole
<b>KAGRA</b>	Kamioka Gravitational-Wave Detector
<b>LIGO</b>	Laser Interferometer Gravitational-Wave Observatory
<b>LISA</b>	Laser Interferometer Space Antenna
<b>LSC</b>	LIGO Scientific Collaboration
<b>LVK</b>	LIGO–Virgo–KAGRA Collaboration
<b>MREFC</b>	NSF’s Major Research Equipment and Facilities Construction
<b>NASA</b>	National Aeronautics and Space Administration
<b>NEMO</b>	Neutron-Star Extreme Matter Observatory
<b>NIST</b>	National Institute of Standards and Technology
<b>NSF</b>	National Science Foundation
<b>PMO</b>	Postmerger-optimized detector configuration
<b>QCD</b>	Quantum chromodynamics
<b>SACNAS</b>	Society for Advancement of Chicanos/Hispanics and Native Americans in Science

## Abbreviations

**SMBH** Supermassive black hole

**SNR** Signal-to-noise ratio

**UHV** Ultrahigh vacuum

**USD** US dollars

## References

1. *GWIC-3G Subcommittee Reports on Next Generation Ground-based Observatories*, Gravitational Wave International Committee, <https://gwic.ligo.org/3Gsubcomm/documents.html> (visited on 5 July 2021) (cit. on pp. 6, 10, 27, 29, 80, 112).
2. ET Steering Committee, *ET Design Report Update 2020*, tech. rep. ET-0007A-20 (Einstein Telescope, Nov. 2020) (cit. on pp. 6, 15).
3. NSF Large Facilities Office, *Major Facilities Guide*, NSF 19–68 (National Science Foundation, Sept. 2019) (cit. on pp. 6, 117, 118, 125).
4. *Future Ground-Based Gravitational-Wave Observatories: Synergies with Other Scientific Communities*, tech. rep. (GWIC, Apr. 2021) (cit. on pp. 6, 104).
5. B. S. Sathyaprakash et al., “Multimessenger Universe with Gravitational Waves from Binaries”, (2019), [arXiv:1903.09277](https://arxiv.org/abs/1903.09277) [astro-ph.HE] (cit. on p. 10).
6. V. Kalogera et al., “The Yet-Unobserved Multi-Messenger Gravitational-Wave Universe”, (2019), [arXiv:1903.09224](https://arxiv.org/abs/1903.09224) [astro-ph.HE] (cit. on p. 10).
7. V. Kalogera et al., “Deeper, Wider, Sharper: Next-Generation Ground-Based Gravitational-Wave Observations of Binary Black Holes”, (2019), [arXiv:1903.09220](https://arxiv.org/abs/1903.09220) [astro-ph.HE] (cit. on p. 10).
8. B. S. Sathyaprakash et al., “Cosmology and the Early Universe”, (2019), [arXiv:1903.09260](https://arxiv.org/abs/1903.09260) [astro-ph.HE] (cit. on p. 10).
9. B. S. Sathyaprakash et al., “Extreme Gravity and Fundamental Physics”, (2019), [arXiv:1903.09221](https://arxiv.org/abs/1903.09221) [astro-ph.HE] (cit. on p. 10).
10. M. Maggiore et al., “Science case for the Einstein telescope”, *J. Cosmology Astropart. Phys.* **2020**, 050 (2020) (cit. on p. 10).
11. H.-Y. Chen et al., “Distance measures in gravitational-wave astrophysics and cosmology”, *Classical and Quantum Gravity* **38**, 055010 (2021) (cit. on p. 12).
12. P. Madau and M. Dickinson, “Cosmic Star Formation History”, *Ann. Rev. Astron. Astrophys.* **52**, 415–486 (2014) (cit. on pp. 13, 19, 51).
13. J. Aasi et al. (LIGO Scientific), “Advanced LIGO”, *Class. Quant. Grav.* **32**, 074001 (2015) (cit. on p. 14).
14. B. P. Abbott et al. (LIGO Scientific, Virgo), “Observation of Gravitational Waves from a Binary Black Hole Merger”, *Phys. Rev. Lett.* **116**, 061102 (2016) (cit. on pp. 14, 26).
15. B. P. Abbott et al. (LIGO Scientific, Virgo), “GW151226: Observation of Gravitational Waves from a 22-Solar-Mass Binary Black Hole Coalescence”, *Phys. Rev. Lett.* **116**, 241103 (2016) (cit. on p. 14).
16. B. P. Abbott et al. (LIGO Scientific, Virgo), “Binary Black Hole Mergers in the first Advanced LIGO Observing Run”, *Phys. Rev. X* **6**, [Erratum: *Phys.Rev.X* **8**, 039903 (2018)], 041015 (2016) (cit. on p. 14).

## References

17. B. P. Abbott et al. (LIGO Scientific, Virgo), “The Rate of Binary Black Hole Mergers Inferred from Advanced LIGO Observations Surrounding GW150914”, *Astrophys. J. Lett.* **833**, L1 (2016) (cit. on p. 14).
18. B. P. Abbott et al. (LIGO Scientific, Virgo), “Tests of general relativity with GW150914”, *Phys. Rev. Lett.* **116**, [Erratum: *Phys.Rev.Lett.* 121, 129902 (2018)], 221101 (2016) (cit. on pp. 14, 26).
19. F. Acernese et al. (VIRGO), “Advanced Virgo: a second-generation interferometric gravitational wave detector”, *Class. Quant. Grav.* **32**, 024001 (2015) (cit. on p. 14).
20. B. P. Abbott et al. (LIGO Scientific, Virgo), “GW170817: Observation of Gravitational Waves from a Binary Neutron Star Inspiral”, *Phys. Rev. Lett.* **119**, 161101 (2017) (cit. on pp. 14, 26).
21. B. P. Abbott et al. (LIGO Scientific, Virgo, Fermi GBM, INTEGRAL, IceCube, AstroSat Cadmium Zinc Telluride Imager Team, IPN, Insight-Hxmt, ANTARES, Swift, AGILE Team, IM2H Team, Dark Energy Camera GW-EM, DES, DLT40, GRAWITA, Fermi-LAT, ATCA, ASKAP, Las Cumbres Observatory Group, OzGrav, DWF (Deeper Wider Faster Program), AST3, CAASTRO, VINROUGE, MASTER, J-GEM, GROWTH, JAGWAR, CaltechNRAO, TTU-NRAO, NuSTAR, Pan-STARRS, MAXI Team, TZAC Consortium, KU, Nordic Optical Telescope, ePESSTO, GROND, Texas Tech University, SALT Group, TOROS, BOOTES, MWA, CALET, IKI-GW Follow-up, H.E.S.S., LOFAR, LWA, HAWC, Pierre Auger, ALMA, Euro VLBI Team, Pi of Sky, Chandra Team at McGill University, DFN, ATLAS Telescopes, High Time Resolution Universe Survey, RIMAS, RATIR, SKA South Africa/MeerKAT), “Multi-messenger Observations of a Binary Neutron Star Merger”, *Astrophys. J. Lett.* **848**, L12 (2017) (cit. on p. 14).
22. B. P. Abbott et al. (LIGO Scientific, Virgo, Fermi-GBM, INTEGRAL), “Gravitational Waves and Gamma-rays from a Binary Neutron Star Merger: GW170817 and GRB 170817A”, *Astrophys. J. Lett.* **848**, L13 (2017) (cit. on p. 14).
23. B. P. Abbott et al. (LIGO Scientific, Virgo, IM2H, Dark Energy Camera GW-E, DES, DLT40, Las Cumbres Observatory, VINROUGE, MASTER), “A gravitational-wave standard siren measurement of the Hubble constant”, *Nature* **551**, 85–88 (2017) (cit. on p. 14).
24. M. R. Drout et al., “Light curves of the neutron star merger GW170817/SSS17a: Implications for r-process nucleosynthesis”, *Science* **358**, 1570–1574 (2017) (cit. on p. 14).
25. S. De et al., “Tidal Deformabilities and Radii of Neutron Stars from the Observation of GW170817”, *Phys. Rev. Lett.* **121**, 091102 (2018) (cit. on p. 14).
26. B. P. Abbott et al., “GWTC-1: A Gravitational-Wave Transient Catalog of Compact Binary Mergers Observed by LIGO and Virgo during the First and Second Observing Runs”, *Physical Review X* **9**, 031040 (2019) (cit. on pp. 14, 26).
27. A. H. Nitz et al., “1-OGC: The First Open Gravitational-wave Catalog of Binary Mergers from Analysis of Public Advanced LIGO Data”, *ApJ* **872**, 195 (2019) (cit. on p. 14).
28. A. H. Nitz et al., “2-OGC: Open Gravitational-wave Catalog of Binary Mergers from Analysis of Public Advanced LIGO and Virgo Data”, *ApJ* **891**, 123 (2020) (cit. on p. 14).
29. T. Venumadhav et al., “New binary black hole mergers in the second observing run of Advanced LIGO and Advanced Virgo”, *Phys. Rev. D* **101**, 083030 (2020) (cit. on p. 14).



## References

30. B. P. Abbott et al. (LIGO Scientific, Virgo), “Low-latency Gravitational-wave Alerts for Multimessenger Astronomy during the Second Advanced LIGO and Virgo Observing Run”, *Astrophys. J.* **875**, 161 (2019) (cit. on p. 14).
31. R. Abbott et al. (LIGO Scientific, Virgo), “Population Properties of Compact Objects from the Second LIGO-Virgo Gravitational-Wave Transient Catalog”, *Astrophys. J. Lett.* **913**, L7 (2021) (cit. on pp. 14, 18, 51).
32. T. Akutsu et al. (KAGRA), “KAGRA: 2.5 Generation Interferometric Gravitational Wave Detector”, *Nature Astron.* **3**, 35–40 (2019) (cit. on p. 14).
33. J. Miller et al., “Prospects for doubling the range of Advanced LIGO”, *Phys. Rev. D* **91**, 062005 (2015) (cit. on p. 14).
34. T. Souradeep et al., “LIGO-India - a unique adventure in Indian science”, *Current Science* **113**, 672 (2017) (cit. on p. 14).
35. R. X. Adhikari et al., “A cryogenic silicon interferometer for gravitational-wave detection”, *Classical and Quantum Gravity* **37**, 165003 (2020) (cit. on pp. 14, 41, 80, 83, 92).
36. B. Shapiro et al., “Cryogenically cooled ultra low vibration silicon mirrors for gravitational wave observatories”, *Cryogenics* **81**, 83–92 (2017) (cit. on pp. 14, 89).
37. A. Brooks, *Mariner-40m: Current Status*, tech. rep. LIGO–G2100910 (LIGO, 2021) (cit. on pp. 14, 77).
38. ETpathfinder Team, *ETpathfinder Design Report*, tech. rep. (Nikhef, Maastricht University, University of Antwerp, Ghent University, Katholieke Universiteit Leuven, Universite Catholique de Louvain, Hasselt University, Vrije Universiteit Brussel, Fraunhofer Institute for Laser Technology, RWTH Aachen, University of Twente, Eindhoven University of Technology, Liege Universite, VITO, TNO, 2021) (cit. on pp. 14, 77).
39. *ESFRI announces the 11 new Research Infrastructures to be included in its Roadmap 2021*, European Strategy Forum on Research Infrastructures, (2021) <https://www.esfri.eu/latest-esfri-news/new-ris-roadmap-2021> (visited on 5 July 2021) (cit. on p. 15).
40. *ET*, Einstein Telescope, <http://www.et-gw.eu> (visited on 11 May 2021) (cit. on p. 15).
41. K. Ackley et al., “Neutron Star Extreme Matter Observatory: A kilohertz-band gravitational-wave detector in the global network”, *PASA* **37**, e047 (2020) (cit. on pp. 15, 43, 111).
42. D. Reitze et al., “Cosmic Explorer: The U.S. Contribution to Gravitational-Wave Astronomy beyond LIGO”, *Bull. Am. Astron. Soc.* **51**, 035 (2019) (cit. on pp. 15, 110, 116).
43. B. P. Abbott et al. (LIGO Scientific), “Exploring the Sensitivity of Next Generation Gravitational Wave Detectors”, *Class. Quant. Grav.* **34**, 044001 (2017) (cit. on p. 15).
44. J. P. Ostriker and N. Y. Gnedin, “Reheating of the Universe and Population III”, *ApJ* **472**, L63 (1996) (cit. on p. 16).
45. V. Bromm, P. S. Coppi and R. B. Larson, “The Formation of the First Stars. I. The Primordial Star-forming Cloud”, *ApJ* **564**, 23–51 (2002) (cit. on p. 16).
46. <https://www.jwst.nasa.gov/index.html> (cit. on p. 17).

## References

47. E. Zackrisson et al., “Detecting gravitationally lensed Population III galaxies with the Hubble Space Telescope and the James Webb Space Telescope”, *MNRAS* **427**, 2212–2223 (2012) (cit. on p. 17).
48. C.-E. Rydberg et al., “Detection of isolated Population III stars with the James Webb Space Telescope”, *MNRAS* **429**, 3658–3664 (2013) (cit. on p. 17).
49. S. E. Woosley and T. A. Weaver, “The Evolution and Explosion of Massive Stars. II. Explosive Hydrodynamics and Nucleosynthesis”, *ApJS* **101**, 181 (1995) (cit. on p. 17).
50. D. Schaerer, “On the properties of massive Population III stars and metal-free stellar populations”, *A&A* **382**, 28–42 (2002) (cit. on p. 17).
51. A. Heger and S. E. Woosley, “The Nucleosynthetic Signature of Population III”, *ApJ* **567**, 532–543 (2002) (cit. on p. 17).
52. G. Costa et al., “Formation of GW190521 from stellar evolution: the impact of the hydrogen-rich envelope, dredge-up, and  $^{12}\text{C}(\alpha, \gamma)^{16}\text{O}$  rate on the pair-instability black hole mass gap”, *MNRAS* **501**, 4514–4533 (2021) (cit. on p. 17).
53. K.-J. Chen et al., “Pair Instability Supernovae of Very Massive Population III Stars”, *ApJ* **792**, 44 (2014) (cit. on p. 17).
54. <https://www.lynxobservatory.com/> (cit. on p. 17).
55. <https://www.the-athena-x-ray-observatory.eu/> (cit. on p. 17).
56. P. Amaro-Seoane et al. (LISA), “Laser Interferometer Space Antenna”, (2017), [arXiv:1702.00786](https://arxiv.org/abs/1702.00786) [astro-ph.IM] (cit. on p. 17).
57. S. Babak et al., “Science with the space-based interferometer LISA. V. Extreme mass-ratio inspirals”, *Phys. Rev. D* **95**, 103012 (2017) (cit. on p. 17).
58. J. R. Gair et al., “Prospects for observing extreme-mass-ratio inspirals with LISA”, in *Journal of Physics Conference Series*, Vol. 840, *Journal of Physics Conference Series* (May 2017), p. 012021, [arXiv:1704.00009](https://arxiv.org/abs/1704.00009) [astro-ph.GA] (cit. on p. 17).
59. L. Ferrarese and D. Merritt, “A Fundamental relation between supermassive black holes and their host galaxies”, *Astrophys. J. Lett.* **539**, L9 (2000) (cit. on p. 17).
60. J. Kormendy and L. C. Ho, “Coevolution (Or Not) of Supermassive Black Holes and Host Galaxies”, *Ann. Rev. Astron. Astrophys.* **51**, 511–653 (2013) (cit. on p. 17).
61. F. Wang et al., “A Luminous Quasar at Redshift 7.642”, *ApJ* **907**, L1 (2021) (cit. on p. 17).
62. J. E. Greene, J. Strader and L. C. Ho, “Intermediate-Mass Black Holes”, *ARA&A* **58**, 257–312 (2020) (cit. on p. 18).
63. A. Sesana, “Prospects for Multiband Gravitational-Wave Astronomy after GW150914”, *Phys. Rev. Lett.* **116**, 231102 (2016) (cit. on p. 18).
64. S. Vitale, “Multiband Gravitational-Wave Astronomy: Parameter Estimation and Tests of General Relativity with Space- and Ground-Based Detectors”, *Phys. Rev. Lett.* **117**, 051102 (2016) (cit. on p. 18).

## References

65. E. Barausse, N. Yunes and K. Chamberlain, “Theory-Agnostic Constraints on Black-Hole Dipole Radiation with Multiband Gravitational-Wave Astrophysics”, *Phys. Rev. Lett.* **116**, 241104 (2016) (cit. on p. 18).
66. C. Cutler et al., “What can we learn from multi-band observations of black hole binaries?”, *BAAS* **51**, 109 (2019) (cit. on p. 18).
67. R. Abbott et al., “GW190814: Gravitational Waves from the Coalescence of a 23 Solar Mass Black Hole with a 2.6 Solar Mass Compact Object”, *ApJ* **896**, L44 (2020) (cit. on p. 18).
68. R. Abbott et al., “GW190521: A Binary Black Hole Merger with a Total Mass of 150  $M_{\odot}$ ”, *Phys. Rev. Lett.* **125**, 101102 (2020) (cit. on p. 18).
69. T. Damour, “Coalescence of two spinning black holes: an effective one-body approach”, *Phys. Rev. D* **64**, 124013 (2001) (cit. on p. 18).
70. E. Racine, “Analysis of spin precession in binary black hole systems including quadrupole-monopole interaction”, *Phys. Rev. D* **78**, 044021 (2008) (cit. on p. 18).
71. R. Abbott et al. (LIGO Scientific, Virgo), “GWTC-2: Compact Binary Coalescences Observed by LIGO and Virgo During the First Half of the Third Observing Run”, *Phys. Rev. X* **11**, 021053 (2021) (cit. on pp. 18, 25).
72. M. Zevin et al., “One Channel to Rule Them All? Constraining the Origins of Binary Black Holes Using Multiple Formation Pathways”, *Astrophys. J.* **910**, 152 (2021) (cit. on p. 18).
73. M. Mapelli, “Astrophysics of stellar black holes”, [arXiv:1809.09130](https://arxiv.org/abs/1809.09130) (cit. on p. 18).
74. I. Mandel and A. Farmer, “Merging stellar-mass binary black holes”, [arXiv:1806.05820](https://arxiv.org/abs/1806.05820) (cit. on p. 18).
75. M. Mapelli, “Formation channels of single and binary stellar-mass black holes”, [arXiv:2106.00699](https://arxiv.org/abs/2106.00699) (cit. on p. 18).
76. E. P. J. van den Heuvel, “Late Stages of Close Binary Systems”, in *Structure and Evolution of Close Binary Systems*, Vol. 73, edited by P. Eggleton, S. Mitton and J. Whelan (Jan. 1976), p. 35 (cit. on p. 18).
77. B. Paczynski, “Common Envelope Binaries”, in *Structure and Evolution of Close Binary Systems*, Vol. 73, edited by P. Eggleton, S. Mitton and J. Whelan (Jan. 1976), p. 75 (cit. on p. 18).
78. L. L. Smarr and R. Blandford, “The binary pulsar: physical processes, possible companions, and evolutionary histories.”, *ApJ* **207**, 574–588 (1976) (cit. on p. 18).
79. A. V. Tutukov and L. R. Yungelson, “The merger rate of neutron star and black hole binaries.”, *MNRAS* **260**, 675–678 (1993) (cit. on p. 18).
80. M. Dominik et al., “Double Compact Objects I: The Significance of the Common Envelope on Merger Rates”, *Astrophys. J.* **759**, 52 (2012) (cit. on p. 18).
81. S. R. Kulkarni, P. Hut and S. McMillan, “Stellar black holes in globular clusters”, *Nature* **364**, 421–423 (1993) (cit. on p. 18).
82. S. Sigurdsson and L. Hernquist, “Primordial black holes in globular clusters”, *Nature* **364**, 423–425 (1993) (cit. on p. 18).

## References

83. S. F. Portegies Zwart and S. L. W. McMillan, “Black Hole Mergers in the Universe”, *ApJ* **528**, L17–L20 (2000) (cit. on p. 18).
84. C. L. Rodriguez, S. Chatterjee and F. A. Rasio, “Binary Black Hole Mergers from Globular Clusters: Masses, Merger Rates, and the Impact of Stellar Evolution”, *Phys. Rev. D* **93**, 084029 (2016) (cit. on p. 18).
85. S. Rastello et al., “Stellar Black Hole Binary Mergers in Open Clusters”, *Mon. Not. Roy. Astron. Soc.* **483**, 1233–1246 (2019) (cit. on p. 18).
86. I. Bartos et al., “Rapid and Bright Stellar-mass Binary Black Hole Mergers in Active Galactic Nuclei”, *Astrophys. J.* **835**, 165 (2017) (cit. on p. 18).
87. M. J. Graham et al., “Candidate Electromagnetic Counterpart to the Binary Black Hole Merger Gravitational Wave Event S190521g”, *Phys. Rev. Lett.* **124**, 251102 (2020) (cit. on pp. 18, 27).
88. D. Gerosa and E. Berti, “Are merging black holes born from stellar collapse or previous mergers?”, *Phys. Rev. D* **95**, 124046 (2017) (cit. on p. 18).
89. M. Fishbach, D. E. Holz and B. Farr, “Are LIGO’s Black Holes Made From Smaller Black Holes?”, *Astrophys. J. Lett.* **840**, L24 (2017) (cit. on p. 18).
90. K. Chatziioannou et al., “On the properties of the massive binary black hole merger GW170729”, *Phys. Rev. D* **100**, 104015 (2019) (cit. on p. 18).
91. C. Kimball et al., “Evidence for Hierarchical Black Hole Mergers in the Second LIGO–Virgo Gravitational Wave Catalog”, *Astrophys. J. Lett.* **915**, L35 (2021) (cit. on p. 18).
92. K. Belczynski, V. Kalogera and T. Bulik, “A Comprehensive study of binary compact objects as gravitational wave sources: Evolutionary channels, rates, and physical properties”, *Astrophys. J.* **572**, 407–431 (2001) (cit. on p. 18).
93. R. O’Shaughnessy, D. Gerosa and D. Wysocki, “Inferences about supernova physics from gravitational-wave measurements: GW151226 spin misalignment as an indicator of strong black-hole natal kicks”, *Phys. Rev. Lett.* **119**, 011101 (2017) (cit. on p. 18).
94. T. Callister et al., “Shouts and Murmurs: Combining Individual Gravitational-Wave Sources with the Stochastic Background to Measure the History of Binary Black Hole Mergers”, *Astrophys. J. Lett.* **896**, L32 (2020) (cit. on p. 19).
95. K. K. Y. Ng et al., “Probing Multiple Populations of Compact Binaries with Third-generation Gravitational-wave Detectors”, *ApJ* **913**, L5 (2021) (cit. on pp. 19, 37, 38, 51).
96. B. P. Abbott et al., “GW190425: Observation of a Compact Binary Coalescence with Total Mass  $\sim 3.4 M_{\odot}$ ”, *ApJ* **892**, L3 (2020) (cit. on p. 19).
97. É. É. Flanagan and T. Hinderer, “Constraining neutron-star tidal Love numbers with gravitational-wave detectors”, *Phys. Rev. D* **77**, 021502 (2008) (cit. on p. 20).
98. T. Hinderer et al., “Tidal deformability of neutron stars with realistic equations of state and their gravitational wave signatures in binary inspiral”, *Phys. Rev. D* **81**, 123016 (2010) (cit. on p. 20).
99. T. Damour, A. Nagar and L. Villain, “Measurability of the tidal polarizability of neutron stars in late-inspiral gravitational-wave signals”, *Phys. Rev. D* **85**, 123007 (2012) (cit. on p. 20).

## References

100. K. Chatziioannou, “Neutron-star tidal deformability and equation-of-state constraints”, *General Relativity and Gravitation* **52**, 109 (2020) (cit. on p. 20).
101. C. Schmidt and S. Sharma, “The phase structure of QCD”, *Journal of Physics G Nuclear Physics* **44**, 104002 (2017) (cit. on p. 20).
102. G. Baym et al., “From hadrons to quarks in neutron stars: a review”, *Reports on Progress in Physics* **81**, 056902 (2018) (cit. on p. 20).
103. B. P. Abbott et al., “GW170817: Measurements of Neutron Star Radii and Equation of State”, *Phys. Rev. Lett.* **121**, 161101 (2018) (cit. on p. 20).
104. I. Tews, J. Margueron and S. Reddy, “Confronting gravitational-wave observations with modern nuclear physics constraints”, *European Physical Journal A* **55**, 97 (2019) (cit. on p. 20).
105. T. Dietrich et al., “Multimessenger constraints on the neutron-star equation of state and the Hubble constant”, *Science* **370**, 1450–1453 (2020) (cit. on p. 20).
106. F. Hernandez Vivanco et al., “Measuring the neutron star equation of state with gravitational waves: The first forty binary neutron star merger observations”, *Phys. Rev. D* **100**, 103009 (2019) (cit. on pp. 20, 90).
107. P. Landry, R. Essick and K. Chatziioannou, “Nonparametric constraints on neutron star matter with existing and upcoming gravitational wave and pulsar observations”, *Phys. Rev. D* **101**, 123007 (2020) (cit. on p. 20).
108. A. W. Shaw et al., “The radius of the quiescent neutron star in the globular cluster M13”, *MNRAS* **476**, 4713–4718 (2018) (cit. on p. 20).
109. J. Nattila et al., “Neutron star mass and radius measurements from atmospheric model fits to X-ray burst cooling tail spectra”, *A&A* **608**, A31 (2017) (cit. on p. 20).
110. M. C. Miller et al., “PSR J0030+0451 Mass and Radius from NICER Data and Implications for the Properties of Neutron Star Matter”, *ApJ* **887**, L24 (2019) (cit. on p. 20).
111. G. Raaijmakers et al., “Constraining the Dense Matter Equation of State with Joint Analysis of NICER and LIGO/Virgo Measurements”, *ApJ* **893**, L21 (2020) (cit. on p. 20).
112. J.-L. Jiang et al., “PSR J0030+0451, GW170817, and the Nuclear Data: Joint Constraints on Equation of State and Bulk Properties of Neutron Stars”, *ApJ* **892**, 55 (2020) (cit. on p. 20).
113. P. S. Ray et al., “STROBE-X: X-ray Timing and Spectroscopy on Dynamical Timescales from Microseconds to Years”, *arXiv:1903.03035* (cit. on p. 20).
114. R. Essick et al., “Direct astrophysical tests of chiral effective field theory at supranuclear densities”, *Phys. Rev. C* **102**, 055803 (2020) (cit. on p. 20).
115. K. Chatziioannou and S. Han, “Studying strong phase transitions in neutron stars with gravitational waves”, *Phys. Rev. D* **101**, 044019 (2020) (cit. on p. 20).
116. W. C. G. Ho and D. Lai, “Resonant tidal excitations of rotating neutron stars in coalescing binaries”, *MNRAS* **308**, 153–166 (1999) (cit. on p. 20).
117. N. N. Weinberg, P. Arras and J. Burkart, “An Instability due to the Nonlinear Coupling of p-modes to g-modes: Implications for Coalescing Neutron Star Binaries”, *ApJ* **769**, 121 (2013) (cit. on p. 20).

## References

118. G. Pratten, P. Schmidt and T. Hinderer, “Gravitational-wave asteroseismology with fundamental modes from compact binary inspirals”, *Nature Communications* **11**, 2553 (2020) (cit. on p. 20).
119. E. Poisson, “Gravitomagnetic tidal resonance in neutron-star binary inspirals”, *Phys. Rev. D* **101**, 104028 (2020) (cit. on p. 20).
120. N. Andersson, “A gravitational-wave perspective on neutron-star seismology”, *Universe* **7**, 97 (2021) (cit. on p. 20).
121. K. Riles, “Recent searches for continuous gravitational waves”, *Mod. Phys. Lett. A* **32**, 1730035 (2017) (cit. on p. 20).
122. N. Andersson, “A New class of unstable modes of rotating relativistic stars”, *Astrophys. J.* **502**, 708–713 (1998) (cit. on p. 20).
123. M. Sieniawska and M. Bejger, “Continuous gravitational waves from neutron stars: current status and prospects”, *Universe* **5**, 217 (2019) (cit. on pp. 20, 22).
124. G. Woan et al., “Evidence for a Minimum Ellipticity in Millisecond Pulsars”, *ApJ* **863**, L40 (2018) (cit. on p. 22).
125. D. Chakrabarty et al., “Nuclear-powered millisecond pulsars and the maximum spin frequency of neutron stars”, *Nature* **424**, 42–44 (2003) (cit. on p. 22).
126. D. Chakrabarty, “The spin distribution of millisecond X-ray pulsars”, in *A Decade of Accreting MilliSecond X-ray Pulsars*, Vol. 1068, edited by R. Wijnands et al., American Institute of Physics Conference Series (Oct. 2008), pp. 67–74, arXiv:0809.4031 [astro-ph] (cit. on p. 22).
127. A. Patruno, B. Haskell and N. Andersson, “The Spin Distribution of Fast-spinning Neutron Stars in Low-mass X-Ray Binaries: Evidence for Two Subpopulations”, *ApJ* **850**, 106 (2017) (cit. on p. 22).
128. M. Sieniawska and M. Bejger, “Continuous Gravitational Waves from Neutron Stars: Current Status and Prospects”, *Universe* **5**, 217 (2019) (cit. on p. 22).
129. N. Yasutake, T. Maruyama and T. Tatsumi, “Hot hadron-quark mixed phase including hyperons”, *Phys. Rev. D* **80**, 123009 (2009) (cit. on p. 22).
130. A. Kurkela and A. Vuorinen, “Cool Quark Matter”, *Phys. Rev. Lett.* **117**, 042501 (2016) (cit. on p. 22).
131. M. Oertel et al., “Hyperons in neutron stars and supernova cores”, *European Physical Journal A* **52**, 50 (2016) (cit. on p. 22).
132. E. R. Most et al., “Signatures of Quark-Hadron Phase Transitions in General-Relativistic Neutron-Star Mergers”, *Phys. Rev. Lett.* **122**, 061101 (2019) (cit. on p. 22).
133. H. Miao, H. Yang and D. Martynov, “Towards the design of gravitational-wave detectors for probing neutron-star physics”, *Phys. Rev. D* **98**, 044044 (2018) (cit. on p. 22).
134. H. Yang et al., “Gravitational wave spectroscopy of binary neutron star merger remnants with mode stacking”, *Phys. Rev. D* **97**, 024049 (2018) (cit. on p. 22).
135. D. Martynov et al., “Exploring the sensitivity of gravitational wave detectors to neutron star physics”, *Phys. Rev. D* **99**, 102004 (2019) (cit. on pp. 22, 43).



## References

136. R. Oechslin, H. .-. Janka and A. Marek, “Relativistic neutron star merger simulations with non-zero temperature equations of state. I. Variation of binary parameters and equation of state”, *A&A* **467**, 395–409 (2007) (cit. on p. 22).
137. A. Bauswein, H. .-. Janka and R. Oechslin, “Testing approximations of thermal effects in neutron star merger simulations”, *Phys. Rev. D* **82**, 084043 (2010) (cit. on p. 22).
138. K. Hotokezaka et al., “Binary neutron star mergers: Dependence on the nuclear equation of state”, *Phys. Rev. D* **83**, 124008 (2011) (cit. on p. 22).
139. A. Bauswein et al., “Equation-of-state dependence of the gravitational-wave signal from the ring-down phase of neutron-star mergers”, *Phys. Rev. D* **86**, 063001 (2012) (cit. on p. 22).
140. A. Bauswein, N. Stergioulas and H. .-. Janka, “Revealing the high-density equation of state through binary neutron star mergers”, *Phys. Rev. D* **90**, 023002 (2014) (cit. on p. 22).
141. K. Takami, L. Rezzolla and L. Baiotti, “Spectral properties of the post-merger gravitational-wave signal from binary neutron stars”, *Phys. Rev. D* **91**, 064001 (2015) (cit. on p. 22).
142. C. Palenzuela et al., “Effects of the microphysical equation of state in the mergers of magnetized neutron stars with neutrino cooling”, *Phys. Rev. D* **92**, 044045 (2015) (cit. on p. 22).
143. W. Kastaun and F. Galeazzi, “Properties of hypermassive neutron stars formed in mergers of spinning binaries”, *Phys. Rev. D* **91**, 064027 (2015) (cit. on p. 22).
144. L. Rezzolla and K. Takami, “Gravitational-wave signal from binary neutron stars: A systematic analysis of the spectral properties”, *Phys. Rev. D* **93**, 124051 (2016) (cit. on p. 22).
145. J. M. Lattimer and M. Prakash, “The equation of state of hot, dense matter and neutron stars”, *Phys. Rep.* **621**, 127–164 (2016) (cit. on p. 22).
146. G. B. Cook, S. L. Shapiro and S. A. Teukolsky, “Rapidly Rotating Neutron Stars in General Relativity: Realistic Equations of State”, *ApJ* **424**, 823 (1994) (cit. on p. 22).
147. I.-S. Suh and G. J. Mathews, “Cold Ideal Equation of State for Strongly Magnetized Neutron Star Matter: Effects on Muon Production and Pion Condensation”, *ApJ* **546**, 1126–1136 (2001) (cit. on p. 22).
148. A. Bauswein et al., “Identifying a First-Order Phase Transition in Neutron-Star Mergers through Gravitational Waves”, *Phys. Rev. Lett.* **122**, 061102 (2019) (cit. on pp. 22, 43).
149. S. Blacker et al., “Constraining the onset density of the hadron-quark phase transition with gravitational-wave observations”, *Phys. Rev. D* **102**, 123023 (2020) (cit. on p. 22).
150. A. Bauswein, T. W. Baumgarte and H. .-. Janka, “Prompt Merger Collapse and the Maximum Mass of Neutron Stars”, *Phys. Rev. Lett.* **111**, 131101 (2013) (cit. on p. 22).
151. M. Hanauske et al., “Rotational properties of hypermassive neutron stars from binary mergers”, *Phys. Rev. D* **96**, 043004 (2017) (cit. on p. 22).
152. A. Bauswein and N. Stergioulas, “Semi-analytic derivation of the threshold mass for prompt collapse in binary neutron-star mergers”, *MNRAS* **471**, 4956–4965 (2017) (cit. on p. 22).
153. S. Köppel, L. Bovard and L. Rezzolla, “A General-relativistic Determination of the Threshold Mass to Prompt Collapse in Binary Neutron Star Mergers”, *ApJ* **872**, L16 (2019) (cit. on p. 22).

## References

154. D. Wysocki et al., “Inferring the neutron star equation of state simultaneously with the population of merging neutron stars”, [arXiv:2001.01747](#) (cit. on p. 22).
155. I. Mandel et al., “Binary population synthesis with probabilistic remnant mass and kick prescriptions”, *MNRAS* **500**, 1380–1384 (2021) (cit. on p. 22).
156. M. W. Coughlin et al., “Constraints on the neutron star equation of state from AT2017gfo using radiative transfer simulations”, *MNRAS* **480**, 3871–3878 (2018) (cit. on p. 22).
157. B. P. Abbott et al., “All-sky search for short gravitational-wave bursts in the second Advanced LIGO and Advanced Virgo run”, *Phys. Rev. D* **100**, 024017 (2019) (cit. on p. 22).
158. B. P. Abbott et al., “Optically targeted search for gravitational waves emitted by core-collapse supernovae during the first and second observing runs of advanced LIGO and advanced Virgo”, *Phys. Rev. D* **101**, 084002 (2020) (cit. on p. 22).
159. R. Abbott et al. (LIGO Scientific, Virgo, KAGRA), “Constraints on Cosmic Strings Using Data from the Third Advanced LIGO–Virgo Observing Run”, *Phys. Rev. Lett.* **126**, 241102 (2021) (cit. on pp. 22, 35).
160. The LIGO Scientific Collaboration et al., “Search for Gravitational Waves Associated with Gamma-Ray Bursts Detected by Fermi and Swift During the LIGO-Virgo Run O3a”, [arXiv:2010.14550](#) (cit. on p. 22).
161. V. Srivastava et al., “Detection prospects of core-collapse supernovae with supernova-optimized third-generation gravitational-wave detectors”, *Phys. Rev. D* **100**, 043026 (2019) (cit. on p. 22).
162. B. Abi et al., “Supernova neutrino burst detection with the deep underground neutrino experiment”, *European Physical Journal C* **81**, 423 (2021) (cit. on p. 22).
163. E. Abdikamalov, G. Pagliaroli and D. Radice, “Gravitational Waves from Core-Collapse Supernovae”, [arXiv:2010.04356](#) (cit. on p. 22).
164. V. Morozova et al., “The Gravitational Wave Signal from Core-collapse Supernovae”, *ApJ* **861**, 10 (2018) (cit. on p. 22).
165. C. Afle and D. A. Brown, “Inferring physical properties of stellar collapse by third-generation gravitational-wave detectors”, *Phys. Rev. D* **103**, 023005 (2021) (cit. on p. 22).
166. R. Jardine, J. Powell and B. Müller, “Gravitational Wave Signals from Two-Dimensional Core-Collapse Supernova Models with Rotation and Magnetic Fields”, (2021), [arXiv:2105.01315 \[astro-ph.HE\]](#) (cit. on p. 22).
167. C. J. Neijssel et al., “The effect of the metallicity-specific star formation history on double compact object mergers”, *MNRAS* **490**, 3740–3759 (2019) (cit. on p. 23).
168. M. Chruslinska, G. Nelemans and K. Belczynski, “The influence of the distribution of cosmic star formation at different metallicities on the properties of merging double compact objects”, *MNRAS* **482**, 5012–5017 (2019) (cit. on p. 23).
169. F. Santoliquido et al., “The Cosmic Merger Rate Density Evolution of Compact Binaries Formed in Young Star Clusters and in Isolated Binaries”, *ApJ* **898**, 152 (2020) (cit. on p. 23).
170. R. Farmer et al., “Constraints from Gravitational-wave Detections of Binary Black Hole Mergers on the  $^{12}\text{C}(\alpha, \gamma)^{16}\text{O}$  Rate”, *ApJ* **902**, L36 (2020) (cit. on p. 23).

## References

171. E. Symbalisty and D. N. Schramm, “Neutron Star Collisions and the r-Process”, *Astrophys. Lett.* **22**, 143 (1982) (cit. on p. 23).
172. L.-X. Li and B. Paczyński, “Transient Events from Neutron Star Mergers”, *ApJ* **507**, L59–L62 (1998) (cit. on p. 23).
173. B. Côté et al., “The Origin of r-process Elements in the Milky Way”, *ApJ* **855**, 99 (2018) (cit. on p. 23).
174. K. Ackley et al., “Observational constraints on the optical and near-infrared emission from the neutron star-black hole binary merger candidate S190814bv”, *A&A* **643**, A113 (2020) (cit. on p. 23).
175. S. Adhikari et al., “The Binary-Host Connection: Astrophysics of Gravitational-Wave Binaries from Host Galaxy Properties”, *ApJ* **905**, 21 (2020) (cit. on p. 23).
176. S. J. Kapadia et al., “Of Harbingers and Higher Modes: Improved Gravitational-wave Early Warning of Compact Binary Mergers”, *ApJ* **898**, L39 (2020) (cit. on p. 23).
177. E. A. Chase et al., “Kilonova Detectability with Wide-Field Instruments”, [arXiv:2105.12268](https://arxiv.org/abs/2105.12268) (cit. on p. 23).
178. R. Fernández and B. D. Metzger, “Electromagnetic Signatures of Neutron Star Mergers in the Advanced LIGO Era”, *Annual Review of Nuclear and Particle Science* **66**, 23–45 (2016) (cit. on p. 23).
179. B. Margalit and B. D. Metzger, “The Multi-messenger Matrix: The Future of Neutron Star Merger Constraints on the Nuclear Equation of State”, *ApJ* **880**, L15 (2019) (cit. on p. 23).
180. J. Kalirai, “Scientific discovery with the James Webb Space Telescope”, *Contemporary Physics* **59**, 251–290 (2018) (cit. on p. 23).
181. M. Gullieuszik et al., “Exploring high-z galaxies with the E-ELT”, *A&A* **593**, A24 (2016) (cit. on p. 23).
182. P. J. McCarthy et al., “Overview and status of the Giant Magellan Telescope project”, in *Ground-based and Airborne Telescopes VII*, edited by R. Gilmozzi, H. K. Marshall and J. Spyromilio (July 2018) (cit. on p. 23).
183. W. Skidmore, G. C. Anupama and R. Srianand, “The Thirty Meter Telescope International Observatory Facilitating Transformative Astrophysical Science”, *Current Science* **113**, 639 (2017) (cit. on p. 23).
184. Y. Ishimaru, S. Wanajo and N. Prantzos, “Neutron Star Mergers as the Origin of r-process Elements in the Galactic Halo Based on the Sub-halo Clustering Scenario”, *ApJ* **804**, L35 (2015) (cit. on p. 23).
185. R. Duque et al., “Probing binary neutron star mergers in dense environments using afterglow counterparts”, *A&A* **639**, A15 (2020) (cit. on p. 23).
186. E. Berger, “Short-Duration Gamma-Ray Bursts”, *ARA&A* **52**, 43–105 (2014) (cit. on p. 24).
187. R. Ciolfi, “Short gamma-ray burst central engines”, *International Journal of Modern Physics D* **27**, 1842004 (2018) (cit. on p. 24).
188. A. Rowlinson et al., “Signatures of magnetar central engines in short GRB light curves”, *MNRAS* **430**, 1061–1087 (2013) (cit. on p. 24).
189. B. Giacomazzo and R. Perna, “Formation of Stable Magnetars from Binary Neutron Star Mergers”, *ApJ* **771**, L26 (2013) (cit. on p. 24).

## References

190. M. M. Kasliwal et al., “Illuminating gravitational waves: A concordant picture of photons from a neutron star merger”, *Science* **358**, 1559–1565 (2017) (cit. on p. 24).
191. J. D. Lyman et al., “The optical afterglow of the short gamma-ray burst associated with GW170817”, *Nature Astronomy* **2**, 751–754 (2018) (cit. on p. 24).
192. E. Troja et al., “The outflow structure of GW170817 from late-time broad-band observations”, *MNRAS* **478**, L18–L23 (2018) (cit. on p. 24).
193. K. P. Mooley et al., “A mildly relativistic wide-angle outflow in the neutron-star merger event GW170817”, *Nature* **554**, 207–210 (2018) (cit. on p. 24).
194. B. Zhang, “The delay time of gravitational wave — gamma-ray burst associations”, *Frontiers of Physics* **14**, 64402 (2019) (cit. on p. 24).
195. A. Murguia-Berthier et al., “The Fate of the Merger Remnant in GW170817 and Its Imprint on the Jet Structure”, *ApJ* **908**, 152 (2021) (cit. on p. 24).
196. Y. B. Yu et al., “Bimodal distribution of short gamma-ray bursts: Evidence for two distinct types of short gamma-ray bursts”, *New A* **75**, 101306 (2020) (cit. on p. 24).
197. B. P. Gompertz, A. J. Levan and N. R. Tanvir, “A Search for Neutron Star-Black Hole Binary Mergers in the Short Gamma-Ray Burst Population”, *ApJ* **895**, 58 (2020) (cit. on p. 24).
198. W. Yuan et al., “Einstein Probe - a small mission to monitor and explore the dynamic X-ray Universe”, *arXiv:1506.07735* (cit. on p. 24).
199. M. Hernanz et al. (eXTP), “The Wide Field Monitor onboard the eXTP mission”, in *SPIE Astronomical Telescopes + Instrumentation 2018* (July 2018), *arXiv:1807.09330 [astro-ph. IM]* (cit. on p. 24).
200. J. Wei and B. Cordier, “The Deep and Transient Universe in the SVOM Era: New Challenges and Opportunities - Scientific prospects of the SVOM mission”, in (Oct. 2016), *arXiv:1610.06892 [astro-ph. IM]* (cit. on p. 24).
201. R. Willingale et al., “The Hot and Energetic Universe: The Optical Design of the Athena+ Mirror”, (2013), *arXiv:1307.1709 [astro-ph. IM]* (cit. on p. 24).
202. L. Amati et al., “The THESEUS space mission concept: science case, design and expected performances”, *Advances in Space Research* **62**, 191–244 (2018) (cit. on p. 24).
203. J. Camp et al., “Transient Astrophysics Probe”, in *Bulletin of the American Astronomical Society*, Vol. 51 (Sept. 2019), p. 85 (cit. on p. 24).
204. S. Mereghetti, J. A. Pons and A. Melatos, “Magnetars: Properties, Origin and Evolution”, *Space Sci. Rev.* **191**, 315–338 (2015) (cit. on p. 24).
205. D. M. Palmer et al., “A giant  $\gamma$ -ray flare from the magnetar SGR 1806 - 20”, *Nature* **434**, 1107–1109 (2005) (cit. on p. 24).
206. B. Giacomazzo et al., “Producing Magnetar Magnetic Fields in the Merger of Binary Neutron Stars”, *ApJ* **809**, 39 (2015) (cit. on p. 24).
207. C. Thompson, “Electrodynamics of Magnetars. IV. Self-Consistent Model of the Inner Accelerator with Implications for Pulsed Radio Emission”, *ApJ* **688**, 499–526 (2008) (cit. on p. 24).

## References

208. B. P. Abbott et al., “Tests of general relativity with the binary black hole signals from the LIGO-Virgo catalog GWTC-1”, *Phys. Rev. D* **100**, 104036 (2019) (cit. on pp. 25, 26).
209. N. Yunes, K. Yagi and F. Pretorius, “Theoretical physics implications of the binary black-hole mergers GW150914 and GW151226”, *Phys. Rev. D* **94**, 084002 (2016) (cit. on p. 26).
210. B. P. Abbott et al., “Search for intermediate mass black hole binaries in the first and second observing runs of the Advanced LIGO and Virgo network”, *Phys. Rev. D* **100**, 064064 (2019) (cit. on p. 26).
211. B. Bruggmann, “Fundamentals of numerical relativity for gravitational wave sources”, *Science* **361**, 366–371 (2018) (cit. on p. 26).
212. B. P. Abbott et al., “Tests of General Relativity with GW170817”, *Phys. Rev. Lett.* **123**, 011102 (2019) (cit. on p. 26).
213. M. Isi, K. Chatziioannou and W. M. Farr, “Hierarchical Test of General Relativity with Gravitational Waves”, *Phys. Rev. Lett.* **123**, 121101 (2019) (cit. on p. 26).
214. B. P. Abbott et al., “Search for Tensor, Vector, and Scalar Polarizations in the Stochastic Gravitational-Wave Background”, *Phys. Rev. Lett.* **120**, 201102 (2018) (cit. on p. 26).
215. K. Pardo et al., “Limits on the number of spacetime dimensions from GW170817”, *J. Cosmology Astropart. Phys.* **2018**, 048 (2018) (cit. on p. 26).
216. M. Isi et al., “Testing the No-Hair Theorem with GW150914”, *Phys. Rev. Lett.* **123**, 111102 (2019) (cit. on p. 26).
217. R. Nair et al., “Fundamental Physics Implications for Higher-Curvature Theories from Binary Black Hole Signals in the LIGO-Virgo Catalog GWTC-1”, *Phys. Rev. Lett.* **123**, 191101 (2019) (cit. on p. 26).
218. C. M. Will, *Theory and Experiment in Gravitational Physics, Second Edition* (Cambridge University Press, Cambridge, UK, 2018) (cit. on p. 26).
219. G. J. Whitrow and G. E. Morduch, “Relativistic theories of gravitation : A comparative analysis with particular reference to astronomical tests”, *Vistas in Astronomy* **6**, 1–67 (1965) (cit. on p. 26).
220. F. Pretorius, “Relativity Gets Thorough Vetting from LIGO”, *Physics Online Journal* **9**, 52 (2016) (cit. on pp. 26, 27).
221. B. P. Abbott et al., “Multi-messenger Observations of a Binary Neutron Star Merger”, *ApJ* **848**, L12 (2017) (cit. on p. 26).
222. H. Yang and D. Martynov, “Testing Gravitational Memory Generation with Compact Binary Mergers”, *Phys. Rev. Lett.* **121**, 071102 (2018) (cit. on p. 26).
223. D. Mattingly, “Modern tests of Lorentz invariance”, *Living Rev. Rel.* **8**, 5 (2005) (cit. on p. 27).
224. A. Ashtekar, A. P. Balachandran and S. Jo, “The CP Problem in Quantum Gravity”, *Int. J. Mod. Phys. A* **4**, 1493 (1989) (cit. on p. 27).
225. M. Okounkova et al., “Constraining gravitational wave amplitude birefringence and Chern-Simons gravity with GWTC-2”, *arXiv:2101.11153* (cit. on p. 27).
226. C. Palenzuela et al., “Dynamical scalarization of neutron stars in scalar-tensor gravity theories”, *Phys. Rev. D* **89**, 044024 (2014) (cit. on p. 27).

## References

227. M. Shibata et al., “Coalescence of binary neutron stars in a scalar-tensor theory of gravity”, *Phys. Rev. D* **89**, 084005 (2014) (cit. on p. 27).
228. C. M. Will, “The Confrontation between General Relativity and Experiment”, *Living Rev. Rel.* **17**, 4 (2014) (cit. on pp. 27, 32, 33).
229. D. A. Brown et al., “Prospects for detection of gravitational waves from intermediate-mass-ratio inspirals”, *Phys. Rev. Lett.* **99**, 201102 (2007) (cit. on p. 27).
230. P. Amaro-Seoane, “Detecting Intermediate-Mass Ratio Inspirals From The Ground And Space”, *Phys. Rev. D* **98**, 063018 (2018) (cit. on p. 27).
231. A. Loeb, “Electromagnetic Counterparts to Black Hole Mergers Detected by LIGO”, *Astrophys. J. Lett.* **819**, L21 (2016) (cit. on p. 27).
232. N. C. Stone, B. D. Metzger and Z. Haiman, “Assisted inspirals of stellar mass black holes embedded in AGN discs: solving the ‘final au problem’”, *MNRAS* **464**, 946–954 (2017) (cit. on p. 27).
233. E. Michaely and H. B. Perets, “Supernova and Prompt Gravitational-wave Precursors to LIGO Gravitational-wave Sources and Short GRBs”, *ApJ* **855**, L12 (2018) (cit. on p. 27).
234. V. Cardoso and P. Pani, “Testing the nature of dark compact objects: a status report”, *Living Reviews in Relativity* **22**, 4 (2019) (cit. on p. 27).
235. A. Tsokaros et al., “Great Impostors: Extremely Compact, Merging Binary Neutron Stars in the Mass Gap Posing as Binary Black Holes”, *Phys. Rev. Lett.* **124**, 071101 (2020) (cit. on p. 27).
236. P. O. Mazur and E. Mottola, “Gravitational vacuum condensate stars”, *Proceedings of the National Academy of Science* **101**, 9545–9550 (2004) (cit. on p. 27).
237. V. Cardoso, E. Franzin and P. Pani, “Is the Gravitational-Wave Ringdown a Probe of the Event Horizon?”, *Phys. Rev. Lett.* **116**, 171101 (2016) (cit. on p. 27).
238. C. Chirenti and L. Rezzolla, “Did GW150914 produce a rotating gravastar?”, *Phys. Rev. D* **94**, 084016 (2016) (cit. on p. 27).
239. C. B. M. H. Chirenti and L. Rezzolla, “How to tell a gravastar from a black hole”, *Classical and Quantum Gravity* **24**, 4191–4206 (2007) (cit. on p. 27).
240. S. L. Liebling and C. Palenzuela, “Dynamical Boson Stars”, *Living Reviews in Relativity* **15**, 6 (2012) (cit. on p. 27).
241. R. Brito et al., “Gravitational wave searches for ultralight bosons with LIGO and LISA”, *Phys. Rev. D* **96**, 064050 (2017) (cit. on pp. 27, 28).
242. D. D. Ivanenko and D. F. Kurdgelaidze, “Hypothesis concerning quark stars”, *Astrophysics* **1**, 251–252 (1965) (cit. on p. 27).
243. C. Rovelli and F. Vidotto, “Planck stars”, *International Journal of Modern Physics D* **23**, 1442026 (2014) (cit. on p. 27).
244. N. Sennett et al., “Distinguishing boson stars from black holes and neutron stars from tidal interactions in inspiraling binary systems”, *Phys. Rev. D* **96**, 024002 (2017) (cit. on pp. 27, 28).
245. S. A. Teukolsky, “The Kerr metric”, *Classical and Quantum Gravity* **32**, 124006 (2015) (cit. on p. 27).



## References

246. E. Berti, “Topical collection: Testing the Kerr spacetime with gravitational-wave and electromagnetic observations”, *General Relativity and Gravitation* **51**, 140 (2019) (cit. on p. 27).
247. E. Berti et al., “Extreme gravity tests with gravitational waves from compact binary coalescences: (II) ringdown”, *General Relativity and Gravitation* **50**, 49 (2018) (cit. on p. 27).
248. R. S. Conklin, “Gravitational wave perturbations on a Kerr background and applications for echoes”, *Phys. Rev. D* **101**, 044045 (2020) (cit. on p. 27).
249. R. S. Conklin and B. Holdom, “Gravitational wave echo spectra”, *Phys. Rev. D* **100**, 124030 (2019) (cit. on p. 27).
250. M. R. Buckley and A. H. G. Peter, “Gravitational probes of dark matter physics”, *Phys. Rep.* **761**, 1–60 (2018) (cit. on p. 28).
251. Y. Wang, “Observational probes of dark energy”, in *Towards New Paradigms*, Vol. 1458, edited by J. Beltrán Jiménez et al., American Institute of Physics Conference Series (July 2012), pp. 285–300, arXiv:1201.2110 [astro-ph.CO] (cit. on p. 28).
252. Planck Collaboration et al., “Planck 2018 results. VI. Cosmological parameters”, *A&A* **641**, A6 (2020) (cit. on p. 28).
253. G. Bertone, D. Hooper and J. Silk, “Particle dark matter: evidence, candidates and constraints”, *Phys. Rep.* **405**, 279–390 (2005) (cit. on p. 28).
254. H. Abramowicz, R. Forty et al., *Physics Briefing Book*, 2020 (cit. on pp. 28, 124).
255. R. K. Ellis et al., “Physics Briefing Book: Input for the European Strategy for Particle Physics Update 2020”, (2019), arXiv:1910.11775 [hep-ex] (cit. on p. 28).
256. G. Bertone et al., “Gravitational wave probes of dark matter: challenges and opportunities”, *SciPost Phys. Core* **3**, 007 (2020) (cit. on p. 28).
257. A. de Lavallaz and M. Fairbairn, “Neutron stars as dark matter probes”, *Phys. Rev. D* **81**, 123521 (2010) (cit. on p. 28).
258. C. Kouvaris and P. Tinyakov, “Can neutron stars constrain dark matter?”, *Phys. Rev. D* **82**, 063531 (2010) (cit. on p. 28).
259. T. Dietrich and K. Clough, “Cooling binary neutron star remnants via nucleon-nucleon-axion bremsstrahlung”, *Phys. Rev. D* **100**, 083005 (2019) (cit. on p. 28).
260. J. Bramante, T. Linden and Y.-D. Tsai, “Searching for dark matter with neutron star mergers and quiet kilonovae”, *Phys. Rev. D* **97**, 055016 (2018) (cit. on p. 28).
261. V. Cardoso et al., “Testing strong-field gravity with tidal Love numbers”, *Phys. Rev. D* **95**, 084014 (2017) (cit. on p. 28).
262. K. Clough, T. Dietrich and J. C. Niemeyer, “Axion star collisions with black holes and neutron stars in full 3D numerical relativity”, *Phys. Rev. D* **98**, 083020 (2018) (cit. on p. 28).
263. T. Dietrich et al., “Neutron star-axion star collisions in the light of multimessenger astronomy”, *MNRAS* **483**, 908–914 (2019) (cit. on p. 28).
264. A. Arvanitaki and S. Dubovsky, “Exploring the string axiverse with precision black hole physics”, *Phys. Rev. D* **83**, 044026 (2011) (cit. on p. 28).

## References

265. S. R. Dolan, “Superradiant instabilities of rotating black holes in the time domain”, *Phys. Rev. D* **87**, 124026 (2013) (cit. on p. 28).
266. R. Brito, V. Cardoso and P. Pani, “Black holes as particle detectors: evolution of superradiant instabilities”, *Classical and Quantum Gravity* **32**, 134001 (2015) (cit. on p. 28).
267. W. E. East and F. Pretorius, “Superradiant Instability and Backreaction of Massive Vector Fields around Kerr Black Holes”, *Phys. Rev. Lett.* **119**, 041101 (2017) (cit. on p. 28).
268. A. Arvanitaki, M. Baryakhtar and X. Huang, “Discovering the QCD axion with black holes and gravitational waves”, *Phys. Rev. D* **91**, 084011 (2015) (cit. on p. 28).
269. K. K. Y. Ng et al., “Searching for ultralight bosons within spin measurements of a population of binary black hole mergers”, *Phys. Rev. D* **103**, 063010 (2021) (cit. on p. 28).
270. K. K. Y. Ng et al., “Constraints on Ultralight Scalar Bosons within Black Hole Spin Measurements from the LIGO-Virgo GWTC-2”, *Phys. Rev. Lett.* **126**, 151102 (2021) (cit. on p. 28).
271. M. Baryakhtar, R. Lasenby and M. Teo, “Black hole superradiance signatures of ultralight vectors”, *Phys. Rev. D* **96**, 035019 (2017) (cit. on p. 28).
272. J. M. Ezquiaga and M. Zumalacárregui, “Dark Energy in light of Multi-Messenger Gravitational-Wave astronomy”, *Front. Astron. Space Sci.* **5**, 44 (2018) (cit. on p. 29).
273. S. M. Feeney et al., “Prospects for resolving the Hubble constant tension with standard sirens”, *Phys. Rev. Lett.* **122**, 061105 (2019) (cit. on p. 29).
274. Z.-Q. You et al., “Standard-siren cosmology using gravitational waves from binary black holes”, *Astrophys. J.* **908**, 215 (2021) (cit. on p. 29).
275. B. F. Schutz, “Determining the Hubble Constant from Gravitational Wave Observations”, *Nature* **323**, 310–311 (1986) (cit. on p. 29).
276. N. Dalal et al., “Short grb and binary black hole standard sirens as a probe of dark energy”, *Phys. Rev. D* **74**, 063006 (2006) (cit. on p. 29).
277. S. R. Taylor and J. R. Gair, “Cosmology with the lights off: standard sirens in the Einstein Telescope era”, *Phys. Rev. D* **86**, 023502 (2012) (cit. on p. 29).
278. R.-G. Cai and T. Yang, “Estimating cosmological parameters by the simulated data of gravitational waves from the Einstein Telescope”, *Phys. Rev. D* **95**, 044024 (2017) (cit. on p. 29).
279. E. Belgacem et al., “Modified gravitational-wave propagation and standard sirens”, *Phys. Rev. D* **98**, 023510 (2018) (cit. on pp. 29, 32).
280. K. I. Kellermann et al., “The Exploration of the Unknown”, in *astro2010: The Astronomy and Astrophysics Decadal Survey*, Vol. 2010 (Jan. 2009), p. 154, [arXiv:0912.4441](https://arxiv.org/abs/0912.4441) [astro-ph.IM] (cit. on p. 30).
281. K. R. Lang, “Serendipitous Astronomy”, *Science* **327**, 39–40 (2010) (cit. on p. 30).
282. S. W. Hawking, “Information loss in black holes”, *Phys. Rev. D* **72**, 084013 (2005) (cit. on p. 32).
283. B. Schulz, “Review on the quantization of gravity”, [arXiv:1409.7977](https://arxiv.org/abs/1409.7977) (cit. on p. 32).
284. G. Dvali, “Quantum black holes”, *Physics Today* **68**, 1, 38–43 (2015) (cit. on p. 32).

## References

285. R. S. Conklin, B. Holdom and J. Ren, “Gravitational wave echoes through new windows”, *Phys. Rev. D* **98**, 044021 (2018) (cit. on p. 32).
286. V. Cardoso et al., “Gravitational-wave signatures of exotic compact objects and of quantum corrections at the horizon scale”, *Phys. Rev. D* **94**, 084031 (2016) (cit. on p. 32).
287. Z. Mark et al., “A recipe for echoes from exotic compact objects”, *Phys. Rev. D* **96**, 084002 (2017) (cit. on p. 32).
288. Y.-T. Wang and Y.-S. Piao, “Searching for gravitational wave echoes in GWTC-1 and O3 events”, (2020), [arXiv:2010.07663 \[gr-qc\]](https://arxiv.org/abs/2010.07663) (cit. on p. 32).
289. K. Pardo et al., “Limits on the number of spacetime dimensions from GW170817”, *JCAP* **07**, 048 (2018) (cit. on p. 32).
290. S. Alexander and N. Yunes, “Chern-Simons Modified General Relativity”, *Phys. Rept.* **480**, 1–55 (2009) (cit. on p. 32).
291. S. H. Alexander and N. Yunes, “Gravitational wave probes of parity violation in compact binary coalescences”, *Phys. Rev. D* **97**, 064033 (2018) (cit. on p. 32).
292. M. Isi and A. J. Weinstein, “Probing gravitational wave polarizations with signals from compact binary coalescences”, (2017), [arXiv:1710.03794 \[gr-qc\]](https://arxiv.org/abs/1710.03794) (cit. on p. 33).
293. A. Arvanitaki et al., “String Axiverse”, *Phys. Rev. D* **81**, 123530 (2010) (cit. on p. 33).
294. R. Brito et al., “Gravitational wave searches for ultralight bosons with LIGO and LISA”, *Phys. Rev. D* **96**, 064050 (2017) (cit. on p. 33).
295. Y. Zel’dovich, “Generation of Waves by a Rotating Body”, *Pis’ma Zh. Eksp. Teor. Fiz.*, *JETP Lett.* **14**, 270 (1971) (cit. on p. 33).
296. R. Penrose and R. M. Floyd, “Extraction of rotational energy from a black hole”, *Nature* **229**, 177–179 (1971) (cit. on p. 33).
297. B. Carr and F. Kuhnel, “Primordial Black Holes as Dark Matter: Recent Developments”, *Ann. Rev. Nucl. Part. Sci.* **70**, 355–394 (2020) (cit. on p. 33).
298. B. P. Abbott et al. (LIGO Scientific, Virgo), “Search for Substellar Mass Ultracompact Binaries in Advanced LIGO’s Second Observing Run”, *Phys. Rev. Lett.* **123**, 161102 (2019) (cit. on p. 33).
299. X.-J. Zhu et al., “Stochastic Gravitational Wave Background from Coalescing Binary Black Holes”, *ApJ* **739**, 86 (2011) (cit. on p. 33).
300. C. Wu, V. Mandic and T. Regimbau, “Accessibility of the gravitational-wave background due to binary coalescences to second and third generation gravitational-wave detectors”, *Phys. Rev. D* **85**, 104024 (2012) (cit. on p. 33).
301. B. P. Abbott et al., “GW150914: Implications for the Stochastic Gravitational-Wave Background from Binary Black Holes”, *Phys. Rev. Lett.* **116**, 131102 (2016) (cit. on p. 33).
302. B. P. Abbott et al., “GW170817: Implications for the Stochastic Gravitational-Wave Background from Compact Binary Coalescences”, *Phys. Rev. Lett.* **120**, 091101 (2018) (cit. on p. 33).
303. B. P. Abbott et al., “Search for the isotropic stochastic background using data from Advanced LIGO’s second observing run”, *Phys. Rev. D* **100**, 061101 (2019) (cit. on p. 33).

## References

304. The LIGO Scientific Collaboration et al., “Upper Limits on the Isotropic Gravitational-Wave Background from Advanced LIGO’s and Advanced Virgo’s Third Observing Run”, [arXiv:2101.12130](#) (cit. on p. 33).
305. T. Regimbau et al., “Digging Deeper: Observing Primordial Gravitational Waves below the Binary-Black-Hole-Produced Stochastic Background”, *Phys. Rev. Lett.* **118**, 151105 (2017) (cit. on p. 33).
306. A. Sharma and J. Harms, “Searching for cosmological gravitational-wave backgrounds with third-generation detectors in the presence of an astrophysical foreground”, *Phys. Rev. D* **102**, 063009 (2020) (cit. on p. 33).
307. S. Sachdev, T. Regimbau and B. S. Sathyaprakash, “Subtracting compact binary foreground sources to reveal primordial gravitational-wave backgrounds”, *Phys. Rev. D* **102**, 024051 (2020) (cit. on p. 33).
308. S. Biscoveanu et al., “Measuring the Primordial Gravitational-Wave Background in the Presence of Astrophysical Foregrounds”, *Phys. Rev. Lett.* **125**, 241101 (2020) (cit. on p. 33).
309. M. Maggiore, “Gravitational wave experiments and early universe cosmology”, *Phys. Rep.* **331**, 283–367 (2000) (cit. on pp. 33, 35, 55).
310. Planck Collaboration et al., “Planck 2015 results. XIII. Cosmological parameters”, *A&A* **594**, A13 (2016) (cit. on p. 33).
311. J. Crowder and N. J. Cornish, “Beyond LISA: Exploring future gravitational wave missions”, *Phys. Rev. D* **72**, 083005 (2005) (cit. on p. 34).
312. S. Kawamura et al., “The Japanese space gravitational wave antenna: DECIGO”, *Classical and Quantum Gravity* **28**, 094011 (2011) (cit. on p. 34).
313. C. Caprini and D. G. Figueroa, “Cosmological backgrounds of gravitational waves”, *Classical and Quantum Gravity* **35**, 163001 (2018) (cit. on p. 34).
314. E. Thrane and J. D. Romano, “Sensitivity curves for searches for gravitational-wave backgrounds”, *Phys. Rev. D* **88**, 124032 (2013) (cit. on p. 34).
315. S. A. Sanidas, R. A. Battye and B. W. Stappers, “Constraints on cosmic string tension imposed by the limit on the stochastic gravitational wave background from the European Pulsar Timing Array”, *Phys. Rev. D* **85**, 122003 (2012) (cit. on p. 34).
316. R. Easther, J. Giblin John T. and E. A. Lim, “Gravitational Wave Production at the End of Inflation”, *Phys. Rev. Lett.* **99**, 221301 (2007) (cit. on pp. 34, 35).
317. R. Allahverdi et al., “Reheating in Inflationary Cosmology: Theory and Applications”, *Annual Review of Nuclear and Particle Science* **60**, 27–51 (2010) (cit. on p. 34).
318. M. A. Amin et al., “Nonperturbative dynamics of reheating after inflation: A review”, *International Journal of Modern Physics D* **24**, 1530003 (2015) (cit. on p. 34).
319. S. Khlebnikov and I. Tkachev, “Relic gravitational waves produced after preheating”, *Phys. Rev. D* **56**, 653–660 (1997) (cit. on p. 34).
320. R. Easther, J. Giblin John T. and E. A. Lim, “Gravitational waves from the end of inflation: Computational strategies”, *Phys. Rev. D* **77**, 103519 (2008) (cit. on p. 34).

## References

321. J. Garcia-Bellido, “Preheating the universe in hybrid inflation”, [arXiv:hep-ph/9804205](#) (cit. on p. 34).
322. R. Easther and E. A. Lim, “Stochastic gravitational wave production after inflation”, *J. Cosmology Astropart. Phys.* **2006**, 010 (2006) (cit. on p. 34).
323. T. W. B. Kibble, “Topology of cosmic domains and strings”, *Journal of Physics A Mathematical General* **9**, 1387–1398 (1976) (cit. on p. 35).
324. T. Vachaspati and A. Vilenkin, “Gravitational radiation from cosmic strings”, *Phys. Rev. D* **31**, 3052–3058 (1985) (cit. on p. 35).
325. E. P. S. Shellard, “Cosmic String Interactions”, *Nucl. Phys. B* **283**, 624–656 (1987) (cit. on p. 35).
326. P. Laguna and R. A. Matzner, “Numerical simulation of bosonic-superconducting-string interactions”, *Phys. Rev. D* **41**, 1751–1763 (1990) (cit. on p. 35).
327. B. Allen and R. R. Caldwell, “Small-scale structure on a cosmic-string network”, *Phys. Rev. D* **43**, 3173–3187 (1991) (cit. on p. 35).
328. B. Allen and P. Casper, “Closed-form expression for the gravitational radiation rate from cosmic strings”, *Phys. Rev. D* **50**, 2496–2518 (1994) (cit. on p. 35).
329. T. Damour and A. Vilenkin, “Gravitational wave bursts from cusps and kinks on cosmic strings”, *Phys. Rev. D* **64**, 064008 (2001) (cit. on p. 35).
330. T. Damour and A. Vilenkin, “Gravitational radiation from cosmic (super)strings: Bursts, stochastic background, and observational windows”, *Phys. Rev. D* **71**, 063510 (2005) (cit. on p. 35).
331. X. Siemens, V. Mandic and J. Creighton, “Gravitational-Wave Stochastic Background from Cosmic Strings”, *Phys. Rev. Lett.* **98**, 111101 (2007) (cit. on p. 35).
332. B. P. Abbott et al., “An upper limit on the stochastic gravitational-wave background of cosmological origin”, *Nature* **460**, 990–994 (2009) (cit. on p. 35).
333. S. Henrot-Versillé et al., “Improved constraint on the primordial gravitational-wave density using recent cosmological data and its impact on cosmic string models”, *Classical and Quantum Gravity* **32**, 045003 (2015) (cit. on p. 35).
334. P. Auclair et al., “Cosmic string loop production functions”, *J. Cosmology Astropart. Phys.* **2019**, 015 (2019) (cit. on p. 35).
335. M. Kamionkowski, A. Kosowsky and M. S. Turner, “Gravitational radiation from first-order phase transitions”, *Phys. Rev. D* **49**, 2837–2851 (1994) (cit. on p. 35).
336. C. Caprini et al., “Science with the space-based interferometer eLISA. II: gravitational waves from cosmological phase transitions”, *J. Cosmology Astropart. Phys.* **2016**, 001 (2016) (cit. on p. 35).
337. S. Iso, P. D. Serpico and K. Shimada, “QCD-Electroweak First-Order Phase Transition in a Supercooled Universe”, *Phys. Rev. Lett.* **119**, 141301 (2017) (cit. on p. 35).
338. D. J. Weir, “Gravitational waves from a first-order electroweak phase transition: a brief review”, *Philosophical Transactions of the Royal Society of London Series A* **376**, 20170126 (2018) (cit. on p. 35).

## References

339. A. Kosowsky, M. S. Turner and R. Watkins, “Gravitational radiation from colliding vacuum bubbles”, *Phys. Rev. D* **45**, 4514–4535 (1992) (cit. on p. 35).
340. S. J. Huber and T. Konstandin, “Gravitational wave production by collisions: more bubbles”, *J. Cosmology Astropart. Phys.* **2008**, 022 (2008) (cit. on p. 35).
341. C. Caprini, R. Durrer and G. Servant, “Gravitational wave generation from bubble collisions in first-order phase transitions: An analytic approach”, *Phys. Rev. D* **77**, 124015 (2008) (cit. on p. 35).
342. C. Caprini, R. Durrer and G. Servant, “The stochastic gravitational wave background from turbulence and magnetic fields generated by a first-order phase transition”, *J. Cosmology Astropart. Phys.* **2009**, 024 (2009) (cit. on p. 35).
343. M. Hindmarsh et al., “Gravitational Waves from the Sound of a First Order Phase Transition”, *Phys. Rev. Lett.* **112**, 041301 (2014) (cit. on p. 35).
344. M. Hindmarsh et al., “Numerical simulations of acoustically generated gravitational waves at a first order phase transition”, *Phys. Rev. D* **92**, 123009 (2015) (cit. on p. 35).
345. D. E. Morrissey and M. J. Ramsey-Musolf, “Electroweak baryogenesis”, *New Journal of Physics* **14**, 125003 (2012) (cit. on p. 35).
346. T. Kahnashvili et al., “Detectability of gravitational waves from phase transitions”, *Phys. Rev. D* **78**, 043003 (2008) (cit. on p. 35).
347. C. Caprini et al., “General properties of the gravitational wave spectrum from phase transitions”, *Phys. Rev. D* **79**, 083519 (2009) (cit. on p. 35).
348. J. T. Giblin and E. Thrane, “Estimates of maximum energy density of cosmological gravitational-wave backgrounds”, *Phys. Rev. D* **90**, 107502 (2014) (cit. on p. 35).
349. K. Belczynski et al., “The first gravitational-wave source from the isolated evolution of two stars in the 40-100 solar mass range”, *Nature* **534**, 512–515 (2016) (cit. on p. 38).
350. K. Belczynski et al., “On the likelihood of detecting gravitational waves from Population III compact object binaries”, *MNRAS* **471**, 4702–4721 (2017) (cit. on p. 38).
351. C. L. Rodriguez and A. Loeb, “Redshift Evolution of the Black Hole Merger Rate from Globular Clusters”, *ApJ* **866**, L5 (2018) (cit. on p. 38).
352. V. De Luca et al., “Bayesian evidence for both astrophysical and primordial black holes: mapping the GWTC-2 catalog to third-generation detectors”, *J. Cosmology Astropart. Phys.* **2021**, 003 (2021) (cit. on p. 38).
353. M. Raidal et al., “Formation and evolution of primordial black hole binaries in the early universe”, *J. Cosmology Astropart. Phys.* **2019**, 018 (2019) (cit. on p. 38).
354. D. W. Hogg, “Distance measures in cosmology”, [arXiv:astro-ph/9905116](https://arxiv.org/abs/astro-ph/9905116) (cit. on p. 38).
355. J. Harms et al., “Low-frequency terrestrial gravitational-wave detectors”, *Phys. Rev. D* **88**, 122003 (2013) (cit. on p. 38).
356. D. Shoemaker et al., “Noise behavior of the Garching 30-meter prototype gravitational-wave detector”, *Phys. Rev. D* **38**, 423–432 (1988) (cit. on p. 39).



## References

357. V. B. Braginsky and F. J. Khalili, “Gravitational wave antenna with QND speed meter”, *Physics Letters A* **147**, 251–256 (1990) (cit. on p. 39).
358. P. Purdue and Y. Chen, “Practical speed meter designs for quantum nondemolition gravitational-wave interferometers”, *Phys. Rev. D* **66**, 122004 (2002) (cit. on p. 39).
359. P. Amaro-Seoane et al., “Laser Interferometer Space Antenna”, [arXiv:1702.00786](https://arxiv.org/abs/1702.00786) (cit. on p. 39).
360. J. Luo et al. (TianQin), “TianQin: a space-borne gravitational wave detector”, *Class. Quant. Grav.* **33**, 035010 (2016) (cit. on p. 39).
361. J. Mei et al. (TianQin), “The TianQin project: current progress on science and technology”, [10.1093/ptep/ptaa114](https://arxiv.org/abs/10.1093/ptep/ptaa114) (2020), [arXiv:2008.10332 \[gr-qc\]](https://arxiv.org/abs/2008.10332) (cit. on p. 39).
362. Y.-L. Taiji Scientific Collaboration Wu et al., “China’s first step towards probing the expanding universe and the nature of gravity using a space borne gravitational wave antenna”, *Communications Physics* **4**, 34 (2021) (cit. on p. 39).
363. S. Kawamura et al., “The Japanese space gravitational wave antenna—DECIGO”, *Classical and Quantum Gravity* **23**, S125–S131 (2006) (cit. on p. 39).
364. S. Kawamura et al., “Current status of space gravitational wave antenna DECIGO and B-DECIGO”, *Progress of Theoretical and Experimental Physics* **2021**, 05A105 (2021) (cit. on p. 39).
365. B. Canuel et al., “Exploring gravity with the MIGA large scale atom interferometer”, *Scientific Reports* **8**, 14064 (2018) (cit. on p. 40).
366. J. Coleman, “MAGIS-100 at Fermilab”, [arXiv:1812.00482](https://arxiv.org/abs/1812.00482) (cit. on p. 40).
367. B. Canuel et al., “ELGAR—a European Laboratory for Gravitation and Atom-interferometric Research”, *Classical and Quantum Gravity* **37**, 225017 (2020) (cit. on p. 40).
368. L. Badurina et al., “AION: an atom interferometer observatory and network”, *J. Cosmology Astropart. Phys.* **2020**, 011 (2020) (cit. on p. 40).
369. J. Hogan et al., “Gravitational Waves in the Mid-band with Atom Interferometry”, *BAAS* **51**, 453 (2019) (cit. on p. 40).
370. B. Canuel et al., “Technologies for the ELGAR large scale atom interferometer array”, [arXiv:2007.04014](https://arxiv.org/abs/2007.04014) (cit. on p. 40).
371. J. Harms, “Terrestrial gravity fluctuations”, *Living Reviews in Relativity* **22**, 6 (2019) (cit. on pp. 40, 70, 88).
372. M. Ando et al., “Torsion-Bar Antenna for Low-Frequency Gravitational-Wave Observations”, *Phys. Rev. Lett.* **105**, 161101 (2010) (cit. on p. 41).
373. T. Shimoda et al., “Torsion-Bar Antenna: A ground-based mid-frequency and low-frequency gravitational wave detector”, *International Journal of Modern Physics D* **29**, 1940003 (2020) (cit. on p. 41).
374. J. A. Clark et al., “Observing gravitational waves from the post-merger phase of binary neutron star coalescence”, *Classical and Quantum Gravity* **33**, 085003 (2016) (cit. on p. 43).
375. B. P. Abbott et al., “Exploring the sensitivity of next generation gravitational wave detectors”, *Classical and Quantum Gravity* **34**, 044001 (2017) (cit. on pp. 44, 47, 80).

## References

376. S. P. Timoshenko and J. M. Gere, *Theory of Elastic Stability*, 2nd ed. (Dover Publications, New York, NY, 1961) (cit. on p. 46).
377. R. X. Adhikari et al., “Astrophysical science metrics for next-generation gravitational-wave detectors”, *Class. Quant. Grav.* **36**, 245010 (2019) (cit. on pp. 50, 51).
378. E. D. Hall and M. Evans, “Metrics for next-generation gravitational-wave detectors”, *Classical and Quantum Gravity* **36**, 225002 (2019) (cit. on pp. 50, 51).
379. C. E. Team, “Cosmic Explorer Trade Study—Goals and Objectives”, In preparation, 1–20 (2021) (cit. on pp. 50, 51).
380. S. Borhanian and B. Sathyaprakash, “Listening to the Universe with Next Generation Gravitational-Wave Observatories”, In preparation, 1–30 (2021) (cit. on pp. 50, 51).
381. I. Mandel and F. S. Broekgaard, “Rates of Compact Object Coalescences”, (2021), arXiv:2107.14239 [astro-ph.HE] (cit. on p. 51).
382. R. Abbott et al., “Population Properties of Compact Objects from the Second LIGO-Virgo Gravitational-Wave Transient Catalog”, *ApJ* **913**, L7 (2021) (cit. on p. 51).
383. V. Srivastava et al., *CEHS: Metric for Black Holes and Neutron Stars throughout Cosmic time, and Testing General Relativity*, tech. rep. CE-T2100009 (Cosmic Explorer, 2021) (cit. on pp. 54–56).
384. S. Vitale and M. Evans, “Parameter estimation for binary black holes with networks of third generation gravitational-wave detectors”, *Phys. Rev. D* **95**, 064052 (2017) (cit. on p. 55).
385. S. Vitale and C. Whittle, “Characterization of binary black holes by heterogeneous gravitational-wave networks”, *Phys. Rev. D* **98**, 024029 (2018) (cit. on p. 55).
386. R. Abbott et al., “Properties and Astrophysical Implications of the 150  $M_{\odot}$  Binary Black Hole Merger GW190521”, *ApJ* **900**, L13 (2020) (cit. on p. 55).
387. V. Srivastava et al., *Understanding Dynamics of Dense Matter Through Observation of Astrophysical Populations*, tech. rep. CE-T2100010 (Cosmic Explorer, 2021) (cit. on p. 59).
388. C. M. Caves, “Quantum-mechanical noise in an interferometer”, *Phys. Rev. D* **23**, 1693–1708 (1981) (cit. on pp. 67, 83).
389. H. J. Kimble et al., “Conversion of conventional gravitational wave interferometers into QND interferometers by modifying their input and / or output optics”, *Phys. Rev. D* **65**, 022002 (2002) (cit. on pp. 67, 68).
390. A. Buonanno and Y. Chen, “Signal recycled laser-interferometer gravitational-wave detectors as optical springs”, *Phys. Rev. D* **65**, 042001 (2002) (cit. on p. 67).
391. L. Barsotti, J. Harms and R. Schnabel, “Squeezed vacuum states of light for gravitational wave detectors”, *Reports on Progress in Physics* **82**, 016905 (2019) (cit. on p. 67).
392. M. Tse et al., “Quantum-Enhanced Advanced LIGO Detectors in the Era of Gravitational-Wave Astronomy”, *Phys. Rev. Lett.* **123**, 231107 (2019) (cit. on pp. 67, 82).
393. M. Evans et al., “Realistic filter cavities for advanced gravitational wave detectors”, *Phys. Rev. D* **88**, 022002 (2013) (cit. on p. 68).

## References

394. P. Kwee et al., “Decoherence and degradation of squeezed states in quantum filter cavities”, *Phys. Rev. D* **90**, 062006 (2014) (cit. on p. 68).
395. S. M. Aston et al., “Update on quadruple suspension design for Advanced LIGO”, *Classical and Quantum Gravity* **29**, 235004 (2012) (cit. on pp. 69, 86).
396. F. Matichard et al., “Seismic isolation of Advanced LIGO: Review of strategy, instrumentation and performance”, *Classical and Quantum Gravity* **32**, 185003 (2015) (cit. on p. 69).
397. P. Kwee et al., “Stabilized high-power laser system for the gravitational wave detector advanced LIGO”, *Optics Express* **20**, 10617 (2012) (cit. on pp. 70, 85).
398. C. Cahillane, G. Mansell and D. Sigg, “Laser Frequency Noise in Next Generation Gravitational-Wave Detectors”, (2021), arXiv:2107.14349 [physics.ins-det] (cit. on pp. 70, 85).
399. J. C. Driggers, J. Harms and R. X. Adhikari, “Subtraction of Newtonian noise using optimized sensor arrays”, *Phys. Rev. D* **86**, 102001 (2012) (cit. on pp. 70, 88).
400. J. Harms and S. Hild, “Passive Newtonian noise suppression for gravitational-wave observatories based on shaping of the local topography”, *Classical and Quantum Gravity* **31**, 185011 (2014) (cit. on pp. 70, 87).
401. S. Brûlé et al., “Experiments on Seismic Metamaterials: Molding Surface Waves”, *Phys. Rev. Lett.* **112**, 133901 (2014) (cit. on pp. 70, 87).
402. A. Palermo et al., “Engineered metabarrier as shield from seismic surface waves”, *Scientific Reports* **6**, 39356 (2016) (cit. on pp. 70, 87).
403. A. Colombi et al., “A seismic metamaterial: The resonant metawedge”, *Scientific Reports* **6**, 27717 (2016) (cit. on pp. 70, 87).
404. P. Roux et al., “Toward seismic metamaterials: The METAFORÉT project”, *Seismological Research Letters* **89**, 582–593 (2018) (cit. on pp. 70, 87).
405. B. Kamai and LIGO Team, “Can we cloak LIGO from Seismic Waves?”, in APS April Meeting Abstracts, Vol. 2019, APS Meeting Abstracts (Jan. 2019), R11.006 (cit. on pp. 70, 87).
406. R. Zaccherini et al., “Locally Resonant Metasurfaces for Shear Waves in Granular Media”, *Physical Review Applied* **13**, 034055 (2020) (cit. on pp. 70, 87).
407. R. Bork et al., “advligorts: The Advanced LIGO real-time digital control and data acquisition system”, *SoftwareX* **13**, 100619 (2021) (cit. on p. 71).
408. A. F. Brooks et al. (LIGO Scientific), “Point absorbers in Advanced LIGO”, *Appl. Opt.* **60**, 4047 (2021) (cit. on pp. 71, 81).
409. A. F. Brooks et al., “Overview of Advanced LIGO adaptive optics”, *Appl. Opt.* **55**, 8256 (2016) (cit. on p. 71).
410. M. E. Zucker and S. E. Whitcomb, “Measurement of Optical Path Fluctuations due to Residual Gas in the LIGO 40 Meter Interferometer”, in Proceedings of the Seventh Marcel Grossman Meeting on recent developments in theoretical and experimental general relativity, gravitation, and relativistic field theories, edited by R. T. Jantzen, G. Mac Keiser and R. Ruffini (Jan. 1996), p. 1434 (cit. on p. 74).

## References

411. A. Cavalleri et al., “Gas damping force noise on a macroscopic test body in an infinite gas reservoir”, *Physics Letters A* **374**, 3365–3369 (2010) (cit. on p. 74).
412. R. Dolesi et al., “Brownian force noise from molecular collisions and the sensitivity of advanced gravitational wave observatories”, *Phys. Rev. D* **84**, 063007 (2011) (cit. on p. 74).
413. R. Weiss, *Postbake Measurements of Module Y2 at Hanford*, tech. rep. LIGO–C982529 (LIGO, Sept. 1998) (cit. on p. 75).
414. Y. Bai, *Cosmic Explorer: Back-scattering Noise and Design Recommendations*, tech. rep. LIGO–T1900854 (LIGO, 2020) (cit. on pp. 76, 91).
415. E. D. Hall et al., “Gravitational-wave physics with Cosmic Explorer: Limits to low-frequency sensitivity”, *Phys. Rev. D* **103**, 122004 (2021) (cit. on pp. 76, 80, 86–89, 92).
416. C. Park, T. Ha and B. Cho, “Thermal outgassing rates of low-carbon steels”, *Journal of Vacuum Science Technology A: Vacuum Surfaces and Films* **34**, 021601 (2016) (cit. on p. 79).
417. R. Weiss, *Third generation beamtube vacuum system study*, tech. rep. LIGO–T1900023 (LIGO Laboratory, 2019) (cit. on p. 79).
418. G. Billingsley, H. Yamamoto and L. Zhang, “Characterization of Advanced LIGO core optics”, *American Society for Precision Engineering (ASPE)* **66**, 78–83 (2017) (cit. on p. 80).
419. A. S. Bell et al., “Anomalous optical surface absorption in nominally pure silicon samples at 1550 nm”, *Class. Quant. Grav.* **34**, 205013 (2017) (cit. on p. 80).
420. G. Vajente et al., “Low Mechanical Loss TiO<sub>2</sub>:GeO<sub>2</sub> Coatings for Reduced Thermal Noise in Gravitational Wave Interferometers”, *Phys. Rev. Lett.* **127**, 071101 (2021) (cit. on p. 81).
421. P. Koch et al., “Thickness uniformity measurements and damage threshold tests of large-area GaAs/AlGaAs crystalline coatings for precision interferometry”, *Optics Express* **27**, 36731 (2019) (cit. on p. 81).
422. P. G. Murray et al., “Ion-beam sputtered amorphous silicon films for cryogenic precision measurement systems”, *Phys. Rev. D* **92**, 062001 (2015) (cit. on p. 81).
423. A. Buikema et al., “Sensitivity and performance of the Advanced LIGO detectors in the third observing run”, *Phys. Rev. D* **102**, 062003 (2020) (cit. on pp. 81, 91).
424. F. Acernese et al., “Increasing the Astrophysical Reach of the Advanced Virgo Detector via the Application of Squeezed Vacuum States of Light”, *Phys. Rev. Lett.* **123**, 231108 (2019) (cit. on p. 82).
425. H. Grote et al., “First Long-Term Application of Squeezed States of Light in a Gravitational-Wave Observatory”, *Phys. Rev. Lett.* **110**, 181101 (2013) (cit. on p. 82).
426. E. Oelker et al., “Audio-Band Frequency-Dependent Squeezing for Gravitational-Wave Detectors”, *Phys. Rev. Lett.* **116**, 041102 (2016) (cit. on p. 82).
427. L. McCuller et al., “Frequency-Dependent Squeezing for Advanced LIGO”, *Phys. Rev. Lett.* **124**, 171102 (2020) (cit. on p. 82).
428. A. R. Wade et al., “A squeezed light source operated under high vacuum”, *Scientific Reports* **5**, 18052 (2015) (cit. on p. 83).

## References

429. E. Oelker et al., “Ultra-low phase noise squeezed vacuum source for gravitational wave detectors”, *Optica* **3**, 682 (2016) (cit. on p. 83).
430. G. L. Mansell et al., “Observation of Squeezed Light in the 2  $\mu$  m Region”, *Phys. Rev. Lett.* **120**, 203603 (2018) (cit. on p. 83).
431. E. Genin et al., “Vacuum-compatible low-loss Faraday isolator for efficient squeezed-light injection in laser-interferometer-based gravitational-wave detectors”, *Appl. Opt.* **57**, 9705 (2018) (cit. on p. 83).
432. E. Knyazev, F. Y. Khalili and M. V. Chekhova, “Overcoming inefficient detection in sub-shot-noise absorption measurement and imaging”, *Optics Express* **27**, 7868 (2019) (cit. on p. 83).
433. Y. Bai et al., “Phase-sensitive optomechanical amplifier for quantum noise reduction in laser interferometers”, *Phys. Rev. A* **102**, 023507 (2020) (cit. on p. 83).
434. L. McCuller et al., “LIGOs Quantum Response to Squeezed States”, *arXiv:2105.12052* (cit. on pp. 83, 85).
435. N. Kijbunchoo et al., “Low phase noise squeezed vacuum for future generation gravitational wave detectors”, *Classical and Quantum Gravity* **37**, 185014 (2020) (cit. on p. 83).
436. H. Miao, N. D. Smith and M. Evans, “Quantum Limit for Laser Interferometric Gravitational-Wave Detectors from Optical Dissipation”, *Physical Review X* **9**, 011053 (2019) (cit. on p. 84).
437. H. T. Cao et al., “Enhancing the dynamic range of deformable mirrors with compression bias”, *Optics Express* **28**, 38480 (2020) (cit. on p. 85).
438. H. T. Cao et al., “High dynamic range thermally actuated bimorph mirror for gravitational wave detectors”, *Appl. Opt.* **59**, 2784 (2020) (cit. on p. 85).
439. B. Willke et al., “Stabilized High Power Laser for Advanced Gravitational Wave Detectors”, in *Journal of Physics Conference Series*, Vol. 32, Journal of Physics Conference Series (Mar. 2006), pp. 270–275 (cit. on p. 85).
440. D. P. Kapasi et al., “Tunable narrow-linewidth laser at 2  $\mu$ m wavelength for gravitational wave detector research”, *Optics Express* **28**, 3280 (2020) (cit. on p. 85).
441. A. Heptonstall et al., “Invited Article: CO<sub>2</sub> laser production of fused silica fibers for use in interferometric gravitational wave detector mirror suspensions”, *Review of Scientific Instruments* **82**, 011301-011301-9 (2011) (cit. on p. 86).
442. K. V. Tokmakov et al., “A study of the fracture mechanisms in pristine silica fibres utilising high speed imaging techniques”, *Journal of Non Crystalline Solids* **358**, 1699–1709 (2012) (cit. on p. 86).
443. K.-H. Lee et al., “Improved fused silica fibres for the advanced LIGO monolithic suspensions”, *Classical and Quantum Gravity* **36**, 185018 (2019) (cit. on p. 86).
444. R. Birney et al., “Coatings and surface treatments for enhanced performance suspensions for future gravitational wave detectors”, *Classical and Quantum Gravity* **34**, 235012 (2017) (cit. on p. 86).
445. A. V. Cumming et al., “Silicon mirror suspensions for gravitational wave detectors”, *Classical and Quantum Gravity* **31**, 025017 (2014) (cit. on p. 86).

## References

446. S. J. Cooper et al., “A compact, large-range interferometer for precision measurement and inertial sensing”, *Classical and Quantum Gravity* **35**, 095007 (2018) (cit. on p. 87).
447. K. Venkateswara et al., “A high-precision mechanical absolute-rotation sensor”, *Review of Scientific Instruments* **85**, 015005 (2014) (cit. on p. 87).
448. M. W. Coughlin et al., “Implications of Dedicated Seismometer Measurements on Newtonian-Noise Cancellation for Advanced LIGO”, *Phys. Rev. Lett.* **121**, 221104 (2018) (cit. on pp. 87, 88).
449. M. P. Ross et al., “Towards windproofing LIGO: reducing the effect of wind-driven floor tilt by using rotation sensors in active seismic isolation”, *Classical and Quantum Gravity* **37**, 185018 (2020) (cit. on p. 87).
450. J. V. van Heijningen, A. Bertolini and J. F. J. van den Brand, “A novel interferometrically read out inertial sensor for future gravitational wave detectors”, in 2018 IEEE Sensors Applications Symposium (SAS) (2018), pp. 1–5 (cit. on p. 87).
451. J. V. van Heijningen, “A fifty-fold improvement of thermal noise limited inertial sensitivity by operating at cryogenic temperatures”, *Journal of Instrumentation* **15**, P06034 (2020) (cit. on p. 87).
452. C. M. Mow-Lowry and D. Martynov, “A 6D interferometric inertial isolation system”, *Classical and Quantum Gravity* **36**, 245006 (2019) (cit. on p. 87).
453. H. Yu et al., “Prospects for Detecting Gravitational Waves at 5 Hz with Ground-Based Detectors”, *Phys. Rev. Lett.* **120**, 141102 (2018) (cit. on p. 87).
454. P. Nguyen et al. (AdvLIGO), “Environmental noise in advanced LIGO detectors”, *Class. Quant. Grav.* **38**, 145001 (2021) (cit. on pp. 88, 91, 92).
455. M. W. Coughlin et al., “Measurement and subtraction of Schumann resonances at gravitational-wave interferometers”, *Phys. Rev. D* **97**, 102007 (2018) (cit. on p. 88).
456. T. Middelmann et al., “Thermal expansion coefficient of single-crystal silicon from 7 K to 293 K”, *Phys. Rev. B* **92**, 174113 (2015) (cit. on p. 89).
457. C. Blair, Y. Levin and E. Thrane, “Constraining temperature distribution inside LIGO test masses from frequencies of their vibrational modes”, *Phys. Rev. D* **103**, 022003 (2021) (cit. on p. 89).
458. L. Sun et al., “Characterization of systematic error in Advanced LIGO calibration”, *Classical and Quantum Gravity* **37**, 225008 (2020) (cit. on pp. 89–91).
459. L. Sun et al., “Characterization of systematic error in Advanced LIGO calibration in the second half of O3”, *arXiv:2107.00129* (cit. on pp. 89, 90).
460. Virgo Collaboration et al., “Calibration of Advanced Virgo and reconstruction of detector strain  $h(t)$  during the Observing Run O3”, *arXiv:2107.03294* (cit. on p. 89).
461. F. Acernese et al. (Virgo), “Calibration of Advanced Virgo and Reconstruction of the Gravitational Wave Signal  $h(t)$  during the Observing Run O2”, *Class. Quant. Grav.* **35**, 205004 (2018) (cit. on p. 89).
462. I. Bartos et al., “The Advanced LIGO timing system”, *Classical and Quantum Gravity* **27**, 084025 (2010) (cit. on p. 89).
463. Y. Asali, S. Countryman and Z. Marka, *aLIGO Timing System Checks During O3A*, tech. rep. LIGO–T1900799 (LIGO, 2019) (cit. on p. 89).



## References

464. L. Lindblom, “Optimal calibration accuracy for gravitational-wave detectors”, *Phys. Rev. D* **80**, 042005 (2009) (cit. on p. 89).
465. M. Agathos et al., “TIGER: A data analysis pipeline for testing the strong-field dynamics of general relativity with gravitational wave signals from coalescing compact binaries”, *Phys. Rev. D* **89**, 082001 (2014) (cit. on p. 89).
466. S. Vitale et al., “Effect of calibration errors on Bayesian parameter estimation for gravitational wave signals from inspiral binary systems in the advanced detectors era”, *Phys. Rev. D* **85**, 064034 (2012) (cit. on p. 89).
467. E. D. Hall et al., “Systematic calibration error requirements for gravitational-wave detectors via the Cramér-Rao bound”, *Classical and Quantum Gravity* **36**, 205006 (2019) (cit. on pp. 89–91).
468. S. Vitale et al., “Physical approach to the marginalization of LIGO calibration uncertainties”, *Phys. Rev. D* **103**, 063016 (2021) (cit. on pp. 89, 91).
469. E. Payne et al., “Gravitational-wave astronomy with a physical calibration model”, *Phys. Rev. D* **102**, 122004 (2020) (cit. on pp. 89, 91).
470. H.-Y. Chen et al., “A Program for Multimessenger Standard Siren Cosmology in the Era of LIGO A+, Rubin Observatory, and Beyond”, *ApJ* **908**, L4 (2021) (cit. on p. 89).
471. B. F. Schutz, “Gravitational-wave astronomy: delivering on the promises”, *Philosophical Transactions of the Royal Society of London Series A* **376**, 20170279 (2018) (cit. on p. 90).
472. D. Tuyenbayev et al., “Improving LIGO calibration accuracy by tracking and compensating for slow temporal variations”, *Classical and Quantum Gravity* **34**, 015002 (2017) (cit. on p. 90).
473. A. D. Viets et al., “Reconstructing the calibrated strain signal in the Advanced LIGO detectors”, *Classical and Quantum Gravity* **35**, 095015 (2018) (cit. on p. 90).
474. S. Karki et al., “The Advanced LIGO photon calibrators”, *Review of Scientific Instruments* **87**, 114503 (2016) (cit. on p. 90).
475. D. Estevez et al., “The Advanced Virgo photon calibrators”, *Classical and Quantum Gravity* **38**, 075007 (2021) (cit. on p. 90).
476. D. Bhattacharjee et al., “Fiducial displacements with improved accuracy for the global network of gravitational wave detectors”, *Class. Quant. Grav.* **38**, 015009 (2021) (cit. on p. 90).
477. M. Spidell et al., “A Bilateral Comparison of NIST And PTB Laser Power Standards for Increased Calibration Confidence at LIGO”, in, Vol. OR (14th International Conference on New Developments and Applications in Optical Radiometry, 2021), p. 017 (cit. on p. 90).
478. A. Vaskuri et al., “Microfabricated bolometer based on a vertically aligned carbon nanotube absorber”, in *Synthesis and Photonics of Nanoscale Materials XVII*, Vol. 11269, edited by J. J. Dubowski, D. B. Geohegan and A. V. Kabashin (International Society for Optics and Photonics, 2020), pp. 41–52 (cit. on p. 90).
479. E. Goetz and R. L. Savage Jr, “Calibration of the LIGO displacement actuators via laser frequency modulation”, *Class. Quant. Grav.* **27**, 215001 (2010) (cit. on p. 90).
480. B. P. Abbott et al., “Calibration of the Advanced LIGO detectors for the discovery of the binary black-hole merger GW150914”, *Phys. Rev. D* **95**, 062003 (2017) (cit. on p. 90).

## References

481. J. Abadie et al. (LIGO Scientific), “Calibration of the LIGO Gravitational Wave Detectors in the Fifth Science Run”, *Nucl. Instrum. Meth. A* **624**, 223–240 (2010) (cit. on p. 90).
482. T. Accadia et al., “Calibration and sensitivity of the Virgo detector during its second science run”, *Classical and Quantum Gravity* **28**, 025005 (2011) (cit. on p. 90).
483. R. Essick and D. E. Holz, “Calibrating gravitational-wave detectors with GW170817”, *Classical and Quantum Gravity* **36**, 125002 (2019) (cit. on p. 90).
484. B. F. Schutz and B. S. Sathyaprakash, “Self-calibration of Networks of Gravitational Wave Detectors”, (2020), [arXiv:2009.10212 \[gr-qc\]](https://arxiv.org/abs/2009.10212) (cit. on p. 90).
485. M. P. Ross et al., “Initial Results from the LIGO Newtonian Calibrator”, [arXiv:2107.00141](https://arxiv.org/abs/2107.00141) (cit. on p. 90).
486. D. Estevez, B. Mours and T. Pradier, “Newtonian calibrator tests during the Virgo O3 data taking”, *Class. Quant. Grav.* **38**, 075012 (2021) (cit. on p. 90).
487. Y. Inoue et al., “Improving the absolute accuracy of the gravitational wave detectors by combining the photon pressure and gravity field calibrators”, *Phys. Rev. D* **98**, 022005 (2018) (cit. on p. 90).
488. M. Rakhmanov et al., “Dynamic resonance of light in Fabry-Perot cavities [rapid communication]”, *PhLA* **305**, 239–244 (2002) (cit. on p. 91).
489. M. Rakhmanov, J. D. Romano and J. T. Whelan, “High-frequency corrections to the detector response and their effect on searches for gravitational waves”, *Class. Quant. Grav.* **25**, edited by S. Hughes and E. Katsavounidis, 184017 (2008) (cit. on p. 91).
490. R. L. Ward, *Length Sensing and Control of a Prototype Advanced Interferometric Gravitational Wave Detector*, PhD thesis (Caltech, 2010) (cit. on p. 91).
491. K. Izumi and C. Cahillane, *DARM response with a small detuning*, tech. rep. LIGO–T1600278 (LIGO, 2016) (cit. on p. 91).
492. E. Hall, *Calibrating optical springs*, tech. rep. LIGO–G1601599 (LIGO, 2016) (cit. on p. 91).
493. C. Cahillane et al. (LIGO Scientific), “Calibration uncertainty for Advanced LIGO’s first and second observing runs”, *Phys. Rev. D* **96**, 102001 (2017) (cit. on p. 91).
494. D. Davis et al., “Improving the sensitivity of Advanced LIGO using noise subtraction”, *Classical and Quantum Gravity* **36**, 055011 (2019) (cit. on p. 91).
495. G. Vajente et al., “Machine-learning nonstationary noise out of gravitational-wave detectors”, *Phys. Rev. D* **101**, 042003 (2020) (cit. on p. 91).
496. G. Vajente and J. Marque, “Stray light issues in advanced interferometers and the search for gravitational waves”, *Astrophys. Space Sci. Libr.* **404**, 275–290 (2014) (cit. on p. 91).
497. D. J. Ottaway, P. Fritschel and S. J. Waldman, “Impact of upconverted scattered light on advanced interferometric gravitational wave detectors”, *Optics Express* **20**, 8329 (2012) (cit. on p. 91).
498. S. Soni et al. (LIGO), “Reducing scattered light in LIGO’s third observing run”, *Class. Quant. Grav.* **38**, 025016 (2020) (cit. on p. 91).
499. M. Waş, R. Gouaty and R. Bonnard, “End benches scattered light modelling and subtraction in advanced Virgo”, *Classical and Quantum Gravity* **38**, 075020 (2021) (cit. on p. 91).

## References

500. E. Flanagan and K. Thorne, *Noise Due to Backscatter Off Baffles, the Nearby Wall, and Objects at the Far end of the Beam Tube, and Recommended Actions*, tech. rep. LIGO–T940063–00–R (LIGO, 1994) (cit. on p. 91).
501. J. Smith and G. Vajente, *Cosmic Explorer Scattering Update*, GWADW, 2021 (cit. on p. 92).
502. A. Ananyeva, *Stray light control upgrades for LIGO 4th Observation run*, GWADW, 2021 (cit. on p. 92).
503. J. Degallaix et al., “Bulk optical absorption of high resistivity silicon at 1550 nm”, *Optics Letters* **38**, 2047 (2013) (cit. on p. 92).
504. J. Eichholz et al., “Practical test mass and suspension configuration for a cryogenic kilohertz gravitational wave detector”, *Phys. Rev. D* **102**, 122003 (2020) (cit. on p. 93).
505. K. Kuns and M. Evans, *Cosmic Explorer Site Search*, tech. rep. CE-T2000016 (Cosmic Explorer Project, 2020) (cit. on p. 95).
506. D. P. Henkel, *MIT Steel Consulting Services*, tech. rep. CE-T2000009 (Rimkus Consulting Group, 2020) (cit. on p. 95).
507. K. Jotania, S. R. Valluri and S. V. Dhurandhar, “A study of the gravitational wave form from pulsars.”, *A&A* **306**, 317 (1996) (cit. on p. 100).
508. T. Adams et al., “Low-latency analysis pipeline for compact binary coalescences in the advanced gravitational wave detector era”, *Classical and Quantum Gravity* **33**, 175012 (2016) (cit. on p. 100).
509. S. Sachdev et al., “The GstLAL Search Analysis Methods for Compact Binary Mergers in Advanced LIGO’s Second and Advanced Virgo’s First Observing Runs”, *arXiv:1901.08580* (cit. on p. 100).
510. K. Cannon et al., “GstLAL: A software framework for gravitational wave discovery”, *SoftwareX* **14**, 100680 (2021) (cit. on p. 100).
511. B. J. Owen and B. S. Sathyaprakash, “Matched filtering of gravitational waves from inspiraling compact binaries: Computational cost and template placement”, *Phys. Rev. D* **60**, 022002 (1999) (cit. on p. 100).
512. A. K. Lenon, D. A. Brown and A. H. Nitz, “Eccentric Binary Neutron Star Search Prospects for Cosmic Explorer”, *arXiv:2103.14088* (cit. on p. 100).
513. N. J. Cornish, “Fast Fisher Matrices and Lazy Likelihoods”, *arXiv:1007.4820* (cit. on p. 100).
514. B. Zackay, L. Dai and T. Venumadhav, “Relative Binning and Fast Likelihood Evaluation for Gravitational Wave Parameter Estimation”, *arXiv:1806.08792* (cit. on p. 100).
515. D. Finstad and D. A. Brown, “Fast Parameter Estimation of Binary Mergers for Multimessenger Follow-up”, *ApJ* **905**, L9 (2020) (cit. on p. 100).
516. E. Pizzati et al., “Bayesian inference of overlapping gravitational wave signals”, *arXiv:2102.07692* (cit. on p. 100).
517. M. Purrer and C.-J. Haster, “Gravitational waveform accuracy requirements for future ground-based detectors”, *Physical Review Research* **2**, 023151 (2020) (cit. on p. 102).
518. D. Ferguson et al., “Assessing the Readiness of Numerical Relativity for LISA and 3G Detectors”, *arXiv:2006.04272* (cit. on p. 102).

## References

519. K. Barkett et al., “Gravitational waveforms for neutron star binaries from binary black hole simulations”, *Phys. Rev. D* **93**, 044064 (2016) (cit. on p. 102).
520. M. Hendry, *LSC EPO White Paper and Executive Summary 2019-20 (public version)*, tech. rep. LIGO-T1900780-v1 (LIGO, Nov. 2019) (cit. on p. 104).
521. *Science Education Center*, Laser Interferometer Gravitational-Wave Observatory, <https://www.ligo.caltech.edu/LA/page/Science-Education-Center> (visited on 5 July 2021) (cit. on p. 104).
522. *Gravity Discovery Centre*, Gravity Discovery Centre, <https://gravitycentre.com.au/> (visited on 5 July 2021) (cit. on p. 104).
523. *A Brief History of Fermilab*, Fermilab, <https://history.fnal.gov/history-fermi.html> (visited on 5 July 2021) (cit. on p. 105).
524. D. Richardson, ed., *APS CSWP & COM Gazette* 39 (2 2020) (cit. on p. 105).
525. K. Kimura et al., “A Hua He Inoa: Hawaiian Culture-Based Celestial Naming”, in *Bulletin of the American Astronomical Society*, Vol. 51 (Sept. 2019), p. 135 (cit. on pp. 105, 107).
526. *Malalo o Ka Po Lani*, Maunakea Visitor Information Station, (2021) <http://www.ifa.hawaii.edu/info/vis/visiting-mauna-kea/saturday-night-programs/malalo-o-ka-po-lani.html> (visited on 5 July 2021) (cit. on p. 105).
527. New Mexico Water Resources Research Institute, ed., *Community Teach-In: Animas and San Juan Watersheds Week*, YouTube, (19 June 2020) [https://youtu.be/KV5Q-i\\_ae88](https://youtu.be/KV5Q-i_ae88) (visited on 5 July 2021) (cit. on p. 105).
528. R. Dunbar-Ortiz, *An Indigenous Peoples’ History of the United States* (Beacon Press, 2014) (cit. on p. 106).
529. L. Swanner, “Contested Spiritual Landscapes in Modern American Astronomy”, *Journal of Religion and Society Supplement* **11** *Religion and the Sciences: Opportunities and Challenges*, edited by R. A. Simkins and T. M. Kelly, 149–62 (2015) (cit. on p. 106).
530. S. Kahanamoku et al., “A Native Hawaiian-led summary of the current impact of constructing the Thirty Meter Telescope on Maunakea”, *arXiv:2001.00970* (cit. on p. 106).
531. M. A. Nash, “Entangled Pasts: Land-Grant Colleges and American Indian Dispossession”, *History of Education Quarterly* **59**, 437–467 (2019) (cit. on p. 106).
532. R. Lee and T. Ahtone, “Land-grab universities”, *High Country News* **52** (2020) (cit. on p. 106).
533. F. S. Hodge, “No meaningful apology for American Indian unethical research abuses”, *Ethics & Behavior* **22**, 431–444 (2012) (cit. on p. 106).
534. K. Gardner-Vandy et al., “Relationships First and Always: A Guide to Collaborations with Indigenous Communities”, in *Bulletin of the American Astronomical Society*, Vol. 53 (May 2021), p. 471 (cit. on p. 106).
535. D. Clery, “No safe haven for the Thirty Meter Telescope”, *Science* **365**, 960–961 (2019) (cit. on p. 106).
536. B. Barbu, “Where science meets the sacred”, *Symmetry* (2021) (cit. on p. 107).
537. N. Greenfieldboyce, “How A Cosmic Collision Sparked A Native American Translator’s Labor Of Love”, *National Public Radio* (2019) (cit. on p. 107).

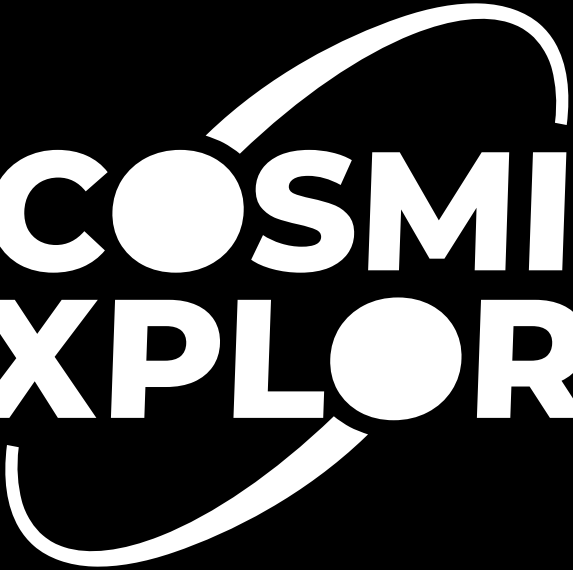
## References

538. *Abuduuxbiisiya o?bigimskAAsts noo?gutsiisaduubya giibiibui agessduuyiists Apstiixisamu EIN-STEIN'S iigayissxinim*, (2016) <https://www.ligo.org/detections/GW150914/press-release/siksika.pdf> (cit. on p. 107).
539. A. Good and A. Johnson, “NASA’s Perseverance Mars Rover Mission Honors Navajo Language”, (2021) (cit. on p. 107).
540. National Science Foundation, *Action Plan of the National Science Foundation to Enhance Tribal Consultation*, <https://www.nsf.gov/geo/opp/arctic/ace/TribalEngagementActionPlan.PDF>, 2021 (cit. on p. 108).
541. *SU LIGO Project*, Southern University, <https://www.subr.edu/subhome/73> (visited on 5 July 2021) (cit. on p. 108).
542. GWIC, Gravitational Wave International Committee, <https://gwic.ligo.org/> (cit. on pp. 109, 111).
543. *Gravitational Wave Agencies Correspondents*, National Science Foundation, <https://www.nsf.gov/mps/phy/gwac.jsp> (visited on 5 July 2021) (cit. on pp. 109, 112).
544. <https://www.roster.cosmicexplorer.org> (cit. on p. 109).
545. E. Hall, “The Next Generation of Ground-Based Gravitational-Wave Detectors”, in APS April Meeting Abstracts, Vol. 2019, APS Meeting Abstracts (Jan. 2019), p. C02.003 (cit. on p. 109).
546. J. Smith, “Cosmic Explorer: the proposed US contribution to the third-generation gravitational-wave detector network.”, *Bulletin of the American Physical Society* **65** (2020) (cit. on p. 109).
547. [https://www.snowmass21.org/docs/files/summaries/CF/SNOWMASS21-CF7\\_CF6-AF6\\_AF0-IF1\\_IF0-010.pdf](https://www.snowmass21.org/docs/files/summaries/CF/SNOWMASS21-CF7_CF6-AF6_AF0-IF1_IF0-010.pdf) (cit. on p. 109).
548. D. Reitze et al., “The US Program in Ground-Based Gravitational Wave Science: Contribution from the LIGO Laboratory”, *Bull. Am. Astron. Soc.* **51**, 141 (2019) (cit. on p. 110).
549. A. Cho, “Giant detectors could hear murmurs from across universe”, *Science* **371**, 1089–1090 (2021) (cit. on p. 110).
550. *What’s next for LIGO? Report from the 1st Dawn Workshop* (Silver Spring MD, USA, May 2015) (cit. on p. 111).
551. *What’s next for LIGO? Report from the 2nd Dawn Workshop* (Atlanta GA, USA, July 2016) (cit. on p. 111).
552. *What’s next for LIGO? Report from the 3rd Dawn Workshop* (Syracuse NY, USA, July 2017) (cit. on p. 111).
553. *Global strategies for gravitational wave astronomy: Report from the 4th Dawn Workshop* (Amsterdam, the Netherlands, Aug. 2018) (cit. on p. 111).
554. *Report from the 5th Dawn Workshop* (Cascina, Italy, May 2019) (cit. on p. 111).
555. GWIC-3G, Gravitational Wave International Committee, <https://gwic.ligo.org/3Gsubcomm/documents.html> (visited on 5 July 2021) (cit. on p. 111).
556. <http://www.et-gw.eu/index.php/letter-of-intent> (cit. on p. 112).

## References

557. National Science Foundation, *Diversity and Inclusion Strategic Plan 2012–2016*, <https://www.nsf.gov/od/odi/reports/StrategicPlan.pdf>, 2021 (cit. on p. 112).
558. F. Dylla, R. Weiss and M. E. Zucker, *Proceedings: NSF Workshop on Large Ultrahigh-Vacuum Systems for Frontier Scientific Research*, tech. rep. LIGO–P1900072 (LIGO, 2019) (cit. on p. 114).
559. D. Shoemaker, *Advanced LIGO Project Risk Registry*, tech. rep. LIGO–M080359–v29 (LIGO, 2015) (cit. on p. 121).
560. D. Shoemaker and C. Wilkinson, *Advanced LIGO Risk Management Plan*, tech. rep. LIGO–M060045–v1 (LIGO, 2006) (cit. on p. 121).
561. R. Gaume, NSF/Astronomy Presentation to the Astronomy & Astrophysics Advisory Committee, Unpublished presentation, 2020 (cit. on p. 124).
562. D. Caldwell, NSF/Physics Division Presentation to the Astronomy & Astrophysics Advisory Committee, Unpublished presentation, 2020 (cit. on p. 124).
563. V. Papitashvilli, NSF/Office of Polar Programs Presentation to the Astronomy & Astrophysics Advisory Committee, Unpublished presentation, 2020 (cit. on p. 124).
564. K. Turner, DOE/HEP Presentation to the Astronomy & Astrophysics Advisory Committee, Unpublished presentation, 2020 (cit. on p. 125).
565. S. Ritz et al., Report of the Particle Physics Project Prioritization Panel, U.S. Department of Energy, Office of Science, 2014 (cit. on p. 125).
566. National Research Council, *Nuclear Physics: Exploring the Heart of Matter* (The National Academies Press, Washington, DC, 2013) (cit. on p. 125).
567. P. Hertz, NASA Astrophysics Presentation to the Astronomy & Astrophysics Advisory Committee, Unpublished presentation, 2020 (cit. on p. 125).
568. *Laser Interferometer Space Antenna for the detection and observation of gravitational waves: Pre-phase A report, 2nd Edition*, tech. rep. (Max-Planck Institut für Quantenoptik) (cit. on p. 125).
569. M. Abernathy et al. (ET Science Team), *Einstein Gravitational Wave Telescope Conceptual Design Study*, tech. rep. ET–0106C–10 (Einstein Telescope, 28 June 2011) (cit. on p. 125).
570. D. H. Shoemaker, “Advanced Interferometric Gravitational-Wave Detectors”, in (World Scientific, 2019) Chap. Planning, managing and executing the design and construction of Advanced LIGO, pp. 655–684 (cit. on p. 125).





**COSMIC  
EXPLORER**